# The centriole in evolution: from motility to mitosis

*Amy Elisabeth Smith*

Department of Zoology, University of Oxford

and

Merton College, Oxford

Thesis submitted for the degree of Doctor of Philosophy

October 2013

# Contents

## Abstract

Centrioles and basal bodies with their characteristic 9+2 structure are found in all major eukaryotic lineages. The correlation between the occurrence of centrioles and the presence of cilia/flagella, but not centrosome-like structures, suggests that the ciliogenesis function of centrioles is ancestral. Here, it is demonstrated that the centriole domain of centrosomes emerged within the Metazoa from an ancestral state of possessing a centriole with basal body function but no functional association with a centrosome. Centrosome structures involving a centriole are metazoan innovations.

When an axoneme is still present but no longer fully functional, such as the sensory cilia of *Caenorhabditis elegans* or, as depicted here, the flagellum of the intracellular amastigote stage of the *Leishmania mexicana* parasite, the basal body structure is less constrained and can depart from the canonical structure. A general view has emerged that classifies axonemes into canonical motile 9+2 and noncanonical, sensory 9+0 structures. This study reveals this view to be overly simplistic, and additional axonemal architectures associated with potential sensory structures should be incorporated into prevailing models. Here, a striking similarity between the axoneme structure of *Leishmania* amastigotes and vertebrate primary cilia is revealed. This striking conservation of ciliary structure, despite the evolutionary distance between *Leishmania* and mammalian cells, suggests a sensory function for the amastigote flagellum. Adding weight to a sensory hypothesis, close examination of *Leishmania* positioning inside the parasitophorous vacuole revealed frequent contact between the flagellum tip and the vacuole membrane. A sensory function could also explain the retention of a flagellum in

*Trypanosoma cruzi* amastigotes, an intracellular stage that, as shown in this study, emerged independently to the *Leishmania* amastigote.

Basal body appendages, such as pro-basal bodies and microtubule rootlets, also vary widely in their structure. Choanoflagellates, a sister group to the Metazoa, posses an extensive microtubule rootlet system that provides support for their characteristic collar tentacles. This atypical structure is reflected in the underlying molecular components of the choanoflagellate basal body. The importance of choanoflagellates as the closest known relative of metazoans was first revealed by their similarity to choanocytes, the feeding cells of sponges. Although phylogenetic analyses leave little doubt that choanoflagellates are a sister group of animals, comparisons of molecular and structural components of appendages associated with the collar tentacles highlight significant differences and questions the extent to which the collar structures of choanoflagellates and choanocytes can be assumed to be homologous.

Finally, the confinement of a centriole-based centrosome to the Metazoa provides little support for the flagellar synthesis constraint as an explanation for the origin of multicellularity. There is, indeed, an apparent constraint; no flagellated or ciliated metazoan cell ever divides. This constraint, however, did not arise until after the incorporation of centrioles into the centrosome in the metazoan lineage and the co-option of centrioles as a structural and functional component of the centrosome. The flagellar synthesis constraint is therefore not an explanation for the origin of multicellularity but a consequence of it.

## Acknowledgements

My sincere and immense thanks go to Peter Holland, my supervisor, for his continuous support and constant enthusiasm. I wholeheartedly appreciate all the effort and advice you have provided over the years.

Thank you to Eva Gluenz and Keith Gull, of the Sir William Dunn School of Pathology, for supervising the *Trypanosoma* research. Thank you to Mike Shaw for his assistance with the electron microscopy, to Helen Dawe for her work on vertebrate primary cilia and to Johanna Höög for the electron tomography images. I thank Barry Leadbeater, from the University of Birmingham, for the gift of various choanoflagellate cultures and the London School of Hygiene and Tropical Medicine for the donation of *Trypanosoma* cultures. Thank you to Sally Leys, from the University of Alberta, for her collaboration on the choanocyte project, and for the supply of Canadian Maple Syrup.

For my many questions regarding choanoflagellates, microscopy, phylogenetics and bioinformatics I turned to Seb, Michiel, Jordi, Kyle and other members of the Holland and Shimeld laboratories. Thank you. Special thanks to Ying-Fu for his patient assistance with the rather repetitive coiled-coil screening.

Thanks to the Jackson Scholarship Fund of Merton College for keeping me fed and watered. And to all the staff of Merton College for putting up with me for so long. Special thanks to Simon for his advice and support.

On a more personal note, many warm thanks to Amir and Claire. If it weren't for you both I'd have remained "90.2 percent done" forever. Thanks to Oli and Laura for your helping hands along the way. To my parents and brother, for knowing when to ask about the thesis, and when to keep quiet. And to all those, too many to list here, who helped (and occasionally hindered) my progress.

Special thanks to Andy, Emma and Gareth, for understanding that beyond the marking and lesson planning there was also a thesis to be finished.

Finally, to the students of Lodge Park Academy. For always being in awe of and maintaining my enthusiasm for science. And for never handing in any homework for me to mark.

*All work presented here is my own, except where identified and acknowledged in the text.*

# List of text-figures

## *Chapter One: Introduction*



## *Chapter Three*

4.12. Immunofluorescence localisation of alpha-tubulin in a pinacocyte cell of the developing sponge epidermis in a juvenile *Ephydatia mulleri* grown from an asexual gemmule.

4.13. Effect of cytochalasin D on the actin-based collar tentacles of *Monosiga brevicollis*.

4.14. Disruption of the gene encoding δ-tubulin results in a doublet rather than triplet basal body arrangement due to a specific loss of the C-tubule.

4.15. Structural association of the basal body, microtubule rootlets and microvilli collar tentacles in choanoflagellates.

## *Chapter Five*

5.1. Occurrence of closed and open mitosis in eukaryotes.

5.2. Phylogenetic distribution of basal body, PCM and centriole proteins among 27 eukaryotes.

5.3. Phylogenetic distribution of γ-tubulin complex proteins among 27 eukaryotes.

5.4. Schematic diagram of the domain organization of the *Monosiga brevicollis* cadherin MBCDH8 showing domain content and arrangement.

5.5. Diagram showing best BLAST hit relationships between human centrosome-associated proteins and MBCDH8 *in Monosiga brevicollis*.

5.6. The number of coiled-coil proteins per genome.

5.7. The number of proteins predicted to contain extended coiled-coil domains.

5.8. The percentage of total proteins in a range of eukaryotic and prokaryotic taxa that are predicted to contain coiled-coil domains.

5.9. The percentage of total proteins in a range of eukaryotic and prokaryotic taxa that are predicted to contain extended coiled-coil domains.

5.10. The results of immunofluorescence on *Monosiga brevicollis* using anti-α-tubulin and anti-γ-tubulin antibodies and DNA-binding dye (DAPI).

## *Supplementary Material*

S5.1. Phylogenetic tree of the Opisthokonta, including the Metazoa, Filasterea and Choanozoa (Choanoflagellata); the Apusozoa; and the Amoebozoa.

# List of tables

## *Chapter Three*



## *Chapter Five*



## *Supplementary Material*

# Chapter 1: Introduction

## 1.1 Basal bodies and centrioles: similar structure, discrete functions

Basal bodies and centrioles are highly conserved cellular organelles that share the same basic microtubule-based structure. They consist of a symmetrical array of nine peripheral microtubule triplets positioned around a cylindrical core (Fig. 1.1.). Despite the similarity in overall organisation, basal bodies and centrioles differ in function and cellular location. Basal bodies are located near the cell surface and function in the nucleation of a cilium or flagellum. The inner core of cilia and flagella consists of a cytoskeletal structure called the axoneme which, in its most widely distributed arrangement, consists of nine peripheral doublets arranged around two central microtubules (the "9+2" axoneme). The nine doublet microtubules of the ciliary axoneme extend from the nine triplet microtubules of the basal body. Centrioles are located in the centrosome of animal cells. The animal centrosome consists of two closely associated centrioles, usually in an orthogonal configuration, surrounded by an electron dense cloud of pericentriolar material (PCM). The centrosome functions as the major microtubule organising centre (MTOC) during interphase and generates the mitotic spindle during cell division.

**Figure 1.1.** Schematic of a transverse section through a basal body or centriole.

Basal bodies and centrioles can interconvert, as indicated in vertebrate cells by the migration of a pre-existing centriole to the apical cell surface in the formation of a primary cilium or a sperm flagellum (Beisson and Wright, 2003). Once a centriole has docked with the cell membrane, it is referred to as a basal body. Conversely, a basal body that anchors a cilium during interphase can migrate to a position near the nucleus and transform into a centriole when the cell re-enters the cell cycle (Kobayashi and Dynlacht, 2011).

## 1.2 Cilia and flagella

Eukaryotic cilia and flagella are cytoskeletal organelles that protrude from the cell body into the external medium and are used by a great diversity of species and cell types to generate motion. Many aspects of animal physiology also require cilia and flagella to function in a sensory capacity. The underlying ultrastructure of these organelles is highly similar and both are composed of many of the same proteins. Although the terms cilia and flagella are, for the most part, interchangeable, several differences do exist (Dawe *et al.*, 2007). For example, whilst only one or two flagella are usually present on a cell, motile cilia are usually found in higher numbers. There are exceptions to this, however. The sperm of the gymnosperms *Ginkgo biloba* and *Zamia pumila,* for example, are equipped with 1000 and 50,000 flagella respectively (Southworth and Cresti, 1997). Flagella are also commonly viewed as longer projections compared to cilia and, unlike flagella, cilia can fuse to form specialised cirri or membranelles, typically found in the heterotrich and spirotrich ciliate protozoa. Flagella motility is distinguished by successive waves that propagate along the length of the flagellum, originating at either the base or tip. Cilia, in contrast, move with a characteristic beat that consists of an effective stroke

followed by a recovery stroke. The parasitic protozoan *Trypanosoma brucei*, however, has been observed to display both flagellar and ciliary beating (Dawe *et al.*, 2007).

### 1.2.1 Cilia ultrastructure and motility

Eukaryotic cilia and flagella are complex macromolecular structures that contain more than 250 polypeptides (Dutcher, 1995). They consist of a highly ordered basic structure of microtubules known as the axoneme. The most widely distributed arrangement of the axoneme, the 9+2 axoneme, consists of nine peripheral microtubule doublets arranged around a central pair of singlet microtubules (Fig. 1.2.). Each outer doublet is comprised of an incomplete “B”-tubule which is fused with a complete “A”-tubule. Dyneins are large motor enzymes that transduce chemical energy into mechanical energy to power flagellum motility through ATP-dependent microtubule sliding. Dyneins are connected to the A-tubules of the peripheral doublets whilst their motor heads interact with the B-tubule of the adjacent doublet (Satir, 1989). Complexes of dynein motors, known as dynein arms are periodically distributed along the axoneme; inner arms with a 96nm periodicity and outer arms with a 24nm periodicity (Ibanez-Tallon *et al.*, 2003; Marshall and Nonaka, 2006). Microtubule sliding is converted into flagellar bending as a result of nexin links, protein cross-links which lie between adjacent doubles and constrain interdoublet sliding (Summers and Gibbons, 1971). Protein complexes, termed radial spokes, project from the A-tubule of each outer doublet towards the central pair and regulate motility by connecting the movement of the central pair to the activity of the dynein arms (Summers and Gibbons, 1971). In general, this molecular mechanism of motion is conserved from single-celled protists to humans.

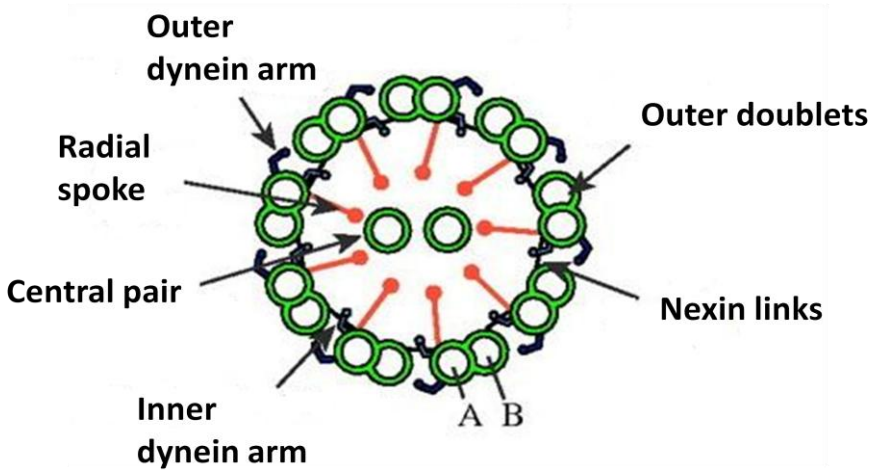


**Figure 1.2.** The structure of the canonical motile "9+2" axoneme. Adapted from Dawe *et al.* (2007).

Although cilia and flagella have been studied extensively, much remains to be understood about the mechanical and regulatory mechanisms that underlie flagellar movement. Technological advances in the last decade, most notably in cryo-electron tomography, have produced high-resolution information about the 3D arrangement of axonemal elements involved in flagellar motility and have generated insights into the precise control of dynein action that is required to generate the complex waveforms typical of beating cilia and flagella (Nicastro *et al.*, 2005; Oda *et al.*, 2007; Nicastro, 2006; Heuser *et al.*, 2009). Recently, cryo-electron tomography revealed that the nexin link, as part of a dynein regulatory complex (DRC), acts as a key regulator of motor activity (Heuser *et al.*, 2009).

The conserved 9+2 structure characteristic of motile cilia and flagella is thought to be the structure that was present in the last common eukaryotic ancestor over 800 million years ago (Mitchell, 2004). Many present-day organisms have retained this original model with few modifications and, as the origin of the eukaryotic flagellum and cilium predates the

radiation that gave rise to extant eukaryotes, its absence in yeast, red algae and higher plants are considered examples of secondary loss. Bacterial flagella, however, are structurally completely different organelles.

Some present-day organisms or cell types demonstrate deviations from this ancestral 9+2 structure. The axoneme of primary cilia, for example, lack the central microtubule pair thus having a "9+0" arrangement (Dawe *et al.*, 2007). Primary cilia, which are almost ubiquitous among vertebrate cells, are generally non-motile and act as sensory organelles that are essential for development and physiology (Pazour and Witman, 2003; Marshall and Nonaka, 2006). The components necessary for motility, such as the central pair and dynein arms, may be absent in immotile sensory cilia but the nine doublet microtubules remain, perhaps to support intraflagellar transport (IFT) and receptor localisation (Mitchell, 2007).

### 1.2.2 Variations in cilia structure and function

Cilia are often broadly classified as "9+2 motile cilia" or "9+0 immotile sensory cilia" (Dawe *et al.*, 2007), although there are several notable exceptions. 9+0 motile cilia found at the embryonic node during development are capable of a simplified rotary motion involved in the establishment of morphogen gradients necessary for the formation of left-right asymmetry (Hirokawa *et al.*, 2006). 9+0 axonemes are also assembled by the gametes of male centric diatoms, a major group of marine algae (Jensen *et al.*, 2003). Although the helical motility of such axonemes is different from the waveforms normally associated with 9+2 axonemes, the existence of such motile 9+0 cilia suggests that the central pair is not a prerequisite for motility. Comparative genomics has also revealed

that one centric diatom, *Thalassiosira pseudonana*, builds motile gametes that lack inner-dynein arms as well as the central pair and radial spokes (Wickstead and Gull, 2007).

Other variations in the structure of cilia and flagella include the addition of paraflagellar rods in protozoa or extra microtubules in spermatozoa (Mitchell, 2007). Some insect sperm, for example, lack the central-pair and radial-spoke apparatus and possess cylindrical axonemes of 12 or 14 doublets or spirals of hundreds of doublets (Baccetti, 1986). Therefore, if the central pair is no longer used by an organism or cell type, successful axonemes with alternative doublet arrangements can evolve (Mitchell, 2007). Axonemes with very simple ultrastructure are also able to produce regular beating of a flagellum. Motile "3+0" and "6+0" axonemes have been reported in the flagella of the male gametes of the parasitic protozoans *Diplauxis hatti* and *Lecudina tuzetae* respectively (Prensier *et al.*, 1980; Schrevel and Besse, 1975). Although these motile flagella lack the central pair and appear to have a simplified bending pattern, it is likely that these parasitic flagellates do not depend on flagellar motility for locomotion in their complex environment.

### 1.2.3 Cilia as a sensory organelle

The membrane surrounding flagella is continuous with the cell plasma membrane but is often selectively different from the cell membrane in protein composition (Fridberg *et al.*, 2007). Intraflagellar transport (IFT) is essential for the assembly and maintenance of flagella. IFT moves non-membrane bound particles from the cell body, along the axonemal doublets, to the tip of the flagellum (Rosenbaum and Witman, 2002). IFT and the associated "flagellar pore complex" at the boundary between the matrix of the

flagellum and the cell body cytoplasm enables the targeting of axonemal and membrane proteins to the flagellar compartment in a selective manner. A large number of receptor proteins have been localised within flagella, consistent with the sensory functions of this organelle in some cell types (Fridberg *et al.*, 2007).

Fluid immediately bordering a cell body membrane may be uncharacteristic of the surrounding fluid due the presence of a glycocalyx or due to the electrostatic effects caused by charged lipids on the cell membrane (Marshall and Nonaka, 2006). By projecting a sensory "probe" into the extracellular medium cells may obtain a more accurate analysis of their surrounding environment. Extension of ciliary membranes into the external medium also increases the area within which cells and tissues can detect and respond to environmental cues.

A great variety of species and cell types require cilia to function in a sensory capacity. Cilia have now been documented as both chemosensory and mechanosensory organelles and have been shown to display unique sets of selected signal transduction molecules including receptors, ion channels, effector proteins and transcription factors that convey physical and chemical stimuli from the external medium in order to control cellular processes during development and homeostasis (Davis *et al.*, 2006; Christensen *et al.*, 2007). For example, primary cilia on kidney epithelial cells can detect extracellular fluid flow rates as a consequence of cilium bending (Praetorius and Spring, 2001).

Compartmentalisation may facilitate the use of the flagellum as a sensory organelle. The high surface area to volume ratio of flagellum would facilitate signal transduction by

enabling a small number of surface receptors to produce a high concentration of second messengers in the flagellar lumen. A larger number of receptors would be required to produce the same concentration in the cell body cytoplasm.

With so many species and cell types recruiting cilia to fulfil essential sensory roles, it is perhaps unsurprising that defects in cilium assembly or function are so often implicated in disease. Defects in cilium formation or function in humans are associated with a wide range of inherited pathologies including infertility, chronic respiratory disease and polycystic kidney disease (Fliegauf *et al.*, 2007). Ciliary defects have also been implicated in cancer, diabetes and obesity (Ainsworth, 2007).

## 1.3 The centrosome

### 1.3.1 Defining a centrosome

The definition of a centrosome is often dependent upon the cell system under study. Some authors use the term to describe any single-copy organelle that represents the main microtubule-organising centre (MTOC) of a cell such as the centriole-containing centrosomes of animal cells, the acentriolar centrosomes of *Dictyostelium discoideum* or the spindle pole bodies (SPBs) of yeast. All of these organelles, though strikingly divergent morphologically, share three basic properties: they are maintained in a central position of the cell due to their microtubule nucleating properties; are physically associated with the nucleus and duplicate only once during the cell cycle (Bornens, 1992). A common debating point concerns the status of centrioles. For some authors, centrioles are integral components of the centrosome whilst, for others that largely equate centrosomes with MTOCs, centrioles are viewed as dispensable “passengers”(Zimmerman *et al.*, 1999).

Indeed, acentriolar pathways of spindle formation have been observed even in vertebrate cells (Khodjakov *et al.*, 2000).

### 1.3.2 The animal centrosome

Centrosomes of animal cells (Fig. 1.3.) are composed of a pair of centrioles surrounded by an amorphous matrix, the pericentriolar material (PCM). The two centrioles, one designated the mother centriole and the other the daughter, lie in an orthogonal configuration so that the long axis of one is almost perpendicular to the long axis of the other. The mother centriole is distinguished from the daughter centriole by distal and subdistal appendages that are lacking on the daughter centriole and are thought to anchor cytoplasmic microtubules at the centriole and enable docking of the centriole to the cell membrane during ciliogenesis (Ishikawa *et al.*, 2005). An intercentriolar link that connects the mother and daughter pair is lost at the initiation of a duplication process during early interphase and both mother and daughter centrioles give rise to their own daughter centrioles (known as procentrioles) resulting in two centriole-procentriole pairs. At the onset of mitosis, the PCM is divided and the duplicated centrosomes migrate apart along the nuclear envelope. Nuclear envelope breakdown enables microtubules to invade the nuclear area and interact with the chromosomes in the formation of the bipolar spindle. The exact sequence of these events and the exact stage of the cell cycle at which each step occurs can differ between cell types (Hinchcliffe and Sluder, 2001; Callaini and Riparbelli, 1990; Delattre and Gonczy, 2004).

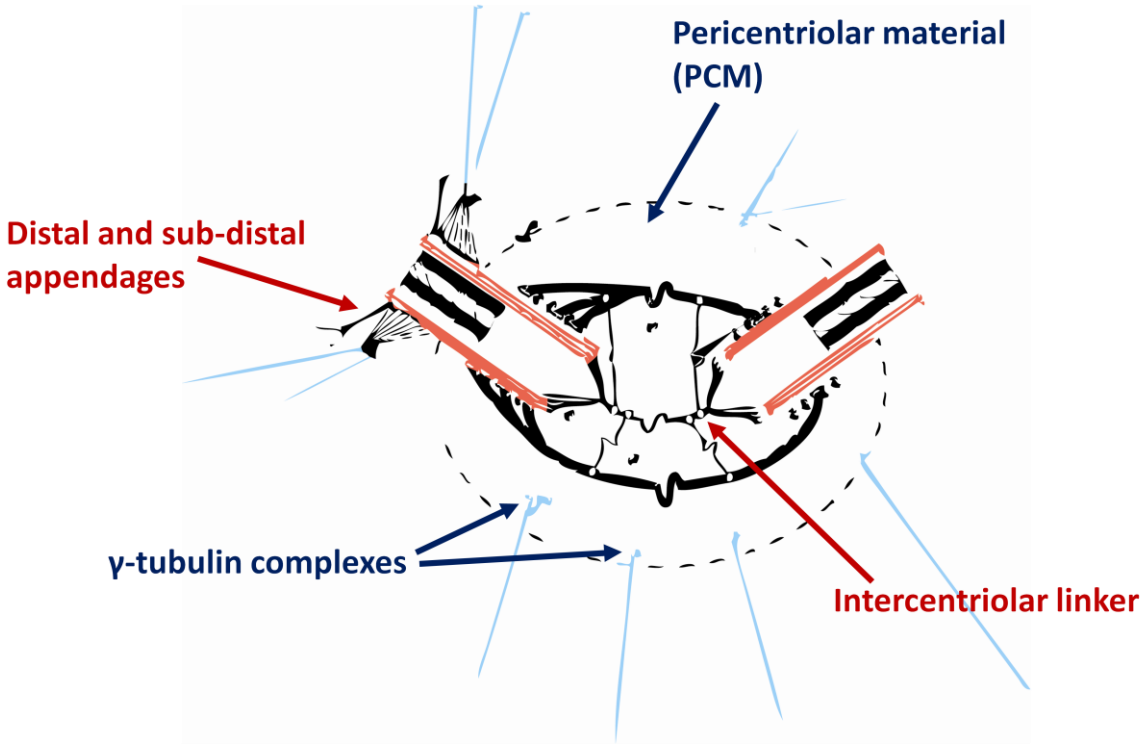


**Figure 1.3. Organisation of the centrosome in a typical animal somatic cell.** Two centrioles (mother and daughter) are embedded in clouds of the pericentriolar material (PCM).

The PCM is a fibrous scaffolding lattice that contains a large number of centrosome proteins and it is this domain that anchors and nucleates cytoplasmic microtubules during interphase and mitosis. The PCM consists of a fibrous scaffolding matrix with a large number of coiled coil proteins and γ-tubulin complexes (Moritz *et al.*, 1995). The centrioles are important for centrosome integrity and aid recruitment of centrosomal proteins to the PCM (Varmark *et al.*, 2007).

## 1.4 Aims and objectives: the evolution of the centriole from motility to mitosis

The conserved 9+2 structure characteristic of centrioles and basal bodies is found in all major eukaryotic groups, either as a centriole, in the context of a centrosome, and/or as a basal body tethered to the membrane (Cavalier-Smith, 2002; Carvalho-Santos *et al.*, 2011). This suggests that the structure was present in the last common eukaryotic ancestor over 800 million years ago (Mitchell, 2004) with secondary loss in specific lineages such as yeasts and higher plants. Centrioles and basal bodies are indispensable for a variety of cellular and developmental processes including motility, sensory perception and centrosome organisation. It is likely that early flagella performed both motile and sensory functions, as these features are observed in multiple branches of the eukaryotic tree of life (Carvalho-Santos *et al.*, 2011; Satir *et al.*, 2008; Bloodgood, 2010). But how, and when, did the structure's myriad roles extend to mitosis? And what role, if any, did the centriole play in the origin of metazoan multicellularity?

Variations on the ancestral 9+2 axoneme configuration are observed among eukaryotes and these alterations often correlate with changes in cilia function. A common view has emerged, for example, that classifies axonemes into motile 9+2 and immotile sensory 9+0 structures. Other structures associated with the centriole structure, such as microtubule rootlets and sub-distal appendages, are even more divergent according to function. Information about the morphology and molecular composition of these accessory structures allows us to pinpoint instances of acquired function of the centriole structure in the evolution of eukaryotes and helps to discriminate between possible scenarios of homology and convergent evolution.

The aims of this study are two-fold. Firstly, to highlight three notable examples where the basal body structure has been co-opted to actively participate in acquired cellular structures or processes:

I. Sensory perception in intracellular parasitism.

II. The anchoring of microvilli tentacles required for feeding by choanoflagellates, the sister group of the Metazoa. The role of the centriole in the origins of multicellularity will also be discussed.

III. A functional component of the metazoan centrosome.

In tandem, this study will utilise the ubiquity of the centriole and divergences in its structure and/or that of accessory structures to discriminate between three scenarios of either homology or convergent evolution:

I. The origins of intracellular invasion during the evolution of two groups of Trypanosomatidae parasites.

II. The collar tentacles of choanoflagellates and choanocytes and their association with the basal body. The importance of choanoflagellates as the closest living relative of metazoans was first revealed by their striking similarity to choanocytes, the feeding cells of sponges, but to what extent are their basal body appendages homologous?

III. Eukaryotic centrosomal structures and their association with centrioles.

# Chapter 2: Materials and methods

## 2.1 Cell culture

*Leishmania mexicana* promastigotes (WHO strain MNYC/BZ/62/M379) were maintained at 28°C in M199 medium supplemented with 10% foetal calf serum (FCS). J774 mouse macrophages were cultured at 37°C in RPMI medium supplemented with 10% FCS.

The population growth rate of the promastigote-form was monitored by measuring cell density with a CASY model TT cell counter.

## 2.2 Propagation of amastigotes

*L. mexicana* amastigotes were obtained though the infection of J774 macrophages with stationary phase *L. mexicana* promastigotes. Macrophage cultures in multi-well plates were prepared at a cell density of approximately $10^6$ cells per ml in RPMI medium supplemented with 20% FCS and incubated at 37°C. Cover-slips sterilised in 100% ethanol were added to each well. *L. mexicana* parasites were added at a parasite to macrophage ratio of 10 to 1.

After parasites were added to macrophage monolayers and maintained for 2 hours, non-adherent parasites were removed by washing the monolayers with culture medium and fresh medium added. Cultures were maintained for 1-, 3- or 4-days post-infection.

Following these procedures cells were fixed with 2% paraformaldehyde for 10 minutes, washed with PBS and permeabilised with 0.01% NP-40 for 5 minutes. Cover-slips were mounted on glass sides using VectaShield Mounting Medium with DAPI. For Giemsa

staining cells that were settled on coverslips were fixed with methanol at -20°C for 5 minutes before staining with Giemsa reagent (Sigma) according to the manufacturer's instructions. Infection efficiency was determined 1-, 3- and 4-days post-infection. The percentage of infected cells was determined by examining at least 100 macrophages by phase-contrast microscopy with an oil immersion lens at 100x magnification.

*Trypanosoma cruzi* amastigotes were obtained through the infection of Vero cells by collaborators at the London School of Hygiene and Tropical Medicine.

## 2.3 Sample preparation for transmission electron microscopy

3-day and 5-day post-infection Vero cultures, a *T. cruzi* epimastigote suspension culture, 3-day post infection J774 cultures and a J774 culture were chemically fixed by the addition of 2.5% glutaraldehyde and 2% formaldehyde for 5 minutes at room temperature, repeated with fresh fixative. Cells were post-fixed in 1% osmium tetroxide in 100mM cacodylate buffer, pH 7 for 1 hour at 4°C, washed several times in distilled water and stained en bloc with 0.5% aqueous uranyl acetate for 16 hours at 4°C. After staining, samples were washed with distilled water and cells released by scraping or propylene oxide as appropriate. Released cells were pelleted and dehydrated through an ethanol series and embedded in Agar 100 resin.

Plastic embedded cells were thin-sectioned, collected on formvar coated copper-rhodium slot grids and then post-stained with aqueous uranyl acetate and lead citrate. Sections were viewed in an FEI Tecnai-F12 electron microscope operating at 80KeV and images recorded digitally.

## 2.4 Geometric correction of electron micrographs

Micrographs showing near transverse cross-sections through an axoneme cannot be directly superimposed due to a discrepancy between the angle of the section and the true transverse plane. This results in an apparent deformation of the axoneme from a circular to an elliptical cross-section. To compensate for axonemal sections not being true perpendicular cross-sections, a mathematical transformation that moves data into the transverse plane was used to correct any elliptical cross-sections to circular ones that represent a true transverse section. The circularity of each corrected image could be confirmed by nine-fold rotation of each image with superposition of the axoneme doublets at each rotation. This mathematical transformation (detailed in Gadelha *et al.,* 2006) was applied through the use of a bespoke macro run through ImageJ software. In addition to correcting for any elliptical deformation, this macro also normalised the axoneme to a specified size to allow comparison of measurements between images.

## *2.5* Systematic review of intracellular and amastigote forms of *Trypanosoma*

A literature search for scientific articles and book chapters containing descriptions of intracellular and amastigote forms of Trypanosoma was conducted using a number of online databases including Google Scholar, Web of Science, JSTOR, PubMed, Scopus and ScienceDirect. Searches included various combinations of the keywords: “amastigote”, “leishmanial”, “leishmaniform”, “Leishman-Donovan bodies”, “intracellular”, “trypanosoma” and “trypanosome”. Additional studies were subsequently obtained from reference lists to include print-only holdings. Both natural- and experimental- infection studies were considered.

Interpretation of early ultrastructure studies is hampered by the myriad of terms used to define different developmental stages of trypanosomes. These terms were often used inconsistently between authors, especially prior to a revision of terminology in 1966 (Hoare and Wallace). Each reference was carefully read and images examined to determine whether the study describes true intracellular amastigotes or extracellular amastigote-like forms.

## 2.6 Phylogenetic analysis

Putative orthologs were searched for using BLASTP and iterative BLASTP in non-redundant protein databases using the full human sequence, except in the case of proteins with coiled-coil domains (see below). Reciprocal best hits in BLASTP were considered to be orthologues. Negative results were investigated further by querying protein databases using protein family members of closely related species. Top-scoring hits that were bidirectional best hits to members of the family in closely related species or to the most conserved regions in the human sequence, although not obeying the first criterion for orthology (reciprocal best hits in BLASTP), were further considered as orthologues. Where possible, orthology assignments were aided by phylogenetic analysis. Multiple sequence alignments were performed using the ClustalW program, followed by manual adjustment. Phylogenetic trees were inferred by maximum-likelihood (ML) using PhyML (http://www.atgc-montpellier.fr/phyml/). All analyses were performed using the LG amino acid substitution model with one invariable and four gamma distributed variable rate categories – assessed as the best fitting model available under all criteria employed in the ProtTest software (Abascal et al., 2005). Bootstrap analysis was carried out to assess support for individual nodes.

Proteins were annotated for conserved domains using a variety of domain- and fold-recognition software including the Pfam database (Punta *et al.*, 2011), the Simple Modular Architecture Research Tool (SMART) (Letunic *et al.*, 2011) and NCBI's Conserved Domain Database (CDD) (Marchler-Bauer *et al.*, 2011). All query sequences were human. Scores represent the confidence level of the domain prediction in the protein query sequence when compared to the conserved domain model curated by the NCBI Conserved Domain Database.

## 2.7 Identification of proteins with coiled-coil domains

Proteome sequence sets of fully sequenced genomes were downloaded from public sequence databases. For details of sources, as well as information regarding numbers of protein predictions see supplementary material (Table S5.4). Where available, UniProtKB complete proteomes, a combination of manually reviewed (Swiss-Prot) and automatically annotated (TrEMBLE) proteins sets, were used. An initial pre-processing of the FASTA files was conducted to remove all proteins sequences shorter than 30 amino acids. To estimate the number of full-length proteins in the individual proteomes that contain coiled-coils, the predictor COILS (Lupas *et al.*, 1991) was ran using default settings. COILS, a commonly used predictor of coiled-coil structure, uses a position-specific scoring matrix containing amino acid frequencies in the seven heptad positions.

To obtain a picture of the predictive power of the algorithm, the COILS output for the human proteome was compared to outputs from two other prediction algorithms, PairCoil2 (McDonnell *et al.*, 2006) and SpiriCoil (Rackham *et al.*, 2010).

The COILS output was post-processed and used to establish a database of coiled-coil prediction data for each organism. Selectivity criteria were applied to select sequences predicted to contain coiled-coil domains longer than or equal to 75, 100, 150, 200, 250 and 400 amino acids.

## 2.8 Masking of coiled-coil domains

To reduce interference of the coiled-coil repeat motif with sequence homology analysis, coiled-coil domains, as predicted by the COILS2 algorithm, were removed from sequences before subjection to sequence similarity searches.

## 2.9 Statistical analysis of coiled-coil content

All statistical tests were carried out in SPSS Version 20.0. Alpha was set at 0.05 and all tests were two-tailed. The Shapiro-Wilk test was used to test the hypothesis of normal distribution. The Wilcoxon signed-rank test was used to compare the number of coiled-coil proteins predicted by the two coiled-coil predictor algorithms, PairCoil2 and COILS. Comparisons of the coiled-coil content of various phylogenetic groupings were made using the Mann-Whitney U test.

## 2.10 Cell culture (choanoflagellates)

20ml cultures of *Monosiga brevicollis* were maintained in 25cm² tissue culture flasks at 15°C. Growth medium consisted of autoclaved seawater enriched with cereal wheatgrass (0.6g per 1l of seawater), and syringe filtered through 0.22µm filter paper. Cultures were maintained by passaging 1ml of culture into 20ml of fresh medium every 3-4 weeks. Cells were dislodged from culture flasks using disposable, sterile cell scrapers.

Cultures of *Monosiga ovata* were passaged as for *Monosiga brevicollis* but maintained at room temperature.

*Stephanoeca diplocostata* and *Diaphanoeca grandis* cultures were maintained at 15°C and 13.6°C respectively. Medium comprised of 30ml of autoclaved seawater and two autoclaved rice grains. All media was cooled prior to passaging to prevent temperature shock. Cultures were maintained by passaging every 3-4 weeks. Parent cultures were diluted in fresh medium between 2x and 5x depending on cell density.

All choanoflagellate cells were fed on bacteria present in the inoculum.

## 2.11 Immunofluorescence (choanoflagellates)

Two anti-peptide antibodies against γ-tubulin were used: a monoclonal mouse antibody, GTU-88 (IgG1), prepared against the EEFATEGTDRKDVFFY peptide corresponding to human γ-tubulin sequence 38-53, a phylogenetically highly conserved region also present in *Monosiga brevicollis*, and an affinity-purified rabbit antibody raised against the same peptide, γ-TUB. Both antibodies were bought from Sigma Aldrich. In double-label immunofluroescence, the microtubule structures were visualised by a monoclonal antibody, TAT1 (IgG2b) specific for α-tubulin (Woods *et al.*, 1989). Secondary antibodies included FITC-conjugated anti-mouse IgG (1:500) and Cy5-conjugated ant-rabbit IgG (1:500).

For immunofluorescence, 1ml aliquots of cell culture were fixed with 37% formaldehyde (125µl per 1ml culture) for 15 minutes at room temperature. After fixation, cells were

harvested by centrifugation, washed and resuspended in 100 µl PBS and settled on poly-L-lysine coated slides for 30 minutes. Slides were rinsed four times in PBS before incubating with blocking buffer (1% BSA and 0.3% Triton X-100 in PBS) for 30 minutes at room temperature. Primary antibodies were diluted in blocking buffer and incubated at room temperature overnight at the following dilutions: GTU-88 (1:1000), γ-TUB (1:1000) and TAT1 (1:100). Slides were washed four times in blocking buffer, followed by incubation with the secondary antibodies overnight at room temperature. Slides were washed four times in blocking buffer and once in PBS. After DAPI (1µl/ml) staining for 10 minutes, coverslips were mounted with 20 µl Mowiol 4-88 mounting medium. Negative controls were obtained by omitting primary antibodies and showed no specific staining.

Slides were examined using a Zeiss Axioskop 2 microscope and photographed with a Zeiss Axiocam camera.

## 2.12 Actin labelling

To label the actin cytoskeleton choanoflagellates were fixed, harvested and settled on poly-L-lysine coated slides as previously described. Either Alexa 594 Phalloidin, Bodipy 591 Phalloidin or Bodipy 505 FL Phallacidin was diluted in PBS with 10% bovine serum albumin (BSA) and incubated for 3 hours at room temperature. Slide preparations were rinsed three times in PBS and mounted as previously described.

## 2.13 Treatment of cells with cytochalasin D

Cytochalasin D was used to disrupt the actin filaments of the microvilli tentacles of the collar. Various incubation times and concentrations of cytochalasin D were tested to

disrupt the actin filaments. An incubation time of 60 minutes and a cytochalasin D concentration of 1µM caused total disruption of actin filaments. A stock solution of cytochalasin D was then prepared by dissolving 5mg of cytochalasin in 1ml of dimethyl sulfoxide (DMSO) producing a 1mM solution. This was stored at -20°C. 1µL of 1mM cytochalasin D was added per 1ml of choanoflagellate culture and incubated for 1 hour in the dark. Controls were untreated cultures to which DMSO alone was added. Post-incubation with cytochalasin D the culture was either fixed immediately with 37% formaldehyde and processed for immunofluorescence labelling as described above, or, in recovery experiments, cells were washed three times with fresh culture medium and incubated in the absence of cytochalasin D for various time periods (see relevant figure legends) before fixation.

## 2.14 Isolation and fixation of choanocytes for fluorescence

Samples of the freshwater sponge *Ephydatia mulleri*, were collected by a collaborator, S. Leys, from Sarita and Rosseau Lakes, Vancouver Island, B.C., Canada. Asexual cysts, called gemmules, were isolated from the parent sponge tissue, washed in 1% hydrogen peroxide solution for 5 minutes and rinsed in distilled water. Single gemmules were transferred using a sterile pipette to glass coverslips in Petri dishes and stored in M-medium (Funayama *et al.*, 2005) in the dark at room temperature before transportation to Oxford.

Juvenile sponges on glass coverslips were fixed using 3.7% paraformaldehyde. Sponge tissues were permeabilized with 0.2% Triton-X100 in PBS for 2 min and washed in cold PBS. To label the actin cytoskeleton, coverslips were inverted onto a drop of solution

containing Alexa 594 Phalloidin, Bodipy 591 Phalloidin or Bodipy 505 FL Phallacidin in PBS with 10% bovine serum albumin (BSA). A 300 µl depression was made in a Parafilm™-covered Petri dish to prevent damage to the soft tissue by the gemmule. After 3 hours at room temperature, preparations were rinsed three times in cold PBS. For mounting, sponges were incubated in a 50:50 v/v glycerine:PBS solution, and mounted in Mowiol 4-88 mounting medium with Vectashield, and allowed to harden overnight. Slides were stored in the dark at 4°C. Preparations were viewed with a Zeiss Axioskop 2 microscope and photographed with a Zeiss Axiocam camera.

Staining of *E. mulleri* for α- and γ-tubulin was conducted as described for choanoflagellate species except that coverslips with gemmules attached were inverted onto solutions in a depression made in a Parafilm™-covered Petri dish. The coverslips were subsequently mounted with 20 µl Mowiol 4-88 mounting medium onto poly-L-lysine coated slides

## 2.15 RNA extraction

40ml of *Monosiga brevicollis* cell suspension were spun for 3 minutes at 3,000rcf, the supernatant removed and cells resuspended in PBS. Cells were pelleted by spinning at 3,000rcf for 3 minutes and lysed with 1ml TRIZOL reagent (approximately 1ml reagent per 5-10x$10^6$ cells) by repetitive pipetting and overnight incubation at -20°C. 0.2ml of chloroform per 1ml of TRIZOL reagent used was added and vortexed vigorously for 20 seconds before incubating for 3 minutes at room temperature. The mixtures were centrifuged at 12,000 rcf for 10 minutes at 4°C before the upper aqueous layer carefully transferred to fresh tubes. 0.5ml of isopropyl alcohol per 1ml of TRIZOL reagent used was added and incubated for 10 minutes at room temperature before centrifugation at

12,000rcf for 10 minutes at 4°C. The pellet was washed twice by the addition of 1ml of 70% ethanol per 1ml of TRIZOL reagent used and subsequent centrifugation at 12,000rcf for 10 minutes at 4°C. The final ethanol supernatant was removed and the pellet air dried for approximately 10 minutes at 60°C before resuspension in 30µl DEPC-treated water. The concentration of RNA was determined by spectrometric analysis (Eppendorf BioSpectrophotometer) at 260nm. All RNA samples were stored at -80°C.

## 2.16 cDNA synthesis and amplification

Reverse transcription was carried out on total RNA using the Invitrogen SuperScript™ III Reverse Transcriptase kit as per the manufacturer's instructions. 1µg of total RNA was used with oligo $(dT)^{12-18}$ primer.

The PCR amplifications were performed in 25µl reactions using Invitrogen's *Taq* polymerase and 0.5µM of each primer. Cycling conditions consisted of initial denaturation (94°C for 5 minutes), 30 cycles of denaturation and annealing and extension (94°C for 1 minute, 51.1°C for 1 minute and 72°C for 1 minute) and final extension (72°C for 5 minutes). The PCR products from PCR reactions were resolved by 1% agarose gel electrophoresis. All PCR experiments were performed at least three times.

# Chapter 3: Divergent basal body structure and bifunctionality in unicellular eukaryotes

Parts of this chapter have been included in publication as:

Gluenz, E., Höög, J.L., Smith, A.E., Dawe, H.L., Shaw, M.K., and Gull, K. (2010) "Beyond 9+0: noncanonical axoneme structures characterise sensory cilia from protists to humans." The FASEB Journal 24: 3117-3121.

## 3.1 Aims and objectives of this chapter

It is evident that the basal body structure has evolved to help fulfil numerous cellular functions through its involvement in both motile and sensory cilia and through its association with centrosome structures. Although the importance of this structure is well documented across eukaryotes, the short non-motile flagella of the amastigote form of *Leishmania* and *Trypanosoma* trypanosomatid protists have received little attention to date and its role in the life cycle of these parasites is unknown. A definitive description of the amastigote flagellum ultrastructure is currently lacking and reports in the literature are contradictory. To investigate the biology of this basal body structure, a first aim of this study is a description of the amastigote flagellum at the EM-level of resolution.

In addition, there is little comment in the literature about the emergence of the intracellular amastigote form in evolutionary history. Interestingly, there are many clear distinctions between the amastigote form of *Leishmania* and *Trypanosoma* with regards to the types of cells invaded; the method of entry into host cells; and the means by which they survive the harsh environment of the phagolysosome. A thorough survey of

ultrastructural descriptions of trypanosomatid parasite species and the subsequent mapping of the presence of an intracellular form onto a consensus phylogeny would, in conjunction with a definitive comparison of the ultrastructure of *Trypanosoma cruzi* and *Leishmania* amastigotes, help pinpoint the emergence of the intracellular amastigote form in evolutionary history.

## 3.2 Introduction to *Leishmania* and *Trypanosoma*

Trypanosomatids are flagellated protozoan parasites of invertebrates, vertebrates and plants. Trypanosomatids are members of the order Kinetoplastida, which is characterized by several unusual cellular features, most notably the presence of a kinetoplast, a portion of the single large mitochondrion that harbours the mitochondrial DNA and is associated with the flagellar base (Shlomai, 2004). Almost all known kinetoplastids are parasitic, most genera being parasites of insects. *Trypanosoma* and *Leishmania* are the most widely studied trypanosomatids since these genera include organisms that are pathogenic to man and domestic animals.

*Leishmania* species cause a wide spectrum of human diseases collectively known the leishmaniases. These diseases represent a major public health risk and currently threaten over 350 million people in 88 countries around the world (Singh, 2006). The consequences of infection range from the relatively mild, such as localized cutaneous lesions that generally self-heal, to advanced visceral leishmaniasis that is often fatal. Although the different species are almost indistinguishable by their morphology, at least 20 species known to infect man have been identified, mainly according to the clinical features they produce in man and their geographical distributions (Lumsden and Shaw,

1987). A variety of immunological, biochemical and molecular techniques have now been developed for the differentiation between species (Laurent *et al.*, 2009).

Another trypanosomatid parasite of man, *Trypanosoma cruzi*, is the aetiological agent of Chagas disease. Chagas disease is prevalent though the Americas and is the result of persistent infection with *T. cruzi* and complex interactions between the parasite and the host immune response. The cumulative tissue damage characteristic of chronic Chagas disease is thought to be caused by the continuous immune attack on persistent parasites (Stuart *et al.*, 2008).

### 3.2.1 Life cycles

*Leishmania* species lead a digenetic life cycle consisting of an extracellular promastigote stage within a *Phlebotomus* or *Lutzomyia* sandfly vector and an intracellular amastigote stage within the mononuclear phagocytes, for example macrophages, of a mammalian host. In the sandfly digestive tract, *Leishmania* multiply as extracellular promastigotes before undergoing metacyclogenesis, a differentiation process that results in the appearance of infective (or metacyclic) promastigotes. Promastigotes are transmitted to the vertebrate host during a bloodmeal of the sandfly where they are taken up by phagocytic macrophages. Within acidic parasitophorous vacuoles (phagolysosomes) of the macrophages the promastigotes differentiate into the smaller, ovoid amastigote form.

Whilst *Leishmania* species exclusively invade the professional mononuclear phagocytes, of the mammalian host, *T. cruzi* can invade a wide range of nucleated mammalian cells

including mononuclear phagocytes, glial cells, vascular endothelial cells, neurons, and fat cells but muscle cells of all types – cardiac, intestinal, skeletal - are those especially affected (Lumsden, 1974; Tyler and Engman, 2001). Blood-sucking Triatominae insects are the vectors that transmit the parasite, shedding infective metacyclic trypomastigotes in their faeces during feeding. The trypomastigotes invade various cells at the bite wound site, within which they differentiate into intracellular amastigotes that proliferate intracellularly by binary fission. At high densities, amastigotes give rise to bloodstream trypomastigotes which subsequently escape into the blood and lymph. Bloodstream trypomastigotes are able to infect new cells and once again become amastigotes or are ingested by another Triatominae insect in order to continue the parasite life cycle. Amastigotes may also be released from lysed host cells, serving to either propagate the infection through the infection of new cells or contribute to the mixture of trypomastigotes and amastigotes present in the blood meal of the vector. Within the gut of the invertebrate host the trypomastigotes undergo several morphological transformations through proliferative epimastigote stages before a final differentiation results in metacyclic trypomastigotes which are eliminated in the insect's faeces.

### 3.2.2 *Leishmania* and *Trypanosoma* ultrastructure: focussing on the flagellum

Trypanosomatids contain several distinctive organelles. A single mitochondrion spans the length of the cell and contains a subcompartment, the kinetoplast, which houses a catenated DNA network. The membrane-bound flagellum is physically coupled to the kinetoplast and emerges from the flagellar pocket, a deep invagination of the plasma membrane where the flagellum exits the cell body. In trypomastigote and epimastigote

stages of *T. cruzi*, the flagellum runs along almost the entire length of the cell body attached to the cell surface (Sanabria, 1963; Sanabria, 1964). This region of attachment is known as the flagellar attachment zone (FAZ). In contrast, the flagellum of *Leishmania* promastigotes, is attached to only a limited portion of the cell body after its emergence from the flagellar pocket.

The trypomastigote, epimastigote and promastigote flagellum typically has the characteristic 9+2 microtubule axoneme and the associated axonemal components required for motility including dynein arms and radial spokes (Sanabria, 1963; Sanabria, 1966). A semi-crystalline structure, the paraflagellar rod (PFR) is also present in all life cycle stages except for the amastigote.

### *The flagellar pocket*

The flagellar pocket appears to be the sole site for endocytosis and exocytosis of macromolecules (Vickerman, 1994). Whilst the rest of the cell body is supported by a sub-pellicular corset of closely spaced microtubules that are prohibitive for membrane vesicle fusion or fission (Overath *et al.*, 1997), these microtubules are absent from the flagellar pocket, with the exception of four specialised microtubules that run along one surface (Webster and Russell, 1993). Consequently, all vesicular traffic into and out of the cell, as well as the trafficking of protein components between the cell body cytoplasm and the flagellum, occurs via the flagellar pocket (McConville *et al.*, 2002). In order to enter the flagellum, a protein must first proceed through the flagellar pore complex. This cytoskeletal neck region contains several structures including the basal body and transition zone filaments and acts as a selective barrier for protein movement into the

flagellum (Rosenbaum and Witman; 2002; Gull, 2003). The molecular composition of the flagellum can therefore different significantly from that of the cell body.

### *Paraflagellar rod*

A major accessory structure, the paraflagellar rod complex (PFR) has been identified in kinetoplastid flagella and is present in all trypanosomatid life cycle stages except for the amastigote (Gull, 1999). This structure, if present, usually runs adjacent to the axoneme and is attached to axonemal microtubule doublets four to seven (Maga *et al.*, 1999), usually at the point where the flagellum exits the flagellar pocket. The PFR is a lattice-like structure composed of two related major proteins, PFR1 and PFR2, in addition to a number of minor ones (Maga *et al.*, 1999). Although the function of the PFR has been the subject of much speculation, mutant studies have demonstrated an essential role for the PFR in flagellum motility, although the force that causes the flagellar wave is generated entirely by the axoneme. Ablation of the PFR structure in *L. mexicana* and *T. brucei* produces viable cells with either paralyzed flagella (Bastin *et al.*, 1998) or abnormal flagellar movement patterns (Santrich *et al.*, 1997). The PFR is also thought to provide support for metabolic regulators that may influence flagellar beating (Pullen *et al.*, 2004) as well as playing a critical role in the attachment of the pathogen to the invertebrate vector cell surfaces (Gadelha *et al.*, 2005; Tetley and Vickerman, 1985).

The PFR has been divided into three morphologically distinct regions, defined by their position relative to the axoneme (Farina, 1986). This tripartite pattern of construction, however, is not consistently conserved throughout the kinetoplastids. One particular group of endosymbiont-containing trypanosomatid species, for example *Crithidia deanei*,

are actively mobile and able to attach to the cell surfaces of the insect host despite an apparent lack of a PFR. Recent re-examination of the *C. deanei* flagellar ultrastructure revealed a previously unobserved PFR consisting of one proximal domain only (Gadelha *et al.*, 2005). It is therefore possible that a similar cryptic PFR is also present in the amastigote flagellum.

#### *Fixed central pair orientation in protozoan parasites*

In wild-type trypanosomatids, the orientation of the central pair is invariant with no central pair rotation (Gadelha *et al.*, 2006). The central pair also retains a fixed orientation relative to the outer microtubule doublets in human (Ralston and Hill, 2008) and sea urchin sperm (Sale, 1986) axonemes. In *Paramecium* and *Chlamydomonas*, however, the central pair rotates within the axoneme (Omoto *et al.*, 1999; Mitchell, 2003). This rotation of the asymmetrical pair apparatus is hypothesised to activate distinct sets of dyneins on the outer doublets via the radial spokes and a dynein regulation complex (DRC). *In vitro* studies with reactivated *Chlamydomonas* axonemes have demonstrated that the position of the C1 microtubule of the central pair correlates with the position of active dyneins (Wargo and Smith, 2003; Wargo *et al.*, 2004). For many organisms, including *Leishmania* species, it is not yet clear if the central pair rotates. This could be achieved through the analysis of randomly selected thin section transmission electron micrographs showing cross-sections of axonemes.

### 3.2.3 The amastigote flagellum: confusion in the literature

Whilst the promastigote stage possesses a long flagellum that protrudes from the flagella pocket, amastigotes are often described as aflagellate (Garnham, 1971; Lumsden, 1974).

Indeed, the term “amastigote”, proposed by Hoare and Wallace (1966), literally means without a flagellum (-mastigote meaning “whip”). However, the amastigote form does posses a small, non-motile flagellum that transverses but is usually contained within the flagellum pocket (Alexander, 1978; Pan and Pan, 1986). The amastigote form of *T. cruzi* also possesses a short flagellum (Meyer and Queiroga, 1960; Meyer and de Souza, 1976,).

### *Leishmania amastigote flagellum ultrastructure*

Although several early studies on the fine structure of *Leishmania* amastigotes have been published, very few were aimed specifically on the ultrastructure of the flagellum. It is evident from this literature that two key paradigms exist in relation to the axoneme of *Leishmania* amastigotes. A number of studies (Rudzinska *et al.*, 1964; Sanyal and Sen Gupta, 1967; Pham *et al.*, 1970; Gardener, 1974; Bourlond-Reinert and Nicolay, 1975; Simpson *et al.*, 1982) describe the axoneme as consisting of the classical 9+2 configuration with nine peripheral microtubule doublets surrounding a central pair.

Rudinska *et al.,* (1964), for example, cultured *L. donovani* amastigotes isolated from infected hamster spleen and examined morphological changes associated with the transformation of the amastigote to the promastigote form. Observations of amastigotes in macrophages within the spleen revealed a flagellum containing nine peripheral doublets and a central pair of microtubules although this is not apparent in the electron micrographs presented. Examination by electron microscopy of *L. tropica* amastigotes obtained from human skin biopsies also demonstrated a 9+2 structure although, again, the transverse section is not entirely persuasive (Pham *et al.*, 1970).

Sanyal and Sen Gupta (1967) examined the fine structure of *L. donovani* amastigotes obtained from human skin biopsy. Although not discernible in any electron micrographs presented, the investigators note an observation of nine peripheral and a central set of microtubules in which the central microtubules were found to be shorter than the peripheral ones.

In contrast, Alexander (1978) observed an unusual arrangement of the axonemes of *L. mexicana*, *L. enritetti* and *L. major* in which the 9+2 configuration is disrupted. This was suggested to be due to constriction of the flagellum at the flagella pocket opening. In amastigotes of *L. mexicana*, for example, the central microtubule pair was present only for a limited distance before one or two of the peripheral doublet were observed to collapse into the centre of the axoneme. Examination of *L. enrietti* amastigotes revealed similar microtubular arrangements in the axoneme. The two central microtubules of *L. tropica major*, however, were observed to persist along much of the length of the flagellum and only lost at the extreme anterior end.

A similar observation was described by Hentzer and Kabayasi (1977) in a study of *L. tropica* amastigotes obtained from human skin. In this second account the replacement of the central tubules by the peripheral doublets was observed to occur only at the distal end of the flagellum. It is therefore possible that both a 9+2 configuration and a more unusual arrangement, such as that described by Alexander (1978), are present within a single flagellum. Further fine-structural studies that include serial sections along the entire length of the amastigote flagellum are required to clarify this.

Many of the aforementioned ultrastructure studies were performed before the molecular mechanisms of flagellar motility were fully understood. There is, therefore, little reference to the presence of associated axonemal components, such as the dynein arms and nexin links, and it is difficult to determine their presence or absence from the electron micrographs. The recent increase in the knowledge of the molecular components of eukaryotic flagella may aid a more definitive account of the fine structure of *Leishmania* and *T. cruzi* amastigote flagellum. The unpersuasive nature of the electron micrographs presented to date indicates the need for electron microscopy studies that focus specifically on the axonemal arrangement of the flagellum.

Further difficulty arises from the myriad of terms that have been used to define the different developmental stages of the leishmanias and trypanosomes in their vertebrate and insect hosts. In the past the amastigote stage has been referred to “leishmanial", “leishmaniform” and “Leishman-Donovan bodies”; the promastigote stage as “leptomonad”; the trypomastigote as “trypanosome”, “trypanosomal” or “trypanosomatic” and the epimastigote stage as “crithidial”. As these names were originally derived from the genera in which the corresponding stages are the most characteristic, confusion sometimes resulted from the name incorrectly implying a close similarity between a genus and a stage of another organism. Furthermore, these terms have been used indiscriminately and inconsistently by some authors, making interpretation of early ultrastructure studies difficult. The revised terminology proposed by Hoare and Wallace (1966), in which morphological forms are distinguished primarily by the site of origin of the single flagellum and forms the nomenclature in common usage today, is not without its difficulties. The term “amastigote” does not reflect the actual

structure of the intracellular form and may have contributed to the common opinion that the flagellum is not present or unimportant.

Another unresolved dispute surrounds whether the flagellum protrudes beyond the flagella pocket. Although the flagellum is often described as "intracellular" or as terminating at the flagellar pocket opening (Pham *et al.*, 1970; Gardener, 1974; Hentzer and Kobayasi, 1977; Pan and Pan, 1986), some electron micrographs clearly depict amastigote flagella protruding past the flagella pocket opening (Simpson *et al.*, 1982). Eperon and McMahon-Pratt (1989), for example, measured the flagellum terminating 100nm beyond the pocket area. Rudzinska *et al.,* (1964) also observed a flagellum that extends for a short distance beyond the flagellar pocket.

### *Culture and characterisation of Leishmania amastigotes*

Studies of the amastigote stage of *Leishmania* have been hampered by the dependence on parasites obtained from infected animals and the difficulty of obtaining abundant numbers in culture. Furthermore, preparations are often contaminated with host-derived components that could lead to misleading results from, for example, antigen characterisation and gene expression studies.

Amastigotes have been obtained from *in-vitro* cultivation in macrophage cell lines (Chang, 1980), from infected tissues and through axenic culture (Pan, 1984). Axenic cultures are routinely obtained using temperature elevation and/or a reduction in pH as a trigger for the transformation of promastigotes to amastigote-like forms in a cell-free medium (Zilberstein and Shapira, 1994). Axenic amastigotes have been reported by

numerous investigators for many species and strains of *Leishmania* including *L. mexicana, L. panamensis, L. pifanoi, L. donovani, L. amazonensis* and *L. braziliensis* (Pan, 1984; Eperon and McMahon-Pratt, 1989; Doyle *et al.*, 1991; Pan *et al.*, 1993; Bates, 1994; Gupta *et al.*, 1996; Hodgkinson *et al.*, 1996; Balanco *et al.*, 1998). However, each strain or species requires different culture conditions for growth as axenic amastigotes and some have shown to be less amenable to axenic culture. For example, only recently has a long-term propagation of axenic amastigotes of *L. major* been successful (Habibi *et al.*, 2008). The stage of the promastigote, initial population density, medium used, temperature, pH and $CO_2$ concentration all need to considered when optimising culture conditions for different *Leishmania* species (Gupta *et al.*, 2001).

It is important that extracellularly cultivated amastigotes are rigorously evaluated to ensure that the cultured forms are *bona fide* amastigotes and not abnormal promastigotes or transformation intermediates. Various criteria have been used to justify the designation of "amastigote" to cells obtained through axenic culture (Gupta *et al.*, 2001). These criteria include morphological observations: the flagella of amastigote-like forms should not extend far beyond the flagellar pocket opening and should be lacking a paraflagellar rod. Membrane-bound megasomes are also characteristic features of amastigotes of *L. mexicana* (Bates *et al.*, 1992; Pral *et al.*, 1993). Differential expression of stage-specific antigens between promastigotes and amastigotes also enables the identification of potential amastigote-like populations through the detection of amastigote-specific antigens using monoclonal antibodies (Eperon and Mcmahonpratt, 1989). As is the case for intracellular amastigotes, axenic amastigotes should be more infective to host cells than promastigotes and they should be able to differentiate back to

promastigotes upon exposure to promastigote growth conditions (Eperon and McMahon-Pratt, 1989; Pan *et al.*, 1993; Hodgkinson *et al.*, 1996).

Numerous studies have reported axenic amastigotes that are morphologically and biochemically similar to lesion-derived amastigotes or those grown in macrophage cell lines (Pan *et al.*, 1993; Hodgkinson *et al.*, 1996; Balanco *et al.*, 1998; Gupta *et al.*, 2001). However, Holzer *et al.* (2006) identified many genes with significant differences in expression between lesion-derived amastigotes and axenic amastigotes. Even more interesting is the observation that, at least for the set of gene transcripts examined, axenic amastigotes appeared to show transcript abundances that were closer to that of promastigotes than lesion-derived amastigotes. Comparative profiles of intracellular metabolites have also revealed that axenic amastigotes appear to be intermediates between promastigotes and intracellular amastigotes despite their strong resemblance to intracellular amastigotes in morphology and infectivity (Gupta *et al.*, 1999). Therefore, although axenic amastigotes provide an abundant source of cells that closely resemble intracellular amastigotes, caution should be applied when using axenic cultures for the detailed study of amastigotes.

### *Trypanosoma cruzi amastigote flagellum ultrastructure*

Numerous ultrastructural studies of *T. cruzi* have been published but, as is the case for *Leishmania*, few were aimed specifically at the flagellum. Of those describing the axoneme arrangement, all report the presence of a central pair in a canonical 9+2 arrangement (Meyer *et al.*, 1958; Sanabria, 1964; Sanabria, 1968; Sanabria, 1971;

Gardener, 1974). Clear transverse electron micrographs of the axoneme, however, are rare.

### 3.2.4 The amastigote flagellum: a redundant or functional organelle?

*Leishmania* and *T. cruzi* amastigote flagella are often described as non-functional (Singh, 2006). The physiological importance of the amastigote flagellum, if any, may not be immediately apparent and the fact that it is non-motile has reinforced the idea that it is non-functional. Just as many people once considered primary cilia to be vestigial, it is possible that a function of amastigote flagella is yet to come to light.

Other eukaryotic organisms, such as the amoeba-flagellate *Physarum polycephalum,* can switch between fully flagellated and completely non-flagellated forms depending upon environmental conditions (Glyn and Gull, 1990). The ability of organisms to retract flagellum and depolymerise the axoneme suggests that retention of the flagellum in amastigote parasites is an important feature of their life cycle.

### 3.2.5 Potential roles of the amastigote flagellum

An ultrastructure study by electron microscopy of extracellular lines of *Leishmania* amastigotes showed that the extremity of the flagellum lies just 100nm outside the flagellar pocket (Eperon and McMahon-Pratt, 1989). If the flagellar tip of amastigotes does protrude beyond the flagellar pocket it is possible that the flagellum may function as a sensory organelle in a way that is analogous to the vertebrate primary cilium. Some cells, however, do possess a primary cilium that does not project from the apical surface

of the cell but is present in a membrane invagination below the surface of the cell (Barnes, 1961). Therefore, if the amastigote flagellum does not protrude from the flagellar pocket, it may have a sensory function nonetheless.

A large number of proteins that target to the flagellum and the flagellar pocket have been identified in trypanosomatids and ongoing investigations are attempting to elucidate the biological functions of these proteins. Flagellar receptor-adenylate cyclases and flagellar calcium-binding proteins, for example, are thought to be involved in signal transduction, suggesting a probable function of trypanosomatid flagella in sensing the extracellular environment in addition to their conventional role in motility (Landfear and Ignatushchenko, 2001). Perhaps the simplest observation to suggest that flagellum sensing is a feature of trypanosomatid biology is exhibited by *T. brucei* and *Leishmania* spp., for example, which swim with their flagellum leading (Ginger *et al.*, 2008).

Another possible role for sensing relates to parasite-vector interactions. In their invertebrate vectors, trypanosomatid parasites attach to epithelial surfaces via the length of the flagellum. In *Leishmania* amastigotes, the targeting of flagellar membrane proteins may define a polarity that could be used by the parasite to orientate itself in the macrophage phagolysosmes. Amastigotes are commonly observed to orientate themselves around the periphery of the phagolysosme with their flagella orientated towards the phagolysosme membrane. Amastigotes of *L. amazonensis*, *L. mexicana* and *L. donovani*, for example, have all been observed to adhere tightly to the membrane of the parasitophorous vacuole via their posterior pole (Benchimol and de Souza, 1981).

The amastigote flagellum, which terminates in a region of extensive desmosomal junction development at the flagellar pocket opening, may serve to ensure closure of the flagellar pocket and therefore compartmentalisation of the flagellar pocket lumen. This "junctional complex" (Balber, 1990), sometimes also referred to as the "zone of adhesion" (Overath *et al.*, 1997), may restrict access of material to the lumen of the pocket area from the parasitophorous vacuole of the host macrophage (Webster and Russell, 1993).The semi-permeable junction could limit the rate of diffusion into the flagellar pocket thus maintaining a low concentration of potentially harmful molecules, such as hydrolases and antibodies, in the lumen of the flagellar pocket. Furthermore, compartmentalisation of molecules within the flagellar pocket prior to uptake may facilitate prelysosomal processing as indicated by the presence of certain enzymes (Bates *et al.*, 1989). Although much of the research on exocytosis and endocytosis by trypanosomatids has focused on the bloodstream forms of African salivarian trypanosomes, a few endocytosis studies have been conducted on *Leishmania* amastigotes. For example, amastigote uptake of intra-vacuolar material has been demonstrated by the detection of biotinylated markers both in the flagellar pocket and inside the amastigotes (Webster and Russell, 1993). Macromolecules present in the parasitophorous vacuole can therefore be endocytosed by the amastigote via its flagellar pocket as further demonstrated by the endocytosis and degradation of MHC class II molecules by *L. amazonesis* and *L. mexicana*, perhaps to help prevent the presentation of *Leishmania*-derived antigens (Antoine *et al.*, 1999).

### 3.2.6 Intracellular parasitism in trypanosomes: an example of convergent evolution?

Although *Leishmania* and *T. cruzi* share the characteristic of an essential life cycle stage within the cells of their vertebrate hosts, there are many clear distinctions between them as regards to the types of cells invaded, the method of entry into host cells and the means by which they survive the harsh environment of the phagolysosome.

#### *Entry of intracellular parasites into host cells*

After inoculation of infective promastigotes into the mammalian dermis by a sandfly parasitized with *Leishmania*, the promastigotes rapidly bind to the cell surface of macrophages via numerous complement receptors (Brittingham and Mosser, 1996). Promastigotes enter host cells via phagocytosis and the internalised parasites are compartmentalised by membrane originating from the macrophage plasma membrane. These *Leishmania*-containing phagosomes then fuse with lysosomes of the macrophage to form parasitophorous vacuoles (PVs). PVs exhibit some features of the lysosmal compartment and have an acidic luminal pH containing various active acidic hydolyases (Lang *et al.*, 1994). During this remodelling of the phagosome, differentiation of promastigotes to amastigotes occurs.

Trypomastigote forms of *T. cruzi* can invade a variety of cell types, including macrophages, muscle cells and fat cells. Unlike *Leishmania* parasites, trypomastigotes appear to actively enter host cells. Invasion is not inhibited by cytochalasin D, a drug that blocks actin polymerisation and phagocytosis (Schenkman *et al.*, 1991). Host-cell lysosmes are actively recruited to the site of parasite entry and fuse with the host cell

plasma membrane, providing material for the formation of a parasitophorous vacuole (Rodríguez *et al*., 1999).

There is evidence for the existence of a second pathway by which trypomastigotes can enter non-phagocytic cells. In addition to lysosome recruitment, trypomastigotes can also enter cells enveloped by invaginated plasma membrane, producing an intracellular vacuole that subsequently fuses with a lysosome (Woolset *et al.*, 2003). This second entry pathway is also independent of host-cell actin polymerisation, thus distinguishing it from phagocytosis.

### *The parasitophorous vacuole inhabited by intracellular Leishmania amastigotes*

The morphology of the parasitophorous vacuole differs according to the species of *Leishmania.* There are two types of vacuole: small, individual vacuoles referred to as type I and large, communal vacuoles referred to as type II (Chang and Dwyer, 1978; Castro *et al.*, 2006). Old World Species of *Leishmania* (*L. major, L. tropica* and *L. donovani*) typically reside in type I vacuoles (Akiyama and McQuillen, 1972; Berman *et al.*, 1981; Blank *et al.*, 1993; Castro *et al.*, 2006). As only a single amastigote is ever present in a type I vacuole, this suggests that the vacuole replicates in synchrony with the amastigote. In contrast, New World Species (*L. mexicana* and *L. amazonensis*) typically reside in type II vacuoles which can contain multiple amastigotes that are usually attached to the vacuolar membrane (Gardener, 1974; Alexander and Vickerman, 1975; Lewis and Peters, 1977; Castro *et al.*, 2006,).

After cell invasion, lysosomes fuse with the parasite-containing phagosome and release their toxic substances and digestive enzymes. Whilst many intracellular parasites, *Toxoplasma gondii* and *Mycobacterium tuberculosis* for example, inhibit lysosomal fusion with the parasitophorous vacuole thereby preventing the delivery of lysosomal material (Jones and Hirsch, 1972, Armstrong and Hart, 1971), lysosomal fusion appears uninhibited in *Leishmania* infections and the phagolysosome is the final intracellular site in which the parasite resides and multiplies (Alexander and Vickerman, 1975; Chang and Dwyer, 1976; Lewis and Peters, 1977). *Leishmania* parasites must therefore be able to withstand the harsh environment of the parasitophorous vacuole.

The major cell surface glycoconjugate of the *Leishmania* promastigote, covering its entire surface including the flagellum, is lipophosphoglycan (LPG). LPG protects the parasite from hydrolases and oxygen radicals within the macrophage phagolysosome and may even prevent activation of the oxidative burst by macrophages (Mcneely and Turco, 1990; Mcconville and Ferguson, 1993). *Leishmania* amastigotes synthesise glycosyl-inositol phospholipids (GIPLs) which are left as the major glycocalyx component after the surface expression of LPG is down-regulated during parasite transformation (Mcconville and Ferguson, 1993). GIPLs, through the inhibition of kinase-mediated signal transduction pathways, may also prevent the activation of the oxidative burst (Schneider *et al.*, 1993). The amastigote stage is well adapted to the acidic environment of the phagolysosome with their metabolic optimum being equal to the acidic pH of the phagolysosome. They exhibit stage-specific proton pumps and stage-specific metabolite transporters that are optimally active at an acidic pH (Zilberstein and Shapira, 1994).

#### *Escape from the phagosome: Trypanosoma cruzi*

An alternative way for an intracellular parasite to avoid the consequences of lysosome-phagosome fusion is for it to escape from the phagosome soon after cell invasion, as demonstrated by *T. cruzi* (Kress *et al.*, 1975). After transformation into amastigotes the parasite multiplies by binary fission whilst free in the cytoplasm where, presumably, macrophages have no specially developed mechanisms for parasite killing.

### 3.2.7 The evolutionary relationships among *Trypanosoma* and *Leishmania* spp.

Early molecular studies of kinetoplastid phylogeny were limited by uneven sampling of species across lineages with a bias towards taxa of medical importance and the fact that the popular molecular marker, small subunit (SSU) rRNA, underwent massive evolutionary change early in kinetoplastid history. Correct estimation of relationships with kinetoplastids was therefore made difficult by the short internal branches within kinetoplastids compared to the long branch that connect kinetoplastids to other eukaryotes in phylogenetic trees estimated from SSU rRNA sequences (Simpson *et al.*, 2006). Several studies of SSU rRNA genes and the majority of phylogenetic analyses involving protein-coding genes support the notion that trypanosomatids are monophyletic (Hashimoto *et al.*, 1995; Alvarez *et al.*, 1996; Lukes *et al.*, 1997; Haag *et al.*, 1998; Stevens *et al.*, 1999; Stevens *et al.*, 2001). Hughes (2003) and Piontkivska (2005), however, presented re-analyses of SSU rRNA data in which trypanosomatids appeared paraphyletic and contended that previous analyses did not include appropriate outgroups and had examined an inadequate taxon selection. More recent extensive analyses settled the debate with high statistical support for trypanosome monophyly (Hamilton *et al.*,

2004; Simpson *et al.*, 2004). Trypanosomatids are descended from within the bodonids and, contrary to early unexpected rRNA phylogenies, the genera *Trypanosoma* and *Leishmania* are both monophyletic (Fig. 3.3.) (Simpson *et al.*, 2006). In contrast, many other genera (*Crithidia*, *Blastocrithidia*, *Herpetomonoas*, *Leptomonas* and *Wallaceina*) do not appear to be monophyletic groups.

Information from several independent sources supports the identification of key phylogenetic groupings of trypanosomes (Fig. 3.1.) (Haag *et al.*, 1998; Stevens *et al.*, 1999; Overath *et al.*, 2001; Hamilton *et al.*, 2004; Hamilton *et al.*, 2007). These include the "Aquatic clade", comprising trypanosomes of mainly aquatic and amphibious vertebrates; the *T. cruzi* clade, which contains two human-infective mammalian trypanosomes (*T. cruzi* and *T. rangeli*), bat trypanosomes and a trypanosome from a kangaroo; the *T. brucei* clade which includes African mammalian trypanosomes (e.g. *T. brucei*, *T. evansi*, and *T. vivax*); the *T. lewisi* clade, which contains trypanosomes from a wide range of rodents, a rabbit and a mole; the *T. theileri* clade, which contains trypanosomes from marsupial and placental mammals (deer cattle and primates); two clades of avian trypanosomes (the *T. avium* clade and the *T. corvi* clade) and the "lizard clade". Other trypanosomatids, including the genus *Leishmania*, branch paraphyletically at the base of the trypanosome clade.

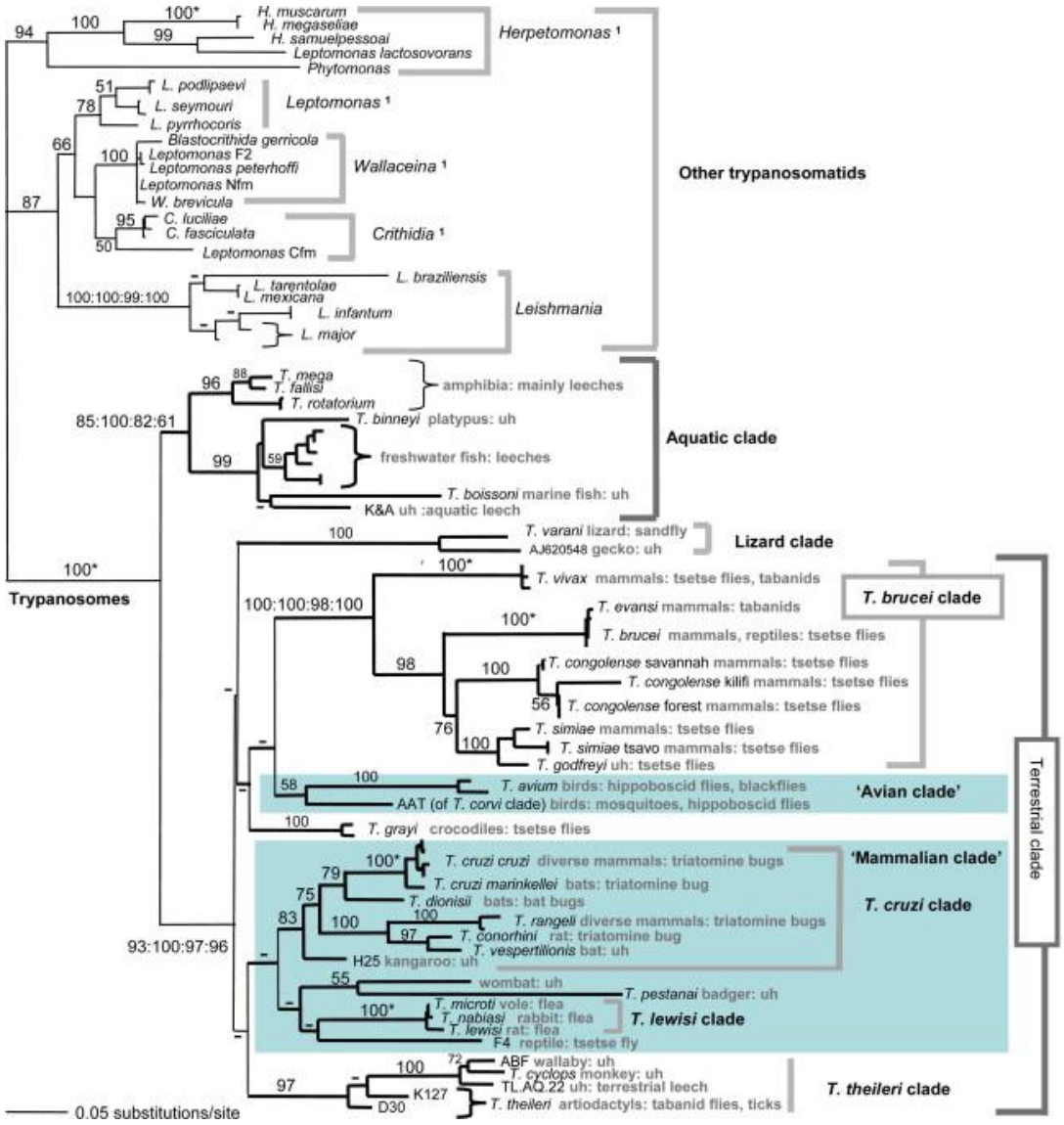


**Figure 3.1. Phylogeny of trypanosomatids.** Maximum-likelihood *gGAPDH* gene tree rooted using non-trypanosome trypanosomatids. Single values at nodes are bootstrap values ("–" denotes a support value <50). Known host taxa are given ("uh" denotes unknown host). [1]Suggested genera for all taxa in these clades. After Hamilton *et al.,* (2007).

*Trypanosoma* and *Leishmania* are thought to have evolved from an ancestral insect parasite, which later adapted to a vertebrate/insect transmission cycle (Hamilton *et al.*, 2004), possibly by transmission into vertebrate host from a blood-sucking insect during feeding (Simpson *et al.*, 2006). *Trypanosoma*, *Leishmania* and *Endotrypanum* (reclassified by some as *Leishmania sp.* (Cupolillo *et al.*, 2000; Hamilton *et al.*, 2007)), are the only lineages to have surviving descendents in warm-blooded vertebrate hosts. *T. cruzi* and

*Leishmania* spp., however, are only distantly related and have distinct evolutionary histories (Hamilton *et al.*, 2004).

## 3.3 Results

### 3.3.1 Growth pattern of *Leishmania mexicana* promastigotes in culture

A population growth rate curve of the promastigote form (Fig. 3.2.) was generated in order to evaluate the growth characteristics of *L. mexicana* promastigotes and to allow calculation of the time point or cell density at which a culture will reach stationary phase. Promastigotes grew logarithmically in the range of 6 x $10^5$ and 2 x $10^7$ cells $ml^{-1}$ (densities under 6 x $10^5$ were not tested). Population growth slowed at densities of greater than 2 x $10^7$ cells $ml^{-1}$ and ceases at approximately 6 x $10^7$ cells $ml^{-1}$. Repeated subculture to maintain promastigotes between 2 x $10^6$ and 2 x $10^7$ cells $ml^{-1}$ gives rise to continuous logarithmic growth with a doubling time of approximately 7 hours.

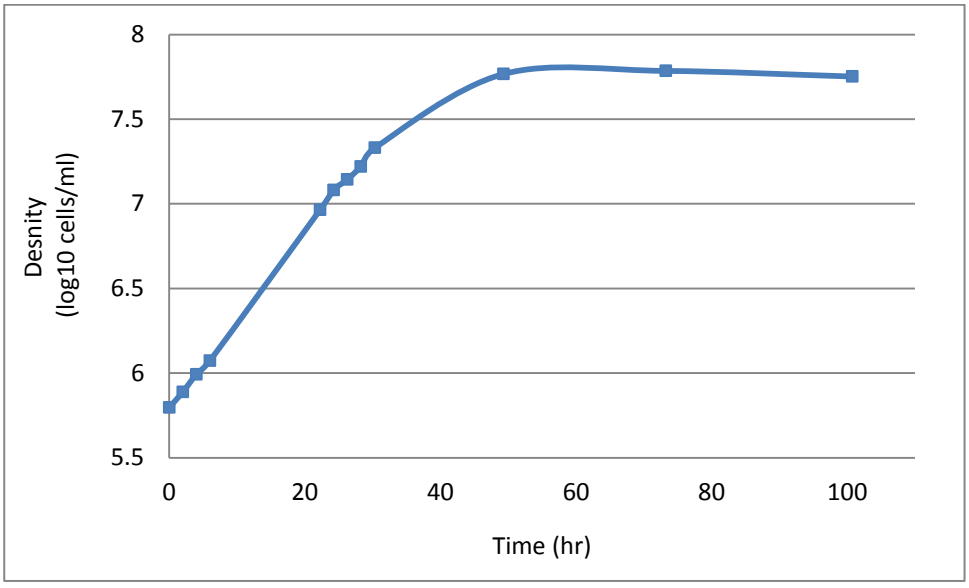


**Figure 3.2.** Growth curve of *Leishmania mexicana* promastigotes at 28°C in M199 with 10% FCS.

### 3.3.2 Validation of the *in vitro* infection protocol: time course and efficiency of infection

Under the culture conditions described promastigotes were observed to gain entry into the macrophages and induce the formation of large type II vacuoles characteristic of *L. mexicana* (Fig. 3.3.a.). The parasites showed dramatic cell restructuring with a reduction of size and readsorption of their flagellum until they reached the typical round shape of tissue-derived amastigotes. The percentage of infected cells peaked at 1-day post-infection with an average of 54% of macrophages containing at least one parasite cell. Infectivity was observed to drop to 26% and 29% 3-days and 4-days post-infection respectively, possibly due to macrophages continuing to undergo mitosis or the digestion of parasites by their host cell. Chang (1980) reported a similar efficiency of infection with 50% infectivity 36 hours post-infection. Due to the occurrence of crowded vacuoles it was not possible to accurately count the number of amastigotes per cell at every time point but the number of parasites per cell was observably higher 1-day post-infection than 4-days post-infection.

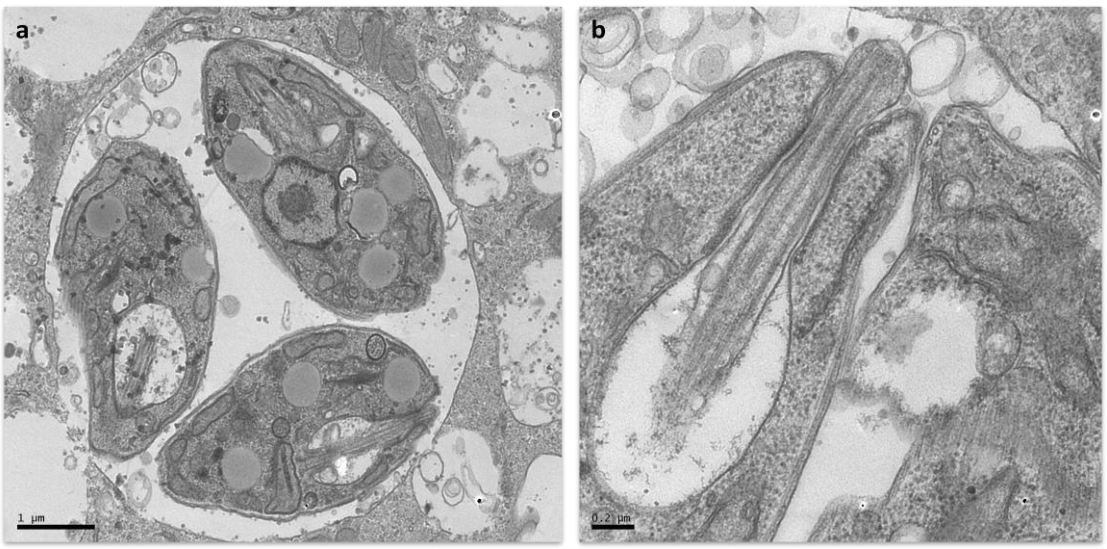


**Fig. 3.3**. **(a-b)** Thin section TEM views of *Leishmania mexicana* amastigotes in a J774 macrophage vacuole. Scale bars = 1µm (a) and 0.2µm (b).

### 3.3.3 The ultrastructure of the *Leishmania mexicana* promastigote flagellum

Stationary phase *L. mexicana* promastigotes were examined by serial thin section transmission electron microscopy (TEM). The axoneme of the promastigote flagellum displays the classical 9+2 microtubule array (Fig. 3.4. and Fig. 3.9.). Associated axonemal components involved in motility including the dynein arms, radial spokes and nexin links, are also evident.

Serial TEM through the flagellum enables the arrangement of the axonemal microtubules to be followed along the flagellum from the basal body to the flagellar tip. The basal body is represented by a proximal end set of microtubule triplets (Fig. 3.4.1.) followed by a more distal doublet microtubule transition zone (Fig. 3.4.2.) and then a basal plate from which the central pair of singlet microtubules extends (Fig. 3.4.3.). After this the 9+2 axoneme extends along the flagellum (Fig. 3.4.4.). The PFR extends from a point halfway along the flagellar pocket to the tip. A pro-basal body, containing triplet microtubules, lies

close to and parallel with the basal body (Fig. 3.6.). The kinetoplast, containing the mitochondrial DNA, is located at the proximal end of the basal body and pro-basal body (Fig. 3.4.).

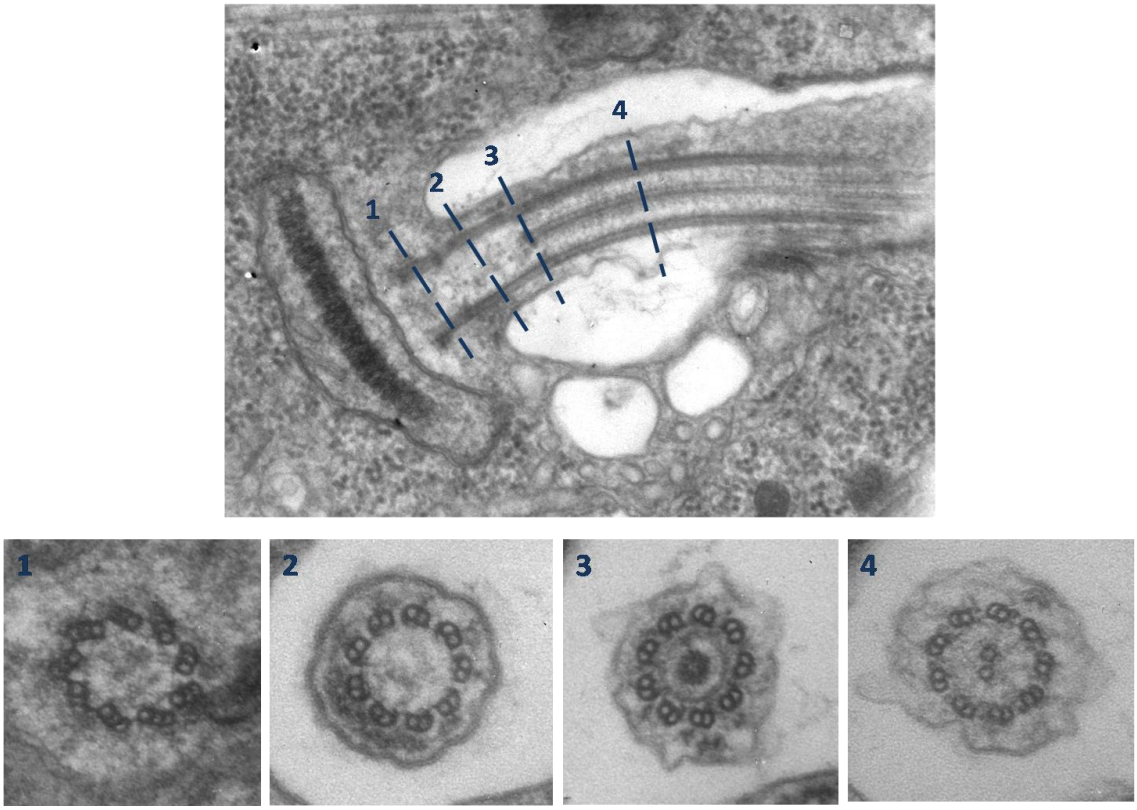


**Figure 3.4. Structure of the *Leishmania mexicana* promastigote flagellum. (1-4)** The serial arrangement of microtubules along the axoneme. The position of these sections is indicated in the longitudinal section.

### 3.3.4 Fixed CP and PFR orientation in *Leishmania mexicana* promastigotes

In all Kinetoplastida examined to date, the PFR runs alongside the axoneme for most of its length (Fuge, 1969; Gull, 1999) and, being permanently connected to a set of four outer doublets, maintains a specific orientation relative to the axoneme (Gull, 1999). The PFR can therefore act as a reference, allowing unambiguous identification of central pair orientation within the flagellum. 20 randomly selected thin section transmission electron

micrographs showing cross-sections of axonemes from *Leishmania mexicana* promastigotes were analysed to determine the orientation of the central pair. Discrepancies between the angle of the axoneme cross-section and the true transverse plane, however, almost always result in apparent elliptical deformation of the axoneme. Geometric transformation of the data from micrographs was used to correct elliptical axoneme cross-sections to circular ones that are representative of a true transverse section (detailed in Materials and Methods). The positions of the central pair were then mapped onto the normalised axonemes (Fig. 3.8.). The positions of all the microtubules were extremely constant from axoneme to axoneme and fell on points predicted by nine-fold symmetry; the circularity of the transformed dataset can therefore be demonstrated by nine-fold rotation of the corrected image, with superposition of the doublets of the axoneme. Using the PFR as an external reference, the axis of the central pair also has a constant orientation. Thus, the orientation of the central pair in *Leishmania mexicana* promastigotes does not vary with respect to the nine outer doublets. Since the dataset comprised cross-sections through axonemes of many different cells and at different positions along the flagellum, this provides strong evidence for a fixed, specific orientation for the central pair in *Leishmania mexicana*, consistent with similar observations in *Trypanosoma brucei* (Gadelha et al., 2006). Given the evolutionary distance between *Trypanosoma brucei* and *Leishmania mexicana* (Fig. 3.1.), it can be assumed that the mechanism by which the central pair rotates relative to the outer nine microtubule doublets in some non-metazoan lineages, does not operate in trypanosomatids.

The PFR, in conjunction with the fixed position of the two central microtubules in the axonemes of trypanosomes (Gadelha *et al.*, 2006), can therefore act as a fixed reference, allowing unambiguous identification of microtubule doublets and triplets. The outer microtubule doublets, as seen in cross-sections through a flagellum, were numbered in clockwise rotation according to Afzelius (1959) with doublet number 1 being that which is equidistant from the two microtubules of the central pair, as shown by a median line that bisects the central pair (Fig. 3.5.). As predicted, the PFR, in all cross-sections examined, extends alongside microtubule doublets 4-7, as concurrent with previous observations in *L. major* (al-Shammary *et al.*, 1995) and other trypanosomatids (Gull, 1999).

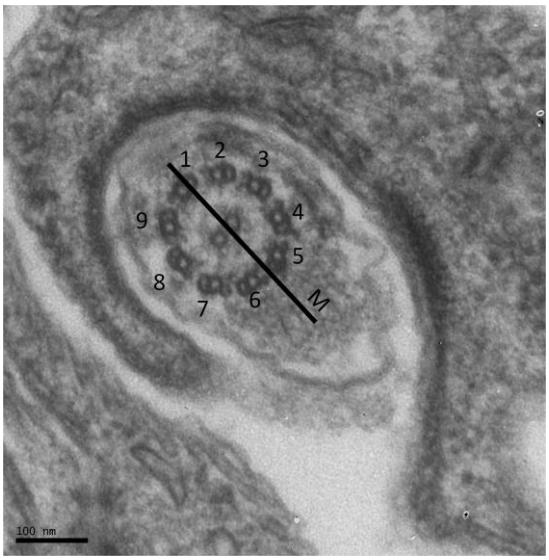


**Figure 3.5.** Cross-section of *Leishmania mexicana* promastigote flagellum showing the axoneme, the PFR, the median line (M) and the doublets numbered according to Afzelius (1959).

### 3.3.5 Invariant positioning of pro-basal body

Using the PFR and central pair as reference points to define doublet number, the position of the pro-basal body relative to the basal body was mapped by serial TEM of promastigote flagella. The pro-basal body was invariably positioned adjacent to triplet 7 (Fig. 3.6.).

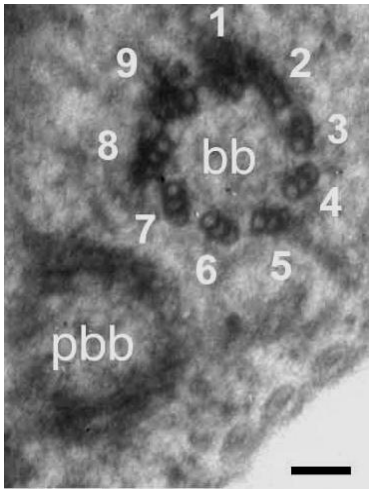


**Figure. 3.6.** The pro-basal body (pbb) of the *Leishmania mexicana* promastigote is invariably positioned adjacent to triplet 7 of the basal body (bb). Scale bar = 100nm.

### 3.3.6 An unusual structure in the axoneme lumen is an extension of central pair microtubules

Of the 24 series that extended along the flagellum between the basal body and the basal plate, approximately half (13, 54%) showed evidence of an unusual microtubule-like structure in the axoneme lumen in sections immediately before the basal plate (Fig. 3.7.). Following geometric transformation of the data from the micrographs to correct for elliptical deformation of the axoneme (detailed in Materials and Methods), the positions of all of these extraordinary structures were mapped onto the normalised axonemes (Fig. 3.8.). Examination of the positioning of the MT-like structures and their appearance immediately before the basal plate from which the central pair extends, suggests that these extraordinary structures are extensions of one or both of the single microtubules of the central pair. Therefore, in some instances, a single microtubule of the central pair may extend from a position slightly proximal to the basal plate.

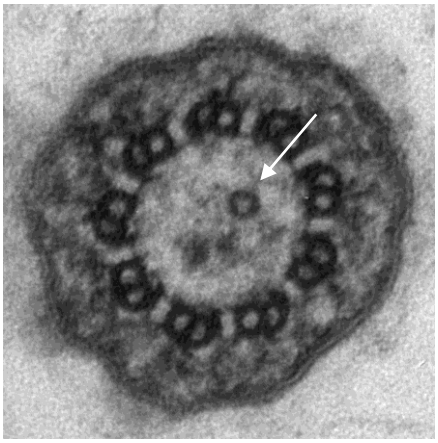

**Figure 3.7.** Unusual microtubule-like structure (arrow) in the axoneme lumen immediately before the basal plate of a *Leishmania mexicana* promastigote.

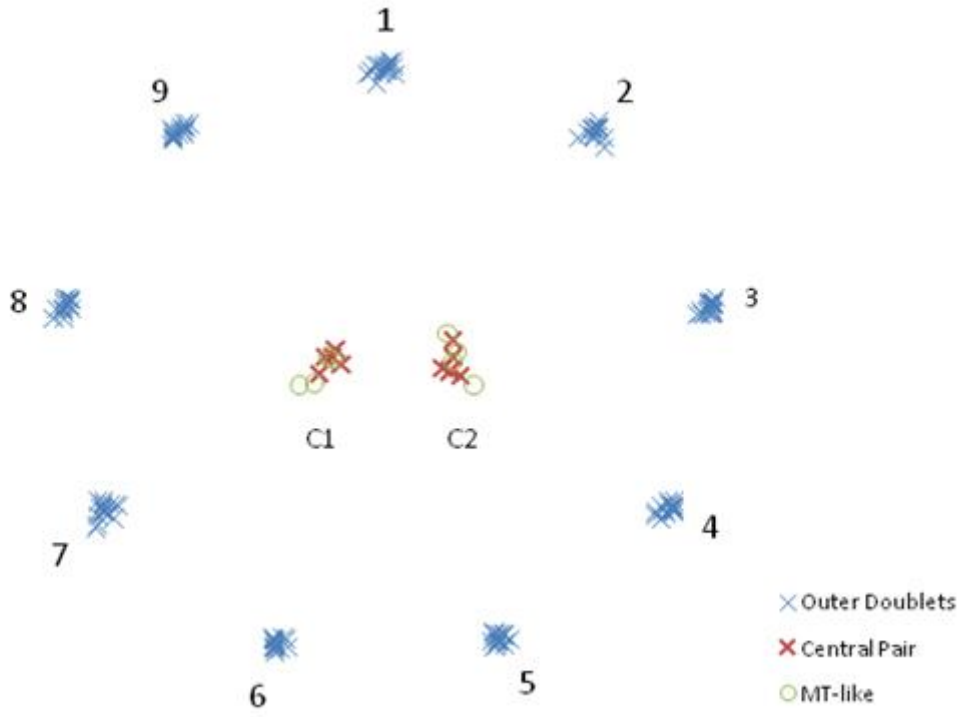


**Figure 3.8. The positions of microtubules in transverse sections of *Leishmania mexicana* promastigotes.** Points show the positions of the centres of the microtubule (MT)-like structure, the central pair microtubules (C1 and C2) or the A-tubules of the outer doublets (1-9).

### 3.3.7 The ultrastructure of *Leishmania mexicana* amastigote flagellum

The amastigote flagellum is short in length (~1.5µm) with only a small bulbous tip exposed to the parasitophorous vacuole environment beyond the flagellar pocket (Fig. 3.9.b and Fig. 3.15.). Analysis of serial sections along the length of the amastigote flagellum shows its structure is distinct from that of the promastigote flagellum and that the nine microtubule doublets are not arranged in a classical 9+2 arrangement (Fig. 3.9).

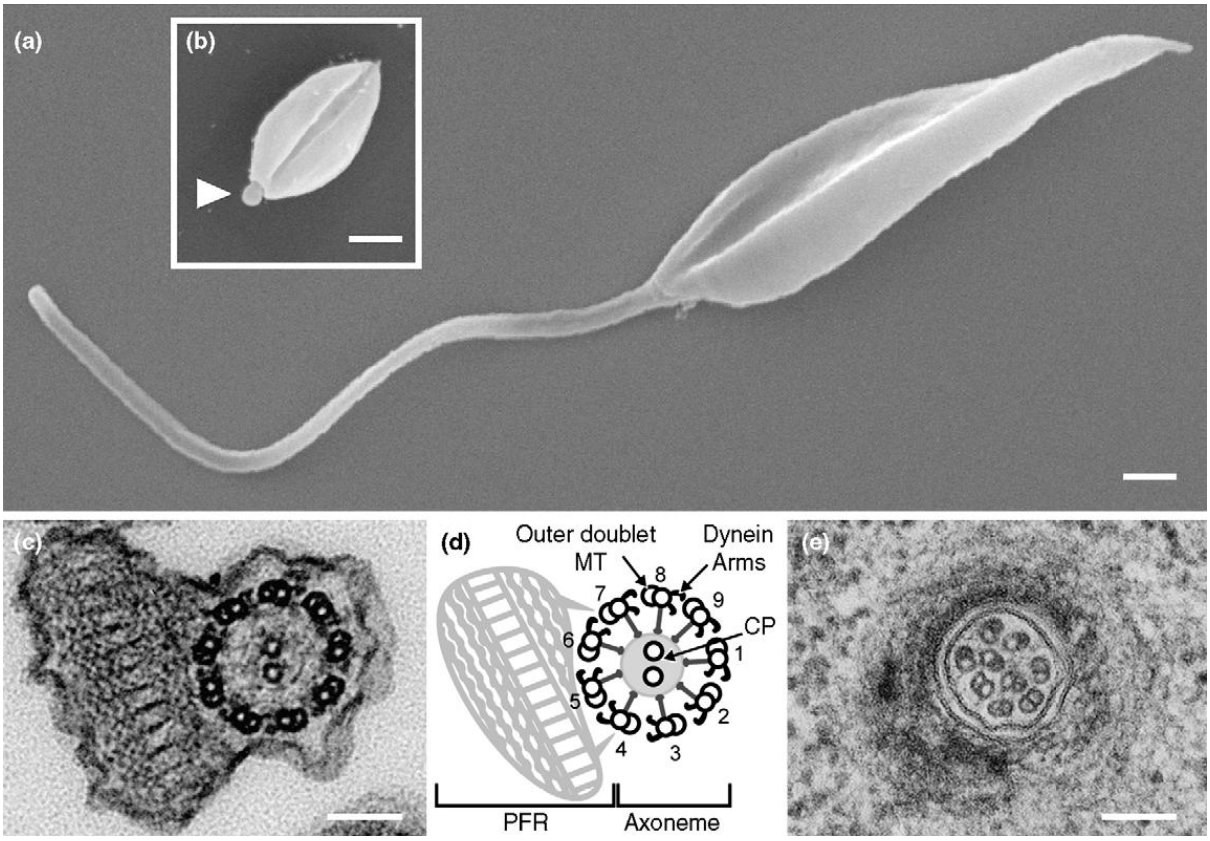


**Figure 3.9. Structure of the *Leishmania mexicana* flagellum in amastigotes and promastigotes.** Scanning electron micrographs show the difference in flagellum length between the *Leishmania mexicana* promastigote **(a)** and amastigote **(b)**. In the amastigote on the tip of the short flagellum is exposed to the environment (arrowhead). Differences between promastigote and amastigote axoneme architecture are clearly visible in transmission electron micrographs of flagellum cross-sections (c and e, respectively). Prominent structural features of the promastigote flagellum **(c)** include the canonical 9+2 microtubule axoneme, forming a ring of nine outer microtubule (MT) doublets around a central pair MT (CP), with associated inner and outer dynein arms, and the PFR. These axonemal structures are shown in the diagram in **d)**. In contrast, the amastigote flagellum **(e)** consists of a collapsed axoneme of nine MT and there is no PFR. Scale bars represent 1µm (a,b) and 0.1µm (c-e). SEM (a and b) by E. Gluenz and M. Shaw.

Similar to the promastigote, the basal body is represented by a set of nine microtubule triplets (Fig. 3.10.a and Fig. 3.11.a), followed by a more distal ring of nine doublet microtubules in the transition zone with associated projections connecting to the flagellar membrane (Fig. 3.10.b-c and Fig. 3.11.b) before nine doublet microtubules surround a basal plate (Fig. 3.10.d and 3.11.c). The amastigote, however, displays a central electron dense core immediately distal to the basal plate (Fig. 3.10.e-f and Fig 3.11.d). Although there is no

evidence of a true central pair, this electron dense core does vary between cells, with the occasional observation of one or two central singlet microtubules that terminate before the neck region. More distally, the nine-fold symmetry of the axoneme is broken by the progressive collapse of one or two of the outer doublets into the centre (Fig. 3.10.f-h; Fig. 3.11.g and Fig. 3.14.). This break of symmetry occurs distal to the basal plate, yet before the narrowing of the flagellum at the pocket neck. Serial examination of doublet displacement in 11 axonemes showed that in five axonemes one doublet was displaced (example shown in Fig. 3.10.), while two doublets were displaced simultaneously in six axonemes (examples shown in Fig. 3.11 and Fig. 3.14.).

There was no evidence of a PFR or outer dynein arms in the amastigote flagellum.

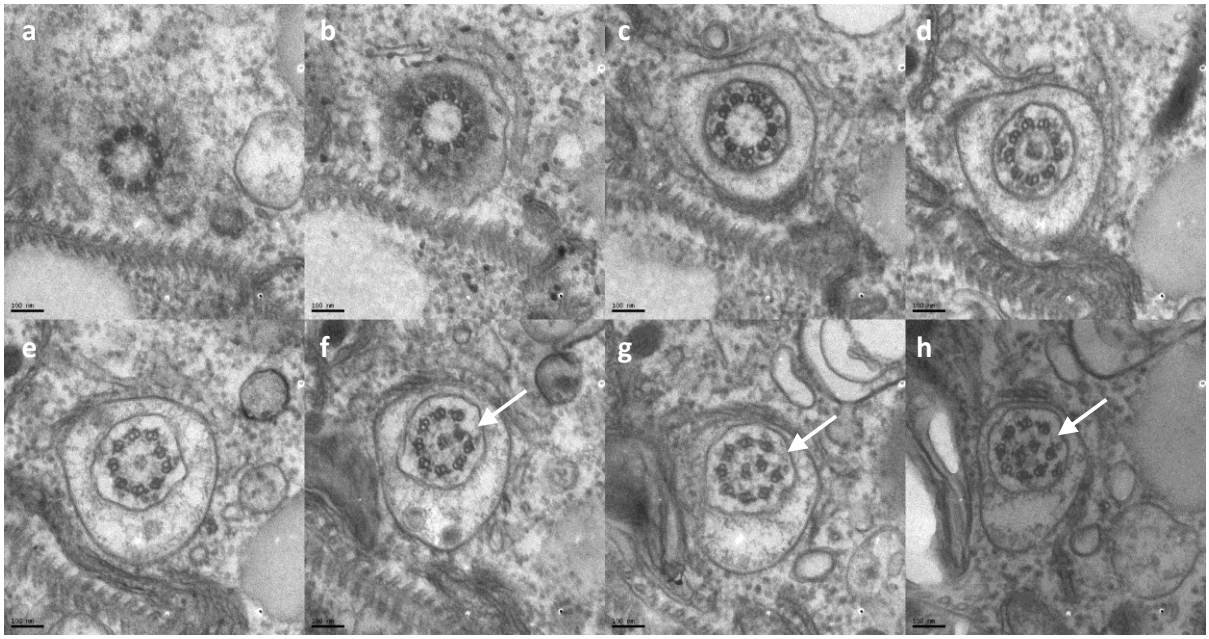


**Figure 3.10. (a-h) Structure of the *Leishmania mexicana* amastigote flagellum.** Serial section TEM from the basal body to the region of symmetry break. Arrows indicate the inward doublet displacement.

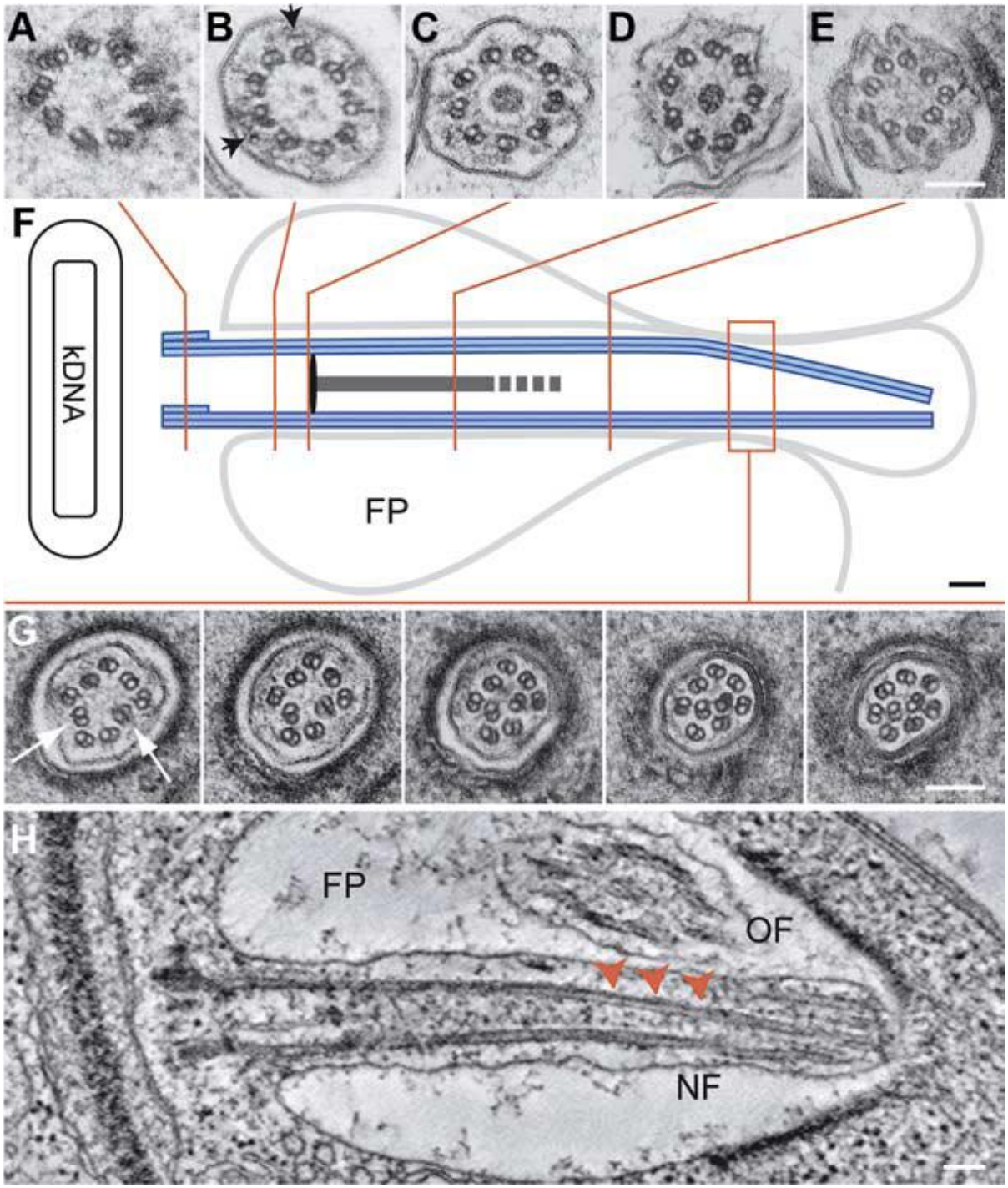


**Figure 3.11. Structure of the *Leishmania mexicana* amastigote flagellum.** J774 macrophages were infected with stationary phase L. mexicana promastigotes. Three days post-infection cells were fixed and processed for TEM. **(A-E,G)** Serial thin sections depicting arrangement of microtubules along the axoneme. Black arrowheads indicate IFT particles. **(F)** Position along the flagellum of sections in A-E and G. **(G)** Displacement of doublets (arrows) shown in serial thin sections through the distal portion. **(H)** Tomographic slice from a reconstructed 3-D volume of a dividing amastigote showing the growing flagellum (NF) in longitudinal section; arrowheads indicate symmetry break. (FP) flagellar pocket; (OF) mature flagellum. Scale bar = 100nm. Electron tomography image (H) by J. L. Höög.

### 3.3.8 No particular doublet initiates axoneme collapse

The absence of both a central pair and a PFR in the *L. mexicana* amastigote flagellum complicates the numbering of doublets and triplets. Numbers were therefore assigned using the pro-basal body as an extra-axonemal reference point. This assumes that the pro-basal body adopts an identical position in both the amastigote and the promastigote, i.e. adjacent to doublet 7 (Fig. 3.12.).

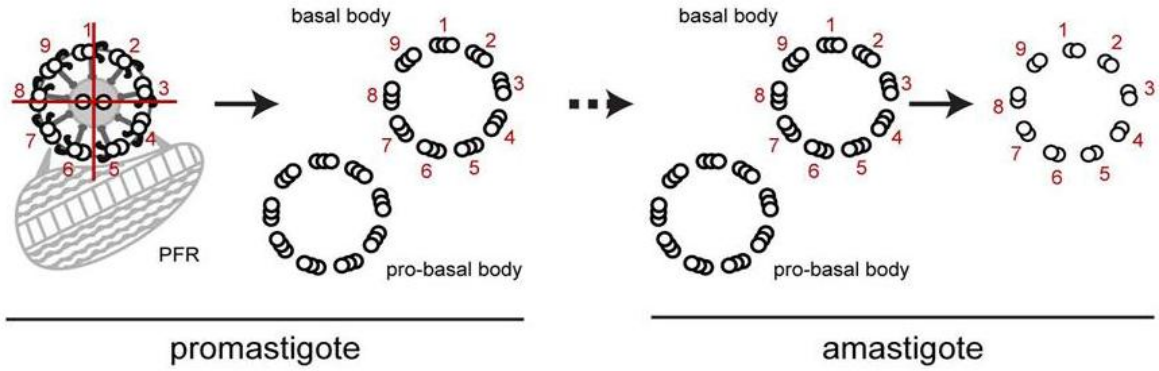


**Figure 3.12. Numbering of microtubule doublets of the *Leishmania mexicana* amastigote flagellum.** Absolute doublet and triplet numbering showed that the *L. mexicana* promastigote pro-basal body is invariably positioned adjacent to triplet 7. These numbers were translated onto the amastigote basal body/pro-basal body pair (dashed arrow) and their positions followed through each series.

Serial sections from the basal body to the flagellum tip demonstrated that no specific doublet(s) are displaced into the centre of the axoneme. Eight of the nine doublets were found to be displaced across the eleven flagella examined (Fig. 3.13.), suggesting essentially stochastic behaviour.

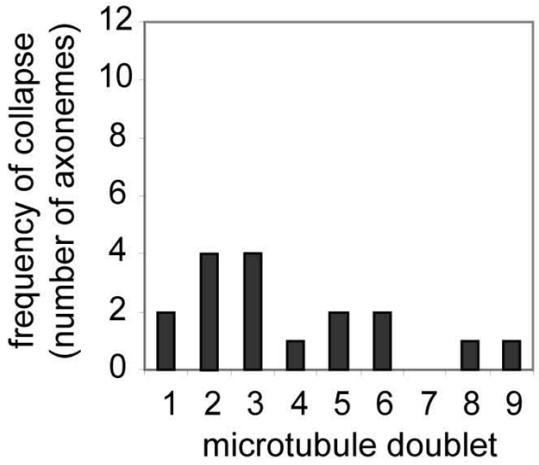


**Figure 3.13.** The frequency of doublet displacement observed for each doublet over 11 *Leishmania mexicana* amastigote axonemes (two doublets were displaced simultaneously in six axonemes).

### 3.3.9 A collapsed axoneme is no impediment to intraflagellar transport.

Axoneme collapse occurs early, as evidence by the structure of a new, still elongating flagellum in a dividing amastigote (Fig. 3.11.h). Almost all cilia and flagella are built by intraflagellar transport (IFT) and the *L. mexicana* amastigote appear to be no exception. IFT particles were observed throughout the flagellum (Fig. 3.11.b and Fig. 3.14.11-14).

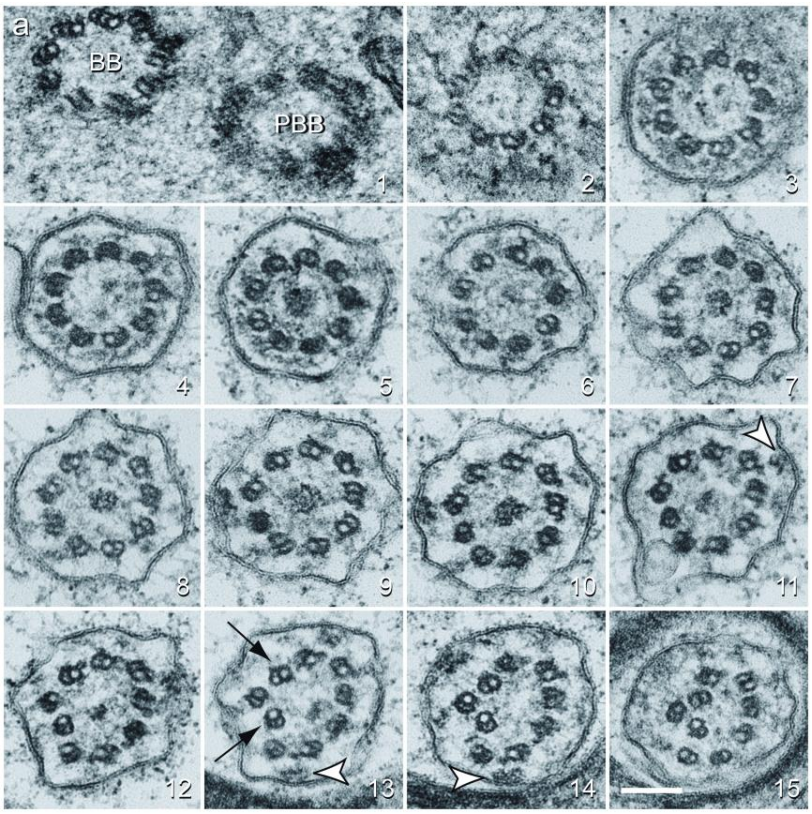


**Figure 3.14**. **(1-15) Serial thin sections depicting arrangement of microtubules and the presence of IFT particles along the *Leishmania mexicana* amastigote flagellum axoneme.** Black arrows indicate displacement of doublets in the distal portion. White arrowheads indicate IFT particles. Scale bar = 100nm.

### 3.3.10 Interaction of the amastigote flagellum tip with the parasitophorous vacuole membrane

The amastigote resides inside the parasitophorous vacuole of the macrophage (Fig. 3.16.a). Close examination of amastigote positioning within this vacuole revealed that the parasite cell is frequently orientated such that the bulbous tip of the flagellum is closely associated with the parasitophorous vacuole membrane (Fig. 3.15. and Fig. 3.16.). Of the 63 individual amastigote flagella examined in serial sections, the tip of over half of these flagella (41, 65%) were associated with the parasitophorous vacuole membrane.

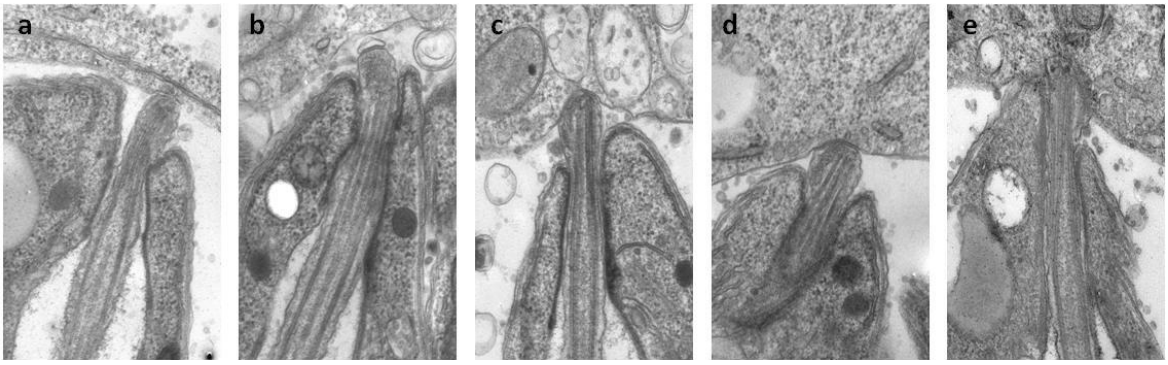


**Figure 3.15. (a-e) Thin section TEM views of *Leishmania mexicana* amastigote flagella in close contact with the J774 vacuole membrane.** The doublet displacement can also be identified in the neck region.

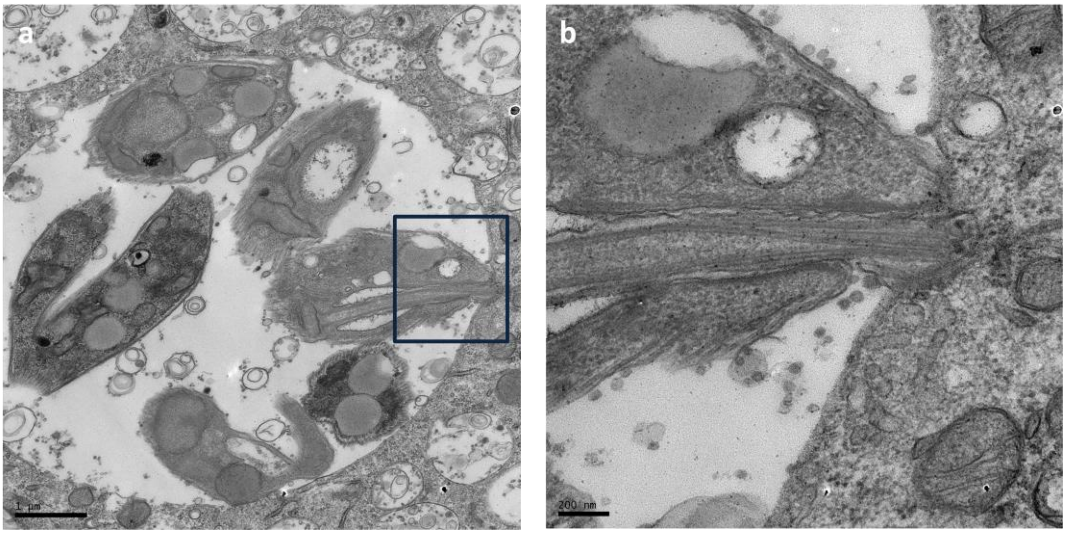


**Figure 3.16. The *Leishmania mexicana* amastigote flagellum tip is closely associated with the parasitophorous vacuole membrane. (a-b)** Thin section TEM views of *L. mexicana* amastigotes in a J774 macrophage vacuole. **(b)** Higher magnification view of the area delineated by the black box in (a). Scale bar 500nm.

### 3.3.11 The ultrastructure of the *Trypanosoma cruzi* amastigote flagellum

Using Vero cells infected with *T. cruzi* the flagellum ultrastructure was analysed by thin section TEM. The *T. cruzi* amastigote flagellum spans the flagellar pocket and protrudes into the Vero cell cytoplasm environment (Fig. 3.17.b). Cross-sections through the axoneme clearly depict a classical 9+2 arrangement of microtubules (Fig. 3.18). Outer dynein arms

and radial spokes are also visible. There was no evidence of a break in the 9-fold symmetry of the outer doublets in the pocket neck (Fig. 3.18.b).

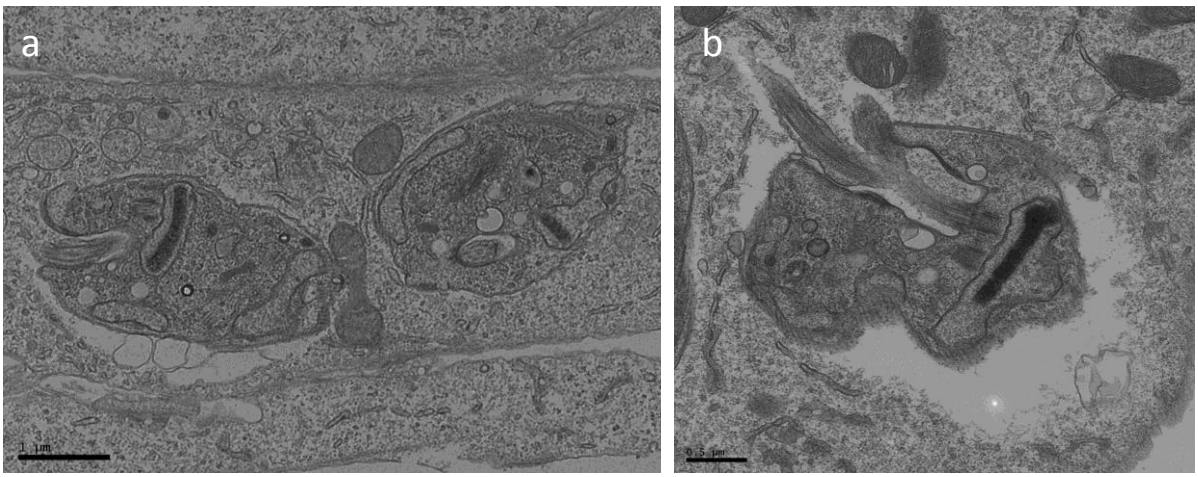


**Figure 3.17. (a) *Trypanosoma cruzi* amastigotes in the cytoplasm of infected Vero cells.** Cells were fixed for TEM 3-days post infection. Scale bar = 1µm. **(b)** The *T. cruzi* amastigote flagellum spans the flagellar pocket and protrudes into the Vero cell cytoplasm environment. Scale bar = 0.5µm.

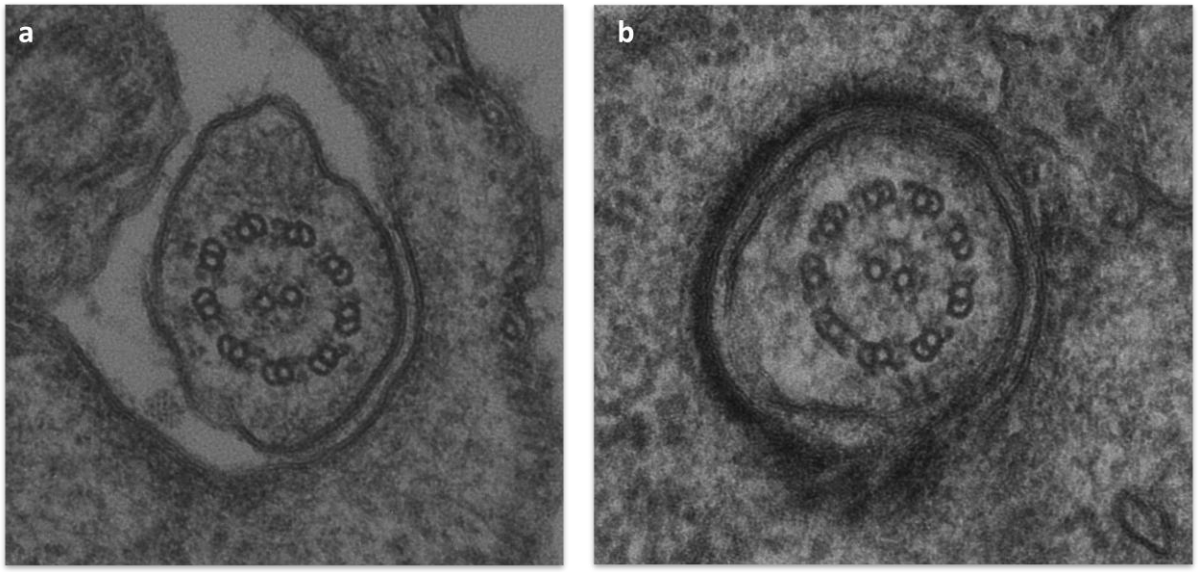


**Figure 3.18. (a-b) Structure of the *Trypanosoma cruzi* amastigote flagellum.** Vero cells infected with *T. cruzi* and fixed for TEM 5-days post infection. **(b)** There is no evidence of a break in the 9-fold symmetry of the outer doublets in the flagellar pocket neck region.

### 3.3.12 A systematic review of the prevalence of intracellular and amastigote forms in the *Trypanosoma* genus

A search of 6 databases yielded a total of 72 references containing ultrastructural and life cycle information on trypanosome parasites. An additional 21 references were obtained by following up reference lists. 81 of these references were either duplications of previously published work or contained no evidence of an intracellular form.

A total of 12 species of trypanosome were found to exist intracellularly at some point in their life cycle (Table 3.1. and supplementary material Table S3.1). All intracellular forms described in the literature were observed in mammalian tissues and are restricted to two of the trypanosome clades, the *T. cruzi* and the *T. lewisi* clade, as identified by modern analyses of trypanosome phylogeny (Fig. 3.1.) (Hamilton *et al.*, 2007).

| *Trypanosoma* clade | Species | Host | References |
|---|---|---|---|
| *T. cruzi* | *T. rangeli* | Various mammals | 1, 2 |
| | *T. dionisii* | European bats | 3 |
| | *T. conorhini* | Rat | 4 |
| *T. lewisi* | *T. xeri* | Ground squirrel | 5 |
| | *T. evotomys* | Bank vole | 6, 7, 8 |
| | *T. zapi* | Jumping mouse | 6, 7, 8 |
| | *T. tiamiasi* | Chipmunk | 6, 7 |
| | *T. microti* | Field vole | 8, 9 |
| | *T. acomys* | Spiny mouse | 10 |
| | *T. musculi* | Mouse | 4, 11, 12, 13 |
| | *T. nabiasi* | Rabbit | 4, 6, 7, 14, 15 |
| | *T. lewisi* | Rat | 4 |

**Table 3.1**. **Occurrence of intracellular forms in *Trypanosoma*.** See Table S3.1 for descriptions of the intracellular form and the methods of observation. References: (1) Urdaneta-Morales and Tejero, 1985 (2) Eger-Mangrich *et al.*, 2001 (3) Glauert *et al.*, 1982 (4) Deane, 1969 (5) Marinkelle and Abdalla, 1978 (6) Molyneux, 1976 (7) Hoare, 1972 (8) Molyneux, 1969a (9) Molyneux, 1969b (10) Abdallah *et al.*, 1989 (11) Krampitz, 1970 (12) Wilson *et al.*, 1973 (13) Molyneux, 1970 (14) Grewal, 1957 (15) Molyneux, 1969c.

## 3.4 Discussion

### *Culture of Leishmania amastigotes*

Many studies of *T. cruzi* and *Leishmania* spp. have focused predominately on the extracellular stages rather than the intracellular amastigote stage. Studies of the amastigote stage have been hampered by a dependence on parasites obtained from infected animals and by the difficulty of obtaining abundant numbers in culture. In the present work, a method to obtain *Leishmania mexicana* amastigote stages through a mouse macrophage line proved successful and provided an abundant source of cells that morphologically resembled amastigotes obtained from infected animals. This protocol therefore provides a more suitable method for the propagation of *L. mexicana* amastigotes for ultrastructural studies than axenic cultures that dominate the field. Differences in gene expression between axenic and lesion-derived cultures have been reported (Holzer *et al.*, 2006). *L. mexicana* amastigotes derived in axenic culture through temperature elevation and pH reduction have been observed with 9+2 and 9+3 axoneme variations (Eva Gluenz, personal communication) that were not observed in this study of infected-macrophage-derived amastigotes. It might be appropriate, however, to verify beyond morphological observation that all cultured forms are *bona fide* amastigotes and not abnormal promastigotes or transformation intermediates. Beyond the morphological criteria adopted in this study, the detection of a stage-specific protein marker, such as PFR2, a major structural protein of the paraflagellar rod absent in the amastigote stage, would further validate this protocol for the propagation of amastigotes. Another stage-specific marker, HASPB, is expressed on the surface membrane of infective parasite stages only, namely metacyclics and amastigotes (Sádlová *et al.,* 2010).

### *Ultrastructure of the Leishmania amastigote flagellum*

A common view has emerged that classifies axonemes into canonical, motile 9+2, and noncanonical, immotile 9+0 sensory structures. This study reveals this view to be overly simplistic, and additional axonemal architectures associated with potential sensory structures should be incorporated into the prevailing models. In this study, serial sectioning of *L. mexicana* amastigote flagella revealed that the 9-fold symmetry of the 9+0 axoneme is broken by the progressive collapse of one or two of the outer doublets into the centre. The structure of the amastigote flagellum is distinct from the promastigote 9+2 flagellum, providing a clear example of differentiation of the axoneme in a unicellular organism's lifecycle.

A strikingly similar arrangement can be observed in vertebrate primary cilia. Although vertebrate primary cilia are generally described as 9+0, various TEM studies indicate a collapse of the microtubule doublet symmetry upon the exit of the primary cilium from the cell. This disarrangement of the peripheral microtubules is commonly observed in the primary cilia of a diverse range of tissues and organisms (Dahl, 1963; Allen, 1965; Breton-Gorius and Stralin, 1967; Gilula and Satir, 1972; Odor and Blandau, 1985; Hagiwara *et al.*, 2008). Primary cilia were once considered a vestigial structure of no functional importance but recent studies indicate that primary cilia act as sensory structures involved in signal transduction and coordination of intra- and intercellular signalling pathways during embryonic and postnatal development in addition to tissue homeostasis in adulthood (Michaud and Yoder, 2006; Singla and Reiter, 2006; Satir and Christensen, 2007).

A parallel project, published in conjunction with this study, revisited the displacement of doublet microtubules in primary cilia through the serial sectioning of the kidney primary cilium. The 9+0 doublet structure distal to the triplet basal body persisted for less than 500nm with doublet repositioning and cilium tapering occurring thereafter (Fig. 3.19.). Ultimately the axoneme contained only one doublet and four singlets. Interestingly, the connections between the microtubule doublets and the ciliary membrane persisted for much of the cilium length, as also observed in the *L. mexicana* amastigote flagellum. As was the case for *L. mexicana* amastigote flagellum, no particular doublet was consistently displaced, suggesting essential stochastic behaviour (Fig. 3.20.).

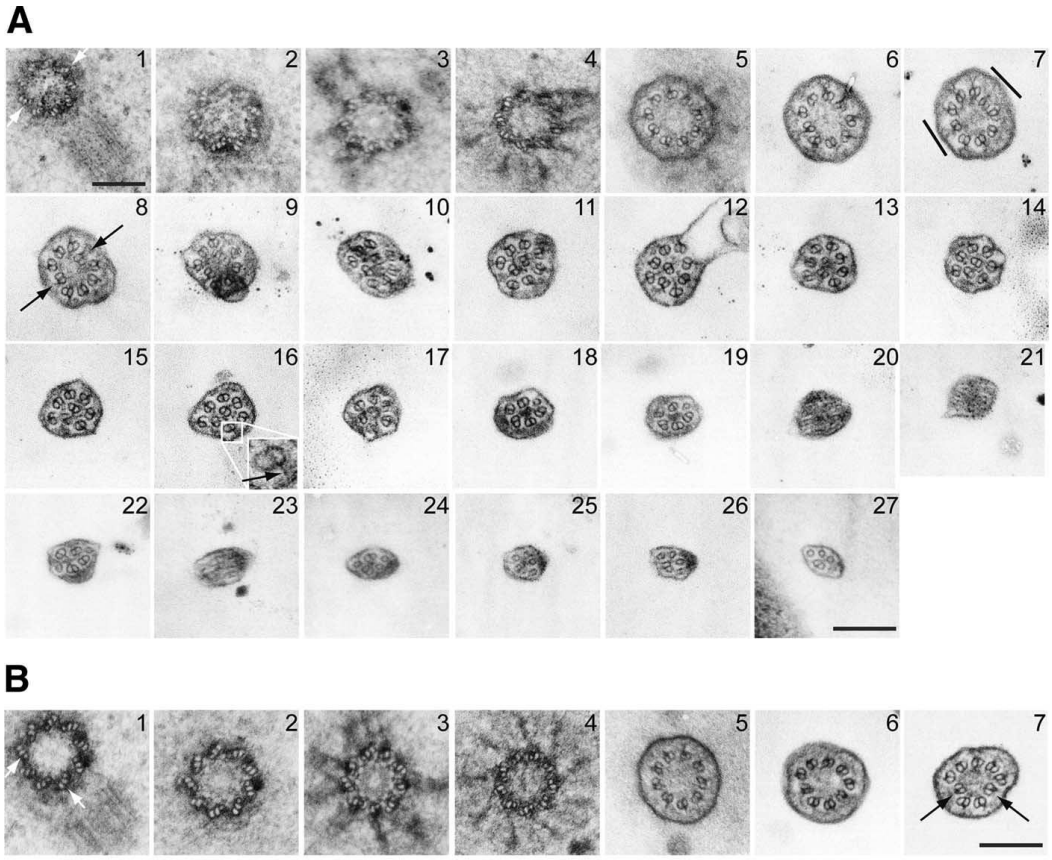


**Figure 3.19**. **Displacement of doublet microtubules in kidney primary cilia of IMCD3 cells.** Numbers indicate adjacent serial sections along the IMCD3 primary cilium. Proximally, the axoneme is 9+0 (A). Flattening (A7, lines) is the first sign of doublet displacement (arrows; A8, B7). Doublet-membrane connections remain for much of the cilium length (e.g. A16, inset, arrow). Scale bars 200nm. TEM of primary cilia by H.R. Dawe.

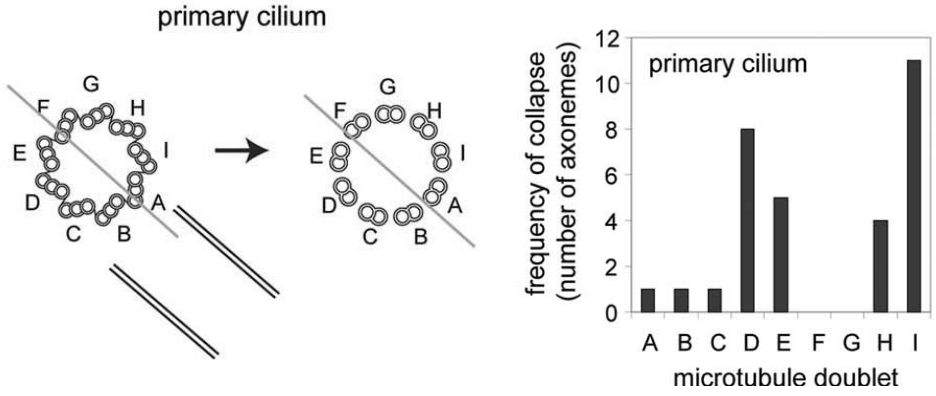


**Figure 3.20. Mapping primary doublet displacement in primary cilia.** (i) The basal body procentriole pair with letters (A-I) assigned to each triplet based on its position relative to the procentriole; these positions were followed (arrow) through each series. (ii) The frequency of doublet displacement observed for each doublet in 18 primary cilium axonemes. Two doublets displaced simultaneously in 14 axonemes; four showed displacement of a single doublet. Primary cilia analysis conducted by H.R. Dawe.

The high level of axoneme organisation required for the generation of flagellar motility imposes tight evolutionary constraints on axoneme structure. Sensory cilia are free from such constraints and, as a result, they may deviate from the canonical 9+0 structure. Mammalian olfactory cilia, for example, exhibit variations in axonemal organization. 9+2, 9+3 and 9+4 axonemes have all been observed in proximal segments of the cilia whilst the tip of the cilium has only two or three singlet microtubules after doublets are progressively lost along its length (Moran *et al.*, 1982). Sensory cilia on *Caenorhabditis elegans* neurons consist of a middle segment containing nine outer microtubule doublets surrounding a few singlets and a distal segment consisting only of microtubule singlets (Evans *et al.*, 2006). Departure from a circular axoneme may also facilitate bending in mechanosensory roles. Primary cilia serve a mechanosensory function in kidney epithelial cells. The primary cilium senses fluid motion through kidney tubules through bending of the cilium and subsequent activation of a mechanosensory cation channel (Praetorius and Spring, 2001). A simplified axoneme with a lack of radial spokes may be important for optimizing transport of signalling molecules along the microtubules. Alternatively, possible secretory functions may be facilitated by a relaxed connection between microtubules and the ciliary membrane.

The striking similarity between the axoneme structure of the *Leishmania* amastigote flagellum and vertebrate primary cilia suggests a common structure for a sensory function. *Leishmania* amastigotes inhabit the parasitophorous vacuoles of host macrophages. The bulbous tip of the flagellum is exposed to the vacuole environment beyond the flagellar pocket and might provide a specialised membrane surface for the targeting of receptor and transport proteins that sense environmental cues and signal or transport molecules across the parasite cell membrane. Interestingly, examination of amastigote positioning within the

parasitophorous vacuole revealed that the parasite cell is frequently orientated such that the tip of the flagellum is closely associated with the vacuole membrane. The targeting of flagellar membrane proteins may define a polarity that could be used by the parasite to orientate itself in the macrophage vacuole. Amastigotes of *L. amazonensis, L. pifanoi* and *L. donovani* have also been observed to adhere tightly to the membrane of the vacuole via their posterior pole (Benchimol and de Souza, 1981). In individual vacuoles, such as those formed by *L. major (Castro et al., 2006)*, the tight association of the membrane with the entire parasite would provide opportunities for engagement of parasite surface molecules, including those on the flagellum tip, with the host cell membrane.

In the *L. mexicana* amastigote flagellum putative intraflagellar transport (IFT) particles were observed throughout the flagellum, including in regions distal to the break of axoneme symmetry. This suggests that a collapsed axoneme does not impede IFT. IFT and an associated "flagellar pore complex" (Rosenbaum and Witman, 2002) at the boundary between the matrix of the flagellum and the cell body cytoplasm would enable the targeting of membrane receptor proteins, for example, to the flagellar membrane compartment. The flagellar pocket neck, where the membranes of the flagellum and cell body are tightly apposed, effectively seals the flagellar pocket. Studies on *T. brucei* suggest that a small luminal space, the "neck channel", provides a direct communication between the flagellar pocket and the external environment (Gadelha *et al.*, 2009). Compartmentalisation of proteins to the amastigote flagellum increases the possibility that it could be used for targeted secretion of vesicles and luminal content into the host cell vacuole, perhaps for the targeted product delivery of macromolecules to the parasitophorous vacuole membrane. A secretory function for cilia has previously been proposed based on observations of vesicles

derived from the flagellum of the green algae *Chlamydomonas reinhardtii* (Baldari and Rosenbaum, 2010) and it is not unrealistic to consider that this phenomenon is widely conserved. Delivery of parasite-derived products to the host cell could contribute to the subversion of the host's immune functions during infection (Kima, 2007, Silverman *et al.*, 2010).

The experimental tractability of trypanosomes facilitates further investigation into the potential sensory role of the amastigote flagellum. The presence and localisation of receptor or transport protein subunits in flagella could be determined through the use of tagged cell lines or antibody localisation. Among other protists there is evidence that flagellar "sensing" is mediated by proteins or pathways that are conserved across eukaryotes. For example, insulin receptor-like proteins have been detected in the ciliary membranes of *Tetrahymena thermophilia* (Christensen *et al.*, 2003). Proteomic studies of isolated flagella have identified many signalling molecules including kinases, phosphatases and ion channels (Ginger *et al.*, 2008). Stable transformation to produce mutant cells in which target genes are subject to RNAi would provide an approach to study gene function and determine whether flagellar signalling proteins are sensing the environment or simply regulating motility.

Alternatively, the amastigote flagellum may be required for correct structure and function of the flagellar pocket. In trypanosomatids the flagellar pocket is the sole site for endocytosis and exocytosis (Vickerman, 1994). This restriction is due to the presence of a sub-pellicular corset of closely spaced microtubules that are prohibitive for membrane fusion or fission at all other surface locations (Gull, 1999). Absence of a flagellar pocket results in multiple cellular defects and is lethal to *T. brucei* cells (Absalon *et al.*, 2008).

Elongation of a new flagellum is not required for flagellar pocket formation *per se*, but is essential for its organisation, orientation and function; without the flagellum to occlude the flagellar pocket neck it is difficult to envisage how the connection between the flagellar pocket and the external environment is maintained. Indeed, a study in *T. brucei* revealed that the flagellar pocket exhibits a smaller and distorted shape in cells with no flagella (Absalon *et al.*, 2008). An amastigote flagellum may therefore be required for the viability of the parasite due to an essential role in flagellar pocket organisation and thereby to regulate macromolecular traffic (Fig. 3.21.). This could be explored through the use of IFT mutants created by RNAi. IFT88 and IFT172, for example, are required for IFT from the base to the flagellar tip and their silencing blocks flagellum assembly (Absalon, 2008, Kohl *et al.*, 2003, Absalon *et al.*, 2008).

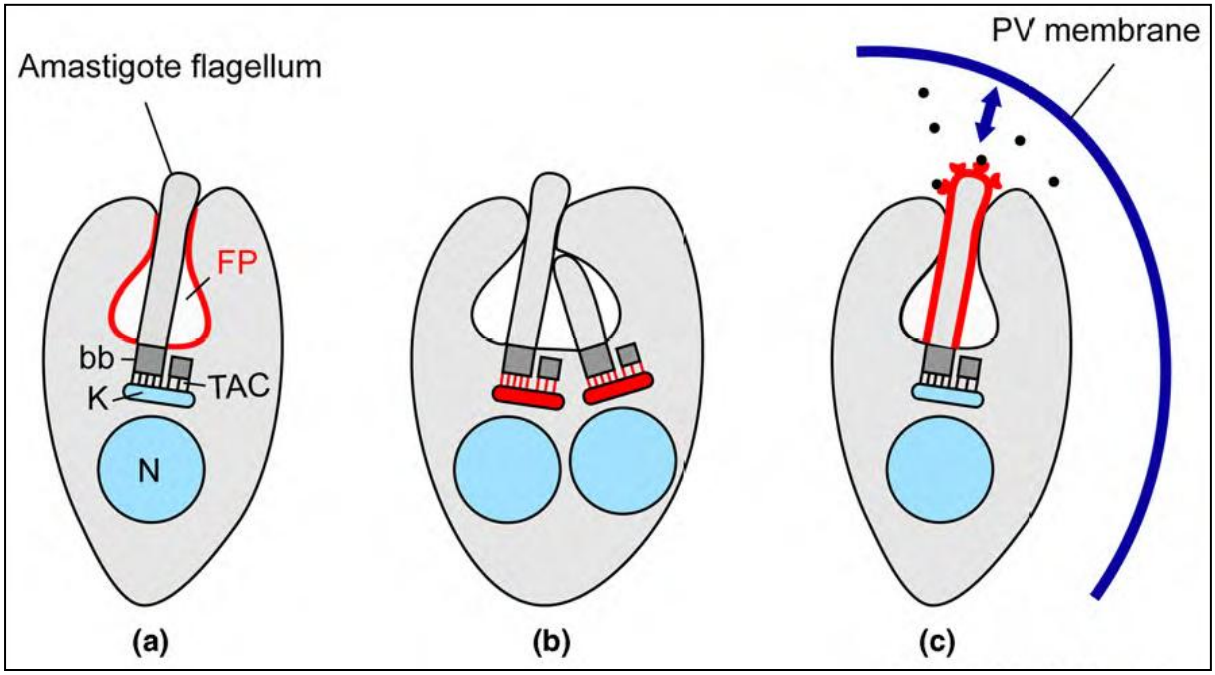


**Figure 3.21. Possible functions of the *Leishmania* amastigote flagellum.** Illustrations showing *Leishmania* amastigotes, possible functions highlighted in red. The flagellum extends from the basal body (bb) through the flagellar pocket (FP), exiting through the narrow FP neck and exposing only the flagellum tip to the environment. The flagellum is connected via a tripartite attachment complex (TAC) to the kinetoplast (K). Possible functions of the amastigote flagellum include the formation of the FP architecture **(a)**;

kinetoplastid segregation during cell division **(b)**; and sensory detection in the parasitophorous vacuole (PV). The tip of the amastigote flagellum could provide a platform for positioning receptors and transporters with roles in environmental sensing and host-parasite interactions **(c)**.

### *Comparing the amastigote flagellum of Leishmani and T. cruzi*

*T. cruzi* cross-sections through the axoneme revealed the presence of a central pair with microtubules arranged in the classical 9+2 configuration. Unlike the *L. mexicana* amastigote flagellum there was no evidence of a break in the 9-fold symmetry of the outer doublets.

An extensive review of the literature revealed that reports of intracellular forms in the trypanosomes are confined to the *T. cruzi* clade. Intracellular forms have been reported in *T. cruzi* and *T. rangeli* which infect a diverse range of mammals and *T. dionisii* which infects bats. The evolutionary relationships among kinetoplastids, as estimated by taxon-rich small subunit rRNA and glycosomal glyceraldehyde phosphate dehydrogenase (*gGAPDH*) sequence data, indicate *Trypanosoma cruzi* and *Leishmania* spp. are only distantly related and do not form a monophyletic group (Fig. 3.1.) (Hamilton *et al.*, 2007). Although it is possible that the ability to invade host cells arose before the *Trypanosoma* and *Leishmania* lineages diverged, this would imply that this trait was then subsequently lost numerous times independently. This evolutionary relationship, in conjunction with the distinctions between *T. cruzi* and *Leishmania* as regards to the types of cells invaded, the method of entry into host cells and the means by which they survive the harsh environment of the phagolysosome, suggests that the ability to invade vertebrate host cells arose at least twice in the evolutionary history of the trypanosomatids (Fig. 3.22.). The different axoneme arrangements observed here in species representative of these two groups, *T. cruzi* and *L. mexicana,* adds further weight to this hypothesis. It would be interesting, therefore, to

investigate the axoneme structure of additional species from each clade. Determination of the axoneme structure of *L. major*, for example, would enable the comparison of flagellar structure between species. *L. major* is an example of an Old World Species that resides in small, individual type I parasitophorous vacuoles (Blank *et al.*, 1993). In contrast, *L. mexicana* resides in large, communal type II vacuoles, as is typical of New World Species. The intimate association between the tip of the *L. mexicana* flagellum and the macrophage vacuole membrane observed in this study may not be present in all species nor both types of vacuole.

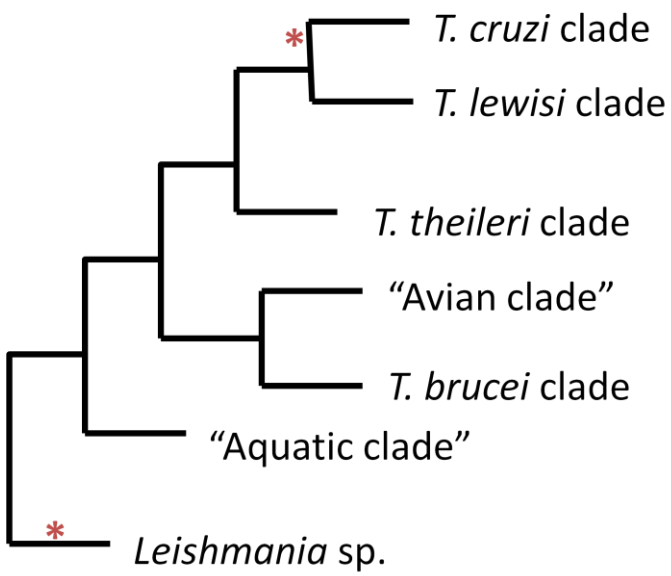


**Figure 3.22. Occurrence of intracellular amastigote forms in trypanosomes.** Asterisks mark the proposed independent appearances of intracellular invasion during evolution. Phylogeny based on *gGAPDH* sequence data rooted using non-trypanosome trypanosomatids (Hamilton *et al.*, 2007).

The existence of intracellular forms in other taxa, however, cannot be excluded. The majority of in-depth studies focus on taxa infecting humans or domestic animals and knowledge of some less-studied species is often limited to simple reports of their isolation. The intraerythrocytic forms of *Endotrypanum* (reclassified by some as *Leishmania* sp.), for example, have only been seen in fresh blood samples from wild sloths and have never been

identified inside erythrocytes in experimental infections (Cupolillo *et al.*, 2000). Even more intriguing, however, is that the occurrence of known intracellular forms appears restricted to mammalian trypanosomes. Although this could be an artefact of biased investigations skewed towards these parasites, it is probable that intracellular replication evolved as an evasion strategy to circumvent the mammalian immune system. Assuming the "invertebrate first" hypothesis of trypanosome evolution, the transition to digenetic parasitism and the subsequent adaption to a vertebrate secondary host is likely to have occurred multiple times in evolutionary history (Kerr, 2006), possibly after transmission from a blood-sucking insect during feeding (Simpson *et al.*, 2006). Interestingly, rounded forms without a free flagellum have been described in the visceral capillaries of hosts of *T. lewisi*, *T. zapi*, *T. nabiasi* and *T. microti* and T*. musculi* (Deane, 1969), all members of the *T. lewisi* clade (Fig. 3.1. and Table 3.1.). Although not intracellular *per se*, this reproductive phase is a common occurrence among species of the *T. lewisi* group of trypanosomes and could have preceded the adaptation of *T. cruzi* to intracellular multiplication. A certain protection may have been provided in the lumen of visceral capillaries and later, as in *T. cruzi*-like species such as *T. dionissii*, the capillary endothelial cells and eventually other cells.

# Chapter 4: Divergent basal body structures between unicellular and multicellular eukaryotes

## 4.1 Aims and objectives of this chapter

Comparisons of flagellar proteomes have revealed that the basal body and axoneme structure of eukaryotes is dependent upon a set of conserved proteins along with lineage-specific elaborations. These additional structures, such as pro-basal bodies and microtubule rootlets, vary widely in their presence or absence and in their structure among taxa, and among cell types in multicellular organisms. Traditionally, the diversity of these components among clades provided a set of characters important in phylogenetic analyses. Choanoflagellates, for example, have extensive basal body appendages that provide support for their characteristic collar tentacles. Is this reflected by diversity in the underlying molecular components of the basal body and axoneme? An aim of this study will be to reveal both conserved and extraordinary characteristics of choanoflagellate flagella through comparisons of protein and species phylogeny.

The importance of choanoflagellates as the closest living relative of metazoans was first revealed by their striking similarity to choanocytes, the feeding cells of sponges. The basic cell morphology and feeding behaviour of all choanoflagellate species observed to date is, at least superficially, structurally and functionally similar to that of choanocytes. Although extensive phylogenetic analysis leaves little doubt that choanoflagellates are the closest known sister group of animals, to what extent are the underlying molecular components of the axoneme, basal body and associated flagellar appendages conserved between the choanoflagellates and choanocytes?

## 4.2 Introduction to choanoflagellates as a sister group of the Metazoa

Choanoflagellates, the closely known living relatives of animals, are a group of single-celled and colony-forming eukaryotes that inhabit a wide range of marine and freshwater environments. Choanoflagellate cells usually posses a single apical flagellum surrounded by a collar of microvilli tentacles (Fig. 4.5. and Fig. 4.8.). Movement of the flagella produces water currents that draw in bacteria onto the outer surface of the collar from where the bacteria are phagocytosed (Pettitt *et al.*, 2002).

The close relationship between choanoflagellates and animals was first postulated after observations of the close resemblance of choanoflagellates to a group of specialised feeding cells, choanocytes, which line the interior of sponges (James-Clark, 1867; Maldonado, 2004). Modern phylogenetic analysis have since confirmed that choanoflagellates are the closest known sister group of animals (Wainright *et al.*, 1993; Lang *et al.*, 2002; Steenkamp *et al.*, 2006; Ruiz-Trillo *et al.*, 2008; Carr *et al.*, 2008; King *et al.*, 2008). Study of the cell biology and genomes of choanoflagellates provides insights into metazoan ancestry and the origins of multicellularity in the animal lineage.

Sponges have always been considered to be the most ‘‘primitive’’ group of animals, as indicated by the old name Parazoa. They are multicellular but have a comparatively small number of cell types. All sponges have ciliated larvae and sessile adults with choanocytes situated in internal chambers. The few exceptions, such as the carnivorous *Asbestopluma*, are clearly specializations (Vacelet and Duport, 2004).

Intriguingly, some choanoflagellates are able to form multi-celled colonies as part of their life cycle. For example, cells within colonies of *Choanoeca perplexa*, previously known as *Proterospongia choanojuncta*, are attached via the pairing of collar micro-villi (Leadbeater, 1983). In other species, such as *Codosiga botrytis*, adjacent cells are connected by thin intercellular bridges (Hibberd, 1975). Some colonies have cells on branched stalks whereas in others the cells are held in a jelly-like matrix. Some colonies are spherical with the collars facing the surrounding environment but *Diaphanoeca sphaerica*, for example, has collars facing the lumen of the colony and resembles a free-swimming choanocyte chamber of a sponge (Nielsen, 2008). Bacterial strains that serve as prey for the choanoflagellates can induce the formation of colonies from a single cell (Fairclough *et al.*, 2010). The formation of colonies in *Salpingoeca rosetta* occurs as a result of incomplete cell division rather than the aggregation of individual cells, a process reminiscent of animal embryology (Dayel *et al*., 2011; Fairclough *et al.,* 2010).

### 4.2.1 A review of choanoflagellate ultrastructure with a focus on the flagellum

Choanoflagellates comprise an ovoid to spherical cell body with a single flagellum surrounded by a collar of actin-based micro-villi tentacles held out rigidly at the anterior end of the cell (Fig. 4.5.). In contrast to the uniform cell body, the morphology of an external covering, the periplast, is extremely varied ranging from simple organic sheaths, or thecas, to complex silica basket-like enclosures named loricas. Periplast morphology formed the basis of the initial classification of choanoflagellates into three families: the Codonosigidae (Kent, 1882) possessing a thin fibrillar coat; the Salpingoecidae (Kent, 1882), possessing a substantial microfibril-based theca; and the Acanthoecidae (Norris, 1965), with a distinctive

lorica construction. A more recent phylogenetic analysis, however, has rejected much of this traditional taxonomy (Carr *et al.*, 2008). The species examined, which included every choanoflagellate species available in culture, fell into one of three well-defined clades (Fig. 4.1.), only one of which, clade 3, corresponds to a traditional taxon, the Acanthoecida, consisting entirely of species that possess a silica-based lorica. The other two clades are both a mixture of thecate and non-thecate taxa with both clades including examples of colony-forming species. In addition, the genera *Monosiga*, *Salpingoeca* and *Stephanoeca* are not monophyletic groups. Elaborations of this revised taxonomy recently divided Choanoflagellata into two orders: Craspedida and Acanthoecida (Nitsche *et al.*, 2011).

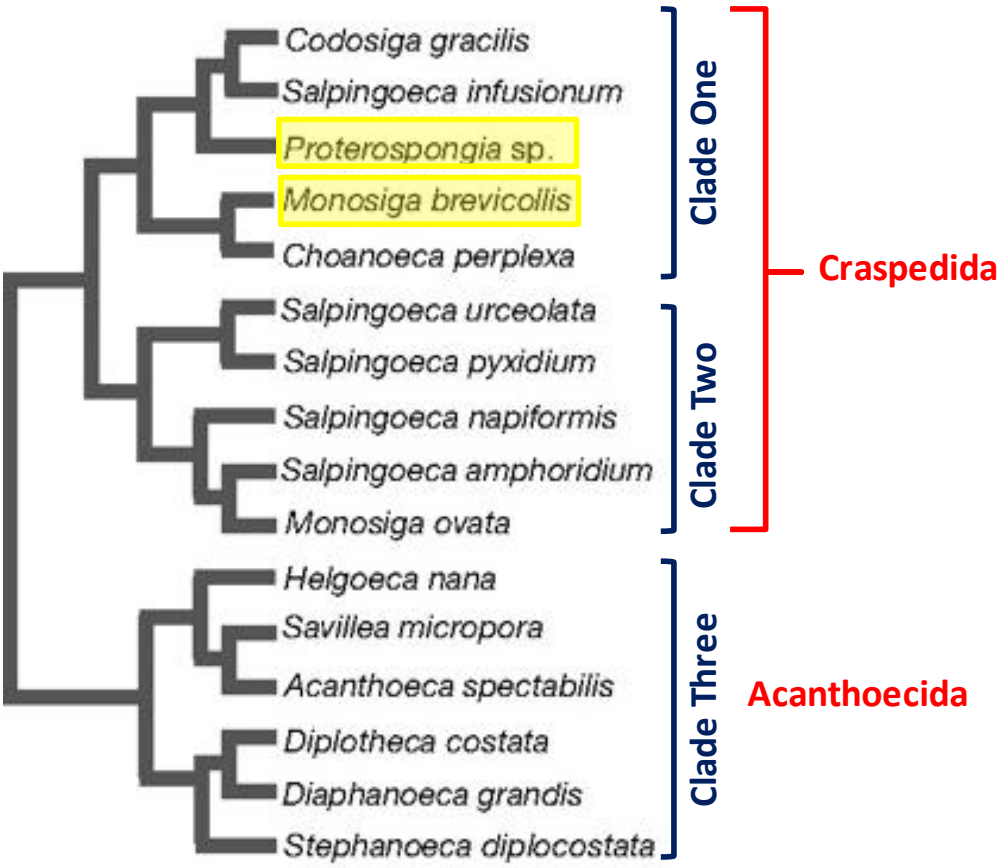


**Figure 4.1. Molecular phylogeny of choanoflagellates.** This phylogeny of 16 choanoflagellate species is based on a concatenated four-gene data set (Carr *et al.*, 2008) and later supported by a successive 29 taxon, multigene phylogeny (Nitsche *et al.*, 2011) that proposed the division of choanoflagellates into two orders. This sampling of choanoflagellate species includes most of those available in culture and represents a broad sample of morphological diversity. Highlighted species represent those choanoflagellates for which genome-sequencing projects have been completed. *Proterospongia* sp. ATCC50818, included in this phylogeny, has been renamed *Salpingoeca rosetta* with "Proterospongia" no longer considered a valid genus. The term is now used to refer to the colonial stage in the life histories of certain choanoflagellates. After Carr *et al.* (2008).

As previously discussed, the 9+2 axonemal structure of flagella and the triplet configuration of basal bodies is ancestral and are considered to have been present in the last common ancestor of eukaryotes. Other characteristic components of the cytoskeleton associated with the flagella, namely microtubule rootlets, also occur almost universally across eukaryotes and, whilst they are believed to fulfil a variety of functions, are often considered

to be homologous (Moestrup, 2000). Individual flagella of many taxonomic groups possess a maximum of two microtubule rootlets, attached to opposite sides of the basal body. The presence of only a single root per flagellum is also relatively common but more than two roots is extremely unusual (Moestrup, 2000). One notable exception to this rule includes the kinetoplastid flagellates, a group that includes the trypanosomatids. Investigations of the *Trypanosoma congolense* flagellar apparatus, for example, revealed four microtubule rootlets (Vickerman, 1969). A second, more notable exception, are the choanoflagellates.

Ultrastructural observations on a number of choanoflagellate species including *Monosiga ovata* (Leadbeater, 1972; Karpov, 1980; Karpov, 1982; Karpov and Leadbeater, 1997), *Kentrosiga thienemanni* (Karpov, 1985), *Codonosiga botrytis* (Hibberd, 1975), *Sphaeroeca volvox* (Karpov, 1981), *Choanoeca perplexa* (Leadbeater, 1977), *Proterospongia choanojuncta* (Leadbeater, 1983) and *Stephanoeca diplocostata* (Leadbeater, 1987) have shown that the main cytoskeletal elements of choanoflagellates are the flagellar apparatus, the microtubule rootlets and the collar tentacles. A non-flagellar pro-basal body lies at approximately right-angles to the flagellar basal body. The flagellar basal body has an extensive rootlet system of radial microtubules that support the anterior end of the cell. These microtubule rootlets, as they radiate outwards from the flagellar basal body, pass close to the microfilament bundles which form the bases of the tentacles (Karpov and Leadbeater, 1998). In most instances, each bundle of microfilaments is located approximately halfway between neighbouring radial microtubules. There are approximately twice the number of radial microtubules than there are tentacles. The collar consists of approximately 15 to 45 microvilli tentacles depending on the species (Leadbeater, 1972; Hibberd, 1975; Karpov and Leadbeater, 1998) and the number for a particular species can

vary by up to five microvilli (Leadbeater, 1972). Differences observed between species therefore concern the number of tentacles composing the collar and the number and arrangement of the microtubule rootlets (Hibberd, 1975; Karpov, 1981; Leadbeater, 1987; Karpov and Leadbeater, 1998). Each microvilli tentacle, approximately 200nm in diameter, is bound by a single membrane and contains electron dense staining material without any trace of microtubules (Leadbeater, 1972).

### 4.2.2 Choanoflagellate and choanocyte structure, a comparison from the literature

The close evolutionary relationship between choanoflagellates and sponges (Porifera) was first postulated on the basis of the similarity in morphology between choanoflagellates and choanocytes. More recently, electron microscope studies of the ultrastructure of choanocytes have revealed finer details of their cytoskeleton and basal body apparatus. A comparison with what is currently known about choanoflagellate cell structure, in particular the cytoskeleton, may indicate several differences in detail between the two groups.

The choanocyte axoneme has a typical 9+2 microtubule organisation. The pro-basal body is not perpendicular to the flagellar basal body but lies at approximately 45° relative to the longest axis of the flagellar basal body (Gonobobleva and Maldonado, 2009). In a minority of species, the pro-basal body is entirely absent (Woollacott and Pinto, 1995) but without a discernible overall phylogenetic pattern. This is in stark contrast with evidence from other metazoans in which a pro-basal body is consistently observed in all flagellated cells (Nielsen, 1987; Woollacott and Pinto, 1995).

The collar consists of approximately 25 to 45 microvilli, the exact number depending on the species, which arise from the distal-lateral “neck” area of the cell (Watanabe, 1978; Vacelet *et al.*, 1989; Gonobobleva and Maldonado, 2009). Exact counts of the number of microvilli tentacles are hindered, however, by the close adherence of adjacent choanocytes. Cross-sections through the collar depict microfibrils connecting adjacent microvilli in individual choanocytes (Fjerdingstad, 1961a) but there are no descriptions of similar connecting fibres in choanoflagellates.

Unlike choanoflagellates, the choanocyte flagellum emerges from the cell surface at the bottom of a cavity formed by an irregular, ring-like protrusion of the cell surface, a periflagellar sleeve, which encloses the base of the axoneme (Woollacott and Pinto, 1995; Gonobobleva and Maldonado, 2009). Although a short system of striated fibrous rootlets arise from the proximal edge of the basal body and run longitudinally to contact the nuclear apex, these are not to be confused with microtubule rootlets. Fibrous rootlets, also present in choanoflagellates (Karpov and Leadbeater, 1998) are heterogenous in comparison to microtubule rootlets with distinguishable composition and characteristics (Andersen *et al.*, 1991). The fibrous rootlets observed in both choanoflagellates and choanocytes extend deep into the cell cytoplasm whilst the microtubule rootlets, described only in choanoflagellates, extend laterally along the cell, close to the cell membrane. In ultrastructure studies completed to date, there is no description of an extensive microtubule rootlet system in choanocytes, nor is it visible on electron micrographs available in publications (Woollacott and Pinto, 1995; Boury-Esnault *et al.*, 1999; Maldonado, 2004; Gonobobleva and Maldonado, 2009). In some larvae of the class Demospongiae, namely *Halichondria melanodocia* and *Haliclona tubifera*, microtubules

were observed associated with the flagella, but not in the extensive radial array consistently observed in choanoflagellates (Woollacott and Pinto, 1995). These microtubules transverse the cytoplasm from the basal body to one side of the cell only.

## 4.3 Results

### 4.3.1 Identification of *Monosiga* and *Amphimedon* axoneme and basal body proteins

Representative genes encoding axoneme proteins were searched for in the *Monosiga brevicollis* and *Amphimedon queenslandica* proteomes (for a full description of methodology, see Materials and Methods). The genes selected included:

i. the central-pair protein PF16, a polypeptide of the C1 microtubule that is essential for flagellum motility in *Chlamydomonas* (Smith and Lefebvre, 1996), *Trypanosoma brucei* (Branche, 2006) and mouse (Sapiro *et al.*, 2002).
ii. PF20, another representative of the central-pair complex that localizes to the bridge between the two singlet microtubules (Smith and Lefebvre, 1997).
iii. RSP3, a protein of the radial spokes; interference leads to complete spoke disruption in *Chlamydomonas* (Williams *et al.*, 1989) and *T. brucei* (Branche, 2006).
iv. intermediate chain protein DNAI1; representative of the outer dynein arm components (Wilkerson *et al.*, 1995).
v. LC1, a light chain component of outer dynein arms required for stable dynein assembly and forward motility in *T. brucei* (Baron *et al.*, 2007).
vi. Trypanin, a subunit of the dynein regulation complex (DRC). This DRC subunit has shown to be required for normal motility in African trypanosomes with knock-down mutants that, although in possession of an actively beating flagellum, are unable to coordinate flagellar beat for productive motion (Hutchings *et al.*, 2002). Trypanin homologues in *Chlamydomonas* (Rupp and Porter, 2003)and zebra fish (Colantonio *et al.*, 2009) are also involved in controlling ciliary beat.
vii. α- and β- tubulin, the major constituents of outer doublet and central pair microtubules.

viii. γ-tubulin, required for microtubule nucleation (Stearns and Kirschner, 1994).

ix. δ- tubulin, required for the formation of the triplet basal body arrangement; gene disruption in *Chlamydomonas* results in a doublet rather than triplet arrangement (Dutcher and Trabuco, 1998).

x. ε-tubulin, required for the assembly of B- and C-tubules of basal bodies and cilium associated centrosomes (Chang and Stearns, 2000).

Alignments of *M. brevicollis* predicted axoneme proteins with orthologues in *Chlamydomonas*, *Nematostella*, mouse and human show a significant conservation degree (supplementary material Table S4.1). Identity was 30-60% between *Nematostella* and *M. brevicollis* orthologues, with the exceptions of PF16 and the α-, β- and γ-tubulins which were all more than 70% identical.

### 4.3.2 Conservation of axoneme and basal body proteins in Monosiga

Incongruity between protein and species phylogenies, including markedly long-branch lengths, may indicate a loss- or change-of-function divergence due to relaxed functional constraints. For most axoneme proteins examined (PFF16, RSP3, Trypanin, DNAI1, LC1 and α-, β-, γ- and ε-tubulins) the protein phylogeny reflects accepted hypotheses for species phylogeny. In these instances, metazoan sequences of a particular protein constitute a monophyletic group which also includes the putative protein identified in the *M. brevicollis* genome. Fig. 4.2., for example, shows the maximum-likelihood (ML) tree derived from eukaryotic γ-tubulin protein sequences. For the *M. brevicollis* axoneme protein sequences that cluster with their metazoan counterparts, they do so with consistently high bootstrap support values (>80%) with the exception of PF16. The grouping of the putative PF16 protein identified in *M. brevicollis* with metazoan PF16 homologues is poorly supported

(25% bootstrap support). This is despite the high percentage identity (65.5%) between the PF16 proteins of human and *M. brevicollis* (Table 4.1.).

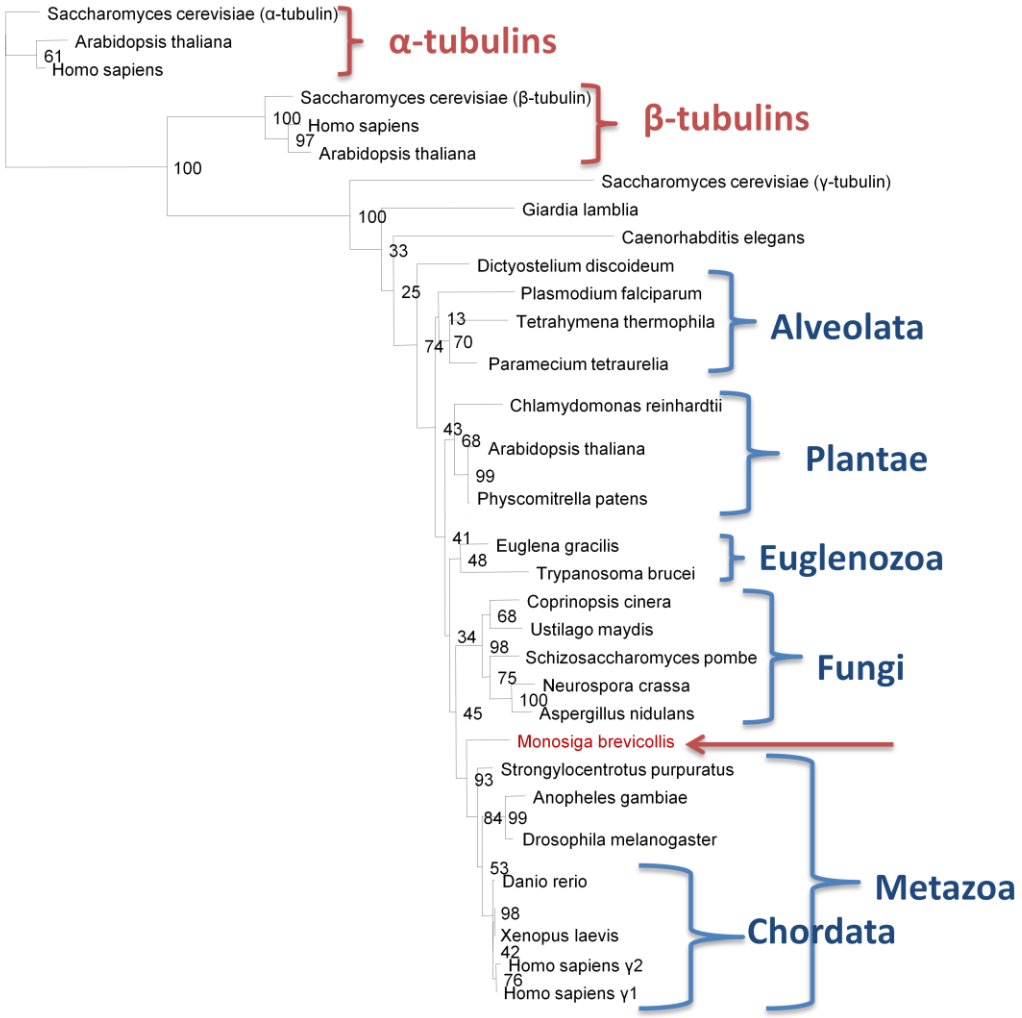


**Figure 4.2. Maximum-likelihood (ML) γ-tubulin protein tree**. Constructed using an alignment of 415 characters and rooted using α-tubulins. Single values at nodes represent ML bootstrap support values. The *M. brevicollis* γ-tubulin protein sequence (arrow) clusters with its metazoan counterparts.

| Protein | % Identity |
|---|---|
| **PF16** | 66.5 |
| **PF20** | 26.7 |
| **DNAI1** | 44.6 |
| **RSP3** | 23.9 |
| **LC1** | 51.5 |
| **Trypanin** | 49.3 |
| **α-tubulin** | 92.9 |
| **β-tubulin** | 94.8 |
| **γ-tubulin** | 74.4 |
| **δ-tubulin** | 33.5 |
| **ε-tubulin** | 51.3 |

**Table 4.1. Percentage of sequence identity between axoneme and basal body proteins from *Monosiga brevicollis* and human.** Alignment was performed using Clustal W.

Fig 4.3. shows the maximum-likelihood tree derived from eukaryotic protein δ-tubulin sequences (24 sequences, 406 aligned amino acid positions). Apparent phylogenetic relationships between eukaryotic δ-tubulin sequences do not reflect currently accepted hypotheses for organism relationships. The δ-tubulin sequence identified in the *M. brevicollis* proteome does not emerge as monophyletic group with the metazoan sequences but appears highly divergent with respect to the metazoan δ-tubulin proteins. The δ-tubulin sequence identified in the *A. queenslandica* genome, however, does emerge as a monophyletic group with other metazoan sequences.

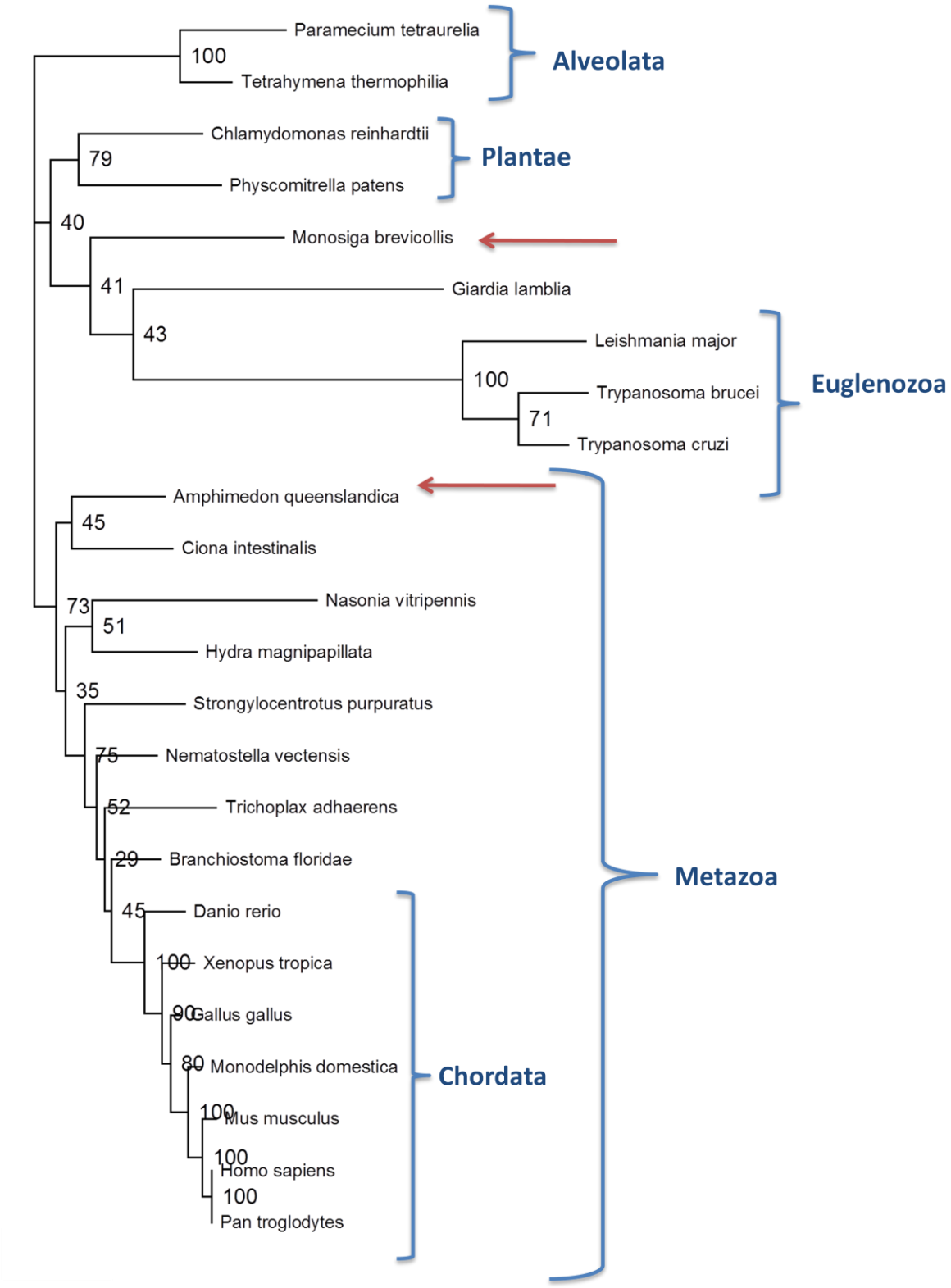


**Figure 4.3. Maximum-likelihood (ML) δ-tubulin protein tree.** Based on an alignment of 406 characters and rooted using non-metazoans. Single values at nodes represent ML bootstrap support values. The *Amphimedon queenslandica* δ-tubulin protein sequence clusters with its metazoan counterparts unlike the protein sequence identified in *Monosiga brevicollis* (arrows).

The Maximum-likelihood tree derived from eukaryotic PF20 sequences (26 sequences, 402 aligned amino acid positions) also exhibits an incongruity between protein and species phylogeny (Fig. 4.4). As was the case for δ-tubulin, the PF20 sequence identified in the *M. brevicollis* proteome does not emerge as monophyletic group with the metazoan sequences but appears highly divergent with respect to the metazoan PF20 protein sequences. Interestingly, an orthologue of PF20 was not detected in *A. queenslandica* in this analysis. It is not possible, however, to discriminate between proteins that have been lost entirely from a lineage, those that have diverged in sequence to such an extent that they are undetectable and those that are not detected due to incomplete genome coverage. The exact phylogenetic placement of the *M. brevicollis* PF20 and δ-tubulin sequences could also be complicated by long-branch attraction, a common cause of errors with respect to the placement of divergent sequences.

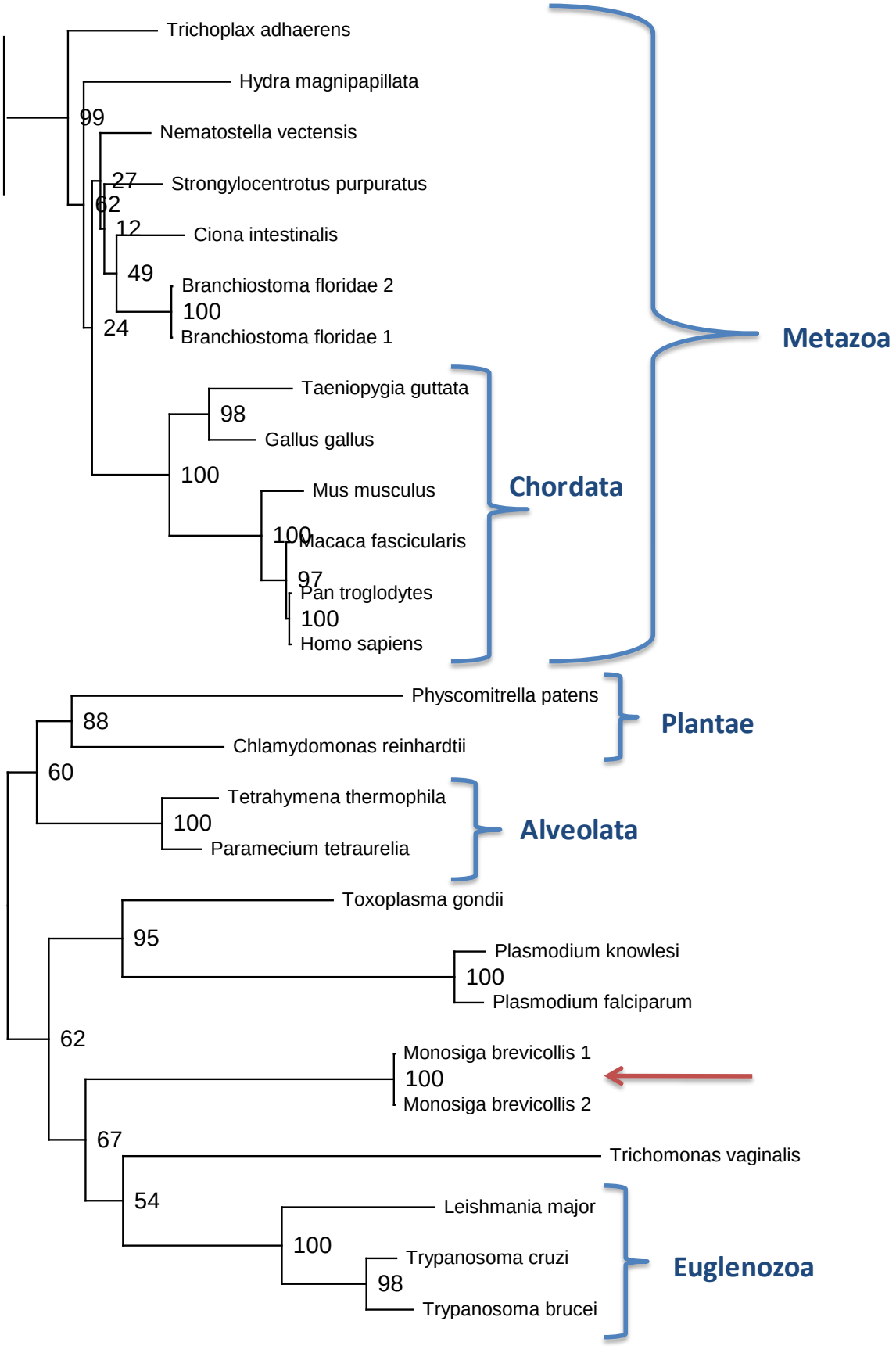


**Figure 4.4. Maximum-likelihood (ML) PF20 protein tree.** Constructed using an alignment of 402 characters and rooted using non-metazoans. Single values at nodes represent ML

bootstrap support values. The *Monosiga brevicollis* PF20 protein sequence (arrow) does not cluster with its metazoan counterparts.

### 4.3.3 Light, immunofluorescence and scanning electron microscopy

#### *Choanoflagellates*

Four species of choanoflagellate were examined: *Monosiga brevicollis*, *Monosiga ovata*, *Stephanoeca diplocostata,* and *Diaphanoeca grandis.* These four species provide representation for each of three clades defined in recent phylogenetic analyses (Fig. 4.1.) (Carr *et al.*, 2008; Nitsche *et al.*, 2011). *Monosiga brevicollis* and *Monosiga ovata* represent the two clades of the newly proposed Craspedida order; species within this order do not typically construct a lorica. *Stephanoeca diplocostata* and *Diaphanoeca grandis* both represent the third clade and second order, Acanthoecida, of which individual cells usually possess a lorica. Note that the genera *Monosiga* and *Stephanoeca* are not monophyletic groups.

The size and shape of the cell body varies between species. The ovoid cell bodies of *Monosiga ovata* and *Monosiga brevicollis* are approximately 4µm long and 2µm wide. The width of the cell body tapers towards the anterior (flagella) end of the cell (Fig. 4.5.). The cells possess single flagella of approximately 6µm in length. The larger cell body of *Diaphanoeca grandis* is comparatively more spherical with a cell length of up to 10µm and flagella of approximately 15µm in length. *Stephanoeca diplocostata* is intermediate in size and shape with a cell length of approximately 6µm and width of 5µm and a single flagellum 8µm in length.

For all species examined the flagellar basal body is surrounded by a considerable number of radial microtubules rootlets comprised, at least in part, of α-tubulin (Fig. 4.6. and Fig. 4.7.). From the flagellar base these microtubules pass outwards and laterally for almost the entire length of the cell. Although it is impossible to determine the number of individual microtubules through immunofluorescence, it is evident that these are considerable in number in every species examined. The density of the microtubule rootlets obscured any observation of the flagellar basal body in most cells.

The size and extent of the microtubule rootlet system, appears to vary between species. Staining of α-tubulin in microtubules rootlets was considerably less extensive in *Stephanoeca diplocostata* and it was possible to identify the flagellar basal body not obscured by an extensive microtubule rootlet array (Fig. 4.7.4b).

The single flagellum is surrounded by a funnel-shaped collar, approximately 4μm long, which originates from the side of the cell, slightly before the anterior end. The collar narrows from a diameter of 150-200ηm to 100-125ηm at the point of attachment to the cell (Fig. 4.5.) Labelling with Bodipy 505 FL Phallacidin confirmed that the microvilli tentacles are actin-based (Fig. 4.13.). It is possible to identify bundles of actin within individual collar tentacles. SEM images show discrete microfibrils connecting individual microvilli (Fig. 4.8.).

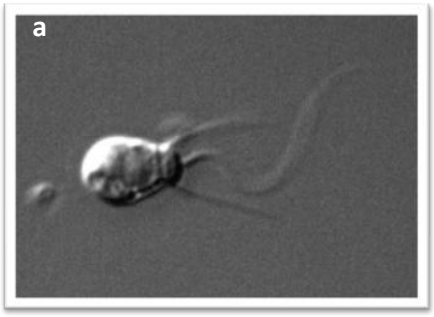


**Figure 4.5. Light microscopy images of live choanoflagellates.** The single flagellum is surrounded by a funnel-shaped collar which originates from the side of the cell, slightly before the anterior end. The nucleus is also visible. **(a)** *Salpingoeca rosetta.* **(b)** and **(c)** a single cell of *Monosiga brevicollis* in two planes of focus. Magnification x100.

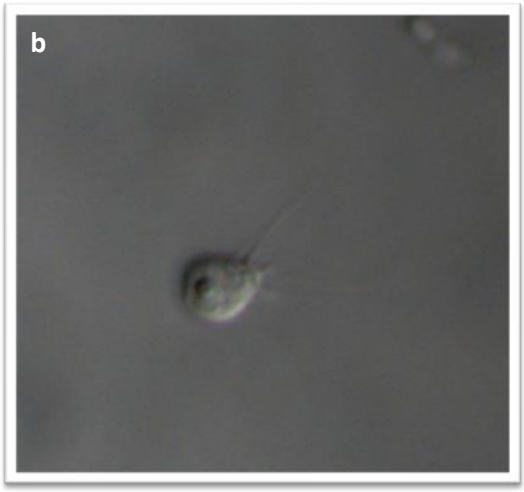


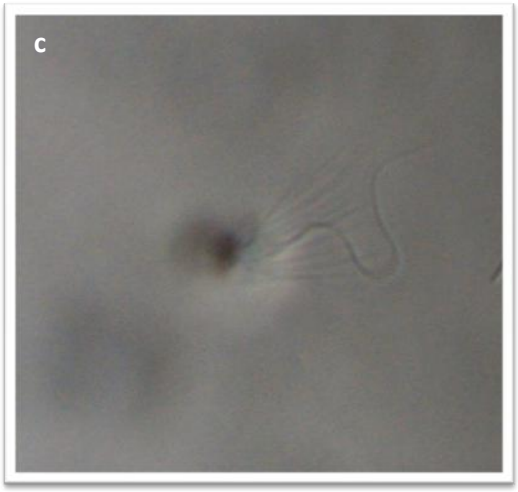


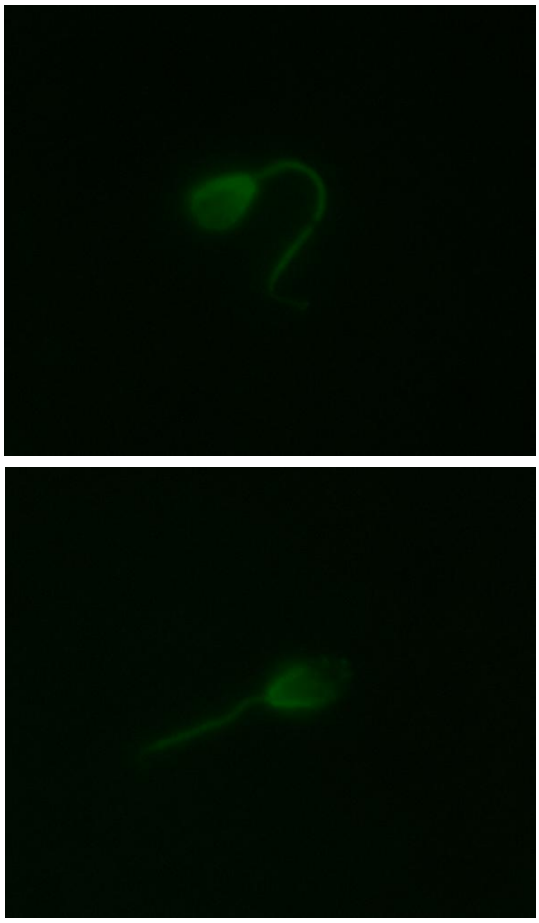

**Figure 4.6. Immunofluoresence localisation of alpha-tubulin in *Monosiga brevicollis*.** The extensive microtubular cytoskeleton shown here is noticeably absent in choanocytes (Fig. 4.11.). Cells were stained with anti-α-tubulin antibodies (green).

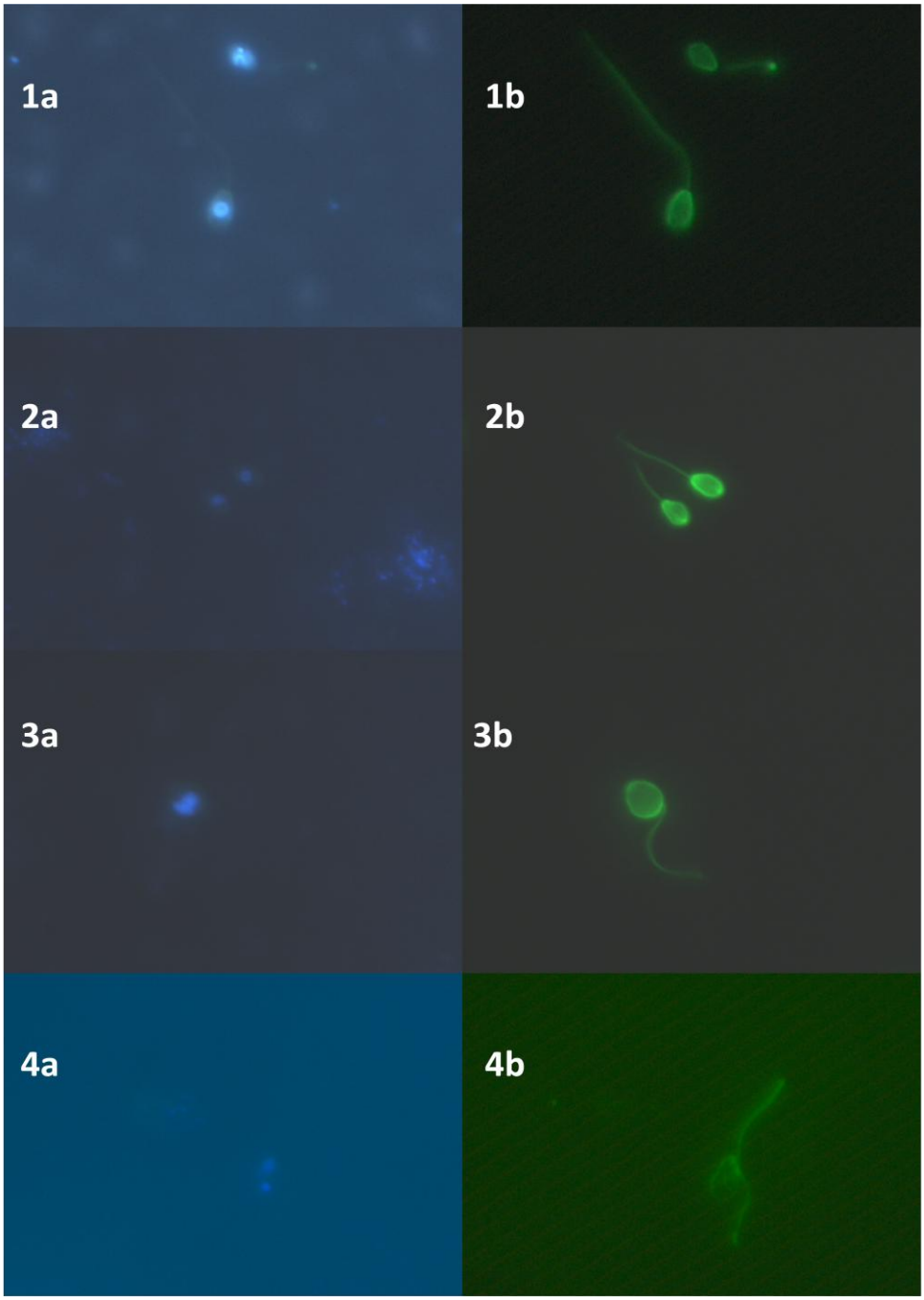


**Figure 4.7. Immunofluorescence localisation of alpha-tubulin in choanoflagellates.** The extensive microtubular cytoskeleton shown here is noticeably absent in choanocytes (Fig. 4.11.). Cells were stained with anti-α-tubulin antibodies (**b**; green) and DAPI (**a**; blue) to indicate the location of the nucleus through staining of the DNA content. 1. *Monosiga brevicollis.* 2. *Monosiga ovata.* 3. *Diaphanoeca grandis.* 4. *Stephanoeca diplocostata.*

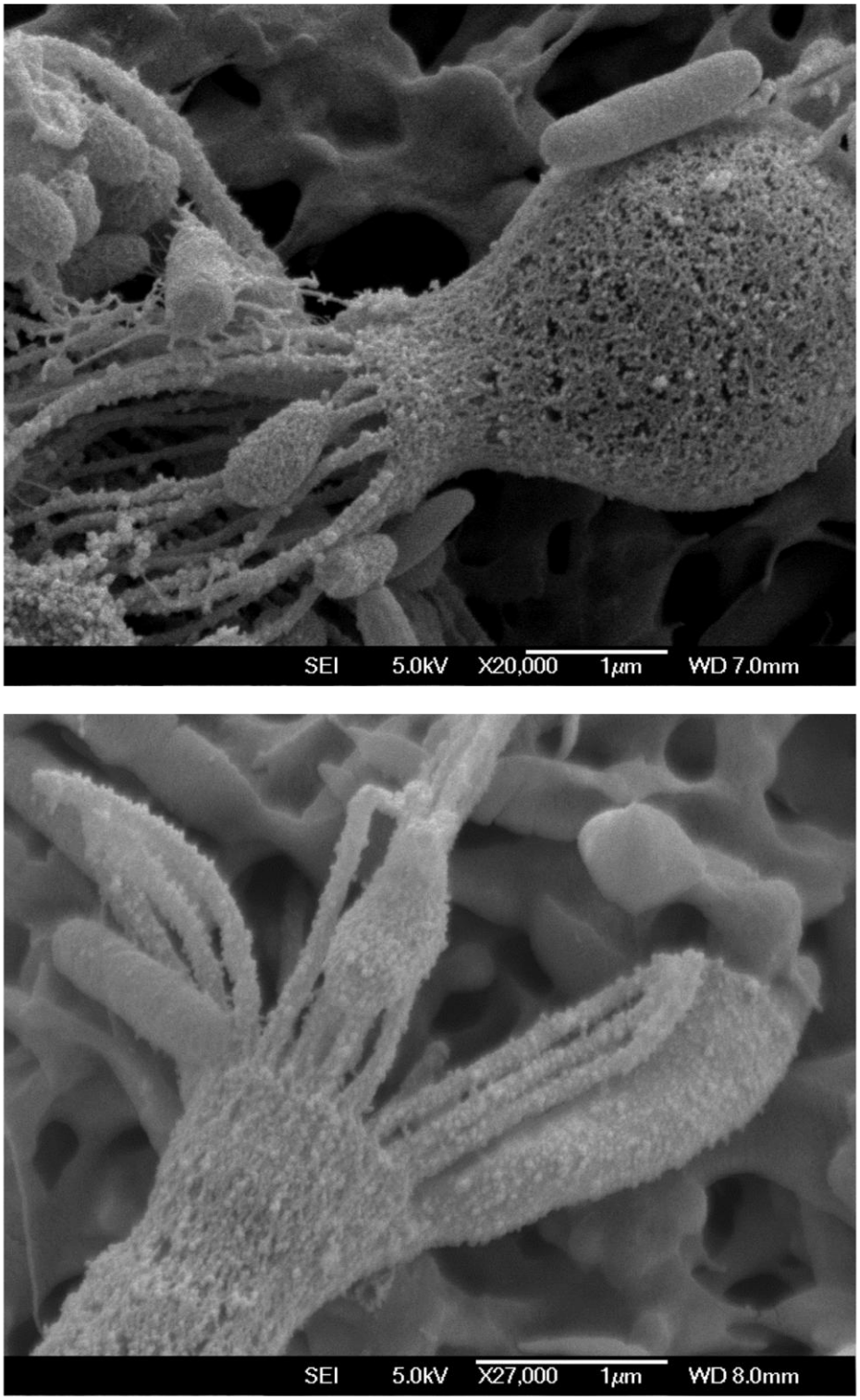


**Figure 4.8. Scanning electron microscope images of *Monosiga brevicollis*.** Discrete microfibrils connecting individual collar microvilli tentacles are visible. Magnification x 20,000; scale bar represents 1µm. Cells prepared by AES. SEM image by S. Leys.

### *Choanocytes*

Choanocytes were extremely difficult to isolate from neighbouring cells of the underlying mesophyl of the developing choanocyte chamber. Special undefined junctions and interdigitations between adjacent choanocytes provide a complex sealing system for the choanoderm leaving cells so tightly juxtaposed that the intercellular spaces can be as narrow as 12nm (Gonobobleva and Maldonado, 2009). The small size and transparency of juvenile *Ephydatia mulleri*, developing from asexual gemmules, did allow the identification and observation of a very small number of choanocytes on the periphery of the gemmules (Fig. 4.9. and Fig. 4.10.).

The cell bodies of *E. mulleri* choanocytes are approximately spherical (width 2.61µm; length 2.17µm) (Fig.4.11.). The single flagellum, of length between 10 and 15µm, is surrounded by a collar, 9 to 10µm in length that encloses and continues for approximately two-thirds the length of the flagellum. The collar width, 2 to 3µm, is typically uniform along its entire length, an almost perfect cylinder (Fig. 4.11.). Labelling with Bodipy 505 FL Phallacidin confirmed that the microvilli tentacles are actin-based.

Alpha-tubulin is localized in the flagella but noticeably absent from the cell body (Fig. 4.11.). This is in contrast to the extensive microtubular cytoskeleton observed in another type of sponge cell, pinacocytes found on the sponge epidermis (Fig. 4.12.).

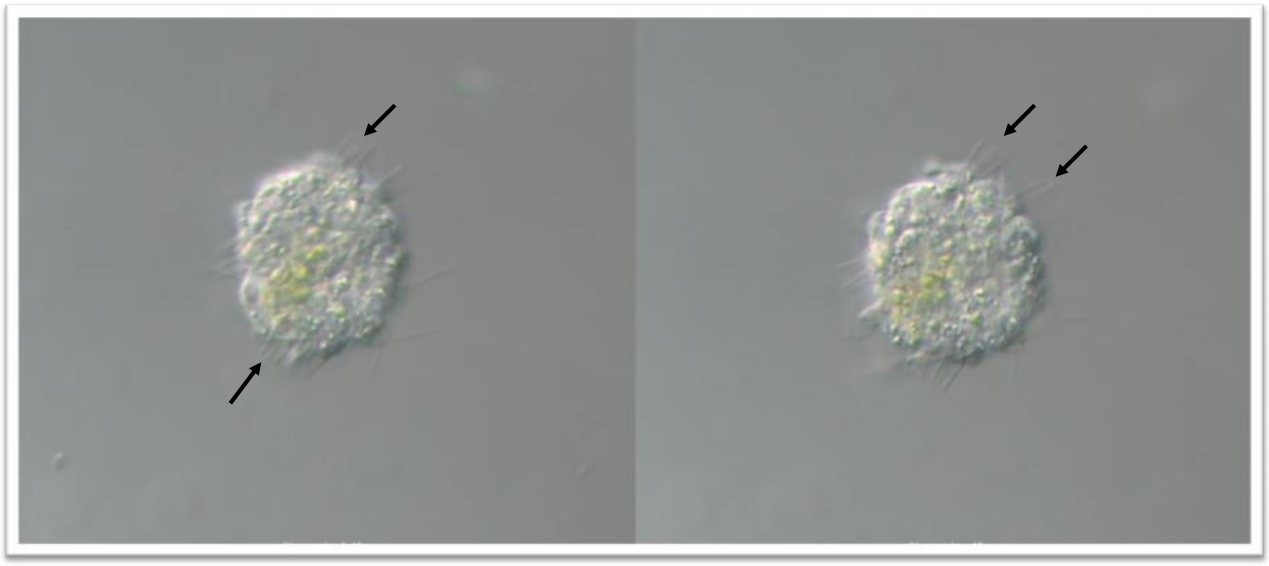

**Figure 4.9. Light microscopy images of juvenile *Ephydatia mulleri* developing from asexual gemmules.** A small number of choanocytes with straight, rigid collars and a single flagellum are visible on the periphery of the gemmules. Arrows indicate choanocyte flagella. Magnification x40.

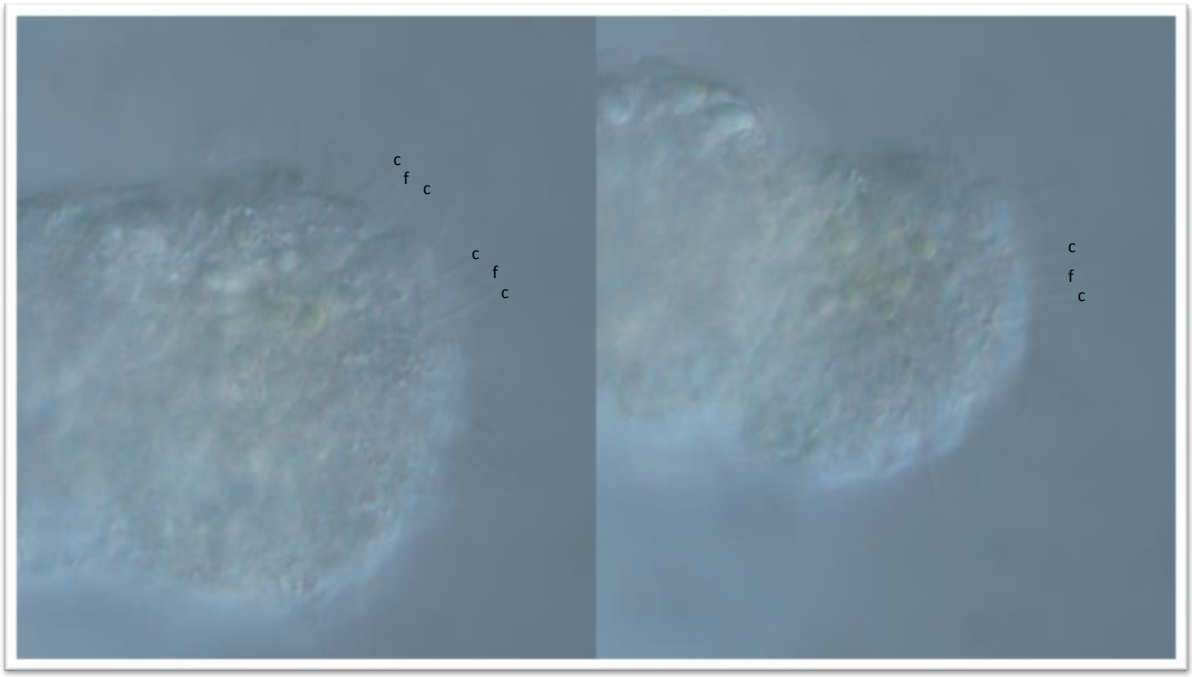


**Figure 4.10. Light microscopy images of juvenile *Ephydatia mulleri* developing from asexual gemmules.** A small number of choanocytes with straight, rigid collars and a single flagellum are visible on the periphery of the gemmules. Abbreviations: f = flagella, c= collar. Magnification x100.

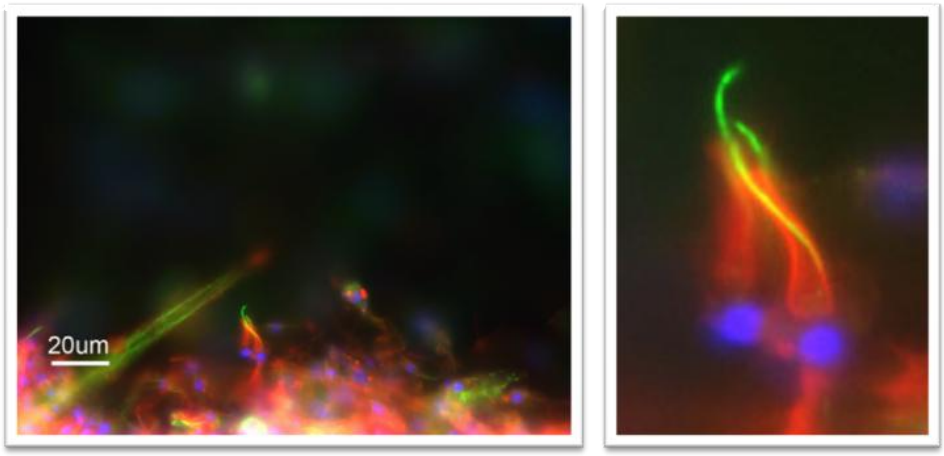


**Figure 4.11. The results of immunofluorescence on *Ephydatia mulleri*** using anti-α-tubulin antibodies (green), Alexa 594 Phalloidin (red) and DNA-binding dye (DAPI; blue). **(a)** Choanocytes with cylindrical actin-based collars and a single flagellum are visible on the periphery of the developing gemmule. Scale bar = 20µm. **(b)** A larger version of the same image. The extensive microtubular rootlet system present in choanoflagellates (Fig. 4.6.) is noticeably absent.

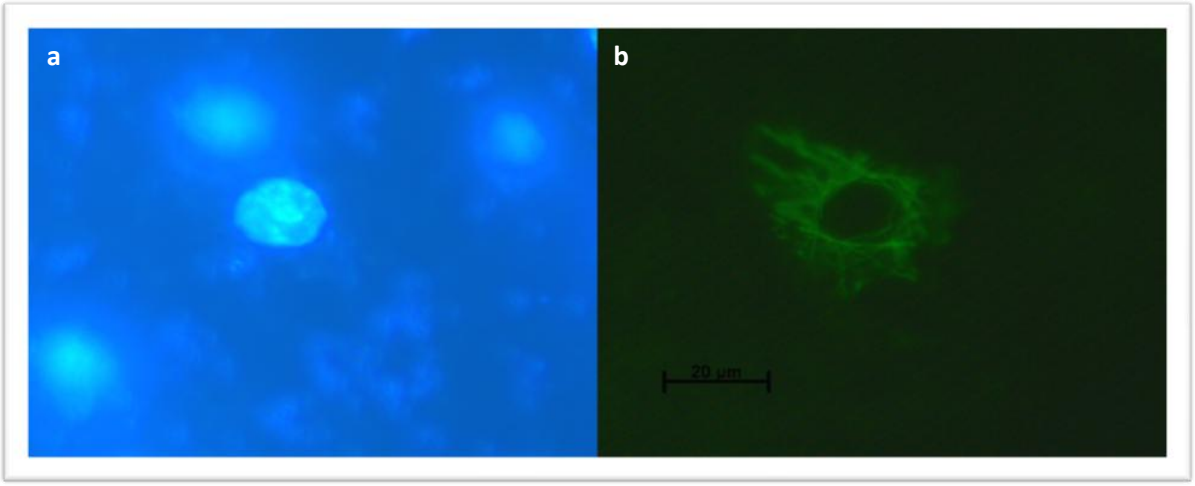


**Figure 4.12. Immunofluorescence localisation of alpha-tubulin in a pinacocyte cell of the developing sponge epidermis in a juvenile *Ephydatia mulleri* grown from an asexual gemmule.** The extensive microtubular cytoskeleton shown here is noticeably absent in choanocytes (Fig. 4.11). Pinacocyte cells contract and expand to help regulate water circulation through the sponge. Cells were stained with anti-α-tubulin antibodies (**b**; green) and DAPI (**c**; blue) to indicate the location of the nucleus through staining of the DNA content. Scale bar = 20µm.

### 4.3.4 Treatment of choanoflagellate cells with cytochalasin D

Cytochalasin D was used to disrupt the actin filaments of the microvilli tentacles of the collar in *Monosiga brevicollis* (experimental procedure detailed in Materials and Methods). Various incubation times and concentration of cytochalasin D were tested to disrupt the actin filaments and the effects were analyzed by double-labelling immunofluorescence microscopy.

An incubation time of 60 minutes and a cytochalasin D concentration of 1µM caused total disruption of actin filaments and disappearance of the collar tentacles (Fig. 4.13.1) As determined from the immunofluorescence signal, shorter incubation times and lower concentrations resulted in incomplete disruption of actin filaments in the collar region. The flagella, where present, appeared normal after treatment. The collar tentacles in untreated control cultures were unaffected (Fig. 4.13.4). After treatment with cytochalasin D, a high intensity immunofluorescence signal at the base of the flagella (Fig. 4.13.1c) suggests that the actin is retracted into the cell body.

The reversibility of cytochalasin D treatment was also investigated. In recovery experiments, cells were washed three times with fresh culture medium and incubated in the absence of cytochalasin D for various time periods before fixation (see legends of figure 4.13.). In the absence of cytochalasin D, cell exhibited a full reorganisation of the actin-based collar within 30 minutes of incubation (Fig. 4.13.3). Fixation after shorter recovery time periods revealed different stages in the re-growth of the collar tentacles. As the collar tentacles extend they do so in an approximately uniform manner; all tentacles appearing approximately the same

length at any point of fixation. Interestingly, in some instances it was possible to see individual bundles of actin filaments (Fig. 4.13.3c).

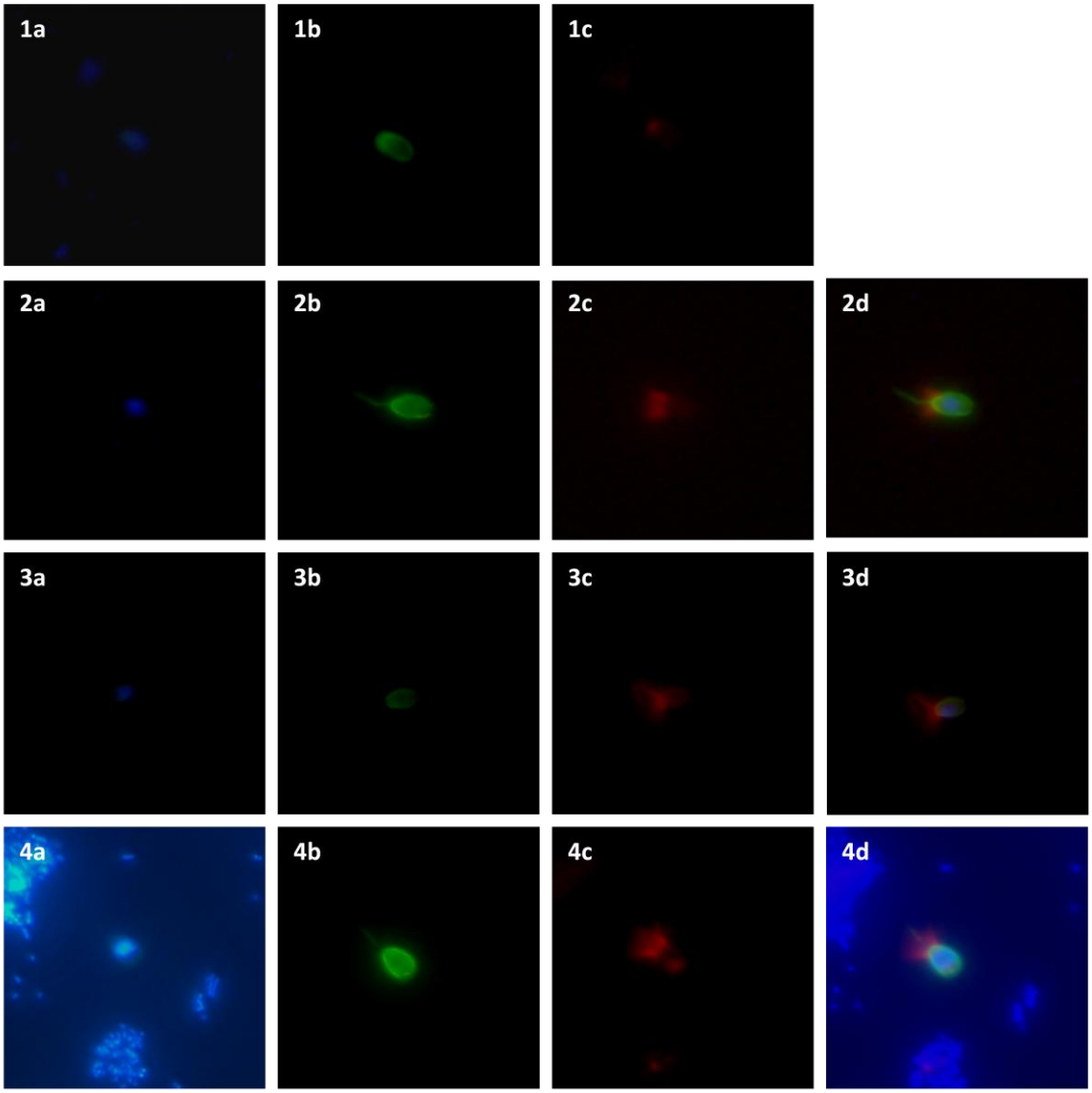


**Figure 4.13. Effect of cytochalasin D on the actin-based collar tentacles of *Monosiga brevicollis*. 1.** Cultures of *Monosiga brevicollis* were exposed to a cytochalasin D concentration of 1µM for 60min, fixed and stained. **2.** Recovery experiment in which treated cells were washed three times with fresh culture medium and incubated in the absence of cytochalasin D for 15 minutes. **3**. Recovery experiment in which treated cells were washed three times with fresh culture medium and incubated in the absence of cytochalasin D for 30 minutes. **4.** Control of untreated culture to which DMSO alone was added.

Cells were stained with DAPI DNA binding-dye (**a**; blue), anti-α-tubulin antibodies (**b**; green) and actin-binding Alexa 594 Phalloidin (**c**; red). The DNA content, α-tubulin and actin staining patterns are shown merged together to show relative positioning (**d**).

## 4.4 Discussion

### *The extensive microtubule rootlet system found in choanoflagellates is reflected in the divergence of underlying molecular components.*

The nine-fold triplet microtubule arrangement of basal bodies is widely conserved across eukaryotes including choanoflagellates. However, comparisons of published flagellar proteomes (Ostrowski *et al.*, 2002; Pazour *et al.*, 2005; Smith *et al.*, 2005) from a range of model organisms have revealed that, although the canonical axoneme and basal body structure is dependent upon a set of conserved proteins, there is a surprising amount of molecular diversity given the structural conservation (Broadhead, 2006). This suggests that the canonical axonemal structure is dependent on a central set of conserved proteins along with organism-, cell- and tissue-specific elaborations. In *M. brevicollis*, the ultrastructural consistency of the axoneme and basal body reflects the conservation of many of the underlying molecular components; proteins representative of key basal body and axoneme components (microtubules, dynein arms, radial spokes) are highly conserved. However, as this study has highlighted, there are several notable exceptions. δ-tubulin and a protein of the central-pair complex, PF20, are divergent in *M. brevicollis* compared to their metazoan counterparts.

In *Chlamydomonas*, disruption of the gene encoding δ-tubulin results in a doublet rather than triplet basal body arrangement due to a specific loss of the C-tubule (Fig. 4.14.) (Dutcher and Trabuco, 1998). This restriction to doublet basal bodies does not appear to have an effect on flagella motility. Knock-down of the δ-tubulin gene in *T. brucei* does result in a loss of flagella motility, however, with basal body structure similarly reduced to doublet microtubules (Gadelha *et al.*, 2006). In *Paramecium,* the C-tubule does not play a direct role

in ciliogenesis: axoneme structure and ciliary activity appears normal in δ-tubulin mutants (Garreau de Loubresse *et al.*, 2001). These gene expression studies highlight the probability that the primary function of δ-tubulin, and the C-tubule for which it is required, is not axoneme motility.

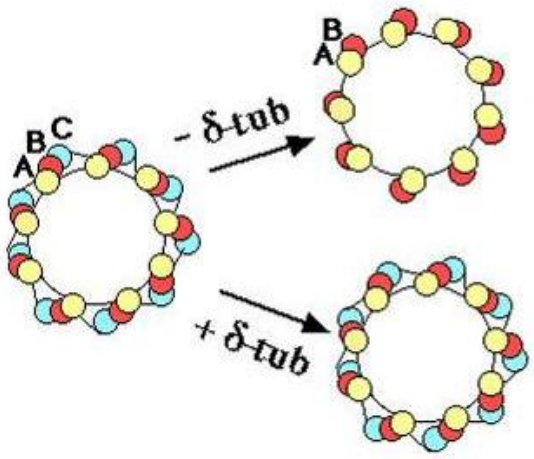


**Figure 4.14.** Disruption of the gene encoding δ-tubulin results in a doublet rather than triplet basal body arrangement due to a specific loss of the C-tubule. After Dutcher and Trabuco (1998).

In both *Paramecium* and *Chlamydomonas*, the C-tubule plays a role in the anchoring, development and positioning of basal body appendages (Garreau de Loubresse *et al.*, 2001). All choanoflagellate species examined, representing each of the three phylogenetic clades, possess an extensive microtubule rootlet system originating from the flagella base. With the magnification and resolution of light microscopy, it was not possible to count the number of individual microtubules. A previous electron microscopy study of *Codosiga botrytis*, however, estimated the presence of between 120-200 microtubule rootlets (Hibberd, 1975). Regardless, it is evident that all species of choanoflagellates examined posses a much greater number of microtubule rootlets than the usual one or two found in most eukaryotes

(Moestrup, 2000). These radiating microtubules extend out under the cell surface and provide support for the collar tentacles that are characteristic of choanoflagellates (Karpov and Leadbeater, 1998). Indeed, there are approximately the same number of microtubule rootlets as there are collar tentacles (Leadbeater, 1994). It is probable, therefore, that this extensive microtubule rootlet system, a specialisation of choanoflagellates, developed in connection with the formation of the collar tentacles and that the emergence of this unusual microtubular system was associated with the evolution of divergent δ-tubulin in *M. brevicollis*.

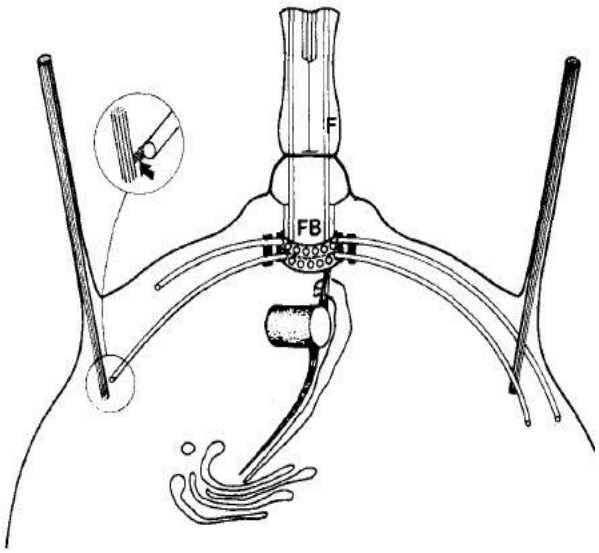


**Figure 4.15. Structural association of the basal body, microtubule rootlets and microvilli collar tentacles in choanoflagellates.** Diagram of the anterior portion of a choanoflagellate cell based on *Monosiga ovata* and *Desmarella moniliformis* showing the arrangement of the flagellar basal body (FB) and the associated cytoskeleton. Arrow (inset) shows the fibrillar connection between the microtubules and tentacle microfilaments of the collar. After Karpov and Leadbeater (1998).

### *Differences in the detail: the central pair of choanoflagellates and choanocytes*

A protein of the central-pair complex, PF20, is also divergent in *M. brevicollis* compared to its metazoan counterpart. PF20 localizes to the bridge between the two singlet microtubules

of the central-pair (Smith and Lefebvre, 1997). A second *M. brevicollis* protein of the central-pair complex, PF16, did group with metazoan PF16 but only with poor bootstrap support (25%). Interestingly, an orthologue of PF20 in *A. queenslandica* was not detected in this analysis. It is not possible, however, to discriminate between proteins that have been lost entirely from a lineage, those that have diverged in sequence to such an extent that they are undetectable and those that are not detected due to incomplete genome coverage.

Is there any unusual structural design in the central pair complex in choanoflagellates and sponges to reflect this underlying molecular divergence? Cross-sections of the flagellum in both choanoflagellates and choanocytes show the canonical 9+2 microtubule arrangement (Fjerdingstad, 1961a; Hibberd, 1975; Gonobobleva and Maldonado, 2009) but within the flagellar transition zone of choanoflagellates the central pair microtubules are replaced by a single central filament of considerable length (Karpov and Leadbeater, 1998). This central filament continues from just above the level of the cell body membrane for approximately 2µm. There are no reports of a similar central filament in choanocytes with the transitional region between the axoneme and the cell body being relatively short (Woollacott and Pinto, 1995; Gonobobleva and Maldonado, 2009).

The central pair plays an important role in regulating axoneme motility: rotation of the asymmetrical pair apparatus is hypothesised to activate distinct sets of dyneins on the outer doublets via the radial spokes and a dynein regulation complex (DRC). *In vitro* studies with reactivated *Chlamydomonas* axonemes have demonstrated that the position of the C1 microtubule of the central pair correlates with the position of active dyneins (Wargo and Smith, 2003; Wargo *et al.*, 2004). Observations of other lineages, however, have revealed a

rotation constraint of the central pair microtubules with the central pair adopting a fixed orientation relative to the outer doublets. In wild-type trypanosomatids, for example, the orientation of the central pair is invariant with no central pair rotation, as demonstrated in this study for *Leishmania mexicana* (chapter 3, section 3.4.) and previously in *Trypanosoma brucei* (Gadelha *et al.*, 2006). The central pair also retains a fixed orientation relative to the outer microtubule doublets in metazoans, as demonstrated in human (Ralston and Hill, 2008), guinea pig (Fawcett, 1968), ctenophore (Tamm and Tamm, 1981), freshwater mussel (Gibbons, 1961; Satir, 1963) and sea urchin sperm (Sale, 1986) axonemes. In *Paramecium tetraurelia, Euglena gracilis* and *Chlamydomonas reinhardtii*, however, the central pair rotates within the axoneme (Melkonian *et al.*, 1982; Omoto *et al.*, 1999; Mitchell, 2003). It is not yet clear if the central pair rotates in choanoflagellates. Examination of the small number of available transmission electron micrographs showing cross-sections of choanoflagellate axonemes, however, all depict the two central pair microtubules as being equidistant from an outer doublet on which it is possible to draw a median line that bisects the two (Leadbeater, 1987, Hibberd, 1975), suggesting a fixed central pair orientation.

The molecular and structural differences regarding the central pair of choanoflagellates and choanocytes may explain the significant different in flagella movement between choanocytes and choanoflagellates. The flagellum movement of sponges is adapted to provide a more powerful pump than the choanoflagellate cell; 80-100 such pumps in a single chamber are needed to create the pressure to overcome the resistance of the extensive sponge canal system (Larsen and Riisgard, 1994).

### *Choanoflagellates and choanocytes: are the collar structures homologous?*

Given the importance of the microtubule rootlets in supporting the collar tentacles in choanoflagellates, it is surprising that no similar structure exists in sponge choanocytes. Immunofluorescence microscopy revealed no extensive microtubule system, as revealed by the restricted localisation of α-tubulin to the axoneme. In published literature there is no description of an extensive microtubule rootlet system in choanocytes, nor is it visible on electron micrographs available in publications (Woollacott and Pinto, 1995; Boury-Esnault *et al.*, 1999; Maldonado, 2004; Gonobobleva and Maldonado, 2009). This absence of a microtubule rootlet system is also reflected in the relative conservation of the underlying molecular components compared to *M. brevicollis*. The δ-tubulin sequence identified in the *A. queenslandica* genome is highly conserved with respect to other metazoans and does not display the divergence in sequence that is present in *M. brevicollis*.

The differences in how the collar is anchored to the cell body may help explain the difference in the shape and relative size of the collar itself. Choanoflagellates appear to have a shorter collar (4μm), approximately the same length of the cell body and covering one third the length of the flagella. The choanoflagellate collar is wide and flaring, with the collar wider apically than basally (150-200ηm to 100-125ηm), reflecting observations made previously of other choanoflagellate species (Fjerdingstad, 1961b; Leadbeater, 1983; Orme *et al.*, 2003). This wide, flaring collar is thought to be what allows relatively fast flow (14-30 $\mu m\ s^{-1}$) through the collar sieve (Fenchel, 1986; Larsen and Riisgård, 1994).

In contrast, choanocytes have long narrow collars. Water is estimated to flow through the sieve relatively slowly at 2-3 $\mu m\ s^{-1}$ (Reiswig, 1975; Riisgård et al., 1993). This narrow collar

may be necessary to fit all the cells into a chamber, and though the flow field around the collar is thought to differ from that around free living choanoflagellates, it is presumed that the alignment of collars and their possible touching at the tips ensures that flow passes through the collar openings (Larsen and Riisgard, 1994). That many choanocytes are arranged within single chambers in a sponge rather than free-living may account for these structural differences.

Microscopy images of choanoflagellate species allowed the identification of individual bundles of actin filaments within each collar tentacle. These bundles, assumed to represent single microvilli, demonstrate a more disorganised arrangement and relative freedom of the choanoflagellate collar. The choanocyte collar, in contrast, appears more uniform and rigid. Previous electron micrographs of cross-sections through the collar reveal connecting fibres between individual microvilli in choanocytes (Fjerdingstad, 1961a, Watanabe, 1978). There are no descriptions of similar connecting fibres in choanoflagellates and cross-sections through the collar tentacles clearly show no such connections (Hibberd, 1975, Karpov and Leadbeater, 1997, Leadbeater, 1977, Karpov and Leadbeater, 1998, Leadbeater, 1972). This study observed only very discrete, if any, microfibrils connecting individual collar microvilli.

This relative freedom of choanoflagellate collar microvilli is evident from the early stages of collar construction. Recovery experiments after treatment with cytochalasin D revealed that as the collar tentacles extend they do so in a uniform manner; all tentacles appearing approximately the same length at any point of fixation. In some instances, as soon as 30 minutes after collar construction began, it was possible to see individual bundles of actin filament, presumably representing individual microvilli. This contrasts with previous

published reports on the formation of the collar in new choanocytes. In sponges, choanocytes differentiate from non-collared cells during embryogenesis and as spent choanocytes are sloughed off daily and replaced. Archaeocytes, totipotent amoeboid cells found in the sponge meosphyl, provide a stem cell population to support this relatively high turnover rate. During collar formation in choanocytes, a continuous membranous tube, essentially a pseudopodial extension, extends from the cell body (Watanabe, 1978; Leys and Hill, 2012,). There are also occasions in the adult choanocyte when the collar consists not of discontinuous microvilli but of a continuous cytoplasmic tube with thin layers of cytoplasm between the continuous plasma membranes. As this continuous collar is more found more often in young flagellated chambers (Watanabe, 1978), and given the high turnover rate of choanocytes in an adult chamber, this situation might represent the collar in the process of differentiation. The microvilli are formed through the fusion of vesicles that contribute new membrane to form the individual microvilli. The vesicles which form the microvilli are derived from the Golgi apparatus which is always located in the apical part of a choanocyte between the collar and the nucleus during collar formation (Watanabe, 1978). Furthermore, unlike demosponge collars, microvilli in the calcareous sponge *Sycon raphanus* are rarely neat filaments. As described in an early study (Duboscq and Tuzet, 1939), the collar microvilli in *S. raphanus* frequently form short, lumpy projections that are often partially fused together.

The formation of collar microvilli in choanocytes occurs during the differentiation of previously larval cells, namely archaeocytes (Leys and Degnan, 2002; Leys and Hill, 2012). Differentiated choanocytes are terminal and therefore each daughter choanocyte possesses newly formed microvilli. This contrasts greatly with the situation in choanoflagellates where,

during cell division, collar tentacles are shared out approximately equitably between the daughter cells (Leadbeater, 1994). A second radial array of microtubule rootlets appears early and provides a framework which ensures the coordination and equal spacing of collar tentacles (Leadbeater, 1994). The regular interspersing of “old” and “new” tentacles highlights further their relative freedom compared to the connected microvilli in choanocytes.

Little is known about how the daughter choanoflagellate cells produce “new” tentacles. As in choanocytes, the Golgi apparatus system is particularly large and active during cell division and, again, is located in the apical part of the cell, close to the anterior surface of the nucleus and the flagellar basal body. During cell division large prominent vesicles containing “fibrillar material”, some of which pass to the juvenile cell after nuclear division, have been observed in the anterior end of the cell body (Leadbeater, 1994). The composition of contents or function of the vesicles has not been commented on, but it is possible that these vesicles contribute to the formation of microvilli tentacles in a similar process to that observed in choanocytes.

One striking difference in collar formation between choanoflagellates and choanocytes is the time required to form a fully-grown collar. Recovery experiments in *M. brevicollis* using cytochalasin D demonstrate that a fully-grown collar can be constructed in less than one hour. This corroborates reports of cell division and cell cycle duration in another choanoflagellate species, *Stephanoeca diplocostata* (Leadbeater, 1994). In contrast, observations of collar formation in *Tetilla serica* choanocytes showed the formation of collar in sponge larva over a period of several days (Watanabe, 1978). At the 28-hour stage, the

larvae consist entirely of undifferentiated cells. By 84-hours initial-stage choanocytes can be observed and by after four days choanocyte collars are observed, but even then they are not yet separated into separate microvilli. The gradual separation of microvilli, and the fusion of vesicles to form the individual microvilli of the collars continues until day 5, when completely formed flagellated choanocyte chambers can be observed.

Cytochalasin D disrupts the organisation of actin filaments by binding to the growing plus ends of microfilaments and inhibiting the addition of individual actin monomers. As actin filament stability depends on a "treadmilling" process in which filament length remains approximately constant while actin monomers are added at the plus end and dissociate from the minus end, blocking of subunit addition at the plus end by cytochalasin D causes loss of the filament as depolymerisation continues at the minus end (Schliwa, 1982; Cooper, 1987). After treatment with cytochalasin D, some actin filaments have been observed to persist, but any organisation is lost with only a focal accumulation of actin remaining (Schliwa, 1982). The high intensity staining spot at the flagellar base observed in *M. brevicollis* may indicate an accumulation of actin, especially as Phalloidin binds specifically at the interface between actin subunits and can therefore bind accumulations of actin monomers as well as filaments (Cooper, 1987).

Given the observed differences in collar formation and structure in choanocytes compared to choanoflagellates, to what extent can these structures be considered homologous? Although extensive phylogenetic analysis leaves little doubt that choanoflagellates are the closest known sister group of animals, comparisons of the underlying molecular and structural components of the appendages associated with the flagella and collar tentacles

highlight significant differences. The traditional hypothesis that an ancestral choanoflagellate-like protist gave rise to choanocyte-bearing metazoan ancestors has also been challenged by the presence of choanocyte-like cells in non-sponge metazoans including corals (Lyons, 1973a; Lyons, 1973b), echinoderms (Norrevang and Wingstrand, 1970) and ribbon worm larvae (Cantell *et al.*, 1982). Given that sponge choanocytes are also specialised cells that arise from non-collared cells during embryogenesis (Maldonado, 2004; Leys and Hill, 2012), colonial choanoflagellates made not provide the best model for the evolution of metazoan multicellularity.

In summary, there are just two common morphological characteristics in the cell structure of choanoflagellates and choanocyte: a single apical flagellum and actin-based microvilli. Given that the radial microtubule rootlet system present in choanoflagellates never occurs in choanocytes and given the observed differences in collar morphology and formation, it is possible that the incorporation of actin-based microvilli into a collar structure in choanoflagellates and choanocytes is not homologous. The presence of actin-based microvilli in choanoflagellates is not surprising. Indeed, microvilli and pseudopodia are related, with microvilli simply reusing part of the pseudopodia toolkit that was present in ancestral eukaryotes despite its loss in multiple lineages (Sebé-Pedrós *et al.*, 2013). The emergence of fascin, a protein required to cross-link actin filaments in microvilli tentacle structures, is also present in earlier holozan lineages including *Capsaspora owczarzaki* (Sebé-Pedrós *et al.*, 2013).

# Chapter 5: Metazoan Origins of a Centriole-Based Centrosome

## 5.1 Aims and objectives of this chapter

In recent years, experimental work on basal bodies, centrioles and centrosomes has revealed a list of constituent proteins that contribute to the formation of these structures and, through localisation and functional analysis, it has become possible to determine if an individual protein has a role in centriole and/or basal-body function. By ascertaining the phylogenetic presence of proteins that have been experimentally linked to either centriole or basal body function, it is possible to determine the evolutionary history of the centriole and its emergence as a structure that is functionally and structurally distinct to basal bodies.

The majority of centrosomal proteins, including those of non-metazoan centrosomes, contain coiled-coil domains. This study will review the phylogenetic occurrence of coiled-coil proteins and assess the role of a reported expansion in coiled-coil protein families in the evolution of the centrosome. This will incorporate the testing and evaluation of several different coiled-coil predictors.

Finally, choanoflagellates, the closest known relatives of animals, will be investigated as an intermediate stage in the evolution of a centriole-based centrosome. The distribution pattern of centrosome proteins will be linked to information from electron microscopy studies on the ultrastructure of mitosis in choanoflagellates. To further characterise the nature of the choanoflagellate MTOCs, data will be collected on the distribution patterns of γ-tubulin, a widely accepted marker of MTOCs, in a variety of choanoflagellate species.

## 5.2 Introduction: Evolution of the centrosome

### 5.2.1 From cilia to centrioles: the basal body is the ancestral structure

The conserved 9+2 axoneme structure characteristic of motile cilia and flagella is thought to have been present in the last eukaryotic ancestor over 800 million years ago (Mitchell, 2004). Examination of the phylogenetic tree of eukaryotes indicates that the centriole structure did not first appear without an axoneme (Azimzadeh and Bornens, 2004). Centrioles localised in a central body and not directly associated with the plasma membrane in a cilium or flagellum can only be observed in more recent lineages, most notably in the animal centrosome.

Lineages in which the motility of cilia or flagella have been lost experience less evolutionary constraint on their basal body/centriole structure. Arthropods and nematodes from the taxon Ecdysozoa, in which cilia are present only as derived sensory organelles, possess divergent centrioles with doublet or singlet microtubules (Azimzadeh and Bornens, 2004). Chapter three of this study described further examples in *Leishmania* amastigotes and vertebrate primary cilia. Where axonemes are entirely absent, centrioles are also absent and centrosomal structures with no association with the plasma membrane, such as the SPBs of yeast, have emerged.

Many protozoa provide a counterbalance to the generally simplified view of a single centrosomal MTOC. Protozoan cells can display a diversity of morphologically distinct and spatially separated MTOCs operating for cytoplasmic, mitotic and flagella/ciliary microtubules (Gull *et al.*, 2004). Whilst the mitotic MTOC of protozoa undergoes usual segregation in the formation of the bipolar spindle, multiple cytoplasmic MTOCs may be

present, each nucleating distinct sets of microtubules, usually with precise number control. Such distinct sets of MTOCs can be easily observed in pathogenic protozoa such as *Giardia*, *Trichomonas*, *Trypanosoma* and *Toxoplasma*.

### 5.2.2 The centriole and multicellularity

Multicellularity has independently evolved multiple times in a wide variety of organisms from distinct evolutionary lineages. The transition to multicellularity that initiated the evolution of animals from a unicellular flagellate is poorly understood and the selective advantages of multicellularity are the matter of many speculations (King, 2004). Multicellularity is thought to have evolved from a colonial state, perhaps favoured through escape from predation (Stanley, 1973) or dividing labour (Michod, 2007). The flagellar synthesis constraint argues that motion and division are mutually exclusive in some lineages due to competition for the same cellular machinery – the centriole/basal body (Margulis, 1981; Buss, 1987; King, 2004). Depending on the phase of the cell cycle and its location in the cell, a solitary MTOC can serve either as a basal body supporting flagellar synthesis or as an organiser of the mitotic spindle. Like animals cells, protozoa with a limited number of MTOCs, would have had to balance the requirements of motility against those of mitosis with flagellum retraction and loss of motility preceding formation of the mitotic spindle. The division of labour between cell fission and motility made possible through colony formation would have avoided this constraint and have granted a selective advantage to multicellular variants. The flagellation constraint appears to hold true for all animal cells: no flagellated or ciliated animal cell ever divides (Margulis, 1981; Buss, 1987).

The association of the basal body with the spindle poles in the unicellular ancestors of animals led to a single MTOC, unlike in organisms such as *Trypanosoma* where the basal bodies retained the unique function of nucleating flagella independent of the mitotic MTOC (Gull *et al.*, 2004). The retraction of the flagellum and the sacrifice of motility during cell division is a constraint that was circumvented by the formation of colonies. In a two-celled organism, for example, one cell could maintain the capacity for cell division while the other retains motility and propels both cells. The balance between motile and immotile cells in primitive multicellular organisms may also have played a role in the origin of gastrulation and differentiation (Buss, 1983).

Centriole-containing centrosomes may have enabled the efficient division of cells that split asymmetrically to produce two daughter cells of different fates. The segregation of differently aged mother centrioles, an asymmetry intrinsic to every animal cell division, can influence the timing of primary cilium formation in the two daughter cells, which in turn can influence their ability to respond to environmental signals and potentially alter the fate of one or both sister cells (Anderson and Stearns, 2009). Asymmetries in centriole inheritance can therefore play a major role in cell differentiation.

### 5.2.3 The origin of open mitosis in the animal lineage

In most unicellular eukaryotes, the nuclear envelope remains intact during mitosis (Heath, 1980). In this closed mitosis, the mitotic MTOC is morphologically and spatially separated to the MTOCs operating for cytoplasmic and/or flagella microtubules; an intranuclear spindle separates the chromosomes before karyokinesis. In contrast, higher eukaryotes undergo an open mitosis in which the nuclear envelope is completely disassembled before or during

spindle formation and reforms around the two daughter nuclei after chromosome separation. Open mitosis is likely to have evolved independently in both the plant and animal kingdoms (Fig. 5.1.) (Rose, 2007). In animal cells undergoing an open mitosis, the centrosome acts as the MTOC during interphase and mitosis. As the centrosome is cytoplasmic, it is necessary to break down the nuclear envelope in order to form a spindle which can interact with chromosomes. The mitotic MTOC of fungi is the spindle pole body, which is embedded in the nuclear envelope of *Saccharomyces cerevisiae* or, in the case of *Schizosaccharomyces pombe*, cytoplasmic during interphase but embedded in the nuclear envelope at the onset of mitosis (Ding *et al.*, 1997; Jaspersen and Winey, 2004).

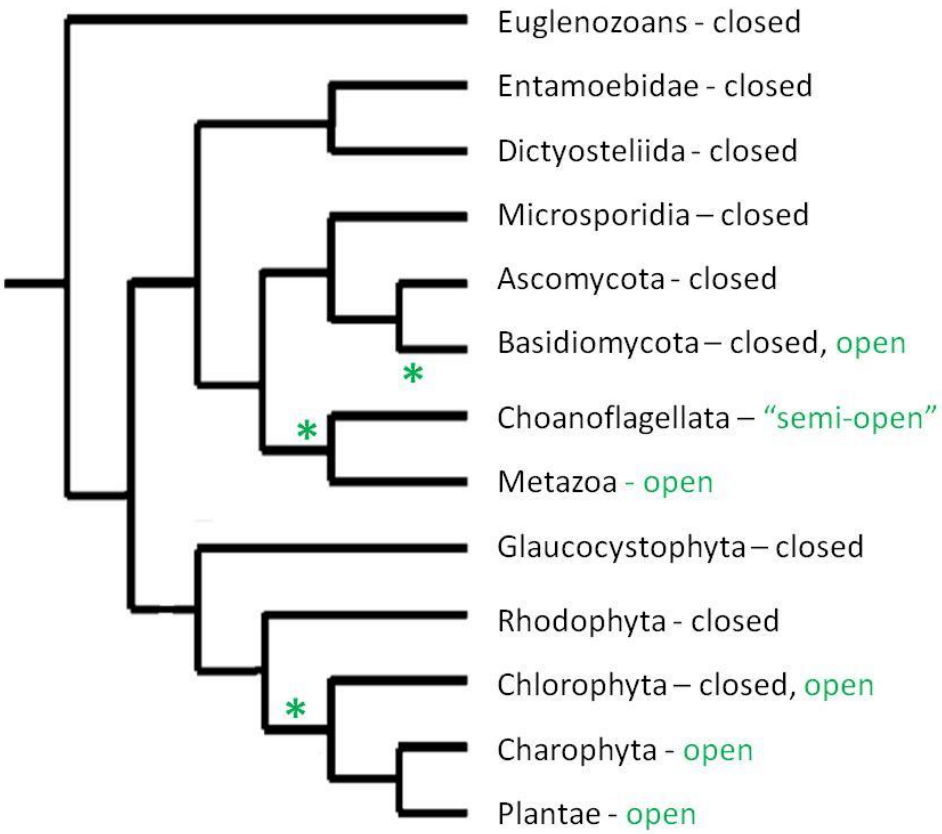


**Figure 5.1. Occurrence of closed and open mitosis in eukaryotes.** Asterisks mark possible independent appearances of open mitosis during evolution. Uncertainty surrounding the emergence of open mitosis in the animal and fungi lineages is discussed in the text. Phylogeny based on Hedges (2002). Adapted from Rose (2000).

Classifying mitosis as either open or closed, however, has limitations. Even in organisms which dismantle their nuclear envelope during mitosis, the phase during which this occurs can vary between organisms (Heath, 1980). Choanoflagellates provide one such example.

Current knowledge of nuclear and cell division in choanoflagellates is limited to some early descriptions based on light microscopy and three more recent electron microscopy studies (Karpov and Mylnikov, 1993; Leadbeater, 1994; Karpov and Leadbeater, 1997). The main stages of nuclear division appear to be similar in marine and freshwater choanoflagellates belonging to different families. In *Monosiga ovata,* mitosis appears to be an intermediate "semi-open" orthomitosis (Raikov, 1982; Karpov and Leadbeater, 1997). Cell division is initiated by the withdrawal of the single anterior flagellum, depolymerisation of the axoneme, and replication of the two parent basal bodies to produce two pairs of basal bodies. The spindle microtubules are assembled within the nucleus but, during early metaphase, as the spindle microtubules do not emerge from the nucleus and do not make contact with the now polar basal bodies, the basal bodies are not thought to act as the mitotic MTOC. As metaphase proceeds, fenestrae appear in the nuclear envelope at each pole and eventually the nuclear envelope disintegrates. It is only when fenestrae have formed that the basal bodies can make contact with the spindle microtubules.

Not all fungi cells undergo mitosis with the nuclear envelope intact (Fig. 5.1.). In the basidiomycete fungus *Ustilago maydis*, a dynein-based mechanism dissembles the mitotic nuclear envelope at the onset of mitosis (Straube *et al.*, 2005). As some aspects of nuclear envelope disassembly are conserved between *Ustilago maydis* and animals (Theisen *et al.*, 2008), it is possible that open mitosis and the removal of the nuclear envelope resemble an

evolutionary ancient mode of chromosome inheritance which was abandoned in ascomycete fungi. In this scenario the semi-open mitosis observed in choanoflagellates would represent a derived rather than an intermediary state. To this effect zygomycete fungi also undergo an open mitosis, (Heath, 1980). This ancient group of fungi is thought to be the ancestors of ascomycetes, including *Saccharomyces cerevisiae*, and of basidiomycetes, such as *Ustilago maydis* (Fitzpatrick *et al.*, 2006).

### 5.2.4 Protein components of the animal centrosome

The exact number of centrosome proteins is difficult to establish with confidence. The animal centrosome is not delineated by a membranous boundary and is a highly dynamic structure that undergoes major structural and compositional changes during the cell cycle. Centrosomes, in addition to their role as MTOCs, act as solid-state platforms for regulatory and signalling molecules (Doxsey *et al.*, 2005). Passive components, with no role in centrosome structure or function, may also use the centrosome as a vehicle to ensure their proper distribution during cell division.

Proteomic studies have therefore revealed a large number of centrosome-associated proteins. A mass spectrometric analysis identified a list of more than 500 proteins which included 47 of the 60 previously described components of the interphase centrosome (Andersen *et al.*, 2003). Of the other proteins identified, 350 had been previously characterised in contexts with no apparent relation to centrosomes. Different methods have identified more conservative numbers, depending upon the centrosome purification protocol used (reviewed by Wilkinson *et al.*, 2004).

Centrosomal proteins can be classified by several parameters. Proteins may either be permanently associated with the centrosome or associate with the structure during distinct stages of the cell cycle. Furthermore, structural proteins may either be directly involved in the centriole structure or localised in the pericentriolar material (PCM; Fig 1.3.).

## 5.3 Phylogenetic distribution of centrosome components

### 5.3.1 Identification of centrosome components across eukaryotes

To gain a deeper understanding of the evolutionary history of a centriole-based centrosome the phylogenetic presence and absence of centrosomal proteins was analysed and the distribution pattern obtained linked to information about the protein. 21 structural proteins were selected (Table 5.1. and supplementary material Table S5.1.), each with known centriolar or PCM localisation, and these protein sequences used to interrogate 30 predicted eukaryotic proteomes for potential orthologues. The proteins selected were all members of the "centrosome core structure": those that are permanently associated with the centrosome structure through cell-cycle dependent structural changes and those that remain after treatment of the centrosome complex with microtubule depolymerising agents (Schatten, 2008). This core set of proteins represent the main structural features of the centrosome, including the intercentriolar linker, centriole appendages, the PCM scaffold matrix and the γ-tubulin complexes.

The 30 eukaryotic organisms selected (Fig. 5.2. and Table S5.2), each with complete or near-complete genome sequencing, represent a wide taxonomic diversity of eukaryotes and include four of the six proposed eukaryotic "supergroups" (Simpson and Roger, 2004; Adl *et al.*, 2005) with a focus on the Opisthokonta that encompasses animals, fungi and

choanoflagellates (Fig. S5.1.). The selected organisms display a variety of centriole/basal body biology with representatives of both ciliated and non-ciliated species (supplementary material Table S5.2.). The approaches and criteria used to identify orthologues are further outlined in Materials and Methods. Ascension numbers of putative homologues are provided in the supplementary material (Table S5.3.).

| Proteins of the centriole domain | Proteins of the PCM domain |
|---|---|
| γ-tubulin | γ-tubulin |
| Cep170 | GCP2 |
| ODF2 (Cenexin) | GCP3 |
| Ninein | GCP4 |
| Rootletin | GCP5 |
| Cep63 | GCP6 |
| C-Nap1(Cep250) | PCM-1 |
| Cep68 | Cep192 |
| CP110 | Pericentrin |
| Cep97 | AKAP450 |
| Cep135* (BLD10) | |
| Cep164* | |

**Table 5.1. Structural classification of core centrosomal proteins.** Rationale for the selection of these proteins is explained in the text. See Table S5.1. for descriptions of function and localisation studies. *****Cep135 and Cep164 are well-documented as essential for the correct function of basal bodies. All other proteins of the centriole domain have been identified as restricted to the centriole structure in a centrosome, and thereby not detected on basal bodies.

### *Focus One: Proteins of the centriole domain*

The nine-fold triple microtubule arrangement of both centrioles and basal bodies is widely conserved in all major eukaryotic groups, suggesting its presence in the last eukaryotic common ancestor (Carvalho-Santos *et al.*, 2011). α-and β-tubulin, the sub-units of centriole and basal body microtubules are found in all eukaryotes with high levels of sequence identity (Dutcher, 2001). In addition to the microtubular cylinder *per se*, other proteins localised on or within the microtubular cylinder have been identified as specifically required

for its assembly and/or function. Although many of these, such as the tetkins, centrin, Sp77, Sp88 and other members of the tubulin family, γ-, δ- and ε-tubulin, are involved in the assembly of both basal bodies and centrioles, a few have been identified, using electron microscopy immunolocalisation, as restricted to centrioles (Beisson and Wright, 2003). These proteins of the centriole domain will form the first focus of this analysis. Cenexin (ODF2), for example, localises to the sub-distal appendages of mature mother centrioles and is required for the recruitment of ninein (Ishikawa *et al.*, 2005; Ibi *et al.*, 2011). Ninein is required for microtubule anchoring and docking of γ-TuRCs at the centrosome (Ou *et al.*, 2002; Delgehyr *et al.*, 2005). Cep170 also localises to the sub-distal appendages of mature centrioles (Guarguaglini *et al.*, 2005). Other centriolar proteins C-NAP1, rootletin and Cep68, are responsible for centriole cohesion by acting as a structural link between centrioles (Fry *et al.*, 1998; Mayor *et al.*, 2000; Bahe *et al.*, 2005; Yang *et al.*, 2006; Graser *et al.*, 2007b). Cep97 and CP110 are recruited to centrioles to inhibit ciliogenesis, the process in which a centriole transforms to a basal body (Chen *et al.*, 2002; Tsang *et al.*, 2006; Spektor *et al.*, 2007; Tsang *et al.*, 2008). Cep63 forms a discrete ring around the proximal end of mature centrioles and is required for normal spindle assembly during mitosis (Sir *et al.*, 2011; Brito *et al.*, 2012).

Two components well-documented as essential for the correct function of basal bodies were also included in the analysis. Cep135 is required for the formation of an intermediate cartwheel structure that enforces the nine-fold symmetry of both basal bodies and centrioles with null mutants lacking the central microtubule pair (Ohta *et al.*, 2002; Matsuura *et al.*, 2004; Hiraki *et al.*, 2007; Kim *et al.*, 2008; Mottier-Pavie and Megraw, 2009; Carvalho-Santos *et al.*, 2010). Cep164 localises to the distal appendages of mature

centrioles, accessory structures required for the docking of the basal body at the apical plasma membrane during ciliogenesis (Graser *et al.*, 2007a).

### *Focus Two: Proteins of the PCM domain and the GCP family of γ-tubulin complex components*

Surrounding the centrioles is an electron-dense matrix, the pericentriolar material (PCM). The size and complexity of the PCM domain is cell-cycle dependent, with a recruitment of material prior to cell division (Rieder and Borisy, 1982). The PCM consists of a fibrous scaffolding matrix with a large number of coiled-coil proteins and γ-tubulin complexes (Moritz *et al.*, 1995).

γ-tubulin itself is a highly conserved protein present in all eukaryotic cell groups and is required for the initiation of microtubule assembly at MTOCs such as the animal centrosome or the yeast spindle body (Pereira and Schiebel, 1997; Schatten, 2008). γ-tubulin forms complexes with several other proteins that act as the essential core of the microtubule nucleating machinery. The γ-tubulin small complex (γ-TuSC) consists of two molecules of γ-tubulin and one molecule each of GCP2 and GCP3. In some eukaryotes several γ-TuSC molecules assemble together with GCP4, GCP5 and GCP6 into a much larger γ-tubulin ring complex (γ-TuRC) that functions as a stable platform in microtubule nucleation with a ring of γ-tubulins acting as a template for α- and β-tubulin (Keating and Borisy, 2000; Moritz *et al.*, 2000; Wiese and Zheng, 2000; Kollman *et al.*, 2011; Erlemann *et al.*, 2012).

γ-tubulin complexes are embedded in a lattice formed by pericentrin, a large protein required for the recruitment and anchoring of PCM components (Dictenberg *et al.*, 1998;

Zimmerman *et al.*, 2004; Lee and Rhee, 2011). Pericentrin binds to PCM-1, a protein that localises in “centriolar satellites” that accumulate near centrosomes during mitosis (Kubo *et al.*, 1999; Dammermann and Merdes, 2002; Kubo and Tsukita, 2003). The recruitment of PCM proteins and the subsequent assembly of γ-TuRCs is controlled by Cep192 (Joukov *et al.*, 2010). Cep192 and pericentrin are mutually dependent for their localisation to the PCM during centrosome maturation (Zhu *et al.*, 2008).

Many PCM domain proteins appear to play no direct role in centrosome structure or function. These passive components are presumed to use to the centrosome to ensure proper distribution during cell division, as has been shown for the surface of the mitotic chromosomes (Rattner, 1992; Mack *et al.*, 2000), and will not be considered further here.

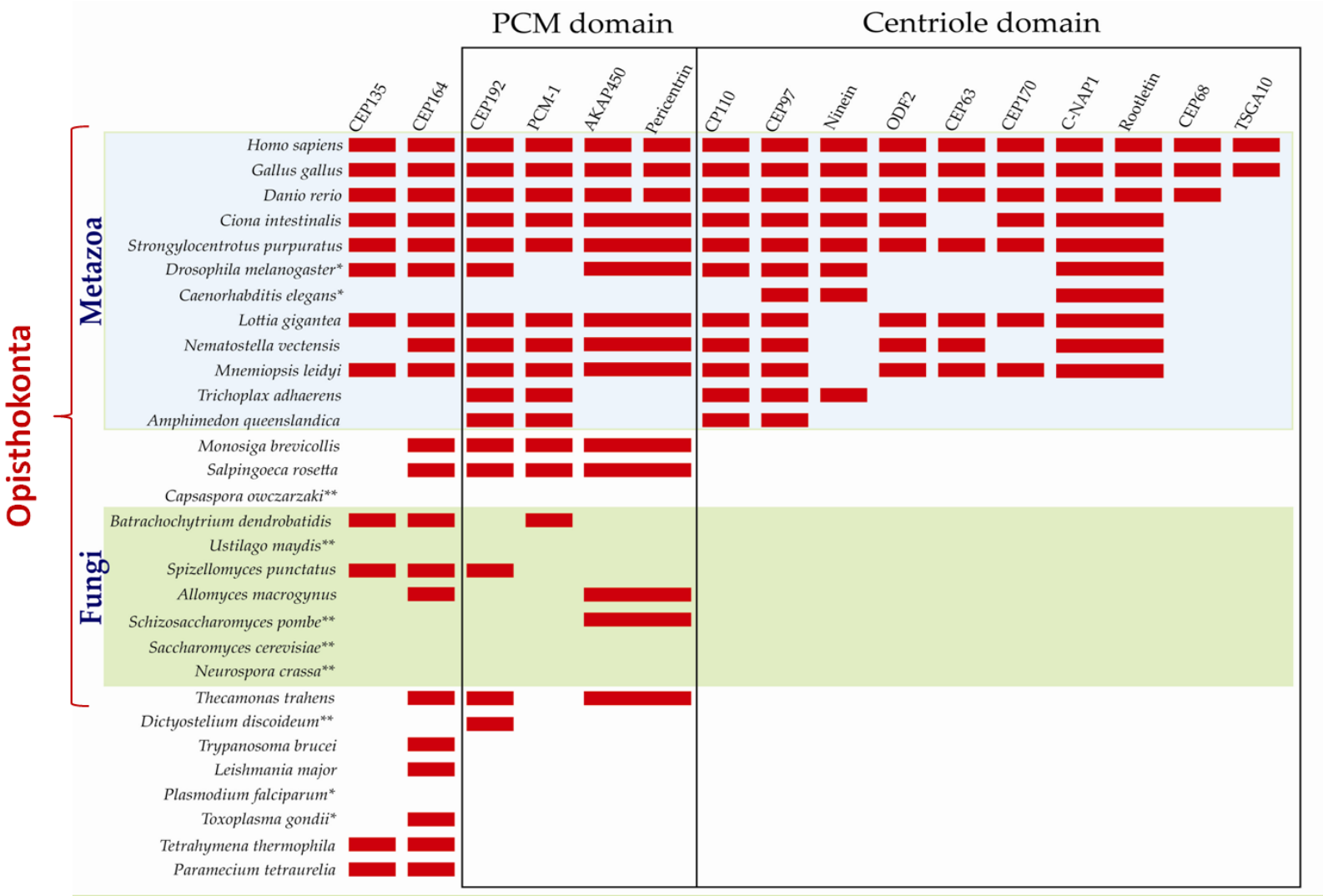


**Figure 5.2. Phylogenetic distribution of basal body, PCM and centriole proteins among 30 eukaryotes.** Red boxes indicate that a homolog was found in the corresponding species (identified in Table S5.3). Rationale for the selection and characterisation of these proteins is explained in the text. TSGA10, not included in the original selection, is a vertebrate paralogue of Cep135. *indicates unusual centriole structure (described in Table S5.2.). **indicates an unciliated taxa with secondary loss of centriole structure. The apusomonad, *Thecamonas trahens,* is considered a sister group to the supergroup Opisthokonta. Phylogeny depicted in Fig. S5.1.

### 5.3.2 Centrioles are primarily essential for axoneme formation and motility

Orthologues of Cep135 and Cep164, two proteins essential for the assembly of both basal bodies and centrioles, were identified in three of the four eukaryotic supergroups analysed, Opisthokonta, Excavata and Chromalveolata (Fig. 5.2.). Within these supergroups Cep135 and Cep164 were restricted to organisms with motile cilia.

Cep135 was detected in a wide diversity of ciliated eukaryotes. Cep135 is required for the formation of an intermediate cartwheel structure that enforces the nine-fold symmetry of basal bodies and centrioles. The presence of Cep135 in ciliated organisms that lack a centriole-based centrosome is presumably required for the formation of basal bodies. Cep135 is retained, for example, in planarian flatworms that use cilia for locomotion yet lack a centriole-based centrosome (Azimzadeh *et al.*, 2012). In contrast, both Cep135 and its associated cartwheel structure are lacking in the nematode *Caenorhabditis elegans*. *Caenorhabditis elegans*, in which cilia are present only as non-motile sensory organelles, possesses derived centrioles with singlet microtubules and shows a correlative loss of a large number of centrosomal proteins from both the centriolar and PCM domain (Fig. 5.2). This all suggests that the ancestral and primary function of Cep135 is to template a motile axoneme.

None of the proteins of the centriole domain of centrosomes, including Cep135 and Cep164, were detected in organisms without motile cilia, namely *Capsaspora owczarzaki*, *Ustilago maydis*, *Schizosaccharomyces pombe*, *Saccharomyces cerevisiae*, *Neurospora crassa* and *Dictyostelium discoideum*. This strict correlation between the occurrence of a basal body or

centriole structure and the presence of a functional axoneme supports the hypothesis that centrioles are primarily and ancestrally essential for axoneme formation. The centriole structure was lost concomitantly with axonemes during the evolution of particular taxa such as the yeasts, *Schizosaccharomyces pombe* and *Saccharomyces cerevisiae*, and the amoeba *Dictyostelium discoideum*.

### 5.3.3 Proteins of the centriole domain are confined to the Metazoa

Strikingly, it was not possible to identify a single orthologue of any of the centriole domain components previously identified as restricted to the centriole structure of a centrosome, and thereby not detected on basal bodies, outside of the Metazoa (Fig. 5.2.). Although comparative analyses cannot discriminate between proteins that have been lost entirely from a lineage and those that have diverged in sequence to such an extent that they are undetectable, it is probable that the centrosome structures to which these components contribute, namely the intercentriolar linker and the sub-distal appendages of the mature centriole, are restricted to the Metazoa. The centriole domain of centrosomes therefore emerged within the Metazoa from an ancestral state of possessing a centriole with basal body function but no association with the centrosome.

Previous studies suggest that the nine-fold symmetry of both centrioles and basal bodies is dependent upon underlying molecular components conserved across ciliated eukaryotes (Carvalho-Santos *et al.*, 2010; Hodges *et al.*, 2010). Nevertheless, the structure of the centriole has appeared particularly insensitive to multiple genes losses and major changes in the ultrastructure of centrioles only occur when the majority of the genes are lost or highly divergent, as demonstrated in the unusual centrioles of *Caenorhabditis elegans* and

*Drosophila melanogaster*. As presented here, only one protein of the centriole domain, Cep97, is present consistently throughout the Metazoa. The majority of the proteins of the centriole domain appear to be been lost, or diverged significantly in sequence, in those organisms with divergent centrioles, notably *Caenorhabditis elegans* and *Drosophila melanogaster*. In a more extreme example, planarians lack a centriole-based centrosome with centrioles only assembled in terminally differentiated ciliated cells through an acentriolar pathway (Azimzadeh *et al.*, 2012). No orthologues of any of the centriole domain components were detected in the planarian genome. This all suggests that the centriole domain is dispensable for cell division in particular lineages.

### 5.3.4 Focusing on the Metazoa: duplication of centriole/basal body proteins in the evolution of the centrosome

As shown above, the centriole domain proteins are characteristic of the Metazoa, but it is also notable that two basal lineages of metazoans have far fewer centriole domain genes. Only two proteins of the centriole domain, CP110 and Cep97, are present in the proteomes of the sponge *Amphimedon queenslandica* and the placazoan *Trichoplax adhaerens* (Fig. 5.2.). Although this suggests an early appearance of a centriole-based centrosome in the Metazoan lineage, other proteins of the centriole domain, for example Cep68 and TSGA10, appear to have originated in vertebrates with gene duplication having played an important role in the evolution of these centrosome components. C-Nap1 is the closest paralogue of rootletin in mammalian genomes with 31% identity and 50% similarity between the human C-Nap1 and rootletin sequences. Both C-Nap1 and rootletin have extended coiled-coil domains with coiled-coil coverage of 77.7% and 78.4% respectively. A single ancestral homolog is detected in basal metazoans and entirely absent in non-metazoans. Given the

key role of C-Nap1 in centrosome cohesion, such a recent evolutionary origin may appear surprising. C-Nap1 is also a substrate of the kinase Nek2, a regulator of centrosome cohesion that is present in basal metazoans (Mardin *et al.*, 2010). The gene encoding C-Nap1 is likely to have arisen from a duplication of the ancestral rootletin gene followed by specialisation. The ancestral gene is likely to have been performing the functions of both rootletin and C-Nap1 for regulating centrosome cohesion.

A paralogue of Cep135, TSGA10, was found only in mammals. TSGA10 is shorter than the ancestral Cep135 present in organisms such as *Paramecium tetraurelia* and the fungi *Spizellomyces punctatus* and contains fewer extended coiled-coil domains.

AKAP450 and pericentrin share a conserved region of homology near their C-termini. A single ancestral homolog was detected in non-vertebrate metazoans and unicellular eukaryotes.

### 5.3.5 Phylogenetic distribution of proteins of the PCM domain

In contrast to proteins of the centriole domain, all proteins of the PCM domain are present in at least some non-Metazoan representatives (Fig. 5.2.). The ancestral homolog of AKAP450/Pericentrin which forms the core structural lattice of the PCM domain was detected in a wide range of opisthokonts including metazoans, choanoflagellates and fungi. Other proteins of the PCM domain, PCM-1 and Cep192, were also detected in choanoflagellates and some fungi species. Proteins of the PCM domain that are not constituents of the γ-tubulin complexes were noticeably absent outside of the opisthokonts.

There appears to be no correlation between the presence of a PCM domain and that of a centriole domain. As discussed above, there is a strict correlation between the occurrence of a centriole structure and the presence of a functional axoneme and yet, unlike the proteins of the centriole domain, centrosome proteins localising to the PCM were detected in non-ciliated eukaryotes. AKAP450/Pericentrin, for example, was detected in the non-ciliated fungi *Schizosaccharomyces pombe* and *Saccharomyces cerevisiae*. Cep192 was also detected in the non-ciliated amoeba *Dictyostelium discoideum*. *Dictyostelium discoideum* has an acentriolar MTOC called the nucleus associated body (NAB) in which Cep192 has been shown to localise (Schulz *et al.*, 2009). This suggests that the function of Cep192, the recruitment of PCM material to the MTOC, is independent of the presence of a centriole structure.

As was the case for proteins of the centriole domain, no proteins of the PCM domain are present consistently throughout the Metazoa and some appear to be been lost, or have diverged significantly in sequence, in some of the representative organisms, especially those with divergent centrioles. PCM-1 appears to be absent in both *Drosophila melanogaster* and *Caenorhabditis elegans*, with all proteins of the PCM domain except for γ-tubulin appearing absent in the later. The ancestral homolog of AKAP450/Pericentrin appears absent in *Amphimedon queenslandica* and *Trichoplax adhaerens*.

*Capsapora owczarzaki,* devoid of centrioles, possesses no recognisable proteins of the PCM domain. PCM-1, for example, was not detected in any of the unciliated organisms represented here.

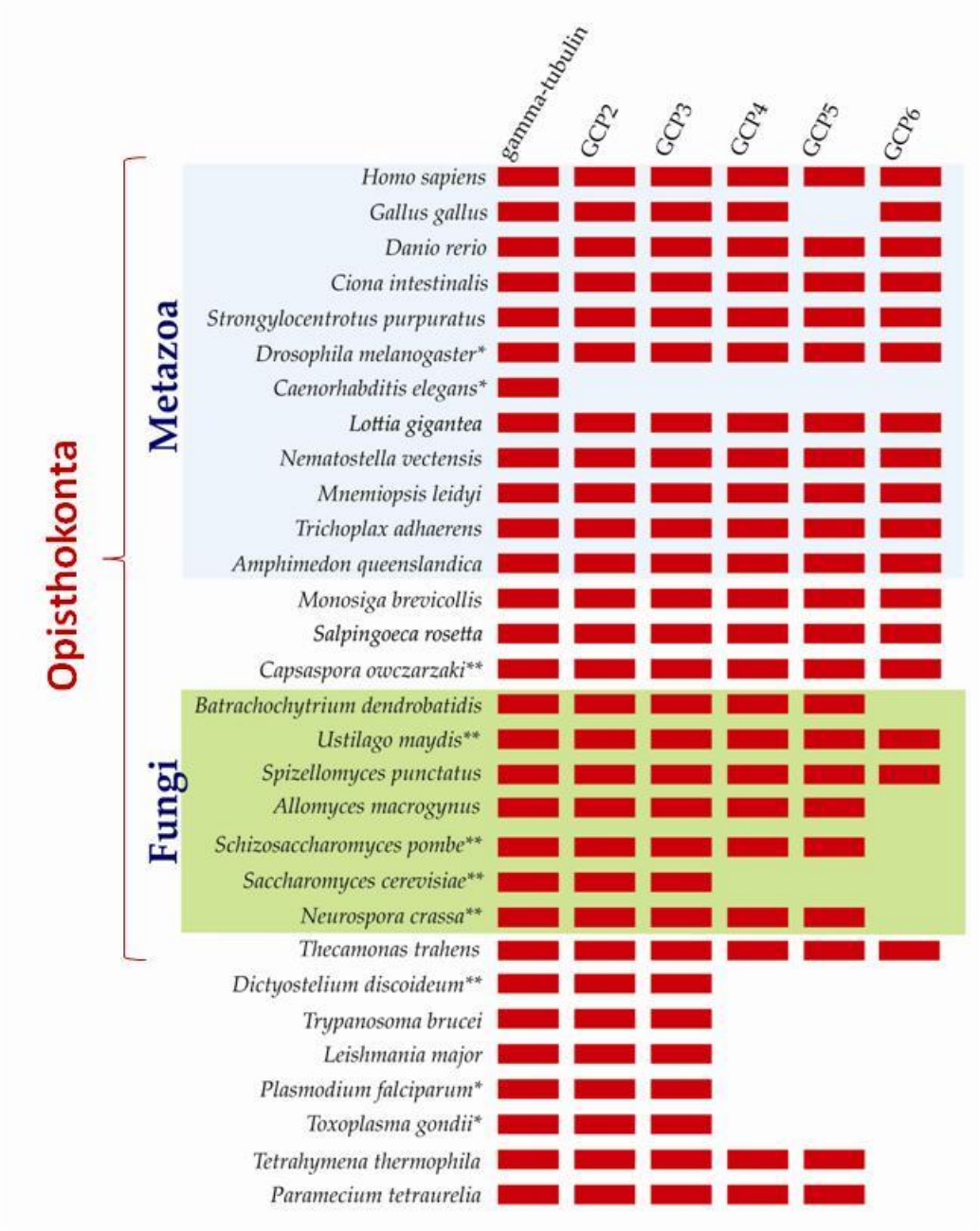


**Figure 5.3. Phylogenetic distribution of γ-tubulin complex proteins among 30 eukaryotes.** Red boxes indicate that a homolog was found in the corresponding species (identified in Table S5.3). Rationale for the selection of these proteins is explained in the text. The γ-tubulin small complex (γ-TuSC) consists γ-tubulin, GCP2 and GCP3. γ-TuSC molecules assemble together with GCP4, GCP5 and GCP6 to form a γ-tubulin ring complex (γ-TuRC). *indicates unusual centriole structure (described in Table S5.2.). **indicates an unciliated taxa with secondary loss of centriole structure. The apusomonad, *Thecamonas trahens,* is considered a sister group to the supergroup Opisthokonta. Phylogeny depicted in Fig. S5.1.

### 5.3.6 Distribution of the GCP family of γ-tubulin complex components across eukaryotes

Components of the γ-tubulin complexes located with the PCM domain of the centrosome appear more widely and consistently conserved (Fig. 5.3.). GCP2 and GCP3, components of the γTuSC, were found in all eukaryotes analysed except *Caenorhabditis elegans*. Representatives from most major groups of eukaryotes (Metazoa, Choanozoa, Fungi, Chromalveolata and Excavata) also possessed GCP4 and GCP5, whereas GCP6 appears to be an addition specific to the Metazoa and Choanozoa lineages. GCP4 and GCP5, two proteins that assemble with multiple γ-TuSCs to form the γTuRC, have identical phylogenetic distributions with the exception of *Gallus gallus* which appears to be missing GCP5.

Although they have been described to duplicate and function in a conventional manner, the centrioles in *Caenorhabditis elegans* are morphologically simple with nine singlet microtubules replacing the usual nine triplet microtubules. The microtubules also possess less prominent appendages (O'Toole et al., 2003). This analysis reveals the PCM domain of *Caenorhabditis elegans* to be either highly divergent or absent with no components of the PCM domain, including components of the γTuSC, detected in the proteome within the parameters of this study. Another study, however, demonstrated the presence of a highly divergent sequence homolog of Cep192, called SPD-2, in *Caenorhabditis elegans* (Pelletier *et al.*, 2004). Although known in the literature, this divergent homologue was not identified within the parameters of this analysis. The presence of highly divergent sequences of both centrioles and the PCM domain in *Caenorhabditis elegans* suggests that the evolution of these two structures is intrinsically linked.

*Saccharomyces cerevisiae* appears to have more basic microtubule-assembly machinery than other fungal representatives. Unlike other fungi, including a second Ascomycota representative, *Schizosaccharomyces. pombe*, *Saccharomyces cerevisiae* does not encode orthologues of the γ-TuRC (GCP-4, GCP-5 and GCP-6). MT nucleation in budding yeast is promoted by a γ-TuSC that is bound to the nuclear and cytoplasmic sides of the SPB with electron microscopy revealing that there are only 21–25 microtubules in haploid cells (Erlemann *et al.*, 2012). In contrast three representatives of the Chytridiomycota division, *Allomyces macrogynus*, *Spizellomyces punctatus* and *Batrachochytrium dendrobatidis*, are all shown here to possess orthologues of GCP-4 and GCP-5, and, in the case of *Spizellomyces punctatus*, GCP-6. Chytrids, which possess centrioles and lack SPDs, are a sister group to the remaining fungal groups and thereby enables reconstruction of the characteristics of ancestral fungi (Wang *et al.*, 2009a). *Thecamonas trahens*, the closest sequenced neighbour to opisthokonts, is also in possession of a full complement of γ-TuRC proteins (Fig. 5.3.).

In summary, there appears to be little correlation between the presence of the constituent proteins of γ-tubulin complexes and a centriole or basal body structure. *Capsapora owczarzaki*, for example, has not been observed to possess centrioles, nor homologues of Cep135 or Cep164, but, as shown here, does possess orthologues of all the main constituents of γ-TuRCs. One exception is *Caenorhabditis elegans*, in which no components of the γ-tubulin complexes excluding γ-tubulin were detected. Furthermore, with the ongoing exception of *Caenorhabditis elegans*, there is no correlation between the presence of the constituent proteins of γ-tubulin complexes and proteins of the PCM domain. The ubiquity of GCP2 and GCP3 in eukaryotes, the components of γ-TuSCs, suggests their presence in the last common ancestor of eukaryotes.

### 5.3.7 Elucidating the ancestry of centriole domain proteins: identification of a potential ancestral protein in *Monosiga brevicollis*: domain organisation and primary structure

Interestingly, six of the selected centriole domain proteins, ninein, C-Nap1, rootletin, ODF2, Cep63, and Cep135, all identified the same putative homologue, named MBCDH8, in the choanoflagellate *Monosiga brevicollis* within an e-value threshold of $<10^{-5}$. Of these six centriole domain proteins all, with the exception of rootletin, a paralogue of C-NAP1, identified MBCDH8 as the most significant match (highest alignment score) in *M. brevicollis*. This putative 8,736 amino-acid protein was analysed with Pfam (Finn *et al.*, 2008) and SMART (Letunic *et al.*, 2009) to detect the presence of any conserved domains. The protein contains 24 cadherin repeats, the defining domain of cadherins (Fig. 5.4.). Cadherins are critical mediators of metazoan cell adhesion and signalling and the cadherin identified in this analysis is one of the 23 cadherins previously identified in the *M. brevicollis* genome (Abedin and King, 2008). Two cohesin domains and two transmembrane domains were also detected.

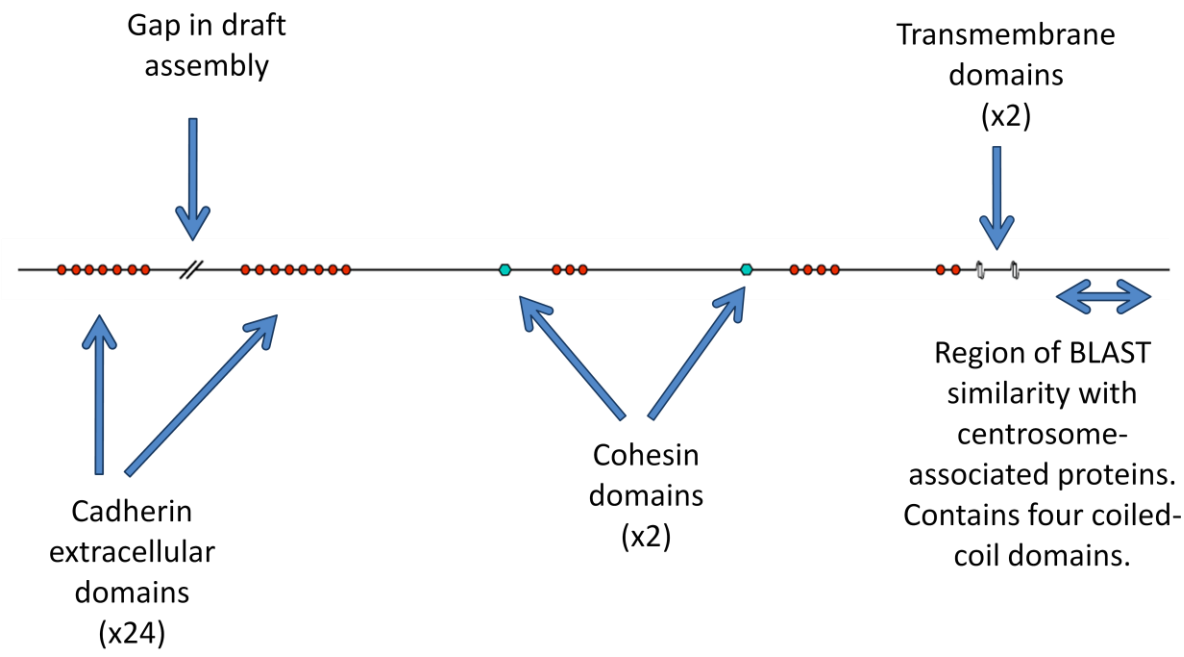


**Figure 5.4. Schematic diagram of the domain organization of the *Monosiga brevicollis* cadherin MBCDH8 showing domain content and arrangement.** The region of BLAST similarity with centrosome-associated proteins is highlighted. Adapted from Abedin and King (2008).

Pairwise sequence alignments of MBCDH8 with human ninein, C-Nap1, rootletin, ODF2, Cep63, and Cep135 indicated that all six of these centrosome-associated proteins aligned with the C-terminus region of MBCDH8 that is free of cadherin, cohesin and transmembrane domains. Removal of the cadherin, cohesin and transmembrane domains, as identified by SMART, and a subsequent BLASTp search using the modified protein sequence in the human proteome, led to the reciprocal identification of the original seven centrosome-associated proteins within an e-value threshold of $<10^{-9}$ (Fig. 5.5.) Two further centrosome-associated proteins not included in the original analysis, testis-specific-10 (TSGA10) and Cep152, were also identified as putative homologues of MBCDH8.

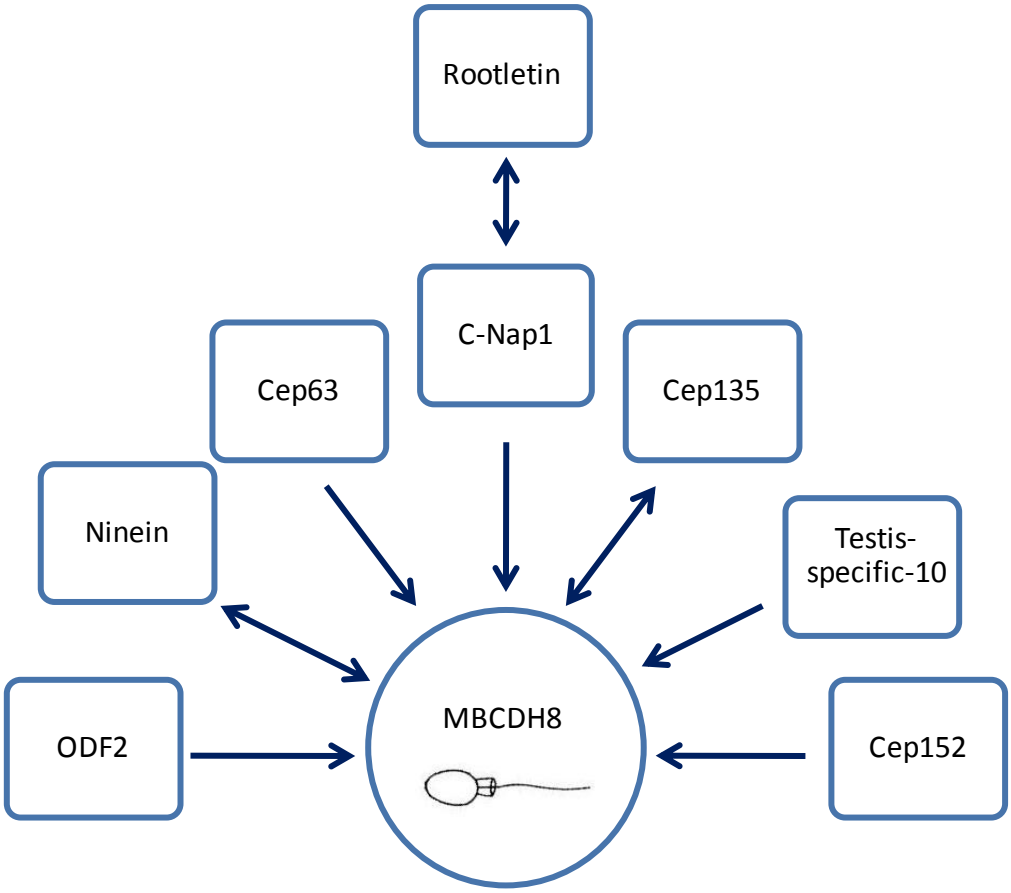


**Figure 5.5. Diagram showing best BLAST hit relationships between human centrosome-associated proteins and MBCDH8 in *Monosiga brevicollis*.** Double ended arrows signify reciprocity after removal of cadherin, cohesin and transmembrane domains in MBCDH8. Testis-specific 10 and Cep152, not included in the original analysis, are two additional centrosome-associated proteins identified as putative homologues of MBCDH8.

The region of sequence homology in MBCDH8 contains four coiled-coil domains, as determined by the Coils2 program (Lupas *et al.*, 1991). Coiled-coil domains consist of two or more alpha-helices winding around each other to form a super coil. On a primary structure level, coiled-coil domains are characterised by a heptad repeat pattern of hydrophobic and polar residues (Burkhard *et al.*, 2001). Residues in the first and fourth position are hydrophobic and residues in the fifth and seventh position are predominately charged or polar. The repeating pattern of hydrophobic and polar residues that characterise coiled-coil domains can interfere with sequence comparison algorithms often leading to false

predictions of homology between long coiled-coil proteins (Rose *et al.*, 2005). Using the Coils2 program, the coiled-coil domains were predicted and removed from each of the human centrosome-associated proteins that identified MBCDH8 as a putative homologue (ninein, C-Nap1, rootletin, ODF2, CEP63, CEP135, testis-specific-10 and CEP152). All nine proteins have high coiled-coil coverage ranging from 57.9% in ninein to 78.7% in rootletin (Table 5.5.).

In BLASTp searches using the modified coiled-coil-free protein sequences, both the modified Ninein and C-Nap1 protein sequences still identified MBCDH8 as a putative homologue. Although the masking of coiled-coil domains in the other human sequences resulted in MBCHD8 no longer being identified as a putative homologue, the high coiled-coil coverage of the proteins resulted in little sequence being available for comparison. The remaining coiled-coil-free protein sequences did not identify any putative homologues with significant alignment scores (e-value threshold of <0).

In the M. brevicollis genome scaffold assembly MBCDH8 spans three contigs encompassing two gaps of 2882 and 6469 base pairs. Attempts at sequence alignments using MBCDH8 revealed the presence of an internal repeat. This 418-amino-acid repeat spans both cohesin domains. The 100% identity between the two repeats suggests the possibility of an assembly error in the draft *M. brevicollis* genome. In addition, MBCDH8, predicted to contain 27 introns, is very intron-rich compared to an average intron density of 6.6 introns/gene in *M. brevicollis* (Westbrook, 2011). With a long open reading frame encoding 5,770 amino acids, most introns are concentrated in the C-terminus region of interest.

### *Validation of cDNA sequence assembly and PCR-determined expression of MBCDH8 in Monosiga brevicollis*

In order to establish whether the unusual constitution of the *M. brevicollis* cadherin MBCDH8 is due to a sequence assembly error, expression of the putative protein was determined through PCR. All available EST data of MBCDH8 is restricted to upstream of the two transmembrane domains and the coiled-coil region of interest. MBCDH8 cDNA was amplified using primer pairs corresponding to various regions of interest (Table 5.2.).

| **Primer** | **Target region of gene** | **Sequence 5' to 3'** | **Use** |
|---|---|---|---|
| **Mb8startF** | Cadherin repeat | CAG GAC AGC GCC ATG GGT GG | Forward |
| **Mb8startR** | Cadherin repeat | TCG CAG ACA CGC TCA GCA GC | Reverse |
| **MbCDH8** | Internal repeat | TTG TAC GGC GGC TGA GTG CG | Forward |
| **MbCDH8a** | Internal repeat | ACA AAG TGT CCG TCG GTC AGC A | Reverse |
| **MbCDH8b** | Internal repeat | GGC ATT CGC TTG GAG CAC GC | Reverse |
| **Mb8tmF** | Transmembrane domain | ATC ATC AGG TGA CCC AGG AG | Forward |

| | | | |
|---|---|---|---|
| **Mb8tmR** | Transmembrane domain | GCT GTT TCT TCG ACC TCG TC | Reverse |
| **Mb8tmccF** | Transmembrane and CC domains | AGT CTG GAC CAG CTT CCT CA | Forward |
| **Mb8tmccR** | Transmembrane and CC domains | ATC GAC TTG CAG TGT TGT CG | Reverse |
| **Mb8ccF** | CC domains | CAA ATT GTC TCG TTG GAG CA | Forward |
| **Mb8ccR** | CC domains | GAG GAC CAG TTG CAC GGT AT | Reverse |

**Table 5.2. PCR primers designed and used in this work.**

Amplification products of the expected sizes were detected as distinct bands on agarose gels for primers targeting the cadherin and coiled-coil domains of MBCDH8. Coiled-coil domains, however, proved too repetitive to allow development of gene-specific primers that are capable of unequivocal discrimination of the target gene, increasing the possibility of false positives. This was partially addressed *in silico* by assessing the specificity of primers against non-target sequences using Primer3 (Rozen and Skaletsky, 2000) and NCBI's Primer-BLAST software and noting the amplicon size of any potential nonspecific products.

No amplicons of the correct size, however, were detected for primers targeting the internal repeat or transmembrane domains supporting the possibility of an assembly error in the draft *M. brevicollis* genome.

### 5.3.8 Centrosomal proteins share homology with SMC domains found in chromosome segregation-related ATPases.

Most proteins are composed from a finite lexicon of evolutionarily conserved functional domains. To further elucidate the evolutionary history of centrosomal proteins, the selected proteins were annotated for conserved domains using a variety of domain- and fold-recognition software including Pfam, SMART and CDD (detailed in Materials and Methods). Subsequent retrieval of proteins that contain a similar protein domain profile may be more effective at finding protein similarities and predicting homology across significant evolutionary distances than by direct sequence similarity searches. Indeed, using conserved domains to find protein homologues can be more effective than standard BLAST searches because the scoring matrices used are tuned to focus on important functional sites and sequence motifs that are highly conserved within the domain (Geer *et al.*, 2002; Marchler-Bauer *et al.*, 2011).

#### *Conserved domains in centrosomal proteins*

Very few conserved domains or structures other than coiled-coils were predicted in the selected centrosomal proteins. The only other domains other than coiled-coils that were predicted by protein annotation software were SMC domains and regions of disorder. The selected centrosome proteins are rich in predicted disordered regions which cover an average of 57% of their length, compared to 39% in the general human proteome (Dos Santos *et al.*, 2013). Regions of disorder, in a similar function to coiled-coil domains, are

thought to facilitate protein interactions (Fong *et al.*, 2009) but, as is the case with coiled-coil domains, are of little use in predicting homology.

10 centrosomal proteins, in addition to MBCDH8, were shown to share homology with the SMC proteins found in chromosome segregation-related ATP-ases within an e-value threshold of less than $<10^{-11}$ (Table 5.3.). All the centrosomal proteins that identified MBCDH8 as a putative homologue in *M. brevicollis* were predicted to contain conserved SMC domains. The masking of coiled-coil domains revealed that all regions of homology with SMC proteins lie within regions of coiled-coil secondary structure.

| **Human centrosomal proteins predicted to contain SMC domains** | **E-value of alignment between the predicted SMC domain in the centrosomal protein and the SMC domain model.** |
|---|---|
| **Pericentrin** | 1.01E-16 |
| **AKAP450** | 1.01E-16 |
| **Ninein** | 1.32E-11 |
| **Cep63** | 2.24E-12 |

| | |
|---|---|
| **C-NAP1** | 5.99E-23 |
| **Rootletin** | 2.07E-11 |
| **ODF-2** | 3.80E-16 |
| **Cep164** | 3.18E-13 |
| **Cep135** | 9.46E-14 |
| **TSGA10** | 1.20E-12 |

**Table 5.3. Centrosomal proteins that are predicted to contain SMC domains.** Scores represent the confidence level of the SMC domain prediction in the protein query sequence when compared to the SMC conserved domain model curated by the NCBI Conserved Domain Database. Query sequences were human.

The presence of shared conserved domains in both centrosomal and SMC proteins, in conjunction with the discovery that a single coiled-coil protein in choanoflagellates, MBCDH8, has potentially eight homologues in the Metazoa, adds further weight to the hypothesis that core centrosomal proteins arose from an expansion of a coiled-coil protein family in the Metazoa. This is particularly interesting given the recent discovery of the functional significance of SMC proteins in centriole cohesion (Schockel *et al.*, 2011).

### *The role of SMC proteins in chromatid cohesion*

SMC proteins are the most widely conserved family of long coiled-coil proteins (Rose *et al.*, 2005). SMC proteins regulate the structural and functional organisation of chromosomes from bacteria to humans with an especially crucial role in chromosome segregation during both mitosis and meiosis (Hirano, 2006). Most bacterial genomes contain a single *smc* gene whose product forms a homodimer. In eukaryotes, there are at least six different SMC proteins (SMC1-6) that form heterodimers in specific combinations. Each SMC subunit self-folds by anti-parallel coiled-coil interactions to form a hinge domain at one end and an ATP-binding head domain the other (Hirano, 2006).

A SMC2-SMC4 pair is a component of the condensin complex that is essential for the condensation of chromatin during chromosome assembly (Hirano, 2005). In metazoans, there are two types of condensin complexes, condensin I and condension II (Ono *et al.*, 2003; Hirano, 2012), whereas non-metazoan eukaryotes including yeasts have a single complex (Bazile *et al.*, 2010). All of the subunits of condensin I are highly conserved across eukaryotes, with the notable exceptions of the nematodes *Caenorhabditis elegans* and *Caenorhabditis briggsae* (Ono *et al.*, 2003). The subunits of condensin II, however, are found only in metazoans (Losada and Hirano, 2005).

A SMC1-SMC3 pair, along with two non-SMC regulatory subunits, Scc1 and Scc3, comprise the core of a cohesin complex that mediates sister-chromatid cohesion (Haering and Nasmyth, 2003). Individual cohesin complexes are predicted to embrace two sister chromatids within their coiled-coil arms and dissociate from the chromosomes prior to

mitosis. Separase, a cysteine protease, dissociates the sister chromatids by cleaving Scc1, a regulatory subunit of the cohesin complex.

### *SMC proteins are conserved across eukaryotes including Monosiga brevicollis*

Homologues of the four main proteins involved in sister-chromatid cohesion, SMC1, SMC3, Scc1 and Scc3, have been found across eukaryotes including metazoans, yeasts and plants (Cobbe and Heck, 2000; Jones and Sgouros, 2001; Losada and Hirano, 2005;). In this study, human SMC complex protein sequences were used to interrogate the proteome of *M. brevicollis* for homologues. Putative homologues of all known subunits of the condensin and cohesin complexes were detected with high sequence identity in choanoflagellates, represented here by *M. brevicollis* (Table 5.4.).

| **SMC complex protein** | **Ascension number of predicted homologues in *Monosiga brevicollis*** | **E-value** |
|---|---|---|
| **Condensin complex:** | | |
| SMC2 | XP_00174499.1 | 0.00 |
| SMC4 | XP_001745611.1 | 0.00E+00 |
| **Cohesin complex:** | | |
| SMC1a | XP_001745611.1 | 1.00E-44 |
| SMC1b | XP_001745612.1 | 2.00E-18 |
| SMC3 | XP_001746007.1 | 3.00E-115 |
| Scc1 | XP_001743156.1 | 3.00E-35 |
| Scc3 | XP_001744374.1 | 7.00E-36 |

**Table 5.4. Predicted protein homologues of components of the condensin and cohesin complexes identified in *Monosiga brevicollis*.** Query sequences were human.

### *Co-option of cohesin enabled synchronisation of the chromosome and centrosome cycles*

Separase, the protease responsible for dissociating the cohesion between sister chromatids by cleaving Scc1, has also been found to be essential for centriole disengagement (Uhlmann *et al.*, 1999; Tsou and Stearns, 2006; Thein *et al.*, 2007). The cohesin subunit Scc1 has been shown to localize to the centrosome and centrosomal Scc1 is cleaved by separase coincidentally with chromatin Scc1 during late mitosis (Nakamura *et al.*, 2009). Studies using engineered cohesin subunits suggested that the cohesin ring complex mediates both the paring of sister-chromatids and the pairing of a newly arising daughter centriole to its mother centriole (Schockel *et al.*, 2011). These pairings are mediated by a cohesin ring which provides a regulatory topological, rather than physical, linkage. The dual use of cohesin ensures coordination of the centrosome and chromosome-cycle and ensures that a newly forming daughter cell will receive one complete set of chromatids and one centrosome.

This cohesin complex between the mother and daughter centriole pair that is lost with mitotic exit is in addition to the protein linker, comprised of rootletin, C-Nap1 and Cep68, that connects the proximal ends of the two mother centrioles. This centriole linker is established with or slightly after centriole disengagement and that persists until the onset of mitosis.

The presence of cohesin proteins across eukaryotes including metazoans, yeasts and plants (Cobbe and Heck, 2000; Jones and Sgouros, 2001; Losada and Hirano, 2005), including non-ciliated organisms such as *Saccharomyces cerevisiae* and *Schizosaccharomyces pombe*,

suggests the ancestral and primary function of the cohesin complex is the pairing of sister-chromatids. Although is it not possible to detect the phylogenetic distribution of this functional duality through bioinformatics, it is interesting to speculate that this co-option of cohesin accompanied the synchronisation of the centrosome cycle with the chromosome cycle as a method to ensure the correct inheritance of centrioles in daughter cells.

## 5.4 Expansion of coiled-coil proteins in Metazoans

13 of the 15 core centrosomal proteins analysed in this study, excluding the GCP family of γ-tubulin complex components, contain coiled-coil domains, as predicted by the Coils2 program (Table 5.5.). Coiled-coil coverage ranges from 1.8% of the protein sequence in Cep170 to 78.4% in rootletin. The discovery that the majority of the core centrosomal proteins contain coiled-coil domains and that a single coiled-coil protein in choanoflagellates, MBCDH8, has potentially eight homologues in the Metazoa both suggest a possible expansion of a coiled-coil protein family in the Metazoa. Is there a significant difference between the number of coiled-coil proteins in metazoans compared to non-metazoans? And to what extent, if any, are centrosome-associated proteins members of a coiled-coil superfamily?

### 5.4.1 Introduction to coiled-coil proteins

The α-helical coiled-coil domain mediates subunit oligomerization of a large number of polymer proteins with analyses of protein sequences predicting that approximately 2-3% of all protein residues form coiled-coils (Wolf *et al.,* 1997). Coiled-coil domains consist of two or more alpha-helices winding around each other to form a super coil. On a primary structure level, coiled-coil domains are characterised by a heptad repeat pattern of

hydrophobic and polar residues (Burkhard *et al.,* 2001). Residues in the first and fourth position are hydrophobic and residues in the fifth and seventh position are predominately charged or polar.

The principal function of coiled-coil domains appears to be related to their ability to act as "cellular velcro"; holding together sub-cellular structures by acting as protein-protein interaction motifs (Rose *et al.*, 2005). Extracellular coiled-coil proteins also include cell adherence factors and components of the extracellular matrix components in metazoans (Odgren *et al.*, 1996). Long coiled-coil domains can also assemble to form mesh-works and scaffolds including the intermediate filaments of the cytoskeleton and nuclear lamina (Strelkov *et al.*, 2003).

| Centrosomal protein | Protein length | Total length of CC domains | % of protein in CC domains |
|---|---|---|---|
| Cep135 | 1140 | 827 | 72.5 |
| Cep164 | 1460 | 469 | 32.1 |
| Cep192 | 2537 | 0 | 0.0 |
| PCM-1 | 2024 | 269 | 13.3 |
| AKAP450 | 3907 | 1945 | 49.8 |
| Pericentrin | 3336 | 1296 | 38.9 |
| CP110 | 1012 | 109 | 10.8 |
| CEP97 | 865 | 34 | 3.9 |
| Ninein | 2046 | 1173 | 57.3 |
| ODF2 | 893 | 566 | 63.4 |
| CEP63 | 703 | 387 | 55.1 |
| Cep170 | 1584 | 28 | 1.8 |
| C-Nap1 | 2442 | 1898 | 77.7 |
| Rootletin | 2017 | 1581 | 78.4 |
| Cep68 | 757 | 0 | 0.0 |
| TSGA10 | 698 | 456 | 65.3 |

**Table 5.5. Prevalence and coverage of coiled-coil (CC) domains in human centrosomal proteins.** In all instances the total length, in amino acids, consists of multiple discontinuous coiled-coil domains.

Multiple coiled-coil predictor programs are available as well as publically-accessible databases of coiled-coil domains for completely sequenced genomes. Reports of coiled-coil predictions are inconsistent with predictions of coiled-coil domains of complete proteomes varying between 10 to 20% for the same organism (Liu and Rost, 2001; Rackham *et al.*, 2010; Szappanos *et al.*, 2010). The number of coiled-coil domains predicted in a protein sequence, or indeed a whole proteome, depends upon both the prediction algorithm and the cut-off for domain length used. Many of published studies do not use a cut-off for domain length to determine coiled-coils yet a minimum length of three to four heptad repeats, equivalent to a minimum domain length of approximately 20 amino acids, is required for the formation of a stable coiled-coil (Su *et al.*, 1994; Litowski and Hodges, 2001; Soppa, 2001).

Previous studies have highlighted a higher percentage of long coiled-coil proteins in eukaryotic genomes compared to prokaryotic genomes (Odgren *et al.*, 1996; Rose *et al.*, 2005). With increasing coiled-coil domain length cut-off, lower percentages of proteins were identified in bacterial genomes. In an analysis of 22 proteomes, including ten bacterial proteome sequence sets, predictions of coiled-coil domains over 400 amino acids in length were completely absent in bacteria but present in eukaryotes (Rose *et al.*, 2005). A study focusing on the occurrence of long coiled-coil domains, defined as domains greater than 75 amino acids, revealed a marked difference between the occurrence of extended coiled-coil domains in metazoans, representing 2.18% of total proteins, compared to 0.55% in non-metazoans (Odgren *et al.*, 1996). The average length of a coiled-coil domain in a metazoan protein sequence was 113 residues, twice the average in non-metazoan proteins at 50 residues. It was suggested that this apparent relationship between coiled-coil proteins and higher-order cell and tissue structure can be explained by the networks or matrixes of coiled-coil interactions that underlie metazoan differentiated cell and tissue structure.

Another study focused on the evolutionary relationships and conservation across phylogenetic groups of proteins with long coiled-coil domains (Rose *et al.*, 2005). Here, long coiled-coil domains were defined to include all sequences with at least one coiled-coil domain with a minimum length of 70 amino acids, two domains with a minimum length of 50, or three or more domains with a minimum length of 30. It revealed families of coiled-coil proteins that are specific to animals, including cytoskeletal components and centrosome-associated proteins. Interestingly, two of the largest clusters, consisting of proteins with coiled-coil domains longer than 250 amino acids or more than 60% coverage, SMC proteins and C-NAP proteins, are two protein families directly involved in centrosome

function. As highlighted previously, many of the centrosomal proteins highlighted in this study contain long coiled-coil domains (Table 5.6.). Proteins of the intercentriolar linker that mediates centriole-centriole cohesion, namely C-Nap1 and rootletin, and proteins that serve as a scaffold for the recruitment of PCM proteins, namely AKAP450 and pericentrin, all contain long coiled-coil domains. An expansion of coiled-coil protein families, and the increasing occurrence of long coiled-coil domains, may have been an important step in the evolution of metazoan cell structure.

| Protein | CC domains | CC domains >75aa | CC domains >100aa | CC domains >150aa | CC domains >200aa | CC domains >250aa | CC domains >400aa |
|---|---|---|---|---|---|---|---|
| CEP135 | Y | Y | Y | Y | Y | Y | Y |
| CEP164 | Y | Y | Y | Y | Y | N | N |
| CEP192 | N | N | N | N | N | N | N |
| PCM-1 | Y | N | N | N | N | N | N |
| AKAP450 | Y | Y | Y | Y | Y | Y | Y |
| Pericentrin | Y | Y | Y | Y | Y | Y | N |
| CP110 | Y | N | N | N | N | N | N |
| Cep97 | Y | N | N | N | N | N | N |
| Ninein | Y | Y | Y | Y | Y | Y | N |
| ODF2 | Y | Y | Y | Y | Y | Y | N |
| CEP63 | Y | Y | N | N | N | N | N |
| CEP170 | Y | N | N | N | N | N | N |
| C-NAP1 (CEP250) | Y | Y | Y | Y | Y | Y | Y |
| Rootletin | Y | Y | Y | Y | Y | Y | Y |
| CEP68 | N | N | N | N | N | N | N |
| TSGA10 | Y | Y | Y | Y | Y | Y | N |

**Table 5.6. Prevalence and coverage of coiled-coil (CC) domains of various lengths in human centrosomal proteins.** "Y" indicates the presence of a continuous coiled-coil domain longer than or equal to 75, 100, 150, 200, 250 and 400 amino acids.

This study will test and evaluate different coiled-coil predictors and review the phylogenetic occurrence of coiled-coil proteins and its relevance for the evolution of particular protein families. Does the appearance of centrosomal proteins in the Metazoa reflect an over-arching expansion of coiled-coil protein families? Given the interference of coiled-coil domains with predictions of homology, to what extent can it be determined that core centrosomal proteins arose from an expansion of a coiled-coil protein family in the Metazoa?

### 5.4.2 Identification of proteins with coiled-coil domains

Proteome sequence sets of 30 fully sequenced genomes were downloaded from public sequence databases. For details of sources, as well as information regarding numbers of protein predictions, see the supplementary material (Table S5.4). Where available, UniProtKB complete proteomes, a combination of manually reviewed (Swiss-Prot) and automatically annotated (TrEMBLE) proteins sets, were used. All proteomes used were non-redundant in the sense that all protein products encoded by one gene in a given species are represented in a single recording including alternative splicing isoforms, fragments, polymorphisms and sequence conflicts. The number of protein sequence entries reflects the annotation at the time of download.

An initial pre-processing of the FASTA files was conducted to remove all proteins sequences shorter than 30 amino acids. To identify proteins in the individual proteomes that contain one or more coiled-coil domains, two separate algorithms were used. First, the predictor COILS (Lupas *et al.*, 1991) was analysed using the web-based SMART (simple modular architecture research tool) program (Letunic *et al.*, 2009) using default settings. COILS, a commonly used predictor of coiled-coil structure, uses a position-specific scoring matrix containing amino acid frequencies in the seven heptad positions. To obtain a picture of the predictive power of the algorithm, the COILS output for the human proteome was compared to outputs from a second prediction algorithm, PairCoil2 (McDonnell *et al.*, 2006), an algorithm that also uses a position-specific scoring matrix. The resulting protein lists were cross-referenced and compared to the recently published SpiriCoil database created using a SUPERFAMILY approach of hidden Markov models (Rackham *et al.*, 2010).

The COILS output was post-processed and used to establish a database of coiled-coil prediction data for each organism. Selectivity criteria were applied to select sequences predicted to contain coiled-coil domains longer than or equal to 75, 100, 150, 200, 250 and 400 amino acids.

| Species | # of protein sequence entries | Total CC domains | | Total CC proteins | | | | CC domain > 75aa | | | | CC domain > 100aa | | | | CC domain > 150aa | | | | CC domain > 200aa | | | | CC domain > 250aa | | | | CC domain > 400aa | | | |
|---|---|---|---|---|---|---|---|---|---|---|---|---|---|---|---|---|---|---|---|---|---|---|---|---|---|---|---|---|---|---|---|
| | | # | | # | | % of proteins | | # | | % of proteins | | # | | % of proteins | | # | | % of proteins | | # | | % of proteins | | # | | % of proteins | | # | | % of proteins | |
| | | PairCoil2 | COILS | PairCoil2 | COILS | PairCoil2 | COILS | PairCoil2 | COILS | PairCoil2 | COILS | PairCoil2 | COILS | PairCoil2 | COILS | PairCoil2 | COILS | PairCoil2 | COILS | PairCoil2 | COILS | PairCoil2 | COILS | PairCoil2 | COILS | PairCoil2 | COILS | PairCoil2 | COILS | PairCoil2 | COILS |
| *Homo sapiens* | 90720 | 33644 | 19686 | 15972 | 12704 | 17.6 | 14.2 | 1089 | 2880 | 1.2 | 3.2 | 519 | 1895 | 0.6 | 2.1 | 207 | 1230 | 0.2 | 1.4 | 92 | 710 | 0.1 | 0.8 | 75 | 465 | 0.1 | 0.5 | 1 | 195 | 0.0 | 0.2 |
| *Gallus gallus* | 22194 | 10544 | 5621 | 4694 | 3498 | 21.1 | 15.9 | 418 | 863 | 1.9 | 3.9 | 206 | 603 | 0.9 | 2.7 | 77 | 386 | 0.3 | 1.8 | 40 | 252 | 0.2 | 1.1 | 24 | 175 | 0.1 | 0.8 | 4 | 91 | 0.0 | 0.4 |
| *Danio rerio* | 41478 | 18529 | 10143 | 8923 | 6629 | 21.5 | 16.0 | 663 | 1584 | 1.6 | 3.8 | 338 | 1103 | 0.8 | 2.7 | 107 | 629 | 0.3 | 1.5 | 61 | 390 | 0.1 | 0.9 | 32 | 273 | 0.1 | 0.7 | 3 | 117 | 0.0 | 0.3 |
| *Ciona intestinalis* | 19858 | 6255 | 3362 | 3133 | 2228 | 15.8 | 11.3 | 165 | 484 | 0.8 | 2.4 | 85 | 315 | 0.4 | 1.6 | 35 | 204 | 0.2 | 1.0 | 22 | 118 | 0.1 | 0.6 | 13 | 80 | 0.1 | 0.4 | 0 | 33 | 0.0 | 0.2 |
| *Strongylocentrotus purpuratus* | 28944 | 10240 | 5594 | 5213 | 3793 | 18.0 | 13.1 | 297 | 752 | 1.0 | 2.6 | 122 | 480 | 0.4 | 1.7 | 36 | 274 | 0.1 | 0.9 | 16 | 172 | 0.1 | 0.6 | 6 | 100 | 0.0 | 0.3 | 0 | 32 | 0.0 | 0.1 |
| *Drosophila melanogaster* | 21899 | 10161 | 6044 | 4750 | 3729 | 21.7 | 17.0 | 226 | 613 | 1.0 | 2.8 | 128 | 395 | 0.6 | 1.8 | 68 | 234 | 0.3 | 1.1 | 16 | 142 | 0.1 | 0.6 | 9 | 102 | 0.0 | 0.5 | 1 | 60 | 0.0 | 0.3 |
| *Caenorhabditis elegans* | 23397 | 5694 | 3900 | 3082 | 2731 | 13.2 | 11.7 | 144 | 493 | 0.6 | 2.1 | 62 | 318 | 0.3 | 1.4 | 26 | 160 | 0.1 | 0.7 | 11 | 99 | 0.0 | 0.4 | 6 | 56 | 0.0 | 0.2 | 0 | 29 | 0.0 | 0.1 |
| *Lottia gigantea* | 23851 | 5642 | 3317 | 3391 | 2439 | 14.2 | 10.2 | 111 | 381 | 0.5 | 1.6 | 39 | 213 | 0.2 | 0.9 | 11 | 94 | 0.0 | 0.4 | 2 | 43 | 0.0 | 0.2 | 1 | 16 | 0.0 | 0.1 | 0 | 2 | 0.0 | 0.0 |
| *Nematostella vectensis* | 27273 | 3764 | 2941 | 2304 | 2125 | 8.4 | 7.8 | 87 | 406 | 0.3 | 1.5 | 40 | 256 | 0.1 | 0.9 | 12 | 122 | 0.0 | 0.4 | 6 | 51 | 0.0 | 0.2 | 2 | 22 | 0.0 | 0.1 | 0 | 5 | 0.0 | 0.0 |
| *Trichoplax adhaerens* | 11520 | 2558 | 1942 | 1510 | 1333 | 13.1 | 11.6 | 51 | 245 | 0.4 | 2.1 | 19 | 147 | 0.2 | 1.3 | 5 | 70 | 0.0 | 0.6 | 1 | 33 | 0.0 | 0.3 | 0 | 12 | 0.0 | 0.1 | 0 | 0 | 0.0 | 0.0 |
| *Amphimedon queenslandica* | 30060 | 9169 | 5059 | 4975 | 3734 | 16.6 | 12.8 | 369 | 959 | 1.2 | 3.3 | 186 | 656 | 0.6 | 2.2 | 44 | 305 | 0.1 | 1.0 | 13 | 140 | 0.0 | 0.5 | 5 | 91 | 0.0 | 0.3 | 0 | 35 | 0.0 | 0.1 |
| *Monosiga brevicollis* | 9196 | 2963 | 2184 | 1557 | 1480 | 16.9 | 16.1 | 95 | 330 | 1.0 | 3.6 | 47 | 236 | 0.5 | 2.6 | 13 | 136 | 0.1 | 1.5 | 8 | 80 | 0.1 | 0.9 | 4 | 48 | 0.0 | 0.5 | 0 | 15 | 0.0 | 0.2 |
| *Salpingoeca rosetta* | 11731 | 7594 | 3827 | 3577 | 2506 | 30.5 | 21.4 | 274 | 517 | 2.3 | 4.4 | 131 | 347 | 1.1 | 3.0 | 45 | 204 | 0.4 | 1.7 | 18 | 143 | 0.2 | 1.2 | 9 | 98 | 0.1 | 0.8 | 3 | 46 | 0.0 | 0.4 |
| *Capsaspora owczarzaki* | 8792 | 3658 | 1961 | 1974 | 1371 | 22.5 | 15.6 | 90 | 234 | 1.0 | 2.7 | 37 | 146 | 0.4 | 1.7 | 12 | 76 | 0.1 | 0.9 | 6 | 40 | 0.1 | 0.5 | 3 | 23 | 0.0 | 0.3 | 1 | 9 | 0.0 | 0.1 |
| *Sphaeroforma arctica* | 25286 | 3354 | 1737 | 2372 | 1425 | 9.4 | 5.6 | 54 | 179 | 0.2 | 0.7 | 21 | 101 | 0.1 | 0.4 | 6 | 42 | 0.0 | 0.2 | 3 | 24 | 0.0 | 0.1 | 1 | 15 | 0.0 | 0.1 | 0 | 4 | 0.0 | 0.0 |
| *Spizellomyces punctatus* | 8804 | 3648 | 1880 | 1835 | 1277 | 20.8 | 14.5 | 86 | 258 | 1.0 | 2.9 | 38 | 167 | 0.4 | 1.9 | 9 | 100 | 0.1 | 1.1 | 5 | 58 | 0.1 | 0.7 | 4 | 42 | 0.0 | 0.5 | 0 | 14 | 0.0 | 0.2 |
| *Batrachochytrium dendrobatidis* | 8732 | 2363 | 496 | 1406 | 339 | 16.1 | 3.9 | 17 | 42 | 0.2 | 0.5 | 4 | 17 | 0.0 | 0.2 | 1 | 11 | 0.0 | 0.1 | 1 | 3 | 0.0 | 0.0 | 1 | 2 | 0.0 | 0.0 | 0 | 0 | 0.0 | 0.0 |
| *Allomyces macrogynus* | 17600 | 5090 | 2741 | 2647 | 1847 | 15.0 | 10.5 | 102 | 344 | 0.6 | 2.0 | 23 | 233 | 0.1 | 1.3 | 3 | 120 | 0.0 | 0.7 | 1 | 56 | 0.0 | 0.3 | 0 | 36 | 0.0 | 0.2 | 0 | 11 | 0.0 | 0.1 |
| *Neurospora crassa* | 9907 | 2747 | 1840 | 1672 | 1410 | 16.9 | 14.2 | 67 | 178 | 0.7 | 1.8 | 31 | 115 | 0.3 | 1.2 | 15 | 76 | 0.2 | 0.8 | 7 | 48 | 0.1 | 0.5 | 2 | 28 | 0.0 | 0.3 | 0 | 8 | 0.0 | 0.1 |
| *Schizosaccharomyces pombe* | 5143 | 1385 | 838 | 863 | 633 | 16.8 | 12.3 | 17 | 87 | 0.3 | 1.7 | 6 | 46 | 0.1 | 0.9 | 2 | 23 | 0.0 | 0.4 | 0 | 13 | 0.0 | 0.3 | 0 | 10 | 0.0 | 0.2 | 0 | 1 | 0.0 | 0.0 |
| *Saccharomyces cerevisiae* | 11081 | 2893 | 1697 | 1860 | 1317 | 16.8 | 12.2 | 44 | 150 | 0.4 | 1.4 | 18 | 78 | 0.2 | 0.7 | 8 | 44 | 0.1 | 0.4 | 4 | 25 | 0.0 | 0.2 | 0 | 18 | 0.0 | 0.2 | 0 | 9 | 0.0 | 0.1 |
| *Ustilago maydis* | 6522 | 1775 | 1198 | 1104 | 909 | 16.9 | 13.9 | 24 | 102 | 0.4 | 1.6 | 12 | 58 | 0.2 | 0.9 | 3 | 33 | 0.0 | 0.5 | 0 | 20 | 0.0 | 0.3 | 0 | 11 | 0.0 | 0.2 | 0 | 4 | 0.0 | 0.1 |
| *Thecamonas trahens* | 11582 | 7332 | 3547 | 2343 | 1733 | 20.2 | 15.0 | 156 | 456 | 1.3 | 3.9 | 70 | 344 | 0.6 | 3.0 | 23 | 215 | 0.2 | 1.9 | 12 | 136 | 0.1 | 1.2 | 9 | 95 | 0.1 | 0.8 | 3 | 39 | 0.0 | 0.3 |
| *Dictyostelium discoideum* | 12315 | 6958 | 4739 | 3335 | 3067 | 27.1 | 24.9 | 192 | 499 | 1.6 | 4.1 | 92 | 278 | 0.7 | 2.3 | 36 | 138 | 0.3 | 1.1 | 16 | 76 | 0.1 | 0.6 | 10 | 51 | 0.1 | 0.4 | 5 | 20 | 0.0 | 0.2 |
| *Entamoeba histolytica* | 9772 | 3425 | 2522 | 2118 | 1953 | 21.7 | 20.0 | 139 | 363 | 1.4 | 3.7 | 90 | 241 | 0.9 | 2.5 | 29 | 128 | 0.3 | 1.3 | 14 | 80 | 0.1 | 0.8 | 6 | 40 | 0.1 | 0.4 | 3 | 15 | 0.0 | 0.2 |
| *Arabidopsis thaliana* | 31921 | 6702 | 4386 | 4368 | 3460 | 13.7 | 10.8 | 102 | 470 | 0.3 | 1.5 | 32 | 276 | 0.1 | 0.9 | 7 | 155 | 0.0 | 0.5 | 3 | 86 | 0.0 | 0.3 | 1 | 51 | 0.0 | 0.2 | 0 | 16 | 0.0 | 0.1 |
| *Leishmania major Friedlin* | 8302 | 2050 | 2207 | 1011 | 1255 | 12.2 | 15.1 | 30 | 251 | 0.4 | 3.0 | 13 | 158 | 0.2 | 1.9 | 8 | 96 | 0.1 | 1.2 | 8 | 62 | 0.1 | 0.7 | 8 | 43 | 0.1 | 0.5 | 7 | 19 | 0.1 | 0.2 |
| *Tetrahymena thermophila* | 27769 | 21181 | 14354 | 8668 | 8177 | 31.2 | 31.0 | 376 | 1440 | 1.4 | 5.5 | 190 | 933 | 0.7 | 3.5 | 59 | 534 | 0.2 | 2.0 | 28 | 347 | 0.1 | 1.3 | 15 | 248 | 0.1 | 0.9 | 5 | 112 | 0.0 | 0.4 |
| *Mycobacterium tuberculosis* | 3975 | 182 | 109 | 147 | 94 | 3.7 | 2.4 | 2 | 4 | 0.1 | 0.1 | 0 | 2 | 0.0 | 0.1 | 0 | 0 | 0.0 | 0.0 | 0 | 0 | 0.0 | 0.0 | 0 | 0 | 0.0 | 0.0 | 0 | 0 | 0.0 | 0.0 |
| *Heliobacter pylori* | 1553 | 324 | 248 | 219 | 199 | 14.1 | 13.1 | 5 | 20 | 0.3 | 1.3 | 1 | 9 | 0.1 | 0.6 | 1 | 3 | 0.1 | 0.2 | 0 | 1 | 0.0 | 0.1 | 0 | 1 | 0.0 | 0.1 | 0 | 0 | 0.0 | 0.0 |

**Table 5.7: The number of coiled-coil (CC) proteins per genome.** The number of protein sequence entries reflects the annotation of ORFs at the time of download. The results from two coiled-coil predictor programmes, PairCoil2 and COILS, are shown. "Total CC domains" includes all domains predicted to form a coiled-coil: many proteins contain multiple coiled-coil domains. "Total CC proteins" represents the number of individual proteins predicted to contain coiled-coil domain(s). "CC domain > 75aa", for example, includes all protein sequences with at least one coiled-coil domain and a minimum domain length of 70 amino acids.

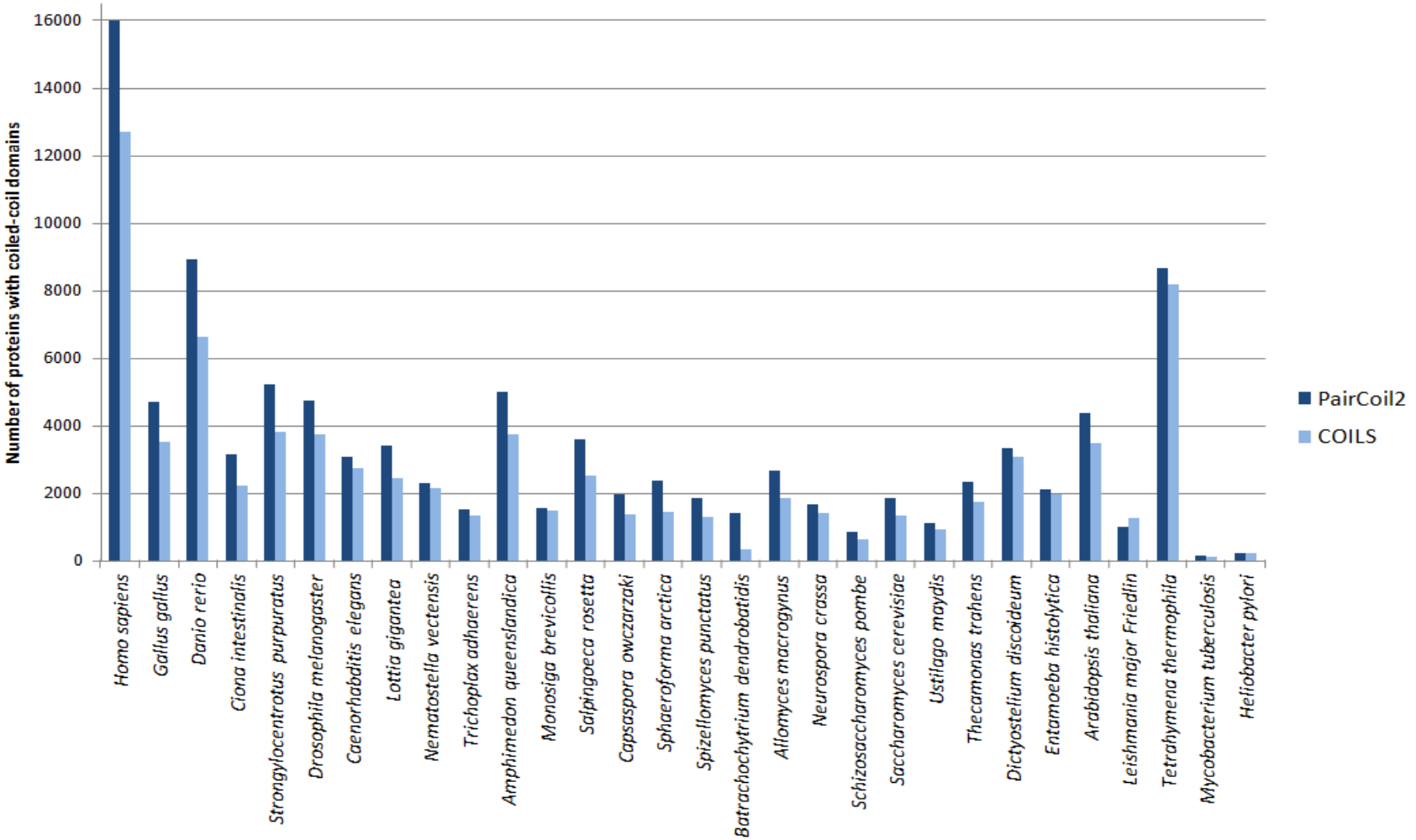


**Figure 5.6. The number of coiled-coil proteins per genome.** The results from two coiled-coil predictor programmes, PairCoil2 and COILS, are shown.

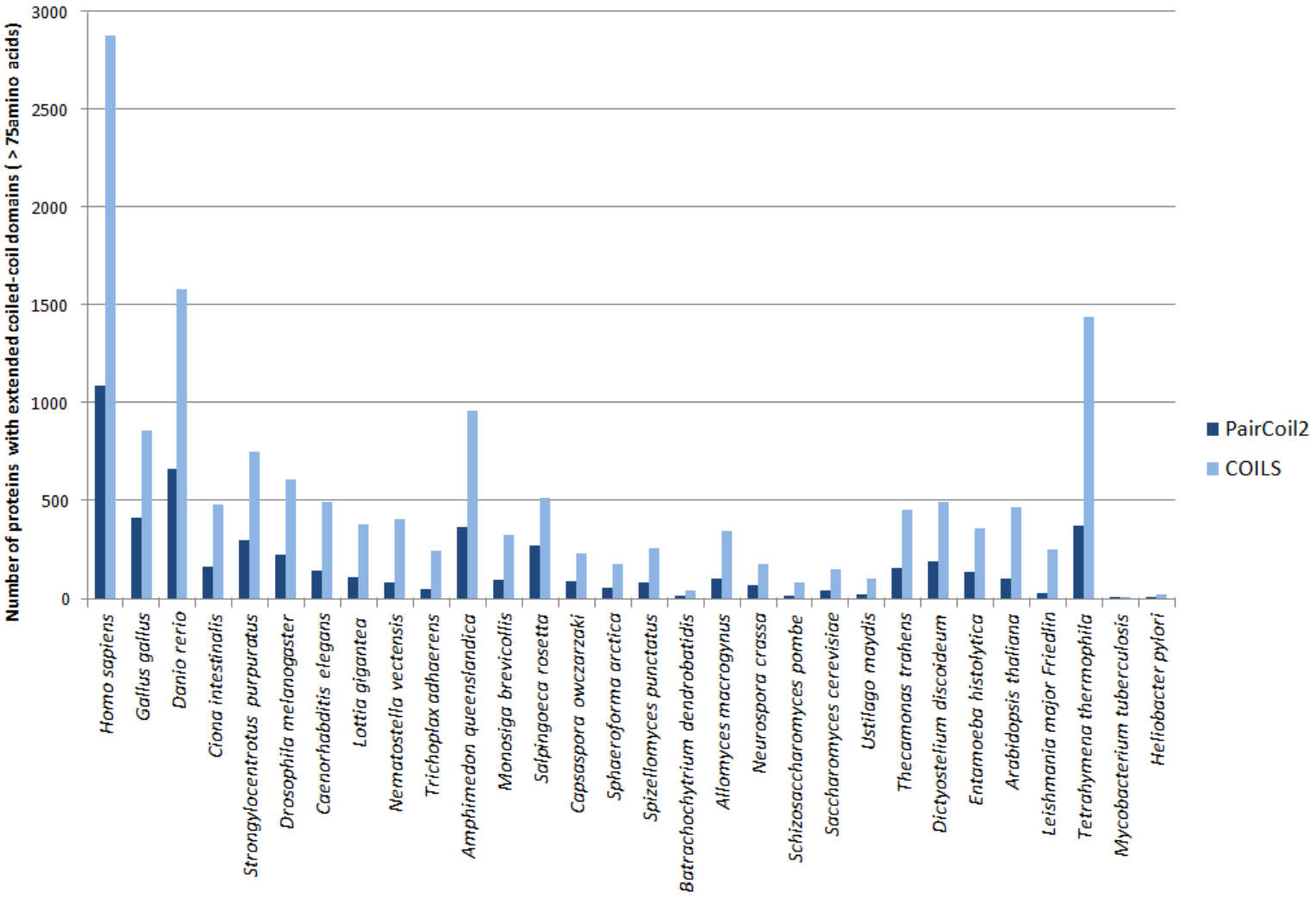


**Figure 5.7. The number of proteins predicted to contain extended coiled-coil domains.** These proteins contain at least one coiled-coil domain with a minimum length of 70 amino acids. The results from two coiled-coil predictor programmes, PairCoil2 and COILS, are shown.

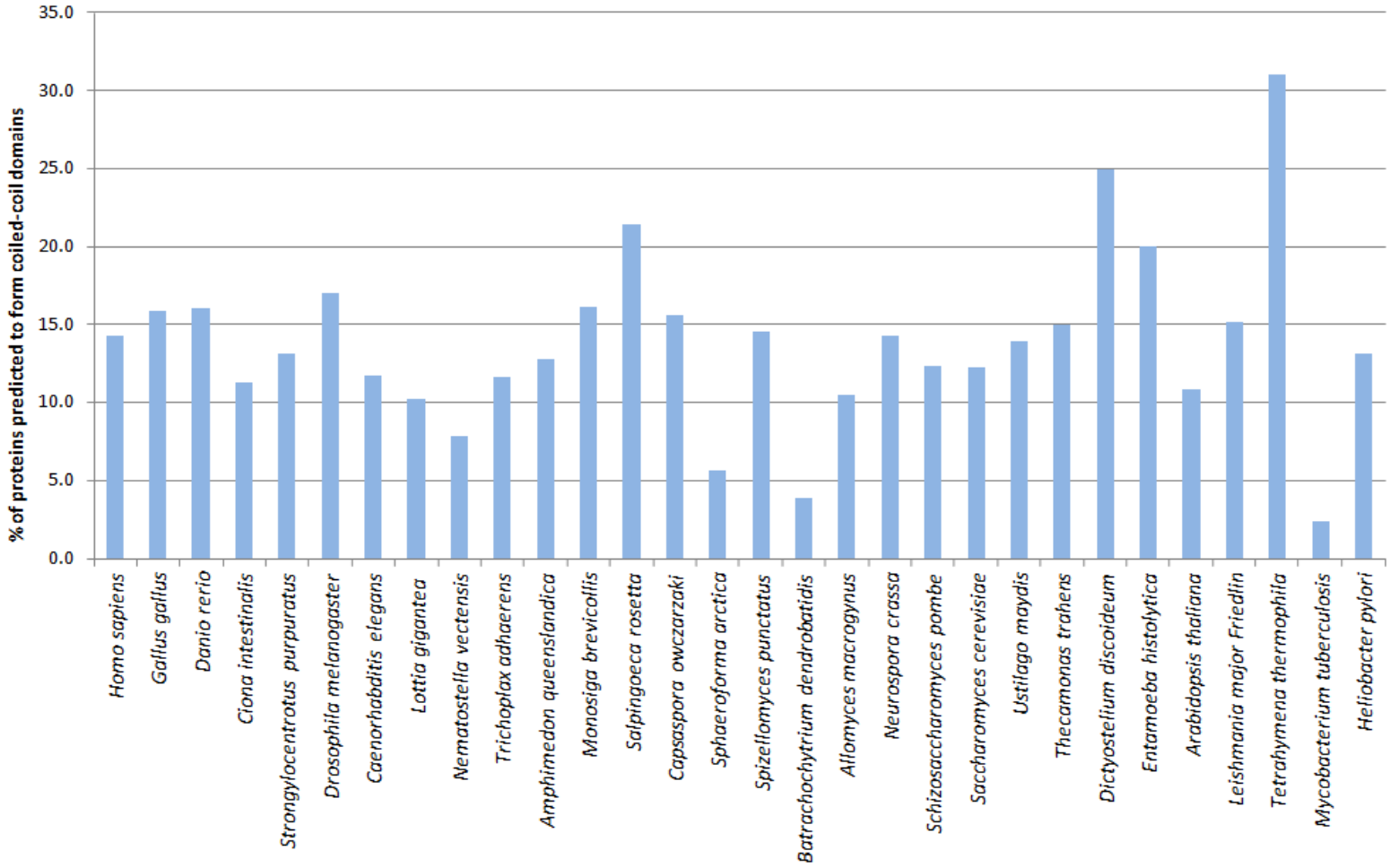


**Figure 5.8. The percentage of total proteins in a range of eukaryotic and prokaryotic taxa that are predicted to contain coiled-coil domains.** Predictions made using the COILS algorithm.

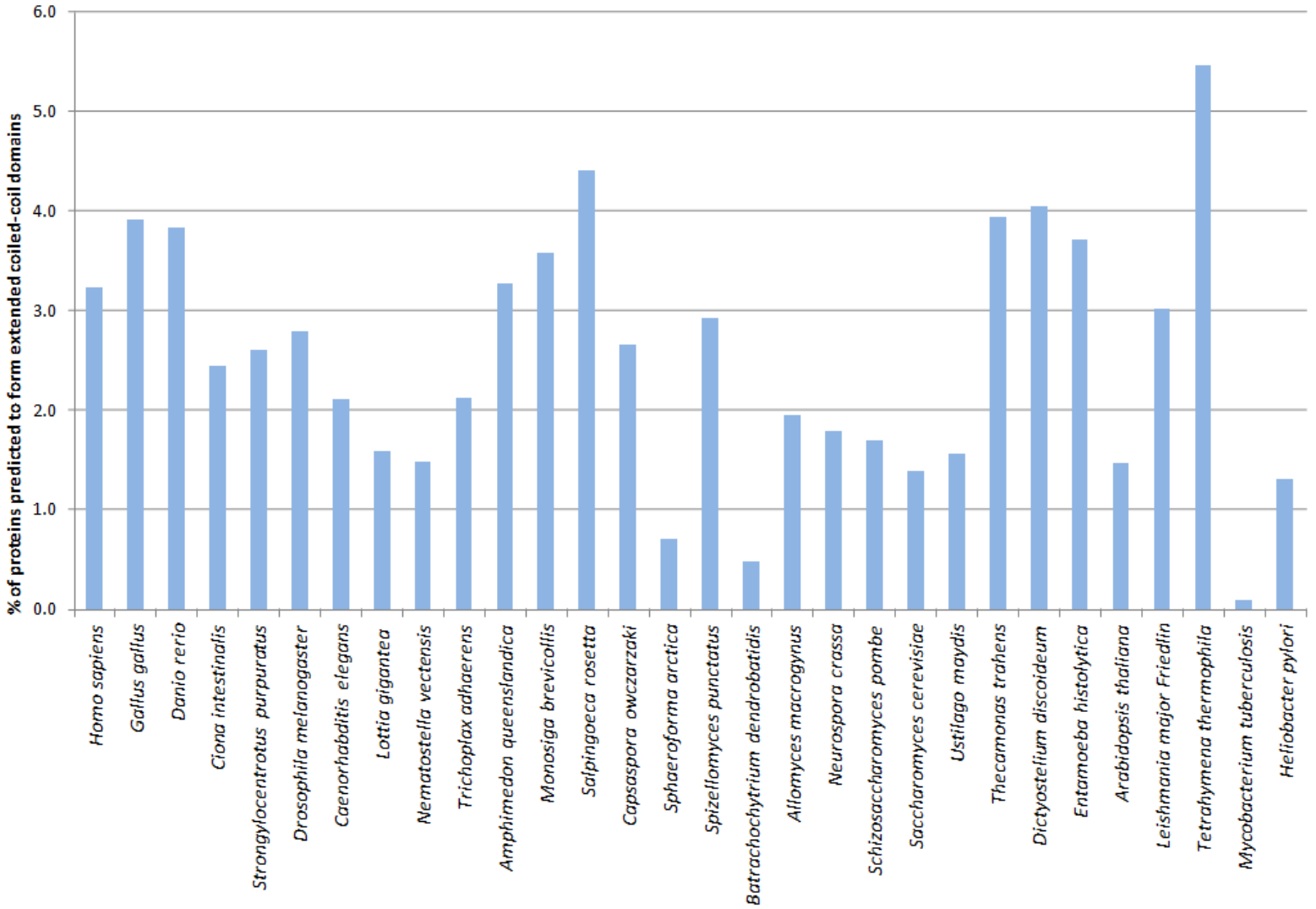


**Figure 5.9. The percentage of total proteins in a range of eukaryotic and prokaryotic taxa that are predicted to contain extended coiled-coil domains.** Includes proteins predicted to contain at least one coiled-coil domain with a minimum length of 70 amino acids. Predictions made using the COILS algorithm.

### 5.4.3 Performance of coiled-coil predictors

The PairCoil2 algorithm predicted a significantly greater number of coiled-coil proteins compared to the COILS algorithm in all proteomes analysed (Table 5.7. and Fig. 5.6.; Wilcoxon Signed Ranks Test: $p$ = 0.00). COILS predicted 14.0% of total proteins (total proteins of all 30 genomes combined) to contain coiled-coil regions compared to 17.7% by PairCoil2. The direction of this observed difference in the sensitivity of predictor programs is reversed when focusing on the number of proteins predicted to contain long coiled-coil domains. COILS predicted the occurrence of extended domains (coiled-coil proteins with at least one domain longer than 75 amino acids) to represent 2.8% of total proteins compared to 1.0% of total proteins predicted by PairCoil (Wilcoxon Signed Ranks Test: $p$ = 0.00). This trend holds true for all proteomes analysed and for all extended coiled-coil domain length cut-offs (100, 150, 200, 250 and 400 amino acids) (Table 5.7. and Fig. 5.7.). Noticeably, PairCoil2 reported no coiled-coil domains over 250 amino acids in *Thecamonas adhaerens* or in four fungi genomes, *Allomyces macrogynus, Schizosaccharomyces pombe, Saccharomyces cerevisiae* and *Ustilago maydis,* despite COILS reporting 12, 36, 10, 18 and 11 respectively (Table 5.7.).

The resulting lists of human proteins predicted to contain coiled-coil domains were examined for each predictor programme and revealed that only the COILS output included all the human centrosomal coiled-coil proteins described in this study (Table 5.5.). Both the PairCoil2 output and the publically available SpiriCoil database are missing the centrosomal proteins rootletin, Cep152 and ninein.

### 5.4.4 Frequency of coiled-coil proteins

Proteins predicted to form coiled-coil domains were present in all proteomes analysed and comprised between 2.4% and 31% of the protein sets (Table 5.7 and Fig. 5.8.). COILS reported that 12.9% of metazoan, 14.2% of eukaryotic and 7.7% of bacterial proteins have coiled-coil regions. There was no significant difference, however, in the proportion of proteins containing coiled-coil domains in metazoans compared to non-metazoans (Mann-Whitney test: U = 88.0, $p$ = 0.478) nor in vertebrates compared to invertebrates (Mann-Whitney U test: U = 3.0, $p$ = 0.07). Comparatively high contents of coiled-coil proteins were detected in *Salpingoeca rosetta*, *Dictyostelium discoideum* and *Tetrahymena thermophila* (Fig. 5.8.).

More significant differences between proteomes were observed in the proportion of proteins predicted to contain long coiled-coil domains (Table 5.7. and Fig. 5.9.). The occurrence of extended domains (coiled-coil proteins with at least one domain longer than 75 amino acids) is significantly higher in vertebrate metazoans with 3.5% of vertebrate proteins containing extended coiled-coil domains compared to 2.3% of invertebrate proteins (Mann Whitney test: U = 1.0, $p$ = 0.024). This trend remains significant for all other coiled-coil domain length cut-offs. There was, however, no significant difference in the proportion of proteins containing extended coiled-coil domains in metazoans compared to non-metazoans (Mann Whitney test: U = 89.5, $p$ = 0.518).

Surprisingly high contents of extended coiled-coils were reported in choanoflagellate proteins (4.0%) compared to metazoans (2.7%) and other unicellular eukaryotes (2.6%). This trend holds true for all other coiled-coil domain length cut-offs.

Lower percentages of bacterial proteins were predicted to contain extended domains: 1.4% of bacterial proteins have coiled-coil domains longer than 75 amino acids. Prediction of coiled-coil domains over 400 amino acids were completely absent in bacterial proteomes (Table 5.7.).

### 5.4.5 Discussion: coiled-coils and the evolution of the centrosome

Here the performance of the programs, PairCoil2, COILS and SpiriCoil were compared and uses to evaluate whether the emergence of core centrosomal proteins in the Metazoa reflects an overarching expansion of coiled-coil proteins

Previous comparative studies have suggested that PairCoil2 shows superior performance to COILS (Delorenzi and Speed, 2002; McDonnell *et al.*, 2006,). Here, PairCoils2 predicted a significantly greater number of coiled-coil proteins compared to the COILS algorithm, yet only for proteins containing short coiled-coil domains. COILS was more sensitive at detecting extended coiled-coil domains.

The performance of a predictor program may therefore depend upon the length as well as the type or family of coiled-coils. Coiled-coils, despite their rather simple structural architecture, are extremely versatile and exist in 16 different oligomeric states organised into 119 super-families (Rackham *et al.*, 2010). Sensitivity and specificity for various coiled-coil predictors has been shown to vary between families of coiled-coil proteins. In this study, long centrosomal proteins in particular were not identified by either SpiriCoil or PairCoil2. These observed differences in sensitivities and specificities may be explained by the size and diversity of the training set that was used to refine a predicator algorithm. Published

improvements to existing predictor programmes describe the increase in the number of families that are used in a new training set that were not included in the training of older programs (McDonnell *et al.*, 2006). For example, the COILS method, shown here to be more sensitive at detecting the long centrosomal proteins, was trained primarily on long, dimeric coiled-coils and therefore may not recognise the wide variety of sequences observed to adopt the coiled-coil fold. Although coiled-coil predictors are frequently reported to have relatively low sensitivity, sometimes recognising less than half of the coiled-coil residues actually present, they do have a high specificity, in which they produce a small number of false positives by mis-predicting residues in other structures as coiled-coils, than other types of protein predictor programs (Szappanos *et al.*, 2010). It is important to note, however, that, in the absence of an analysis of potential false negatives and false positives of all families of coiled-coils, restricted here to centrosomal proteins, the number of predicted proteins does not give an indisputable indication of performance.

This study, in line with previous studies, highlights the pervasive presence of coiled-coil domains. As predicted by the COILS predictor program, 14.2% of eukaryotic and 7.7% of prokaryotic proteins have coiled-coil regions. Where no minimum length of coiled-coil domain is defined, previous studies report a range of values between 10% and 20% for eukaryotic genomes (Liu and Rost, 2001; Barbara *et al.*, 2007) and between 2% and 5% for prokaryotic genomes (Odgren *et al.*, 1996; Liu and Rost, 2001; Rose *et al.*, 2005). Lower percentages of bacterial proteins were predicted to contain extended domains: 1.4% of bacterial proteins have coiled-coil domains longer than 75 amino acids. Prediction of coiled-coil domains over 400 amino acids were completely absent in bacterial proteomes. SMC proteins, the largest group of prokaryotic coiled-coil domain proteins, are characterised by

two coiled-coil domains separated by a hinge domain. The discontinuity of coiled-coil domains in SMC proteins is therefore likely to warrant their omission from counts of extended coiled-coil domains.

A proportion of the coiled-coil proteins exclusive to eukaryotes include those of centrosome structures. In addition to the coiled-coil proteins of the centriole-based centrosome, coiled-coil proteins also constitute significant structural roles in other centrosomal structures. Genetic and biochemical techniques have identified approximately 50 proteins that are either part of or closely associated with the spindle pole body, the microtubule-organising centre of budding yeast (Costanzo *et al.*, 2000). 24 of these proteins are predicted to contain at least one coiled-coil (Newman *et al.*, 2000). The multiple interactions between these proteins, in which 17 of the 24 proteins make 51 interactions amongst themselves, play a major role in organising and anchoring the SPB (Newman *et al.*, 2000). Interestingly, it is a coiled-coil protein of the PCM domain of the animal centrosome, namely pericentrin, that suggests the SPBs of yeast and fungi are the functional homologues of the PCM domain of the centriole-based centrosome. A central SPB structural protein, SPC110, has been identified to contain a calmodulin-binding site that is similar to kendrin, an alternatively spliced product of the same gene of pericentrin that also localises to the centrosome (Flory *et al.*, 2000; Flory and Davis, 2003). Coiled-coil proteins also play an important structural role in the nucleus associated body (NAB) of *Dictyostelium discoideum* (Blau-Wasser *et al.*, 2009). The NAB consists of a box-shaped core surrounded by the corona, an amorphous matrix functionally equivalent to the PCM of the animal centrosome (Ueda *et al.*, 1999).

This study, however, was unable to reproduce previously published reports of a significant difference between the number of extended coiled-coil domains, defined here as at least 75 amino acids in length, in metazoans compared to non-metazoans (Odgren *et al.*, 1996). There was, however, a significant higher number of extended coiled-coil domains in vertebrates compared to invertebrates.

Given the repeat nature of the coiled-coil domain, it is incredibly difficult to clearly determine homology relationships between coiled-coil proteins, especially those with extended coiled-coil domains. The heptad repeats ensures a low complexity of sequence and coiled-coil proteins are more likely to be similar even if they are not homologous in the true evolutionary sense of the term. A SUPERFAMILY approach, successfully applied to another class of "difficult" protein structures, namely membrane proteins (Wilson *et al.*, 2007), has recently been extended to coiled-coil proteins (Rackham *et al.*, 2010). This process groups together domains that share a common evolutionary ancestor, with each superfamily representing a single *de novo* evolution of a protein fold, of which 119 have been identified to contain coiled-coils. The different oligomeric states of coiled-coil domains have not evolved by morphologically changing over evolution from one to another, but rather were each independently created, sometimes more than once. The vast majority of coiled-coils, therefore, having been formed at the point of the *de novo* creation of a whole protein domain containing coiled-coils, and present in 16 different oligomeric states, have been predicted to have arisen independently well over 100 times (Rackham *et al.*, 2010). Given their rather simple structural architecture yet high versatility, this widespread occurrence is perhaps not surprising. Coiled-coils were present in the last universal common ancestor in almost all of the 16 oligomeric states, the exceptions being one eukaryote-

specific state, two states that are missing from the Archaea and three bacteria-specific states (Rackham *et al.*, 2010). The majority of superfamilies were present in the last universal common ancestor but there has been noticeable expansion in eukaryotes, with 22 superfamilies appearing between the eukaryote superkingdom being formed and the divergence into animal, plant and fungi kingdoms. Indeed, SMCs are one of only two large coiled-coil protein families to be present in both eukaryotes and prokaryotes (Rose *et al.*, 2005). Another expansion is noticeable in animals with 12 super-families appearing being the emergence of animals and chordates. This pattern of evolution is not significantly different from that for other superfamilies with different structural characteristics (Chothia and Gough, 2009).

Extended coiled-coil proteins are prevalent in both the centriole and PCM domain of the metazoan centrosome. The two proteins whose function is restricted to basal bodies and which are present across eukaryotes, Cep135 and Cep164, also contain extended coiled-coil proteins. The coiled-coil proteins of the centriole domain restricted to metazoans, CP110, Cep97, ninein, Cep63, Cep170, C-NAP1, rootletin and TSGA10, may have arisen from either the expansion of a pre-existing coiled-coil superfamily or from the de novo creation of the coiled-coil domain. Although interference of the coiled-coil domains with algorithmic predictors of homology hinders a definitive answer, the identification of shared SMC domains between certain centrosomal proteins and the discovery that a single coiled-coil protein in choanoflagellates, MBCDH8, has potentially eight homologues in the Metazoa, both support the former hypothesis that certain core centrosomal proteins, namely Ninein, Rootletin, CNAP-1, Cep63, Cep135 and TSGA10, arose from an expansion of a coiled-coil protein family.

A previous study identified a family of centrosome-associated proteins to be restricted to mammals but, although the cluster is mentioned to include ninein and C-NAP1, no further information on the identity of the other centrosome-associated proteins in this cluster was provided (Rose *et al.*, 2005). An examination of the proteome sequence sets analysed also revealed that *Caenorhabditis elegans* and *Drosophila melanogaster* were the only non-mammalian metazoans included in the data set (Rose *et al.*, 2005). These two organisms are renowned for their unusual centriole structures and, as observed in this study for *Caenorhabditis elegans* in particular, divergent centrosomes.

The SPB of yeast, the NAB of *Dictyostelium discoideum* and the animal centrosome are often stated as functional equivalents yet published reports rarely extended to a discussion of homology. All three structures contain significant coiled-coil proteins yet, with the exception of pericentrin and SPC110 already discussed, this characteristic does not necessarily imply a direct relationship between the proteins of the respective structures. Indeed, most researchers have failed to identify homologues of a respective centrosome's constituent proteins in other lineages (Blau-Wasser *et al.*, 2009). The clear exceptions to this, however, are proteins directly associated with microtubules, namely components of the gamma-tubulin complexes. Some centrosome proteins of *Dictyostelium discoideum*, for example, were identified based on their homology to their mammalian counterparts. All of these proteins, including γ-tubulin (Euteneuer *et al.*, 1998), DdCP224 (Graf *et al.*, 2000), EB1 (Rehberg and Graf, 2002), Spc97 and Spc98 (Daunderer and Graf, 2002) are associated with the microtubule nucleating machinery of the gamma-tubulin complexes. For example, EB1 is a microtubule tracking protein that associates with the plus-end of microtubules, and Spc97 and Spc98 are homologues of components of the gamma-tubulin complex, GCP2 and GCP3

respectively. As shown in the study, this conservation of microtubule nucleation is apparent across the eukaryotes with GCP2 and GCP3, components of the γTuSC, found in all eukaryotes analysed except *Caenorhabditis elegans*. The ubiquity of the components of γ-TuSCs, GCP2 and GCP3 suggests their presence in the last common ancestor of eukaryotes. It is perhaps these components alone that are shared between the different centrosome structures found in eukaryotes.

Given the interference of the repeating pattern of coil domains with sequence comparison algorithms and the subsequent difficulties in predicting homology between coiled-coil proteins, it is therefore difficult to confirm whether the centrosome-associated proteins are indeed part of a coiled-coil superfamily. However, as previously discussed, gene duplication has certainly played a role in the evolution of a centriole proteins of the centrosome. The three pairs of paralogues identified in this study (AKAP450 and pericentrin; C-NAP1 and rootletin; TSGA10 and Cep135) are the result of gene duplications in the metazoan lineage.

## 5.5 Choanoflagellates as a model organism to study MTOCs

All MTOCs, which include centrosomes, basal bodies and spindle pole bodies, have at their centre γ-tubulin. As this study has shown, it is the components of the γ-tubulin complexes that are widely and consistently conserved and the ubiquity of components of γ-TuSCs, namely GCP2 and GCP3, in eukaryotes suggests their presence in the last common ancestor of eukaryotes. Although basal bodies associated with an axoneme were also present in the last common ancestor or eukaryotes, centrioles and their associated centrosomal appendages are present only in the Metazoa.

Choanoflagellates have a number of advantages for studying MTOCs. Firstly, as the closest known relatives of animals, they are a model system for testing specific hypotheses about animal origins and the emergence of animal-specific structures, in this instance the centriole domain of the centrosome. Secondly, sequencing of the *Monosiga brevicollis* and *Salpingoeca rosetta* genomes has facilitated the identification of genes that encode γ-tubulin complex proteins. Thirdly, as this study of the phylogenetic distribution of centrosomal proteins has shown, and as supported by information from previous electron microscopy studies on the ultrastructure of mitosis in choanoflagellates, choanoflagellates are here proposed to posses an intermediate stage in the evolution of a centriole-based centrosome.

As previously discussed, a blast search of the *M. brevicollis* and *S. rosetta* genome databases with human GCP protein sequences revealed strong GCP2-6 homologues exist in both species. Although all the selected components of the PCM domain were identified to be present in choanoflagellates, no single component of the centriolar domain appears to be present outside of the Metazoa. Building on this discovery that the components of the centriole domain originated in the Metazoa, this study also revealed the possibility of a single ancestral gene that duplicated and diverged in the metazoan lineage to form many of the components of the centriole domain. This ancestral coiled-coil protein, represented by an extant homologue in *M. brevicollis*, named MBCDH8, duplicated after the isolation of the Metazoan lineage to form a family of a coiled-coil proteins. These duplication events occurred in a stepwise fashion throughout the evolution of the Metazoa.

### *γ-tubulin and eukaryotic microtubule organising centres*

γ-tubulin is a widely accepted as a marker of MTOCs in diverse eukaryotes (Oakley and Oakley, 1989; Stearns *et al.*, 1991; Zheng *et al.*, 1991; Oakley, 1992; Stearns and Kirschner, 1994). Indeed, it is the most conserved component of MTOCs.

Oakley *et al.* (1990) showed by immunofluorescence microscopy that in *Aspergillus nidulans*, a filamentous fungus, γ-tubulin is located at the fungal MTOC, the spindle pole body. Subsequently, Zheng *et al.* (1991) and Stearns *et al.* (1991) demonstrated that in the Metazoa, represented by *Drosophila melanogaster*, *Xenopus laevis* and mammalian cells, γ-tubulin is located in the centrosome, specifically the pericentriolar material where it is thought to bind to the minus end of microtubules as part of a γ-tubulin complex. Unlike α- and β-tubulin, γ-tubulin is usually restricted to the microtubule nucleation machinery and is undetectable in microtubules *per se* (Oakley, 1992). Immunofluorescence microscopy of *Leishmania tropica* and *Trypanosoma brucei*, however, revealed the presence of γ-tubulin in both the flagellum and the sub-pellicular microtubules of the cell body, as well as the basal body MTOC (Scott *et al.*, 1997; Libusova *et al.*, 2004).

To further characterise the nature of the choanoflagellate MTOCs, data was collected on the distribution patterns of γ-tubulin in a variety of choanoflagellate species.

### 5.5.1 Immunofluorescence microscopy: elucidating the nature of the mitotic MTOC in choanoflagellates

Two anti-γ-tubulin antibodies, GTU-88 and γ-TUB, were used to assign the sub-cellular localization of γ-tubulin in three choanoflagellate species, *Monosiga brevicollis*, *Monosiga ovata* and *Stephanoeca diplocostata* (Fig. 5.10.). For a better orientation, DNA-binding dye was used to visualize the nucleus. Flagella and the array of rootlet microtubules were

stained with a monoclonal antibody TAT1 against α-tubulin. Details regarding cell culture conditions and immunofluorescence microscopy procedure are further outlined in the Materials and Methods.

Immunofluorescence staining with the TAT1 antibody decorated the rootlet microtubules and flagella, as described previously in chapter three. This, along with DAPI staining of the nucleus, allowed individual cells to be identified. Immunofluorescence staining of γ-tubulin with both GTU-88 and γ-TUB showed a different localisation to that for α-tubulin. Cells throughout the population shows a general low level fluorescence, sometimes punctuate, over the cell body. Both anti-γ-tubulin antibodies failed to stain flagella and no γ-tubulin was detected in the nucleus.

Intense staining of the basal body region was observed with both anti-γ-tubulin antibodies for both *M. brevicollis* and *S. diplocostata*. This observation varied throughout the population and was not visible in cells without a flagellum. Although it is possible to establish the orientation of a cell from the outline of its microtubule rootlets and determine whether a flagellum, if present, should be visible, it is not possible to distinguish whether a flagella is absent due to damage during centrifugation or fixation of the culture or whether the flagella has been retracted prior to mitosis. Indeed, it was observed that in *S. diplocostata* the flagellum is not retracted during cell division with two flagella observed within individual cells (Fig. 4.7.4b). The presence or absence of a flagellum, therefore, is not a reliable method for establishing position in the cell cycle. Indeed, any establishment of position in the cell cycle was restricted here to observations of the DAPI-stained nucleus and the rare observation of two pairs of basal bodies. Although staining of the profuse

microtubule rootlets obscured any identification of a basal body structure using an anti-α-tubulin antibody, the intense staining of the basal body region using anti-γ-tubulin antibodies in *M. brevicollis* and *S. diplocostata* enabled the identification of the basal bodies migrating to or at nuclear poles. Given the extremely slow growth rate of choanoflagellate cultures, however, very few cells were discerned to be in mitosis and it was not possible to determine if the intensity of labelling was cell-cycle dependent.

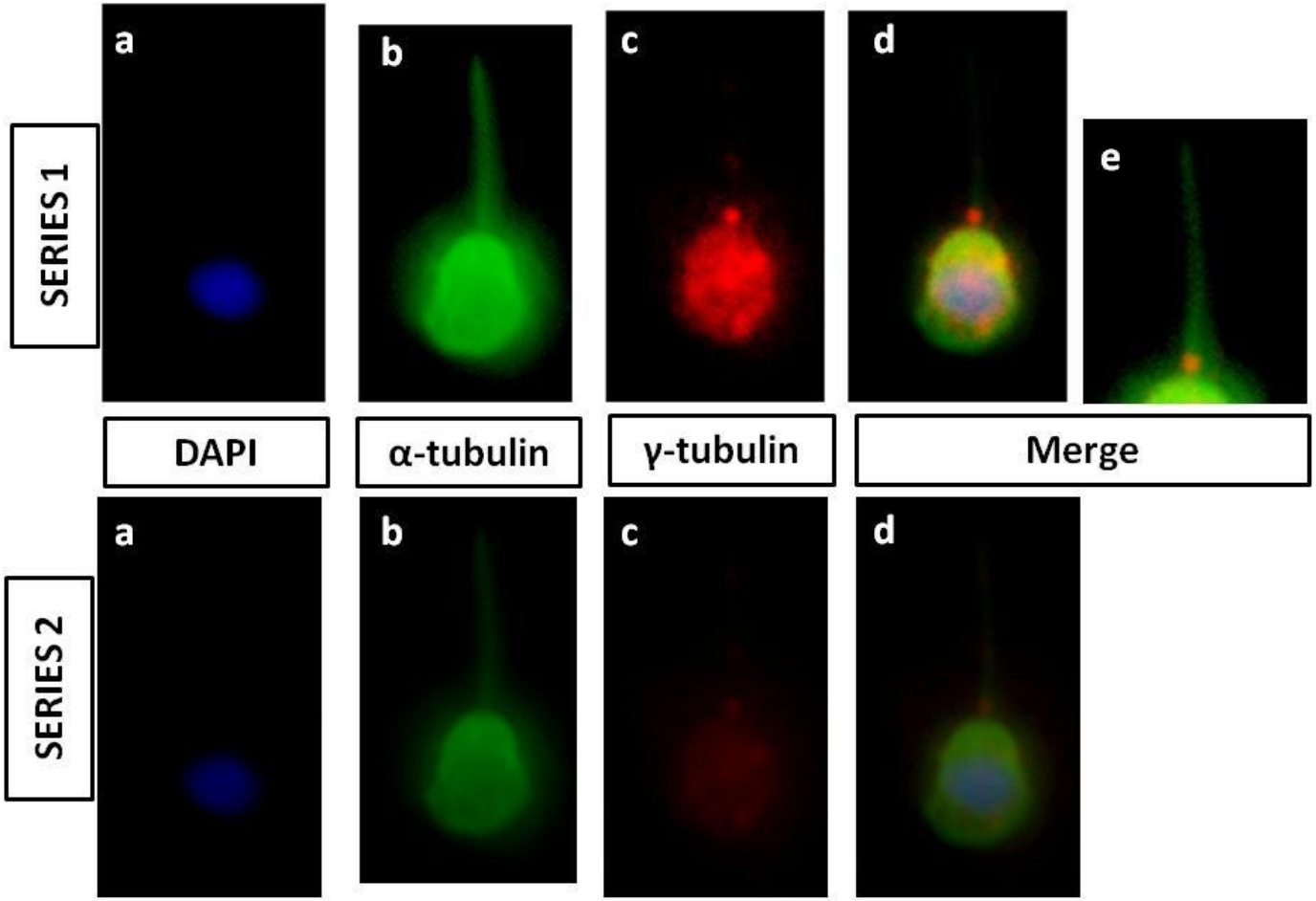


**Figure 5.10.** The results of immunofluorescence on *Monosiga brevicollis* using anti-α-tubulin and anti-γ-tubulin antibodies and DNA-binding dye (DAPI). **Series 1** represents refined images to show the major staining pattern of γ-tubulin (red) more clearly. **Series 2** shows unadjusted images.

(a) DNA content of the cell (blue)

(b) α-tubulin (green)

(c) γ-tubulin (red)

(d) The DNA content, α-tubulin and γ-tubulin staining patterns are shown merged together to show the relative positioning.

(e) Focus on the γ-tubulin staining of the basal body at the base of the flagellum.

### 5.5.2 Discussion: the mitotic MTOC in choanoflagellates

Although it is impossible to demonstrate by immunofluorescence microscopy that γ-tubulin is entirely absent from microtubules, it can be demonstrated that it is predominately associated with other sub-cellular locations, in this instance the basal body and the cell body cytoplasm. This is in agreement with previous reports that report that γ-tubulin is undetectable in microtubules (Oakley, 1992). Irregular findings of γ-tubulin along eukaryotic flagella in *Leishmania major* and *Trypanosoma brucei* may be explained by an interaction between γ-tubulin and proteins of the filamentous paraflagellar rod that lies alongside the whole length of the axoneme in Trypanosomatidae promastigotes (Scott *et al.*, 1997; Libusova *et al.*, 2004).

Whilst at first sight the low intensity of staining using anti-γ-tubulin antibodies over the cell body might be taken as background staining, it was a consistent occurrence and the described staining pattern was similar with both anti-γ-tubulin antibodies, no matter what fixation or staining procedure was applied. The γ-tubulin staining in the cell body may reflect a distributed cytoplasmic pool of γ-tubulin. Moudjou *et al.* (1996) also identified the close association of γ-tubulin with centrioles as well as the fact that in mammalian cells over 80% of total γ-tubulin resides as a cytosolic form. In human cells, this cytosolic pool of γ-tubulin is involved with large complexes, possibly γ-TuRCs, not associated with the centrosome (Moudjou *et al.*, 1996). Similar cytoplasmic pools of γ-tubulin were observed in *Xenopus* egg and somatic cells and in human HEK293 cells (Stearns *et al.*, 1991). The homogenous distribution in the cytoplasm may mean that cytoplasmic pools of γ-tubulin are often not detected by classical immunofluorescence techniques (Moudjou *et al.*, 1996).

No γ-tubulin was detected in the nucleus. Localisation of γ-tubulin to the nucleus, even during interphase, is reminiscent of the inner plaques of SPBs of yeasts and other fungi (Spang *et al.*, 1996; Xiong and Oakley, 2009). Antibody staining of γ-tubulin in other eukaryotes that undergo closed mitosis, in which the nuclear envelope remains intact, also recognises MTOC structures in the nucleus. In fact, nuclear γ-tubulin has only ever been described in organisms with intranuclear mitosis. Intranuclear MTOCs have been identified in, for example, *Entamoeba histolytica* (Gomez-Conde *et al.*, 2000), *Trypanosome brucei* (Scott *et al.*, 1997), *Leishmania tropica* (Libusova *et al.*, 2004), *Paramecium tretraurelia* (Klotz *et al.*, 2003) and *Euplotes octocarinatus* (Curtenaz *et al.*, 1997), all of which display closed mitosis. Although mitosis in choanoflagellates has been observed to be only "semi-open" (Raikov, 1982; Karpov and Mylnikov, 1993; Leadbeater, 1994; Karpov and Leadbeater, 1997) the lack of nuclear γ-tubulin suggests that the MTOC does not lie within the nucleus or embedded in the nuclear envelope, as is the case for the SPB of fungi.

The localisation of γ-tubulin to the basal body is in agreement with previous reports on γ-tubulin presence in the basal bodies of *Tetrahymena thermophila* (Liang *et al.*, 1996), *Paramecium tretraurelia* (Klotz *et al.*, 2003), *Trypanosoma brucei* (Scott *et al.*, 1997), *Leishmania major* (Libusova *et al.*, 2004), *Euplotes octocarinatus* (Curtenaz *et al.*, 1997), *Chlamydomonas reinhardtii* (Silflow et al., 1999), *Giardia intestinalis* (Nohynkova *et al.*, 2000), mice (Palacios *et al.*, 1993) and human (Dibbayawan *et al.*, 1995). This is unsurprising as basal bodies are considered MTOCs in their own right. Basal bodies act as a MTOC and γ-tubulin is essential for the nucleation of the central pair microtubules during flagellum morphogenesis (McKean *et al.*, 2003).

Interestingly, however, the localisation of γ-tubulin to the basal body region does not signify that the basal bodies act as the mitotic MTOC. Previous electron microscope studies of *Monosiga ovata* report that during early metaphase the spindle microtubules do not make contact with the basal bodies (Raikov, 1982; Karpov and Leadbeater, 1997). In *Stephanoeca diplocostata* a spindle of microtubules is observed before a second basal body has migrated to the posterior end of the cell (Leadbeater, 1994). These observations suggest that choanoflagellates may have multiple MTOCs, with the mitotic MTOC distinct from the basal bodies. Indeed, many eukaryotes have secondary MTOCs which co-exist with the primary mitotic MTOC (Luders and Stearns, 2007). Anucleate fission yeast cells, for example, lack spindle pole bodies yet can assemble a normal interphase microtubule array (Carazo-Salas and Nurse, 2006). Polarized epithelial cells also have an extensive non-centrosomal microtubule network with few microtubules associating with the centrosome (Reilein *et al.*, 2005). Another example of a secondary MTOC is the Golgi complex, which nucleates and anchors microtubules at its cytoplasmic face (Chabin-Brion *et al.*, 2001).

In *Monosiga ovata* the earliest indication of an impending cell division is duplication of the flagellar basal bodies followed by the withdrawal and apparent disintegration of the flagellar axoneme (Karpov and Leadbeater, 1997). The flagellar basal body is apparently unaffected by withdrawal of the axoneme and maintains its microtubule rootlet array (Karpov and Leadbeater, 1998). The separation and migration of the two pairs of basal bodies to the nuclear poles is followed by the development of two new flagella on opposite sides of the cell during early metaphase. As previously highlighted, the spindle microtubules present within the nucleus at this time do not make contact with the basal bodies (Karpov and Leadbeater, 1997). In other choanoflagellates, however, the flagellar apparatus has

been observed to duplicate prior to mitosis. In *Choanoeca perplexa*, for example, mitosis is preceded by the appearance of a second anterior flagellum. In this study, this was also observed in *Stephanoeca diplocostata*. The retention of flagella throughout mitosis in some choanoflagellate species, and the lack of contact between the basal bodies and the spindle microtubules, both support a conclusion that basal bodies do not act at the mitotic MTOC in choanoflagellates. Furthermore, this conclusion provides little support for the flagellar synthesis constraint as an explanation for the origin of multicellularity in which the temporal exclusivity of motility and division, brought about by competition for the same cellular machinery - the centriole/basal body – would favour colony formation. Alternately flagellar withdrawal may occur in loricate species undergoing tectiform replication as retention of the flagellum would interfere with subsequent movement of the tentacles and the restrictive external cell covering (Leadbeater, 1994).

So what, exactly, is the nature of the mitotic MTOC in choanoflagellates? Previous electron microscopy studies suggested that the polar basal bodies do not act as the mitotic MTOC with mitosis appearing to be an intermediate semi-open orthomitosis (Karpov and Mylnikov, 1993; Leadbeater, 1994; Karpov and Leadbeater, 1997). This study supports this claim with an analysis of the phylogenetic distribution of centrosome components revealing that no components of the centriole domain of the animal centrosome are detectable in choanoflagellates.

In closed mitoses, the functions of a mitotic MTOC are usually carried out by a specialised portion of the nuclear envelope (Raikov, 1982) yet, as shown in this study, γ-tubulin does not appear to localise in the nuclear periphery. This is supported by the lack of an electron

dense region in the nuclear envelope of choanoflagellate species (Karpov and Leadbeater, 1997), a distinguishing characteristic when the functions of a MTOC are carried out by a specialised portion of the nuclear envelope (Raikov, 1982).

The presence of components of the PCM domain in choanoflagellates, and the high conservation of all known proteins of the γ-TuRCs, suggests that, as is the case for metazoans, γ-tubulin complexes are embedded in a pericentrin lattice. These proteins serve as nucleating sites in all MTOCs studied to date. Localisation of γ-tubulin suggests that in choanoflagellates these γ-TuRCs lie within the cytoplasm of the cell body.

If the basal bodies do not act as the mitotic MTOC when the spindle microtubules are assembled during early metaphase, why do the basal bodies and their associated microtubules rootlets make contact with the spindle poles later, during mid-metaphase? A similar question is raised by numerous studies on animal cells that have observed acentriolar spindle assembly in *Drosophila* cells lines (Debec *et al.*, 1995; Basto *et al.*, 2006; Stevens *et al.*, 2007) and in mammalian cells after disruption of the centriole (Bobinnec *et al.*, 1998). Moreover, in animals there are naturally occurring acentriolar cells: the mouse embryo develops with no centrioles until the 64-cell stage (Courtois *et al.*, 2012).

One hypothesis regarding the evolutionary origin of the animal centrosome proposes that centrioles were initially “hitchhiking” on the spindle poles (Beisson and Wright, 2003), something that would have become possible with the evolution of open mitosis. Association of basal bodies with the spindle poles ensures fidelity in their inheritance into daughter cells and avoids the hazard of multi-polar spindles to which cells with multiple MTOCs and open

mitosis are at risk. The early association of the microtubule rootlet cytoskeleton with the basal bodies at the spindle poles may also ensure that the collar tentacles are shared out equitably and are moved in an orderly and coordinated manner to their new locations on the daughter cells.

Later on in the course of evolution, after the appearance of animals, basal bodies began to participate in the organisation of the mitotic spindle. Indeed, centrioles are instrumental in organizing centrosomal components into a structurally stable organelle. In animals, centrioles facilitate the nucleation of PCM and several centriolar proteins contribute to PCM recruitment, indicating the co-evolution of these two structures in the metazoan lineage (Dobbelaere *et al.*, 2008; Fu and Glover, 2012). This dual function of the centriole/basal body occurs in mammals in which one centriole from the centrosome becomes a basal body in order to generate the primary cilium or the spermatozoon flagellum. The flagellar synthesis constraint is therefore not an explanation for the origin of multicellularity, but a consequence.

## 5.6 Discussion and conclusions: origins of a centriole-based centrosome

### 5.6.1 The cilia function of centrioles is ancestral

Centrioles and basal bodies are found in all major eukaryotic lineages, suggesting their presence in the last common eukaryotic ancestor. The phylogenetic presence of a centriole structure correlates with the occurrence of a flagellated stage: all organisms that possess a basal body/centriole structure also build cilia. When axonemes are absent, basal bodies and centrioles are also absent and centrosomal structures with no centrioles can be observed, such as the spindle pole body in yeasts and the nucleus-associated body in amoeba. When

the axoneme is still present but no longer fully functional, such as the sensory cilia of *Caenorhabditis elegans*, the basal body structure is less constrained and can depart from the canonical structure. Not all basal bodies, when present, associate with spindle poles. In certain species, as is the case of ciliates, centrioles do not associate with the spindle poles but remain at the membrane where they nucleate axonemes.

The correlation between the occurrence of centrioles and the presence of cilia/flagella structures but not centrosome-like structures, suggests that the cilia function of centrioles is ancestral and more essential.

### 5.6.2 Evolution of the centriole-based centrosome

Given that the ancestral function of the centriole/basal body structure is in ciliogenesis, when did a centriole-based centrosome first appear? In *Monosiga brevicollis,* centriole components associated with basal body function are present whilst those restricted to a centrosome function are entirely absent. Proteins of the intercentriolar linker, ninein and C-Nap1, for example, are absent in *M. brevicollis* and other non-metazoans. CP110 and Cep97, proteins that regulate the transformation between centrioles and basal bodies are also restricted to metazoans. This reflects the situation painted by electron microscopy ultrastructure studies of cell division and mitosis in choanoflagellates. Although the basal bodies do associate with the spindle poles they do not act as the mitotic MTOC as the basal bodies make no contact with the spindle microtubules. Instead, mitosis appears to be an intermediate semi-open orthomitosis (Karpov and Mylnikov, 1993; Leadbeater, 1994; Karpov and Leadbeater, 1997). This is reminiscent of the situation in ciliated fungi. In the

aquatic fungus, *Catenaria anguillulae*, for example, the centrioles are associated with but not connected to the mitotic spindle which is intranuclear (Ichida and Fuller, 1968).

The idea of a single MTOC, such as the centrosome in animal cells, is not the generality in unicellular eukaryotes. Instead, they possess a diversity of MTOCs within the same cell with spatially separated and morphologically distinct MTOCs operating for mitotic and flagellar microtubules (Gull *et al.*, 2004). It appears that only within the metazoan lineage did basal bodies emerge to have an explicit function in mitotic spindle formation with a centriole-based centrosome being specific to Metazoa. The innovation of possessing a centriole within a cytoplasmic organelle, no longer permanently associated with an axoneme, occurred in the metazoan lineage.

In contrast, proteins of the PCM domain of the centrosome are present in choanoflagellates, exemplified here by *Monosiga brevicollis* and *Salpingoeca rosetta*. Proteins of the PCM domain are also found in some fungi species and it is these proteins that have generated discussions surrounding the homology between animal centrosomes and other centrosome structures such as the spindle pole body in fungi and the nucleus associated body found in *Dictyostelium discoideum*. At the heart of the PCM domain are the γ-tubulin complexes which, at least in part, are ubiquitously conserved across all eukaryotes.

Gene duplication and loss are major forces of evolutionary innovation, facilitating the development of new functions and the abolition of ancestral ones. Gene duplication is also an important mechanism in the evolution of protein interaction networks and the addition of new components. Gene duplication appears to have played an important role in the

evolution of centrosome components with proteins that contribute to a centriole-based centrosome having appeared in a stepwise manner throughout the evolution of the Metazoa.

The coiled-coil proteins of the centriole domain restricted to metazoans, CP110, Cep97, ninein, Cep63, Cep170, C-NAP1, rootletin and TSGA10, may have arisen from the expansion of a pre-existing coiled-coil superfamily. Seven of the selected centriolar domain proteins all identified the same putative homologue in *M. brevicollis*. However, given the interference of the repeating pattern of coil domains with sequence comparison algorithms and the subsequent difficulties in predicting homology between coiled-coil proteins, it is difficult to confirm whether the centrosome-associated proteins are indeed part of a coiled-coil superfamily. Elsewhere the role of gene duplication in the evolution of a centriole-based centrosome is more clear-cut. Three clear pairs of paralogues were identified in this study (AKAP450 and pericentrin; C-NAP1 and rootletin; TSGA10 and Cep135), the result of gene duplications within the metazoan lineage.

### 5.6.3 Definition of a "centrosome"

The SPB of yeast, the NAB of *Dictyostelium discoideum* and the animal centrosome are often stated as functional equivalents yet published dialogues rarely extend to a discussion of homology. Most researchers have failed to identify homologues of the respective centrosome's constituent proteins in other species (Blau-Wasser *et al.*, 2009). The clear exceptions to this, however, are proteins directly associated with microtubules. Some centrosome proteins of *Dictyostelium discoideum* were identified based on their homology to their mammalian counterparts. All of these proteins, including γ-tubulin (Euteneuer *et al.*,

1998), DdCP224 (Graf *et al.*, 2000), EB1 (Rehberg and Graf, 2002), Spc97 and Spc98 (Daunderer and Graf, 2002), are associated with the microtubule nucleating machinery of the gamma-tubulin complexes. Spc97 and Spc98, for example, are homologues of components of the gamma-tubulin complex, GCP2 and GCP3 respectively. As shown in this study, this conservation of microtubule nucleation and regulation is apparent across the eukaryotes with GCP2 and GCP3, components of the γTuSC, found in all eukaryotes analysed except *Caenorhabditis elegans*. The ubiquity of the components of γ-TuSCs, GCP2 and GCP3, suggests their presence in the last common ancestor of eukaryotes. It is perhaps the components of γ-tubulin complexes alone that are shared between the different centrosome structures found in eukaryotes.

Indeed, numerous experimental studies have demonstrated that γ-tubulin complexes serve as nucleating sites in animal cells that do not display typical centrosomes. In vertebrates, normal bipolar spindle formation can proceed following experimental destruction of centrosomes or in cells lacking centrosomes, suggesting that non-centrosome-associated microtubules can contribute to spindle formation (Szöllösi *et al.*, 1972; Gueth-Hallonet *et al.*, 1993; Bobinnec *et al.*, 1998; Khodjakov *et al.*, 2000). Even in the presence of centrosomes, non-centrosome associated microtubules are utilized in spindle formation (Tulu *et al.*, 2003). In addition, Planarians naturally lack a centriole-based centrosome with centrioles only assembled in terminally differentiated ciliated cells through an acentriolar pathway (Azimzadeh *et al.*, 2012). Here, discussions have focused on “centrosome loss” in the evolution of Planarians but a definition of what is meant by the term “centrosome” is required. Given the usage of the term centrosome to define functional homologues such as the spindle pole body and the nucleus associated body, and given that the centriole domain

was a late metazoan-specific addition to the centrosome structure, the absence of centrioles in proliferating cells does not necessarily imply a lack of a centrosome. The nature of the mitotic MTOC in choanoflagellates and the evolutionary history of the centriole-based centrosome argue against the equivalence of centrioles with centrosomes that pervades the literature.

The strategic position of centrioles in the centrosome has no doubt supported the general belief that centrioles are the division centre of the cell. The ancestry of the centrosome displayed here suggests that, instead, the focus should be on the γ-tubulin complexes with the PCM domain. To this effect Gould and Borisy (1977) demonstrated in hamster ovary cells that spindle microtubules are mostly nucleated from the PCM, the lattice framework upon which γ-tubulin complexes are held, and not by the centrioles themselves. In another example, during early mouse development, whilst centrioles are transiently absent from blastomeres during the first cleavages, γ-tubulin remains present (Gueth-Hallonet *et al.*, 1993). All centrosomes, indeed all MTOCs, rely on γ-tubulin and γ-tubulin complexes are, at least in part, ubiquitously conserved across all eukaryotes. Should a centrosome, therefore, be considered a focal accumulation of PCM or γ-tubulin complexes? And what function, if any, do centrioles contribute to the metazoan centrosome?

### 5.6.4 Role of the centriole in the centrosome

#### *"Flagellar synthesis constraint": consequence rather than cause*

The confinement of a centriole-based centrosome to Metazoa and the absence of a centriole-based centrosome in choanoflagellates, in which the mitotic MTOC is distinct from the basal bodies, provide little support for the flagellar synthesis constraint as explanation

for the origin of multicellularity. The temporal exclusivity of motility and division, brought about by competition for the same cellular machinery - the centriole/basal body – was suggested to favour colony formation. There is indeed an apparent constraint; no flagellated or ciliated metazoan cell ever divides (Margulis, 1981; Buss, 1987; Cavalier-Smith, 1991; King, 2004) but this constraint did not arise until after the incorporation of centrioles into the centrosome in the metazoan lineage and the gradual co-option of centrioles as a structural and functional component of the centrosome, associated with mitosis and cytokinesis completion.

### *The centriole emerges as a poly-functional organelle: centriole function in the centrosome*

Centrioles are not entirely dispensable for cell division in metazoans. In mutant acentriolar *Drosophila,* mitotic spindle assembly continues but with asymmetric divisions of larval neuroblasts appearing abnormal (Basto *et al.*, 2006). There is also no recruitment of PCM proteins to a centrosomal structure and any focal accumulation of γ-tubulin at the spindle poles disperses quickly after microtubule disassembly (Szöllösi *et al.*, 1986). This function of centrioles in the organisation of PCM was also observed in HeLa cells (Bobinnec *et al.*, 1998) and, more recently, through three-dimensional structured illumination microscopy of the interface between the centrioles and the PCM (Fu and Glover, 2012). Other experimental acentriolar *Drosophila* cell lines have failed to undergo cytokinesis (Basto *et al.*, 2006). It appears that centrioles are not essential for the assembly of the mitotic spindle but are needed for the fidelity and asymmetry of cell division, depending on tissue type (Debec *et al.*, 2010).

The role of centrioles in facilitating the nucleation of PCM, with several proteins of the centriole domain appearing to contribute to PCM recruitment, suggests the co-evolution of the centrioles and the centrosome in the metazoan lineage. Some proteins of the centriole domain have two functions and are required for both centriole duplication and centrosome maturation (Dobbelaere *et al.*, 2008). The incorporation of centrioles into the centrosome in the metazoan lineage and the gradual co-option of centrioles as a structural and functional component of the centrosome resulted in the cementation of basal bodies as a poly-functional organelle. This is concurrent with the emergence of the metazoan-specific molecular mechanisms that govern the switch between basal body and centriole function.

### *Centriole function in animal development and cell differentiation*

The significance of centrioles in metazoan cell division is not restricted to centrosome maturation and organisation. The centriole pair of the metazoan centrosome display asymmetry due to the structural and functional differences between the mother and daughter centriole. The mother centriole is distinguished by distal appendages and its ability to transform into a basal body, docking at the plasma membrane to template an axoneme (Palazzo *et al.*, 2000). Prior to cell division the mother and daughter centrioles disengage and duplicate. During cell division one of the two daughter cells receives the older of the two mother centrioles; this centriole was formed prior to the last cell cycle. Even though both mother centrioles can readily assemble primary cilia after mitotic cell division, the cell inheriting the older of the two mother centrioles is able to do so considerably faster (Anderson and Stearns, 2009). As the primary cilium is specialized for hedgehog signal transduction this could lead to a differential response to various signalling cues (Goetz and Anderson, 2010). Centriole age could therefore be associated with pronounced phenotypic

variation with the asymmetry of centrioles contributing to the determining of cell fate during mitotic division (Pelletier and Yamashita, 2012). Asymmetric centrosome inheritance during cell division was first described in the *Drosophila* male germline stem cell (GSC). Male GSCs divide asymmetrically producing one stem cell and one differentiating cell. During this asymmetric cell division the mother centrosome always remains within the stem cell, while the differentiating daughter cell always receives the daughter centrosome (Yamashita *et al.*, 2007). A similar observation was made in the mouse neural cortex, in which the mother centrosome remains in the neural glial progenitor stem cells suggesting that asymmetric centrosome inheritance during stem cell division might be a widespread phenomenon (Wang *et al.*, 2009b). Further evidence from *Drosophila* neuroblasts, in which the daughter centrosome is inherited by the neuroblast rather than the differentiating daughter cells, suggests the presence of a regulatory mechanism that ensures the inheritance of certain chromosomes by certain cells instead of the mother centrosome being passively inherited by stem cells (Conduit and Raff, 2010; Januschke *et al.*, 2011). As fate-determining mRNA has been shown to associate with one pole of the spindle (Lambert and Nagy, 2002), stem cells may be able to regulate the localisation of fate-determining factors by associating them with the mother or daughter centrosomes (Pelletier and Yamashita, 2012). Differences between mother and daughter centrosomes have also been revealed to contribute to asymmetric cytokinesis with only the cell that contains the mother centrosome inheriting the midbody cytokinetic contractile ring (Ettinger *et al.*, 2011; Kuo *et al.*, 2011,). Other studies have shown that even during apparently symmetrical cell divisions, peripheral centrosome material is distributed asymmetrically (Fuentealba *et al.*, 2008), perhaps setting up a pattern for differentiation.

Many of the centriole-domain proteins identified in this study to be restricted to the Metazoa, namely Cenexin and Cep170 of the appendage structures, are selectively associated with the mature mother centriole. These proteins could be important for cell differentiation, perhaps through primary cilia signalling, and provide a mechanism for spatial cell differentiation in an early multicellular life cycle.

Centrioles also enabled the preservation of individual cell polarity in the transitions from a colonial stage of unicellular cells to a multicellular assembly of cells. By internalising the basal body structure of a unicellular choanoflagellate-like ancestor into a centrosome structure, cell polarity and cell individuation was maintained. In metazoans, the centrosome is now required for the stable individualisation of polarised cells and the transmission of this polarity through cell division. Furthermore, the lost of the centriole domain of centrosomes in planarian flatworms supports rather than refutes this theory, as planarian embryonic cleavage has also not retained the stereotypical pattern of cell division orientation (Bornens, 2012).

### *In the beginning; centrioles as inert passengers*

However, given the aforesaid constraint, why and how did a centriole-based centrosome first appear? It is evident from choanoflagellates that, prior to the innovation of a centriole within a cytoplasmic centrosome, the basal body structure appears to associate with the spindle poles during mitosis. A similar situation is observable in green algae including *Chlamydomonas* and other volvocalean algae; the basal bodies associate with the mitotic spindle but are not implicated in its nucleation (Pickett-Heaps, 1973; Coss, 1974; Doonan and Grief, 1987). Similar observations are found in the Metazoa. Observations of meiotic

spindles in spermatocytes of the silkworm *Bombyx mori* revealed centrioles clearly separated from the spindle microtubules (Friedlander and Wahrman, 1970).

The association of basal bodies with the spindle poles ensures their equal distribution between daughter cells. Previous authors have questioned the role of the centriole in the establishment of a mitotic spindle and proposed that, instead, the spindle of Metazoan cells guarantees the accurate segregation of both chromosomes and basal bodies (Dietz, 1966; Friedlander and Wahrman, 1970). Pickett-Heaps (1971) proposed centrioles appear only as inert passengers that, through their attachment to the spindle apparatus, are ensuring equal partitioning between daughter cells during cell division. A related hypothesis regarding the evolutionary origin of the animal centrosome proposes that centrioles were initially "hitchhiking" on the spindle poles (Beisson and Wright, 2003), something that became possible with the evolution of open mitosis. As well as ensuring fidelity in their inheritance into daughter cells, the association of basal bodies with the spindle poles would have avoided the hazard of multi-polar spindles to which cells with multiple MTOCs and open mitosis are at risk. Later on in the course of evolution, basal bodies also participated in the organisation of the mitotic spindle; this bifunctionality of the centriole/basal body occurs in mammals in which one centriole becomes a basal body in order to generate the primary cilium or the spermatozoon flagellum.

The position of the centrioles at the poles of the spindle is therefore more of a consequence than a cause of spindle formation. The separation of centrioles from the spindle microtubules in choanoflagellates, and the absence of any centrosomal proteins pertaining to a functional centriole-domain in non-metazoans, supports these proposals.

Cilia and flagella have important functions in physiology and development across eukaryotes and the correct inheritance of basal body apparatus is essential. The organelle is crucial for motility, survival, differentiation, reproduction, division and feeding, among other activities, of many unicellular eukaryotes and the existence of an accurate mechanism for the equal distribution of basal bodies amongst daughter cells would have been of significant selective advantage. In metazoans it remains paramount that centrioles are generated with high structural fidelity and stringent number control. Abnormalities in centriole number and structure are implicated in an increasing number of different diseases including cystic kidney disease, infertility, retinal degeneration, hydrocephalus, laterality defects and chronic respiratory problems (Dawe *et al.*, 2007; Nigg and Raff, 2009). Recent studies have also identified cilia and basal body dysfunction as the underlying cause of various systemic diseases, including Bardet-Biedl, Alstrom and Meckel syndromes (Andersen *et al.*, 2003; Ansley *et al.*, 2003; Mykytyn and Sheffield, 2004; Romio *et al.*, 2004; Kyttala *et al.*, 2006), and these have expanded the range of ciliopathy phenotypes to include obesity, diabetes, hypertension and cardiac abnormalities (Badano *et al.*, 2006).

### 5.6.5 Conclusions

It is hypothesised that the incorporation of centrioles into the centrosome in the metazoan lineage was made possible as basal bodies began hitchhiking on the spindle poles as a means of ensuring their correct inheritance, something that became possible with the evolution of open mitosis. This proto-centrosome, perhaps visible in choanoflagellates, contained the PCM material and γ-tubulin complexes. The gradual co-option of centrioles as a structural and functional component of the centrosome resulted in the cementation of basal bodies as a poly-functional organelle. This is concurrent with the emergence of the

metazoan-specific molecular mechanisms that govern the switch between basal body and centriole function and of centriole proteins that are specific to centrosomal function.

To decide if all centrosomes are homologous, that is if the centrosome as an organelle already existed in the last common ancestor of eukaryotes, then it is important to define what is meant by the term “centrosome”. It is evident that centrosomal proteins of the centriole domain are specific to the Metazoa, indicating that the animal centrosome is a metazoan innovation. This implies that association of centrioles with the spindle poles has arisen independently in more than one lineage. In contrast, the components of the PCM domain, most notably the γ-tubulin complexes, were present in the last common ancestor of eukaryotes.

# Chapter 6: General discussion and conclusions

## 6.1 Basal bodies and motility: the ancestral state

Centrioles and basal bodies with their characteristic 9+2 structure are found in all major eukaryotic lineages, suggesting their presence in the last common eukaryotic ancestor over 800 million years ago with secondary loss in specific lineages such as yeasts and higher plants. The phylogenetic presence of a centriole structure correlates with the occurrence of a flagellated stage: the centriole structure did not first appear without an axoneme and all organisms that possess a basal body/centriole structure also build cilia. When axonemes are absent, basal bodies and centrioles are also absent and centrosomal structures with no centrioles can be observed, such as the spindle pole body in yeasts and the nucleus-associated body in amoeba. When the axoneme is still present but no longer fully functional, such as the sensory cilia of *Caenorhabditis elegans* and, as depicted here, the flagellum of the *Leishmania mexicana* intracellular amastigote, the basal body structure is less constrained and can depart from the canonical structure. It is likely that early flagella performed both motile and sensory functions, as these features are observed in multiple branches of the eukaryotic tree of life (, Satir *et al.*, 2008; Bloodgood, 2010; Carvalho-Santos *et al.*, 2011).

The correlation between the occurrence of centrioles and the presence of cilia/flagella structures but not centrosome-like structures, suggests that the cilia function of centrioles is ancestral and arguably more indispensable. Centrioles localised in a central body and not directly associated with the plasma membrane in a cilium or flagellum can only be observed in more recent lineages, most notably in the animal centrosome. As this study has show the centriole domain of centrosomes emerged within the Metazoa from an ancestral state of

possessing a centriole with basal body function but no functional association within the centrosome. To this effect, it was not possible to identify a single orthologue of any of the centriole domain components previously identified as restricted to the centriole structure of a centrosome, and thereby not detected on basal bodies, outside of the Metazoa.

## 6.2 Beyond 9+0: non-canonical axoneme structures of sensory cilia

A common view has emerged that classifies axonemes into canonical, motile 9+2, and non-canonical, immotile 9+0 sensory structures. This study revealed this view to be overly simplistic, and additional axonemal architectures associated with potential sensory structures should be incorporated into the prevailing models.

The high level of axoneme organisation required for the generation of flagellar motility imposes tight evolutionary constraints on axoneme structure. Sensory cilia are free from such constraints and, as a result, they may deviate from the canonical 9+0 structure. In this study, a striking similarity between the microtubule axoneme structure of the *Leishmania mexicana* parasite infecting a macrophage and vertebrate primary cilia was revealed. In both, the 9-fold microtubule doublet symmetry is broken by the incursion of one or more microtubule doublets into the centre of the axoneme. This striking observation of conservation of ciliary structure, despite the evolutionary distance between *Leishmania* and mammalian cells, suggests a sensory function for the *L. mexicana* amastigote flagellum. In addition, as the structure of the *Leishmania amastigote* flagellum is distinct from the 9+2 flagellum of the extracellular promastigote stage, it also provides a clear example of differentiation of the axoneme in a unicellular organism's lifecycle.

Adding weight to the sensory hypothesis, close examination of the Leishmania amastigote position inside the parasitophorous vacuole revealed frequent and close contact between the flagellum tip and the vacuole membrane. The collapsed axoneme also does not impede intraflagellar transport, thus enabling the targeting of membrane receptor proteins to the flagellar membrane compartment. A sensory function could also explain the retention of the flagellum in the *Trypanosoma cruzi* amastigote flagellum, an intracellular life cycle stage that, as shown in this study, emerged independently to that of the *Leishmania* amastigote. A sensory role of the flagellum of intracellular parasites could have important and novel functions in the maintenance of host-parasite interactions and signalling.

## 6.3 Diversity of basal body appendages

Comparisons of flagellar proteomes have revealed that the canonical basal body and axoneme structure of eukaryotes is dependent upon a set of conserved proteins along with organism-specific elaborations. Additional structures, such as pro-basal bodies and microtubule rootlets, vary widely in their presence or absence and in their structure among taxa, and among cell types in multicellular organisms. Choanoflagellates, for example, have an extensive microtubule rootlet system that extends out under the cell surface and provides support for the collar tentacles that are characteristic of choanoflagellates. The radial array of microtubule rootlets also provides a framework which ensures the coordination and equal spacing of collar tentacles during collar formation (Leadbeater, 1994).

This extensive microtubule rootlet system, present in all choanoflagellate species examined, is comprised of between 120-200 microtubule rootlets compared to the usual one or two

found in most eukaryotes (Moestrup, 2000). This atypical structure is also reflected in the underlying molecular components of the choanoflagellate basal body. A significant divergence of δ-tubulin, an essential component of the triplet C-tubule and thereby necessary for the anchoring and positioning of basal body appendages, correlates with the presence of an extensive microtubule rootlet system found in choanoflagellates.

The importance of choanoflagellates as the closest living relative of metazoans was first revealed by their striking similarity to choanocytes, the feeding cells of sponges. Although extensive phylogenetic analysis leaves little doubt that choanoflagellates are the closest known sister group of animals, comparisons of the underlying molecular and structural components of the appendages associated with the flagellar and collar tentacles highlight significant differences.

Given the importance of the microtubule rootlets in supporting the collar tentacles in choanoflagellates, it is surprising that no similar structure exists in sponge choanocytes. Immunofluorescence microscopy revealed no extensive microtubule rootlet system in choanocytes. This absence of a microtubule rootlet system is also reflected in the underlying molecular components. The δ-tubulin sequence identified in the *Amphimedon queenslandica* genome is highly conserved with respect to other metazoans and does not display the divergence in sequence that is present in *Monosiga brevicollis*.

These differences in how the collar is anchored to the cell body may explain the observed differences in the shape and relative size of the collar itself. The observation of further structural and developmental differences, such as connections between individual microvilli

tentacles and the time required for collar formation, questions the extent to which the collar structure of choanoflagellates and choanocytes can be assumed to be homologous. Given the disparity in life cycles between the two cell types, where choanocytes are closely arranged within single sponge chamber rather than free-living, these structural differences are unsurprising.

## 6.4 The centriole as a component of the centrosome

Given that the ancestral function of the centriole/basal body structure is in ciliogenesis, when did a centriole-based centrosome first appear? In recent years, through localisation and functional analysis, it has become possible to determine if an individual centriole protein has a role in centrosomal or basal-body functions. By ascertaining the phylogenetic presence of proteins that have been experimentally linked to either centrosome or basal body function, it was possible to determine the evolutionary history of the centriole and its emergence as a structure that is functionally and structurally distinct to basal bodies.

None of the proteins of the centriole domain of centrosomes were detected in organisms without motile cilia. The strict correlation between the occurrence of a basal body or centriole structure and the presence of a functional axoneme supports the hypothesis that centrioles are primarily and ancestrally essential for axoneme formation. In addition, components of the centriole domain of centrosomes are restricted to the Metazoa. Centrosome structures involving a centriole, namely the intercentriolar linker and the sub-distal appendages of the mature centriole, are metazoan innovations. The centriole domain of the centrosomes emerged within the Metazoa from an ancestral state of possessing a centriole with basal body function but no association with the centrosome.

Furthermore, very few proteins of the centriole domain of centrosomes are present consistently throughout the Metazoa and appear to have been lost , or diverged significantly in sequence, in those organisms with divergent centrioles, notably *Caenorhabditis elegans* and *Drosophila melanogaster*. This, in conjunction with the complete lack of a centriole-based centrosome in planarians, suggests that the centriole domain is dispensable for cell division in particular lineages.

In *Monosiga brevicollis,* centriole components associated with basal body function are present whilst those restricted to a centrosome function are entirely absent and restricted to metazoans. In choanoflagellates, although the basal bodies do associate with the spindle poles, they do not act as the mitotic MTOC as the basal bodies make no contact with the spindle microtubules. This is not unusual. The idea of a single MTOC, such as the centrosome in animal cells, is not the generality in unicellular eukaryotes. Instead, they possess a diversity of MTOCs within the same cell with spatially separated and morphologically distinct MTOCs operating for mitotic and flagellar microtubules (Gull *et al.*, 2004). It appears that only within the metazoan lineage did basal bodies emerge to have an explicit function in mitotic spindle formation with a centriole-based centrosome being specific to Metazoa. The innovation of possessing a centriole within a cytoplasmic organelle, no longer permanently associated with an axoneme, occurred in the metazoan lineage. The appearance of a centriole-based centrosome occurred early in the Metazoan lineage, with proteins of the centriole domain present in proteomes representing both the Placazoa and Porifera phyla. Gene duplication appears to have played an important role in the evolution of centrosome components with identifiable paralogues contributing to a centriole-based centrosome in the Metazoa.

In contrast, proteins of the PCM domain of the centrosome are present in choanoflagellates and some fungi species including the non-ciliated *Schizosaccharomyces pombe* and *Saccharomcyces cerevisiae*; a centriole structure is not a prerequisite for functioning PCM. It is PCM proteins that have generated discussions surrounding the homology between animal centrosomes and other acentriolar centrosome structures such as the spindle pole body in fungi and the nucleus associated body found in *Dictyostelium discoideum*. At the heart of the PCM domain are the γ-tubulin complexes which, at least in part, are ubiquitously conserved across all eukaryotes.

A definition of what is meant by the term "centrosome" is required. Given the usage of the term centrosome to define functional homologues such as the spindle pole body and the nucleus associated body, and given that the centriole domain was a late metazoan-specific addition to the PCM centrosome structure, the absence of centrioles in proliferating cells does not necessarily imply a lack of a centrosome. The evolutionary history of the centriole-based centrosome argues against the equivalence of centrioles with centrosomes that pervades the literature. The ancestry of the centrosome reported here suggests that, instead, the focus should be on the γ-tubulin complexes within the PCM domain. The ubiquity of the components of γ-tubulin complexes suggests their presence in the last common ancestor or eukaryotes. It is perhaps these components alone that are shared between the different centrosome structures found in eukaryotes.

## 6.5 The centriole and the origins of multicellularity

The lack of contact between the basal bodies and the spindle microtubules in choanoflagellates and the confinement of a centriole-based centrosome to the Metazoa,

both support a conclusion that basal bodies do not act at the mitotic MTOC in choanoflagellates. Furthermore, this conclusion provides little support for the flagellar synthesis constraint as an explanation for the origin of multicellularity in which the temporal exclusivity of motility and division, brought about by competition for the same cellular machinery - the centriole/basal body – would favour colony formation. Flagellar withdrawal may occur in loricate species as retention of the flagellum would interfere with subsequent movement of the tentacles and the restrictive external cell covering (Leadbeater, 1994).

There is, indeed, an apparent constraint in the metazoan lineage; no flagellated or ciliated metazoan cell ever divides (Margulis, 1981; Buss, 1987; Cavalier-Smith, 1991; King, 2004). This constraint, however, did not arise until after the incorporation of centrioles into the centrosome in the metazoan lineage and the gradual co-option of centrioles as a structural and functional component of the centrosome, associated with mitosis and the cytokinesis completion. The flagellar synthesis constraint is therefore not an explanation for the origin of multicellularity but a consequence of it.

## 6.6 The centriole: the centre of the cell?

As early as 1887, centrosomes containing centrioles were observed at the poles of the mitotic spindle and identified as “the organ for cell division”. More recently, however, a debate has initiated as to whether this is just an epiphenomenon with centrioles acting as inert passengers that are hitchhiking on the mitotic spindle poles to ensure accurate segregation between daughter cells. Although ongoing research is revealing important functions of centrioles in animal development and differentiation, hitchhiking centrioles provides a strong explanation for the origins of a centriole-based centrosome.

In this scenario, the incorporation of centrioles into the centrosome in the metazoan lineage was made possible as basal bodies began hitchhiking on the spindle poles as a means of ensuring their correct inheritance. This proto-centrosome, perhaps visible in choanoflagellates where basal bodies associate with but do not make contact with the spindle poles, contained the PCM material and γ-tubulin complexes. The gradual co-option of centrioles as a structural and functional component of the centrosome in metazoans resulted in the cementation of basal bodies as a poly-functional organelle and the co-evolution of centrioles and the centrosome in the metazoan lineage. This theory is concurrent with the emergence of the metazoan-specific molecular mechanisms that govern the switch between basal body and centriole function.

To decide if all centrosomes are homologous, that is if the centrosome as an organelle already existed in the last common ancestor of eukaryotes, then it is important to define what is meant by the term “centrosome”. It is evident that centrosomal proteins of the centriole domain are specific to the Metazoa, indicating that the centriole-based centrosome is a metazoan innovation. This implies that association of centrioles with the spindle poles may have arisen independently in more than one lineage. In contrast, the components of the PCM domain, most notably the γ-tubulin complexes, were present in the last common ancestor of eukaryotes.

## 6.7 Closing remarks

Despite evidence for the demotion of the centriole as “the organ of cell division” its pervasive role in the construction of cilia and flagella has important functions in physiology and development across eukaryotes. The organelle is crucial for the motility, survival, differentiation, reproduction, division and feeding of many unicellular and multicellular eukaryotes.

The evolution of the centriole, with its myriad and sometimes conflicting functions, is a complicated tale to unravel. Its pervasive nature and functional importance have required, but also enabled, contributions from many biological disciplines. Increased understanding of the centriole in its various guises aids the advancement of countless biological disciplines ranging from unicellular microbiology to human health and disease. Given its functional significance, it is unsurprising that an accurate mechanism for its equal distribution during cell division was of a significant selective advantage.

# Supplementary Material

Table S3.1 Literature review of the phylogenetic distribution of intracellular and amastigote forms in *Trypanosoma*.

Table S4.1. Percentage of identity between axoneme and basal body proteins from *Monosiga brevicollis* with human, mouse, *Nematostella vectensis* and *Chlamydomonas reinhardtii*. Alignment was performed using ClustalW.

Figure S5.1. Phylogenetic tree of the Opisthokonta, including the Metazoa, Filasterea and Choanozoa (Choanoflagellata); the Apusozoa; and the Amoebozoa.

Table S5.1. Function and localisation of basal body, PCM and centriole proteins included in the phylogenetic distribution analysis.

Table S5.2. Basal body and axoneme structure of the 30 eukaryotic organisms selected.

Table S5.3. Ascension numbers of putative homologues of basal body, PCM and centriole proteins identified in this study.

Table S5.4. Proteome sequence data sets downloaded for analysis of coiled-coil content.

| **Table S3.1. Literature review of the phylogenetic distribution of intracellular and amastigote forms in *Trypanosoma*.** | | | | |
|---|---|---|---|---|
| **Species (and host)** | **Trypanosome clade** | **Methods** | **Observations** | **Reference** |
| *T. rangeli*<br><br>(man, various wild and domestic animals) | *T. cruzi* clade | Experimentally-infected male white mice. Various tissues sectioned/stained 3 days post inoculation with metatrypomastigotes of "Dog-82" strain. | Intracellular amastigotes and trypomastigotes were seen in the heart, liver and spleen sections. Amastigotes were rounded or ellipsoidal with an average max diameter of 4.2µm. Intracellular amastigotes but no blood flagellates were seen dividing. | (Urdaneta-Morales and Tejero, 1985) |
| | | Experimental infection of Vero cells, murine macrophages and promonocytes. | Macrophages showed highest infection rate but intracellular forms were no longer observed 48hrs post infection. Infection rates of Vero cells and J774 promonocytes were always below 5%. No evidence of intracellular multiplication. | (Eger-Mangrich *et al.*, 2001) |
| *T. dionisii*<br><br>(European bats) | *T. cruzi* clade | Cultures of bison lung cells infected with *T. dionisii* trypomastigotes derived from *in vitro* cultures and examined by light and electron microscopy. | Intracellular parasites remained as trypomastigotes for 24hrs then transformed into rounded amastigotes with no external flagellum (without passing through any distinguishable intermediate state) and replicated by binary fission. From 3 days onwards elongated parasites were seen. Fully differentiated trypomastigotes were distinguished by day 7 onwards. | (Glauert *et al.*, 1982) |
| *T. conorhini* (rat) | *T. cruzi* clade | | Rounded forms without a free flagellum found within visceral capillaries of the kidney. | (Deane, 1969) |
| *T. xeri* (ground squirrel; *Xerus erythropus*) | *T. lewisi* clade. | Blood and organ smears from wild ground squirrels from Sudan. | "All flagellates found were extracellular". Dividing amastigote forms observed in the liver (tissue and visceral capillaries) – variety of shapes and sizes (3.6-7.2µm in length). No mention of intracellular amastigotes. | (Marinkelle and Abdalla, 1978) |

| | | | | |
|---|---|---|---|---|
| *T. evotomys* (voles, *Clethrionomys spp.)* | *T. lewisi* clade. | | Amastigotes (3-7µm) in spleen and lymphoid tissues are the only dividing stage. | ( Molyneux, 1969a; Hoare, 1972; Molyneux, 1976) |
| *T. zapi* (jumping mice; *Zapus* species) | *T. lewisi* clade. | | Division forms are present in tissues and visceral capillaries. Amastigotes observed in lung and heart capillaries. | ( Hoare, 1972; Molyneux, 1976) |
| *T. tamiasi* (chipmunk, *Tamias striatus*) | *T. lewisi* clade | | Division forms are present in tissues and visceral capillaries. Amastigotes observed in lymphoid tissue. | ( Hoare, 1972; Molyneux, 1976) |
| *T. microti* (vole) | *T. lewisi* clade | | Division forms are present in tissues and visceral capillaries. Amastigotes observed in lymphoid tissue. | ( Molyneux, 1969b; Hoare, 1972; Molyneux, 1976) |
| *T. acomys* (spiny mouse; *Acomys cahirinus*) | *T. lewisi* clade | Mice captured in South Jordan as well as experimentally-infected laboratory-bred mice. | Trypomastigotes in peripheral blood. Amastigote syncytial, ovoid, reproductive forms (10-45µm) observed in thymus (in close association with thymus cells). Transitional trypomastigote-like forms also observed in thymus. No reproductive/dividing forms observed in the blood or any other tissues. | (Abdallah *et al.*, 1989) |
| *T. musculi* (mouse) | *T. lewisi* clade | | Large round/oval syncytical amastigote stages. Amastigotes observed in kidney capillaries. | (Krampitz, 1970; Molyneux, 1970; Wilson *et al.*, 1973) |
| *T. nabiasi* (rabbit) | *T. lewisi* clade | Blood smears and tissue sections from wild and artificially infected rabbits. | The development of the rabbit trypanosome takes place in the capillaries of the spleen (flagellate becomes irregularly rounded). Amastigotes observed in lymphoid tissue. | (Grewal, 1957; Molyneux, 1969c; Hoare, 1972; Molyneux, 1976) |
| *T. lewisi* (rat) | *T. lewisi* clade | | Rounded forms without a free flagellum found within visceral capillaries of the kidney. | (Deane, 1969) |

| Species | PF16 | PF20 | DNAI1 | RSP3 | LC1 | Trypanin | α-tubulin | β-tubulin | γ-tubulin | δ-tubulin | ε-tubulin |
|---|---|---|---|---|---|---|---|---|---|---|---|
| H. sapiens | 66.5 | 26.7 | 44.6 | 23.9 | 51.5 | 49.3 | 92.9 | 94.8 | 74.4 | 33.5 | 51.3 |
| M. musculus | 67.6 | 28.4 | 45.6 | 22.6 | 51.5 | 44.0 | 92.9 | 95.3 | 74.3 | 33.8 | 51.0 |
| N. vectensis | 70.6 | 33.2 | 45.2 | 30.0 | 56.6 | 53.7 | 93.3 | 96.6 | 72.9 | 34.0 | 51.8 |
| C. reinhardtii | 56.8 | 18.5 | 36.8 | 26.5 | 45.0 | 47.7 | 85.8 | 88.7 | 64.8 | 33.3 | 34.8 |

**Table S4.1.** Percentage of identity between axoneme and basal body proteins from *Monosiga brevicollis* with human, mouse, *Nematostella vectensis* and *Chlamydomonas reinhardtii*. Alignment was performed using ClustalW.

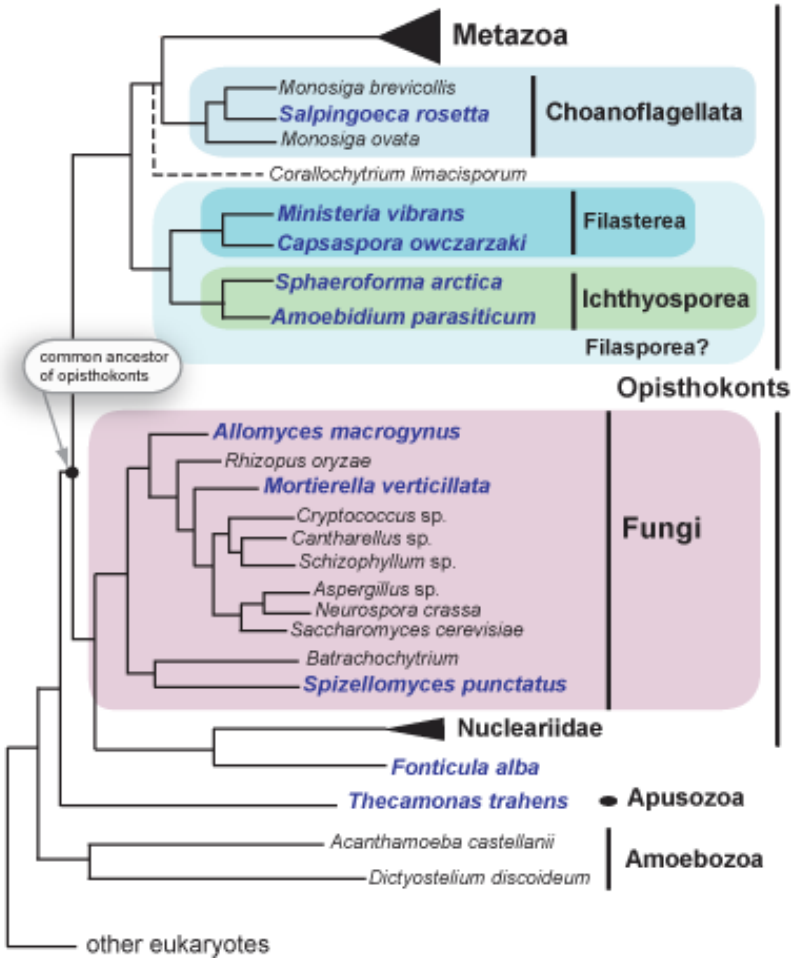


**Figure S5.1. Phylogenetic tree of the Opisthokonta, including the Metazoa, Filasterea and Choanozoa (Choanoflagellata); the Apusozoa; and the Amoebozoa.** The other eukaryotic supergroups also included in this analysis, Excavata and Chromalveolata, can be considered outgroups to those depicted above. Phylogeny based on molecular data. After Ruiz-Trillo et al., (2007) Species highlighted in blue are those for which genome sequencing is to be carried out under the auspices of UNICORN , a multi-taxon genome-sequencing initiative that aims to gain insights into how multicellularity first evolved.

**Table S5.1. Function and localisation of basal body, PCM and centriole proteins included in the phylogenetic distribution analysis.**

| Protein | Localisation in centrosome | Function | References |
|---|---|---|---|
| α-tubulin | Cellular cytoskeletons, centrioles and the axonemes of cilia and flagella. | Sub-unit of microtubules (forms a heterodimer with β-tubulin). Found in all eukaryotes. | (Dutcher, 2001) |
| β-tubulin | Cellular cytoskeletons, centrioles and the axonemes of cilia and flagella. | Sub-unit of microtubules (forms a heterodimer with α-tubulin). Found in all eukaryotes. | (Dutcher, 2001) |
| γ-tubulin | Sites of microtubule nucleation including γ-tubulin ring complexes in the pericentriolar material. | Required for the initiation of microtubule assembly. Component of γ-tubulin small complex (γTuSC). | (Oakley and Oakley, 1989; Pereira and Schiebel, 1997' Kollman *et al.*, 2011) |
| Cep170 | Sub-distal appendages of mature mother centrioles. | Marker for centriole maturation. | (Guarguaglini *et al.*, 2005) |
| ODF2 / Cenexin | Distal and sub-distal appendages of mother centrioles. | Controls recruitment of ninein. Essential for primary cilia formation. | (Ishikawa *et al.*, 2005; Ibi *et al.*, 2011) |
| Ninein | Proximal end of centrioles including the sub-distal appendages of mother centrioles. | Microtubule anchoring and docking of the γ-TuRC at the centrosome. | (Ou *et al.*, 2002; Delgehyr *et al.*, 2005) |
| Rootletin | Proximal end of and in between centrioles. | Interacts with C-NAP1. Essential for maintenance of centrosome cohesion. Acts as physical linker between centrioles. | (Bahe *et al.*, 2005; Yang *et al.*, 2006) |
| Cep63 | Discrete ring around proximal end of mature centrioles. | Recruits Cep152 to the centrosome. Required for normal spindle assembly and maintenance of normal centrosome number. | (Sir *et al.*, 2011; Brito *et al.*, 2012) |
| C-NAP1 / Cep250 | Proximal end of centrioles. | Mediates centriole-centriole cohesion. Holds rootletin, an intercentriolar linker. | (Fry *et al.*, 1998; Mayor *et al.*, 2000; Yang *et al.*, 2006) |

| | | | |
|---|---|---|---|
| Cep68 | Fibres emanating from the proximal end of centrioles. | Cooperates with C-Nap1 and rootletin in the formation of a dynamic linker structure connecting centrioles. | (Graser *et al.*, 2007b) |
| TSGA10 | Mammalian sperm flagella and cilia. | Axoneme assembly in cilia and flagella. | (Modarressi *et al.*, 2004; Behnam *et al.*, 2006; Roghanian *et al.*, 2010) |
| CP110 | Distal end of centrioles. | Collaborates with Cep97 to inhibit ciliogenesis. | (Chen *et al.*, 2002; Tsang *et al.*, 2006; Spektor *et al.*, 2007; Tsang *et al.*, 2008) |
| Cep97 | Centrioles. | Recruits CP110 to the centrosome. Cep97 and CP110 collaborate to inhibit ciliogenesis. | (Spektor *et al.*, 2007) |
| GCP-2 | Sites of microtubule nucleation including γ-tubulin ring complexes in the pericentriolar material. | Component of γ-tubulin small complex (γTuSC). | (Kollman *et al.*, 2011) |
| GCP-3 | Sites of microtubule nucleation including γ-tubulin ring complexes in the pericentriolar material. | Component of γ-tubulin small complex (γTuSC). | (Kollman *et al.*, 2011) |
| GCP-4 | Sites of microtubule nucleation including γ-tubulin ring complexes in the pericentriolar material. | Multiple γTuSCs assemble with GCP4, GCP5 and GCP6 to form the γ-tubulin ring complex (γ-TuRC). | (Kollman *et al.*, 2011) |
| GCP-5 | Sites of microtubule nucleation including γ-tubulin ring complexes in the pericentriolar material. | Multiple γTuSCs assemble with GCP4, GCP5 and GCP6 to form the γ-tubulin ring complex (γ-TuRC). | (Kollman *et al.*, 2011) |
| GCP-6 | Sites of microtubule nucleation including γ-tubulin ring complexes in the pericentriolar material. | Multiple γTuSCs assemble with GCP4, GCP5 and GCP6 to form the γ-tubulin ring complex (γ-TuRC). | (Kollman *et al.*, 2011) |
| PCM-1 | Cytoplasmic “centriolar satellites” that are | Required for the recruitment of centrosomal | (Kubo *et al.*, 1999; Dammermann and |

| | | | |
|---|---|---|---|
| | enriched around the centrosome. | components including centrin, pericentrin and ninein. Also required for the organisation of the cytoplasmic microtubule network. | Merdes, 2002; Kubo and Tsukita, 2003) |
| Cep135 / BLD10 | On the surface of and within the proximal lumen of centrioles. | Role in cartwheel formation, an intermediate structure that enforces the ninefold symmetry of centrioles and basal bodies. Male infertility and lack of central microtubule pair in *Drosophila* CEP135/BLD10 null mutants. Platform protein for C-NAP1; suppression results in premature centrosome splitting. | (Ohta *et al.*, 2002; Matsuura *et al.*, 2004; Hiraki *et al.*, 2007; Kim *et al.*, 2008; Mottier-Pavie and Megraw, 2009; Carvalho-Santos *et al.*, 2010) |
| Cep164 | Distal appendages of mature centrioles. | Required for primary cilia formation. Role in docking of the basal body to the apical plasma membrane. | (Graser *et al.*, 2007a) |
| Cep192 | Pericentriolar material. Accumulates at centrosomes during mitosis. | Regulates centrosome biogenesis by controlling recruitment of PCM proteins and the subsequent assembly of γ-TuRCs (centrosome maturation). | (Zhu *et al.*, 2008; Joukov *et al.*, 2010) |
| AKAP450/Pericentrin | Pericentriolar material. | Required for the recruitment and anchoring of PCM proteins including γ-TuRCs. Serves as a scaffold. | (Zimmerman *et al.*, 2004; Zhu *et al.*, 2008; Lee and Rhee, 2011) |

**Table S5.2. Basal body and axoneme structure of the 30 eukaryotic organisms selected.** * signifies a non-ciliated species. Where possible, information on the type of mitotic microtubule organising centre (MTOC) was included. Ultrastructure information for some of the organisms included in this study was unavailable. In some instances, the structure was inferred using available data from closely related species. The phylogenetic relationship between major groups is shown in Fig. S5.1.

| Eukaryotic "supergroup" | Organism Name | Centriole / Axoneme / MTOC Structure | References |
|---|---|---|---|
| **Opisthokonta**<br>Metazoa | *Homo sapiens* | 9+2 and 9+0 axoneme structures, nucleated from a basal body with 9+0 triplets. Mitosis is open with a centriole-based centrosome. | (Dawe *et al.*, 2007) |
| | *Gallus gallus* | | |
| | *Danio rerio* | | |
| | *Ciona intestinalis* | 9+2 and 9+0 axoneme structures, nucleating from a basal body with 9+0 triplets. | (Fukumoto, 2000; Woollacott, 2005) |
| | *Strongylocentrotus purparatus* | | |
| | *Drosophila melanogaster* | Sensory 9+0 cilia and motile 9+2 flagella. IFT-independent axoneme. Builds centrioles based on either doublet or triplet microtubules (depending on the cell type). | (Callaini and Riparbelli, 1990; Riparbelli *et al.*, 2013) |
| | *Caenorhabditis elegans* | Non-motile sensory 9+0 cilia with distal segment consisting only of microtubule singlets. Unusual basal body architecture with 9 microtubule doublets and 7 inner singlets. Open mitosis. Centrioles are morphologically simple with nine singlet microtubules replacing the usual nine triplet microtubules. Centrioles also lack the 'cartwheel' structure found at the proximal end of most centrioles. | (Perkins *et al.*, 1986; Evans *et al.*, 2006) |
| | *Lottia gigantea* | | |
| | *Nematostella vectensis* | | |

| Eukaryotic "supergroup" | Organism Name | Centriole / Axoneme / MTOC Structure | References |
|---|---|---|---|
| | *Mnemiopsis leidyi* | | |
| | *Trichoplax adhaerens* | 9+2 axoneme structure, nucleated from a basal body with 9+0 triplets. | (Ruthmann *et al.*, 1986) |
| | *Amphimedon queenslandica* | Motile 9+2 flagella | |
| Choanozoa | *Monosiga brevicollis* | Unicellular organisms with a single 9+2 flagellum. The basal body has 9+0 triplets. Mitosis is "semi-open" with the basal bodies associating, but not making connections with, the spindle poles. | (Karpov and Mylnikov, 1993; Leadbeater, 1994; Karpov and Leadbeater, 1997) |
| | *Salpingoeca rosetta* | | |
| Filasterea | *Capsaspora owczarzaki** | Secondary loss of centriole structure. No flagellated stage in life cycle. More than 75% of the 117 genes involved in flagellum construction and motility are lost in the *C. owczarzaki* genome. | (Suga *et al.*, 2013) |
| Fungi | *Batrachochytrium dendrobatidis* | Multicellular fungi with flagellated zoospores. Single flagellum with 9+2 structure. Basal body with 9+0 structure. Mitosis is semi-open with nuclear envelope where fenestrae where spindle microtubules enter. Centrioles associate with spindle poles. | (Longcore, 1999) |
| | *Spizellomyces punctatus* | Zoospores with a single 9+2 flagellum. | (James *et al.*, 2006) |
| | *Allomyces macrogynus* | | |
| | *Schizosaccharomyces pombe** | Secondary loss of centriole structure. No flagellated stage in life cycle. Mitosis is closed with microtubules nucleating from a spindle pole body like structure in the nuclear envelope. | (Beisson and Wright, 2003) |
| | *Saccharomyces cerevisiae** | | |
| | *Neurospora crassa** | | |
| | *Ustilago maydis** | | |

| Eukaryotic "supergroup" | Organism Name | Centriole / Axoneme / MTOC Structure | References |
|---|---|---|---|
| Apusozoa*(sister lineage to the Opisthokonta) | *Thecamonas trahens* | Biflagellate microorganism with 9+2 flagella. No observations of the flagellar apparatus during cell replication. | (Heiss *et al.*, 2013) |
| **Amoebozoa** | *Dictyostelium discoideum** | Secondary loss of centriole structure. No flagellated stage in life cycle. Acentriolar centrosome structure, the nucleus associated body (NAB). | (Ueda *et al.*, 1999) |
| **Excavata** | *Trypanosoma brucei* | 9+2 flagella with 9+0 triplet basal bodies. Mitosis is closed and the mitotic MTOC is a ring-like structure at the poles of the spindle. | (Woodward and Gull, 1990; Gadelha *et al.*, 2006; Gluenz *et al.*, 2010) |
| | *Leishmania major* | 9+2 flagella with 9+0 triplet basal bodies. Collapsed axoneme ("9+v") in intracellular amastigote stage. | (Gluenz *et al.*, 2010) |
| **Chromalveolata** | *Plasmodium falciparum* | 9+2 flagella with 9+0 triplet basal bodies. Closed mitosis with microtubules focussing on a dense structure in the nuclear membrane ("centriolar plaque"). Centrioles, with an unusual structure of 9 single microtubules surrounding a single central microtubule, are located close to but separate from the spindle pole plaque. | (Sinden et al., 1976; Sinden *et al.*, 1978; Morrissette and Sibley, 2002) |
| | *Toxoplasma gondii* | Two distinct MTOCs: the apical polar ring for the sub-pellicular microtubules and spindle pole plaques/centrioles for the spindle microtubules. Centrioles consist of singlet rather than doublet microtubules. | (Morrissette and Sibley, 2001) |
| | *Tetrahymena thermophila* | 9+2 flagella with 9+0 triplet basal bodies. The macronucleus divides by fission and the micronucleus forms a spindle inside the nucleus (closed mitosis) without centrioles at the poles. | (Jaeckel-Williams, 1978) |
| | *Paramecium tetraurelia* | 9+0 triplet basal bodies. 9+2 axoneme structure with only one of the two central tubules persisting along the length of the axoneme. | (Dute and Kung, 1978; Gogendeau *et al.*, 2011) |

**Table S5.3. Ascension numbers of putative homologues of basal body, PCM and centriole proteins identified in this study. (*)**signifies where a single ancestral homolog was detected for two proteins and therefore the same ascension number identified for both (Rootletin and C-Nap1; Cep135 and TSGA10; AKAP450 and Pericentrin). **(-)** indicates that no homologue was detected.

| Species | Cep170 | ODF2 / Cenexin | Ninein | C-Nap1 / Cep250 | Rootletin | Cep63 | Cep68 |
|---|---|---|---|---|---|---|---|
| *Homo sapiens* | NP_055627.2 | NP_702913.1 | NP_891989.2 | NP_009117.2 | NP_055490.3 | NP_079456.2 | NP_055962.2 |
| *Gallus gallus* | XP_001234761.1 | NP_001012817.1 | XP_426482.2 | XP_417323.2 | XP_425750.2 | NP_001161479.1 | XP_419343.2 |
| *Danio rerio* | XP_685634.4 | ABD64539.1 | XP_700610.4 | XP_692550.3 | XP_692550.3 | Q6PGZ0.2 | NP_001007172.1 |
| *Ciona intestinalis* | XP_002120272.1 | XP_002126710.1 | XP_002120842.1 | XP_002119303.1* | XP_002119303.1* | - | - |
| *Strongylocentrotus purparatus* | XP_784848.2 | XP_001184343.1 | XP_788604.2 | XP_001187086.1* | XP_001187086.1* | XP_781747.1 | - |
| *Drosophila melanogaster* | - | - | NP_476916.3<br>NP_723072.1<br>NP_723073.1 | NP_651216.2* | NP_651216.2* | - | - |
| *Caenorhabditis elegans* | - | - | NP_509950.2 | NP_508848.2* | NP_508848.2* | - | - |
| *Lottia gigantea* | ID 174486 | ID 156047 | - | ID 51307* | ID 51307* | ID 156197 | - |
| *Nematostella vectensis* | - | XP_001630242.1 | - | XP_001639189.1* | XP_001639189.1* | XP_001627301.1 | - |

| Species | Cep170 | ODF2 / Cenexin | Ninein | C-Nap1 / Cep250 | Rootletin | Cep63 | Cep68 |
|---|---|---|---|---|---|---|---|
| *Mnemiopsis leidyi* | ML27983 | ML18202 | - | ML092622* | ML092622* | ML011721 | - |
| *Trichoplax adhaerens* | - | - | XP_002109140.1 | - | - | - | - |
| *Amphimedon queenslandica* | - | - | - | - | - | - | - |
| *Monosiga brevicollis* | - | - | - | - | - | - | - |
| *Salpingoeca rosetta* | - | - | - | - | - | - | - |
| *Capsaspora owczarzaki* | - | - | - | - | - | - | - |
| *Batrachochytrium dendrobatidis* | - | - | - | - | - | - | - |
| *Spizellomyces punctatus* | - | - | - | - | - | - | - |
| *Allomyces macrogynus* | - | - | - | - | - | - | - |
| *Schizosaccharomyces pombe* | - | - | - | - | - | - | - |
| *Saccharomyces cerevisiae* | - | - | - | - | - | - | - |
| *Neurospora crassa* | - | - | - | - | - | - | - |

| Species | Cep170 | ODF2 / Cenexin | Ninein | C-Nap1 / Cep250 | Rootletin | Cep63 | Cep68 |
|---|---|---|---|---|---|---|---|
| *Ustilago maydis* | - | - | - | - | - | - | - |
| *Thecamonas trahens* | - | - | - | - | - | - | - |
| *Dictyostelium discoideum* | - | - | - | - | - | - | - |
| *Trypanosoma brucei* | - | - | - | - | - | - | - |
| *Leishmania major* | - | - | - | - | - | - | - |
| *Plasmodium falciparum* | - | - | - | - | - | - | - |
| *Toxoplasma gondii* | - | - | - | - | - | - | - |
| *Tetrahymena thermophila* | - | - | - | - | - | - | - |
| *Paramecium tetraurelia* | - | - | - | - | - | - | - |

| Species | TSGA10 | Cep135 / BLD10 | Cep97 | GCP-2 | GCP-3 | GCP-4 | GCP-5 | GCP-6 |
|---|---|---|---|---|---|---|---|---|
| *Homo sapiens* | NP_079520.1 | NP_079285.2 | NP_078824.2 | NP_006650 | NP_006313.1 | NP_055259.2 | NP_443135.3 | NP_065194.2 |
| *Gallus gallus* | XP_416892.2 | XP_420699.2 | XP_416617.2 | NP_001006496.1 | XP_416949.2 | XP_413958.2 | - | XP_415987.2 |
| *Danio rerio* | NP_001070757.2* | NP_001070757.2* | NP_938185.1 | NP_956416.1 | XP_001004513.1 | NP_001128602.1 | NP_001018151.1 | XP_002667047.2 |
| *Ciona intestinalis* | XP_002126770.1* | XP_002126770.1* | XP_002123564.1 | XP_002120595.1 | XP_002131421.1 | XP_002121664.1 | XP_002131068.1 | XP_002123337.1 |
| *Strongylocentrotus purparatus* | XP_781904.2* | XP_781904.2* | XP_780521.2 | XP_788563.1 | XP_001195981.1 | XP_798348.2 | XP_786630.2 | XP_786939.2 |
| *Drosophila melanogaster* | NP_648749.3* | NP_648749.3* | NP_608811.2 | NP_728264.1 | NP_524919.2 | NP_609412.1 | NP_648537.2 | CAC20097.1 |
| *Caenorhabditis elegans* | - | - | NP_504289.1 | - | - | - | - | - |
| *Lottia gigantea* | ID186653* | ID186653* | ID106866 | ID131294 | ID167139 | ID206938 | ID235580 | ID208649 |
| *Nematostella vectensis* | - | - | XP_001630753.1 | XP_001638168.1 | XP_001625729.1 | XP_001629307.1 | XP_001622681.1 | XP_001631101.1 |
| *Mnemiopsis leidyi* | ML115916* | ML115916* | ML07315 | NA | NA | NA | NA | NA |
| *Trichoplax adhaerens* | - | - | XP_002112891.1 | XP_0021103858.1 | XP_002111743.1 | XP_002111069.1 | XP_002117103.1 | XP_002108898.1 |
| *Amphimedon queenslandica* | - | - | PACid_15702055 | Aqu1.218401 | Aqu1.227457 | Aqu1.227703 | Aqu1.214340 | |

| Species | TSGA10 | Cep135 / BLD10 | Cep97 | GCP-2 | GCP-3 | GCP-4 | GCP-5 | GCP-6 |
|---|---|---|---|---|---|---|---|---|
| *Monosiga brevicollis* | - | - | - | XP_001746401.1 | XP_001745810.1 | XP_001747415.1 | XP_001747754.1 | |
| *Salpingoeca rosetta* | - | - | - | PTSG_01023 | PTSG_01132 | PTSG_03962 | PTSG_07625.2 | PTSG_10110.2 |
| *Capsaspora owczarzaki* | - | - | - | CAOG_06526.2 | CAOG_01240.2 | CAOG_03785.2 | CAOG_01949.2 | CAOG_07819.2 |
| *Batrachochytrium dendrobatidis* | BDEG_01407.1* | BDEG_01407.1* | - | EGF84256.1 | EGF79540.1 | EGF78094.1 | EGF77465.1 | - |
| *Spizellomyces punctatus* | SPPG_08646.2* | SPPG_08646.2* | - | SPPG_08016.2 | SPPG_05284.2 | SPPG_02977.2 | SPPG_04274.2 | SPPG_03883.2 |
| *Allomyces macrogynus* | - | - | - | AMAG_00976.1 | AMAG_02723.1 | AMAG_06891.1 | AMAG_13453.1 | - |
| *Schizosaccharomyces pombe* | - | - | - | NP_596044.1 | XP_001713121.1 | NP_596616.1 | NP_592858.1 | - |
| *Saccharomyces cerevisiae* | - | - | - | NP_012042.1 | NP_014273.1 | - | - | - |
| *Neurospora crassa* | - | - | - | XP_962067.1 | XP_960965.1 | NP_962628.1 | NP_960944.1 | - |
| *Ustilago maydis* | - | - | - | XP_757621.1 | XP_757097.1 | XP_758667.1 | XP_759450.1 | XP_761122.1 |
| *Thecamonas trahens* | - | - | - | AMSG_03572.1 | AMSG_01474.1 | AMSG_02310.1 | AMSG_03640.1 | AMSG_03867.1 |
| *Dictyostelium* | - | - | - | XP_637962.1 | XP_638829.1 | - | - | - |

| Species | TSGA10 | Cep135 / BLD10 | Cep97 | GCP-2 | GCP-3 | GCP-4 | GCP-5 | GCP-6 |
|---|---|---|---|---|---|---|---|---|
| *discoideum* | | | | | | | | |
| *Trypanosoma brucei* | - | - | - | XP_823199.1 | XP_829199.1 | XP_845361.1 | - | - |
| *Leishmania major* | - | - | - | XP_001687023.1 | XP_001684562.1 | - | - | - |
| *Plasmodium falciparum* | - | - | - | XP_001351110.1 | XP_001352200.1 | XP_001348588.1 | - | - |
| *Toxoplasma gondii* | - | - | - | XP_002365451.1 | XP_002364259.1 | XP_002369746.1 | - | - |
| *Tetrahymena thermophila* | - | XP_001027292.1* | - | XP_001013794.2 | XP_001010657.1 | XP_001025759.2 | XP_001014477.1 | - |
| *Paramecium tetraurelia* | - | XP_001453612.1* | | XP_001423927.1 | XP_001456718.1 | XP_001434697.1 | XP_001437351.1 | - |

| Species | CP110 | Cep164 | Cep192 | AKAP450 | Pericentrin |
|---|---|---|---|---|---|
| *Homo sapiens* | NP_001185951.1 | NP_055771.4 | NP_115518.3 | NP_005742.4 | NP_006022.3 |
| *Gallus gallus* | XP_414915.2 | XP_417909.2 | XP_419129.2 | NP_997062.2 | XP_421895.2 |
| *Danio rerio* | XP_002663889.1 | XP_002664791.1 | XP_693893.4 | XP_002665489.1 | XP_002662349.1 |
| *Ciona intestinalis* | XP_002121364.1 | XP_002121669.1 | | XP_002120215.1* | XP_002120215.1* |
| *Strongylocentrotus purparatus* | XP_783709.2\| | XP_784792.2 | XP_002122890.1 | XP_787230.2* | XP_787230.2* |
| *Drosophila melanogaster* | NP_001033857.1 | NP_573095.1 | XP_790994.2 | NP_001027574.1* | NP_001027574.1* |
| *Caenorhabditis elegans* | - | - | - | - | - |
| *Lottia gigantea* | ID157573 | ID 105990 | ID 159239 | ID 174523* | ID 174523* |
| *Nematostella vectensis* | XP_001620551.1 | XP_001625770.1 | XP_001626635.1 | XP_001636860.1* | XP_001636860.1* |
| *Mnemiopsis leidyi* | ML101014 | ML13023 | ML11176 | ML06632* | ML06632* |
| *Trichoplax adhaerens* | XP_002110198.1 | - | XP_002111473.1 | - | - |
| *Amphimedon queenslandica* | PACid_15724243 | - | Aqu1.223035 | - | - |
| *Monosiga brevicollis* | - | XP_001742510.1 | XP_001749822.1 | XP_001746010.1* | XP_001746010.1* |

| Species | CP110 | Cep164 | Cep192 | AKAP450 | Pericentrin |
|---|---|---|---|---|---|
| *Salpingoeca rosetta* | - | PTSG 12024.1 | PTSG 07176.1 | PTSG 02758.1* | PTSG 02758.1* |
| *Capsaspora owczarzaki* | - | - | - | - | - |
| *Batrachochytrium dendrobatidis* | - | BDEG_00990.1 | - | - | - |
| *Spizellomyces punctatus* | - | SPPG 08004.2 | SPPG_06205.2 | - | - |
| *Allomyces macrogynus* | - | AMAG_02111.1 | - | AMSG_00455.1* | AMSG_00455.1* |
| *Schizosaccharomyces pombe* | - | - | - | NP_594115.1* | NP_594115.1* |
| *Saccharomyces cerevisiae* | - | - | - | - | - |
| *Neurospora crassa* | - | - | - | - | - |
| *Ustilago maydis* | - | - | - | - | - |
| *Thecamonas trahens* | - | AMSG_01776.1 | AMSG_05256.1 | AMSG_00455.1* | AMSG_00455.1* |
| *Dictyostelium discoideum* | - | - | XP_638290.1 | - | - |
| *Trypanosoma brucei* | - | XP_001219054.1 | - | - | - |
| *Leishmania major* | - | XP_001682371.1 | - | - | - |

| Species | CP110 | Cep164 | Cep192 | AKAP450 | Pericentrin |
|---|---|---|---|---|---|
| *Plasmodium falciparum* | - | - | - | - | - |
| *Toxoplasma gondii* | - | XP_002364636.1 | - | - | - |
| *Tetrahymena thermophila* | - | XP_001023987.1 | - | - | - |
| *Paramecium tetraurelia* | - | XP_001455899.1 | - | - | - |

**Table S5.4.** Proteome sequence data sets downloaded for analysis of coiled-coil content.

| Species | Common Name | Source | Version | Release / Modification Date | File |
|---|---|---|---|---|---|
| *Homo sapiens* | Human | Ensembl | rel 63 | 20/06/2011 | Homo_sapiens.GRCh37.63.pep.all.fa.gz |
| *Gallus gallus* | Chicken | Ensembl | rel 63 | 17/06/2011 | Gallus_gallus.WASHUC2.63.pep.all.fa.gz |
| *Danio rerio* | Zebrafish | Ensembl | rel 63 | 16/06/2011 | Danio_rerio.Zv9.63.pep.all.fa.gz |
| *Ciona intestinalis* | Sea squirt | Ensembl | rel 63 | 16/06/2011 | Ciona_intestinalis.JGI2.63.pep.all.fa.gz |
| *Strongylocentrotus purpuratus* | Purple sea urchin | HGSC at Baylor College of Medicine | | 09/03/2007 | STRPU_GLEAN3.fa |
| *Drosophila melanogaster* | Fruit fly | Ensembl | rel 63 | 16/06/2011 | Drosophila_melanogaster.BDGP5.25.63.pep.all.fa.gz |
| *Caenorhabditis elegans* | Roundw orm | Uniprot | | | FASTA complete proteome |
| *Lottia gigantea* | Ow l limpet | JGI | v. 1.0 | 24/07/2007 | Lotgi1_GeneModels_FilteredModels1_aa.fasta |
| *Nematostella vectensis* | Sea anemone | JGI | v. 1.0 | | proteins.Nemve1FilteredModels1.fasta.gz |
| *Trichoplax adhaerens* | Placozoa | JGI | v. 1.0 | 22/07/2007 | Triad1_best_proteins.fasta |
| *Amphimedon queenslandica* | Demosponge | JGI | | 27/10/2010 | Aqu1.pep.fa.gz |
| | | | | | |
| *Monosiga brevicollis* | Choanoflagellate | JGI | v. 1.0 | July 2006 | Monbr1_best_proteins.fasta |
| *Salpingoeca rosetta* | Choanoflagellate | Broad Institute Origins of Multicellularity | | 17/02/2010 | salpingoeca_rosetta_1_proteins.fasta.gz |
| | | | | | |
| *Capsaspora owczarzaki* | | Broad Institute Origins of Multicellularity | | 17/02/2011 | capsaspora_ow czarzaki_atcc_30864_2_proteins.fasta.gz |
| | | | | | |
| *Sphaeroforma arctica* | Ichthyosporea | Broad Institute Origins of Multicellularity | | 26/01/2011 | sphaeroforma_artica_jp610_1_proteins.fasta.gz |
| | | | | | |
| *Spizellomyces punctatus* | Chytrid fungus | Broad Institute Origins of Multicellularity | | 14/08/2009 | spizellomyces_punctatus_daom_br117_1_proteins.fasta.gz |
| *Batrachochytrium dendrobatidis* | Chytrid fungus | JGI | v 1.0 | 04/03/2008 | Batde5_best_proteins.fasta.gz |
| *Allomyces macrogynus* | Chytrid fungus | Broad Institute Origins of Multicellularity | | 15/01/2010 | allomyces_macrogynus_atcc_38327_3_proteins.fasta.gz |
| *Neurospora crassa* | Bread mould (Ascomycota) | Broad Institute | | 25/06/2010 | neurospora_crassa_or74a_finished_10_proteins.fasta.gz |
| *Schizosaccharomyces pombe* | Fission yeast | Sanger | v 19.0 | | pompep.fasta |
| *Saccharomyces cerevisiae* | Baker's yeast | Saccharyomyces Genome Database | rel 64 | 03/02/2011 | orf_trans_all.fasta.gz |
| *Ustilago maydis* | Smut fungus | Broad Institute | rel 2 | March 2004 | ustilago_maydis_1_proteins.fasta |
| | | | | | |
| *Thecamonas trahens* | Biflagellate (Apusozoa) | Broad Institute Origins of Multicellularity | | 12/08/2010 | thecamonas_trahens_atcc_50062_1_proteins.fasta.gz |
| | | | | | |
| *Dictyostelium discoideum* | Slime mould (Amoebozoa) | dictyBase | | | dicty_primary_protein |
| *Entamoeba histolytica* | Parasitic protozoan (Amoebozoa) | TIGR | | 22/12/2004 | EHA1.pep |
| | | | | | |
| *Arabidopsis thaliana* | Mouse-ear cress | TAIR | rel 7 | 25/04/2007 | TAIR7_pep_20070425 |
| | | | | | |
| *Trypanosoma brucei* | Parasitic protozoa (Excavata) | TIGR | | 24/07/2005 | TBA1.pep |
| *Leishmania major* Friedlin | Parasitic protozoa (Excavata) | Sanger | | 11/05/2006 | GeneDB_Protein_database_110506 |
| *Tetrahymena thermophila* | Ciliate protozoa (Alveolata) | TIGR | 8313006 | 24/10/2006 | TTA1_08302006.pep |
| | | | | | |
| *Mycobacterium tuberculosis* | Bacteria | Uniprot | | | FASTA complete proteome |
| *Heliobacter pylori* | Bacteria | Uniprot | | | FASTA complete proteome |

# References


Abascal, F., Zardoya, R. and Posada, D. (2005) ProtTest: selection of best-fit models of protein evolution. *Bioinformatics* **21**: 2104-2105.

Abdallah, M.A., Abdelhafez, S.K. and Alyaman, F.M. (1989) *Trypanosoma acomys* (Wenyon, 1909): reproductive forms and course of parasitemia in the natural host *Acomys cahirinus* (Desmarest, 1819). *Parasitology Research* **75**: 439-443.

Abedin, M. and King, N. (2008) The premetazoan ancestry of cadherins. *Science* **319**: 946-948.

Absalon, S. (2008) Intraflagellar transport and functional analysis of genes required for flagellum formation in trypanosomes. *Molecular Biology of the Cell* **19**: 929-944.

Absalon, S., Blisnick, T., Bonhivers, M., Kohl, L., Cayet, N., Toutirais, G., Buisson, J., Robinson, D. and Bastin, P. (2008) Flagellum elongation is required for correct structure, orientation and function of the flagellar pocket in *Trypanosoma brucei*. *Journal of Cell Science* **121**: 3704-3716.

Adl, S.M., Simpson, A.G.B., Farmer, M.A., Andersen, R.A., Anderson, O.R., Barta, J.R., Bowser, S.S., Brugerolle, G., Fensome, R.A., Fredericq, S., James, T.Y., Karpov, S., Kugrens, P., Krug, J., Lane, C.E., Lewis, L.A., Lodge, J., Lynn, D.H., Mann, D.G., McCourt, R.M., Mendoza, L., Moestrup, O., Mozley-Standridge, S.E., Nerad, T.A., Shearer, C.A., Smirnov, A.V., Spiegel, F.W. and Taylor, M.F.J.R. (2005) The new higher level classification of eukaryotes with emphasis on the taxonomy of protists. *Journal of Eukaryotic Microbiology* **52**: 399-451.

Afzelius, B. (1959) Electron microscopy of the sperm tail; results obtained with a new fixative. *Journal of Biophysical and Biochemical Cytology* **5**: 269-278.

Ainsworth, C. (2007) Tails of the unexpected. *Nature* **448**: 638-641.

Akiyama, H.J. and McQuillen, N.K. (1972) Interaction and transformation of *Leishmania donovani* within *in vitro* cultured cells. An electron microscopical study. *American Journal of Tropical Medicine and Hygiene* **21**: 873-879.

al-Shammary, F.J., Shoukrey, N.M., al-Shewemi, S.E., Ibrahim, E.A., al-Zahrani, M.A. and al-Tuwaijri, A.S. (1995) *Leishmania major*: *in vitro* ultrastructural study of the paraxial rod of promastigotes. *International Journal for Parasitology* **25**: 443-452.

Alexander, J. (1978) Unusual axonemal doublet arrangements in the flagellum of *Leishmania* amastigotes. *Transactions of the Royal Society of Tropical Medicine and Hygiene* **72**: 345-347.

Alexander, J. and Vickerman, K. (1975) Fusion of host-cell secondary lysosomes with parasitophorous vacuoles of *Leishmania mexicana* infected macrophages. *Journal of Protozoology* **22**: 502-508.

Allen, R.A. (1965) Isolated cilia in inner retinal neurons and in retinal pigment epithelium. *Journal of Ultrastructure Research* **12**: 730-747.

Alvarez, F., Cortinas, M.N. and Musto, H. (1996) The analysis of protein coding genes suggests monophyly of *Trypanosoma*. *Molecular Phylogenetics and Evolution* **5**: 333-343.

Andersen, J.S., Wilkinson, C.J., Mayor, T., Mortensen, P., Nigg, E.A. and Mann, M. (2003) Proteomic characterization of the human centrosome by protein correlation profiling. *Nature* **426**: 570-574.

Andersen, R.A., Barr, D.J.S., Lynn, D.H., Melkonian, M., Moestrup, O. and Sleigh, M.A. (1991) Terminology and nomenclature of the cytoskeletal elements associated with the flagellar ciliary apparatus in protists. *Protoplasma* **164**: 1-8.

Anderson, C.T. and Stearns, T. (2009) Centriole age underlies asynchronous primary cilium growth in mammalian cells. *Current Biology* **19**: 1498-1502.

Ansley, S.J., Badano, J.L., Blacque, O.E., Hill, J., Hoskins, B.E., Leitch, C.C., Kim, J.C., Ross, A.J., Eichers, E.R., Teslovich, T.M., Mah, A.K., Johnsen, R.C., Cavender, J.C., Lewis, R.A., Leroux, M.R., Beales, P.L. and Katsanis, N. (2003) Basal body dysfunction is a likely cause of pleiotropic Bardet-Biedl syndrome. *Nature* **425**: 628-633.

Antoine, J.C., Lang, T., Prina, E., Courret, N. and Hellio, R. (1999) H-2M molecules, like MHC class II molecules, are targeted to parasitophorous vacuoles of *Leishmania*-infected macrophages and internalized by amastigotes of *L. amazonensis* and *L. mexicana*. *Journal of Cell Science* **112:** 2559-2570.

Armstrong, J.A. and Hart, P.D. (1971) Response of cultured macrophages to *Mycobacterium tuberculosis*, with observations on fusion of lysosomes with phagosomes. *Journal of Experimental Medicine* **134:** 713-740.

Azimzadeh, J. and Bornens, M. (2004) The centrosome in evolution. In: Nigg, E. (ed.) *Centrosomes in Development and Disease*. Weinhein: Wiley-VCH.

Azimzadeh, J., Wong, M.L., Downhour, D.M., Alvarado, A.S. and Marshall, W.F. (2012) Centrosome loss in the evolution of planarians. *Science* **335**: 461-463.

Baccetti, B. (1986) Evolutionary trends in sperm structure. *Comparative Biochemistry and Physiology Part A: Molecular and Integrative Physiology* **85**: 29-36.

Badano, J.L., Mitsuma, N., Beales, P.L. and Katsanis, N. (2006) The ciliopathies: an emerging class of human genetic disorders. *Annual Review of Genomics and Human Genetics* **7**: 125-148.

Bahe, S., Stierhof, Y.D., Wilkinson, C.J., Leiss, F. and Nigg, E.A. (2005) Rootletin forms centriole-associated filaments and functions in centrosome cohesion. *Journal of Cell Biology* **171**: 27-33.

Balanco, J.M.F., Pral, E.M.F., Da Silva, S., Bijovsky, A.T., Mortara, R.A. and Alfieri, S.C. (1998) Axenic cultivation and partial characterization of *Leishmania braziliensis* amastigote-like stages. *Parasitology* **116**: 103-113.

Balber, A.E. (1990) The pellicle and the membrane of the flagellum, flagellar adhesion zone, and flagellar pocket: functionally discrete surface domains of the bloodstream form of African trypanosomes. *Critical Reviews in Immunology* **10**: 177-201.

Baldari, C.T. and Rosenbaum, J. (2010) Intraflagellar transport: it's not just for cilia anymore. *Current Opinion in Cell Biology* **22**: 75-80.

Barbara, K.E., Willis, K.A., Haley, T.M., Deminoff, S.J. and Santangelo, G.M. (2007) Coiled coil structures and transcription: an analysis of the *S. cerevisiae* coilome. *Molecular Genetics and Genomics,* **278**: 135-147.

Barnes, B.G. (1961) Ciliated secretory cells in the pars distalis of the mouse hypophysis. *Journal of Ultrastructure Research* **5**: 453-467.

Baron, D.M., Kabututu, Z.P. and Hill, K.L. (2007) Stuck in reverse: loss of LC1 in *Trypanosoma brucei* disrupts outer dynein arms and leads to reverse flagellar beat and backward movement. *Journal of Cell Science* **120**: 1513-1520.

Bastin, P., Sherwin, T. and Gull, K. (1998) Paraflagellar rod is vital for trypanosome motility. *Nature* **391:** 548.

Basto, R., Lau, J., Vinogradova, T., Gardiol, A., Woods, C.G., Khodjakov, A. and Raff, J.W. (2006) Flies without centrioles. *Cell* **125**: 1375-1386.

Bates, P.A. (1994) Complete developmental cycle of *Leishmania mexicana* in axenic culture. *Parasitology* **108**: 1-9.

Bates, P.A., Hermes, I. and Dwyer, D.M. (1989) *Leishmania donovani*: immunochemical localization and secretory mechanism of soluble acid phosphatase. *Experimental Parasitology* **68**: 335-346.

Bates, P.A., Robertson, C.D., Tetley, L. and Coombs, G.H. (1992) Axenic cultivation and characterization of *Leishmania mexicana* amastigote-like forms. *Parasitology* **105**: 193-202.

Bazile, F., St-Pierre, J. and D'Amours, D. (2010) Three-step model for condensin activation during mitotic chromosome condensation. *Cell Cycle* **9**: 3243-3255.

Behnam, B., Modarressi, M.H., Conti, V., Taylor, K.E., Puliti, A. and Wolfe, J. (2006) Expression of TSGA10 sperm tail protein in embryogenesis and neural development: from cilium to cell division. *Biochemical and Biophysical Research Communications* **344**: 1102-1110.

Beisson, J. and Wright, M. (2003) Basal body/centriole assembly and continuity. *Current Opinion in Cell Biology* **15**: 96-104.

Benchimol, M. and de Souza, W. (1981) *Leishmania mexicana amazonensis*: attachment to the membrane of the phagocytic vacuole of macrophages *in vivo*. *Zeitschrift fur Parasitenkunde* **66**: 25-29.

Berman, J.D., Fioretti, T.B. and Dwyer, D.M. (1981) *In vivo* and *in vitro* localisation of *Leishmania* within macrophage phagolysosomes: use of colloidal gold as a lysosomal label. *Journal of Protozoology* **28**: 239-242.

Blank, C., Fuchs, H., Rappersberger, K., Rollinghoff, M. and Moll, H. (1993) Parasitism of epidermal Langerhans cells in experimental cutaneous leishmaniasis with *Leishmania major*. *Journal of Infectious Diseases* **167**: 418-425.

Blau-Wasser, R., Euteneuer, U., Xiong, H.J., Gassen, B., Schleicher, M. and Noegel, A.A. (2009) CP250, a novel acidic coiled coil protein of the *Dictyostelium* centrosome, affects growth, chemotaxis, and the nuclear envelope. *Molecular Biology of the Cell* **20**: 4348-4361.

Bloodgood, R.A. (2010) Sensory reception is an attribute of both primary cilia and motile cilia. *Journal of Cell Science* **123**: 505-509.

Bobinnec, Y., Khodjakov, A., Mir, L.M., Rieder, C.L., Edde, B. and Bornens, M. (1998) Centriole disassembly *in vivo* and its effect on centrosome structure and function in vertebrate cells. *Journal of Cell Biology* **143**: 1575-1589.

Bornens, M. (1992) Structure and functions of isolated centrosomes. In: Kalnins, V.I. (ed.) *The Centrosome*. San Diego, CA: Academic Press.

Bornens, M. (2012) The centrosome in cells and organisms. *Science* **335**: 422-426.

Bourlond-Reinert, L. and Nicolay, M. (1975) Leishmaniose cutaneé: étude ultrastructurale. *Dermatologica* **151**: 113-124.

Boury-Esnault, N., Efremova, S., Bezac, C. and Vacelet, J. (1999) Reproduction of a hexactinellid sponge: first description of gastrulation by cellular determination in the Porifera. *Invertebrate Reproduction and Development* **35**: 187-201.

Branche, C. (2006) Conserved and specific functions of axoneme components in trypanosome motility. *Journal of Cell Science* **119:** 3443-3455.

Breton-Gorius, J. and Stralin, H. (1967) Formation de cils rudimentaires dans les cellules sanguines primitives du sac vitellin d'embryons de rat et de poulet. *Nouvelle Revue Francaise d'Hematologie* **7**: 79-94.

Brito, D.A., Gouveia, S.M. and Bettencourt-Dias, M. (2012) Deconstructing the centriole: structure and number control. *Current Opinion in Cell Biology* **24**: 4-13.

Brittingham, A. and Mosser, D.M. (1996) Exploitation of the complement system by *Leishmania* promastigotes. *Parasitology Today* **12**: 444-447.

Broadhead, R. (2006) Flagellar motility is required for the viability of the bloodstream trypanosome. *Nature* **440**: 224-227.

Burkhard, P., Stetefeld, J. and Strelkov, S.V. (2001) Coiled coils: a highly versatile protein folding motif. *Trends in Cell Biology* **11**: 82-88.

Buss, L.W. (1983) Evolution, development, and the units of selection. *Proceedings of the National Academy of Sciences of the United States of America-Biological Sciences* **80**: 1387-1391.

Buss, L.W. (1987) *The Evolution of Individuality.* Princeton: Princeton University Press.

Callaini, G. and Riparbelli, M.G. (1990) Centriole and centrosome cycle in the early *Drosophila* embryo. *Journal of Cell Science* **97**: 539-543.

Cantell, C.E., Franzen, A. and Sensenbaugh, T. (1982) Ultrastructure of multi-ciliated collar cells in the pilidium larva of *Lineus bilineatus* (Nemertini). *Zoomorphology* **101**: 1-15.

Carazo-Salas, R.E. and Nurse, P. (2006) Self-organization of interphase microtubule arrays in fission yeast. *Nature Cell Biology* **8**: 1102-1107.

Carr, M., Leadbeater, B.S.C., Hassan, R., Nelson, M. and Baldauf, S.L. (2008) Molecular phylogeny of choanoflagellates, the sister group to Metazoa. *Proceedings of the National Academy of Sciences of the United States of America* **105**: 16641-16646.

Carr, M., Nelson, M., Leadbeater, B.S.C. and Baldauf, S.L. (2008) Three families of LTR retrotransposons are present in the genome of the choanoflagellate *Monosiga brevicollis*. *Protist* **159**: 579-590.

Carvalho-Santos, Z., Azimzadeh, J., Pereira-Leal, J.B. and Bettencourt-Dias, M. (2011) Tracing the origins of centrioles, cilia, and flagella. *Journal of Cell Biology* **194**: 165-175.

Carvalho-Santos, Z., Machado, P., Branco, P., Tavares-Cadete, F., Rodrigues-Martins, A., Pereira-Leal, J.B. and Bettencourt-Dias, M. (2010) Stepwise evolution of the centriole-assembly pathway. *Journal of Cell Science* **123**: 1414-1426.

Castro, R., Scott, K., Jordan, T., Evans, B., Craig, J., Peters, E.L. and Swier, K. (2006) The ultrastructure of the parasitophorous vacuole formed by *Leishmania major*. *Journal of Parasitology* **92**: 1162-1170.

Cavalier-Smith, T. (1991) Cell diversification in heterotropic flagellates. In: Patterson, D.J. and Larsen, J. (eds.) *The Biology of Free-living Heterotropic Flagellates*. Oxford: Clarendon Press.

Cavalier-Smith, T. (2002) The phagotrophic origin of eukaryotes and phylogenetic classification of protozoa. *International Journal of Systematic and Evolutionary Microbiology* **52**: 297-354.

Chabin-Brion, K., Marceiller, J., Perez, F., Settegrana, C., Drechou, A., Durand, G. and Pous, C. (2001) The Golgi complex is a microtubule-organizing organelle. *Molecular Biology of the Cell* **12**: 2047-2060.

Chang, K.-P. and Dwyer, D.M. (1976) Multiplication of a human parasite (*Leishmania donovani)* in phagolysosomes of hamster macrophages *in vitro*. *Science* **193**: 678-680.

Chang, K.P. (1980) Human cutaneous *Leishmania* in a mouse macrophage line: propagation and isolation of intracellular parasites. *Science* **209**: 1240-1242.

Chang, K.P. and Dwyer, D.M. (1978) *Leishmania donovani* - hamster macrophage interactions *in vitro*: cell entry, intracellular survival, and multiplication of amastigotes. *Journal of Experimental Medicine* **147**: 515-530.

Chang, P. and Stearns, T. (2000) Delta-tubulin and epsilon-tubulin: two new human centrosomal tubulins reveal new aspects of centrosome structure and function. *Nature Cell Biology* **2**: 30-35.

Chen, Z.H., Indjeian, V.B., McManus, M., Wang, L.Y. and Dynlacht, B.D. (2002) CP110, a cell cycle-dependent CDK substrate, regulates centrosome duplication in human cells. *Developmental Cell* **3**: 339-350.

Chothia, C. and Gough, J. (2009) Genomic and structural aspects of protein evolution. *Biochemical Journal* **419**: 15-28.

Christensen, S.T., Guerra, C.F., Awan, A., Wheatley, D.N. and Satir, P. (2003) Insulin receptor-like proteins in *Tetrahymena thermophila* ciliary membranes. *Current Biology* **13:** R50-R52.

Christensen, S.T., Pedersen, L.B., Schneider, L. and Satir, P. (2007) Sensory cilia and integration of signal transduction in human health and disease. *Traffic* **8**: 97-109.

Cobbe, N. and Heck, M.M.S. (2000) SMCs in the world of chromosome biology - from prokaryotes to higher eukaryotes. *Journal of Structural Biology* **129**: 123-143.

Colantonio, J.R., Vermot, J., Wu, D., Langenbacher, A.D., Fraser, S., Chen, J.N. and Hill, K.L. (2009) The dynein regulatory complex is required for ciliary motility and otolith biogenesis in the inner ear. *Nature* **457**: 205-209.

Conduit, P.T. and Raff, J.W. (2010) Cnn dynamics drive centrosome size asymmetry to ensure daughter centriole retention in *Drosophila* neuroblasts. *Current Biology* **20**: 2187-2192.

Cooper, J.A. (1987) Effects of cytochalasin and phalloidin on actin. *Journal of Cell Biology* **105**: 1473-1478.

Coss, R.A. (1974) Mitosis in *Chlamydomonas reinhardtii* basal bodies and the mitotic apparatus. *Journal of Cell Biology* **63**: 325-329.

Costanzo, M.C., Hogan, J.D., Cusick, M.E., Davis, B.P., Fancher, A.M., Hodges, P.E., Kondu, P., Lengieza, C., Lew-Smith, J.E., Lingner, C., Roberg-Perez, K.J., Tillberg, M., Brooks, J.E. and Garrels, J.I. (2000) The Yeast Proteome Database (YPD) and *Caenorhabditis elegans* Proteome Database (WormPD): comprehensive resources for the organization and comparison of model organism protein information. *Nucleic Acids Research* **28**: 73-76.

Courtois, A., Schuh, M., Ellenberg, J. and Hiiragi, T. (2012) The transition from meiotic to mitotic spindle assembly is gradual during early mammalian development. *Journal of Cell Biology* **198**: 357-370.

Cupolillo, E., Medina-Acosta, E., Noyes, H., Momen, H. and Grimaldi, G. (2000) A revised classification for *Leishmania* and *Endotrypanum*. *Parasitology Today* **16**: 142-144.

Curtenaz, S., Wright, M. and Heckmann, K. (1997) Localization of gamma-tubulin in the mitotic and meiotic nuclei of *Euplotes octocarinatus*. *European Journal of Protistology* **33**: 1-12.

Dahl, H.A. (1963) Fine structure of cilia in rat cerebral cortex. *Zeitschrift Fur Zellforschung Und Mikroskopische Anatomie* **60**: 369-386.

Dammermann, A. and Merdes, A. (2002) Assembly of centrosomal proteins and microtubule organization depends on PCM-1. *Journal of Cell Biology* **159**: 255-266.

Daunderer, C. and Graf, R. (2002) Molecular analysis of the cytosolic *Didycostelium* gamma-tubulin complex. *European Journal of Cell Biology* **81**: 175-184.

Davis, E.E., Brueckner, M. and Katsanis, N. (2006) The emerging complexity of the vertebrate cilium: new functional roles for an ancient organelle. *Developmental Cell* **11**: 9-19.

Dawe, H.R., Farr, H. and Gull, K. (2007) Centriole/basal body morphogenesis and migration during ciliogenesis in animal cells. *Journal of Cell Science* **120**: 7-15.

Dayel, M.J., Alegado, R.A., Fairclough, S.R., Levin, T.C., Nichols, S.A., McDonald, K. and King, N. (2011) Cell differentiation and morphogenesis in the colony-forming choanoflagellate *Salpingoeca rosetta*. *Developmental Biology* **357**: 73-82.

Deane, M.P. (1969) On the life cycle of trypanosomes of the lewisi group and their relationships to other mammalian trypanosomes. *Revista do Instituto de Medicina Tropical de São Paulo* **11**: 34-43.

Debec, A., Detraves, C., Montmory, C., Geraud, G. and Wright, M. (1995) Polar organization of gamma-tubulin in acentriolar mitotic spindles of *Drosophila* m*elanogaster* cells. *Journal of Cell Science* **108**: 2645-2653.

Debec, A., William, S. and Bettencourt-Dias, M. (2010) Centrioles: active players or passengers during mitosis. *Cell and Molecular Life Sciences* **67**: 2173-2194.

Delattre, M. and Gonczy, P. (2004) The arithmetic of centrosome biogenesis. *Journal of Cell Science* **117**: 1619-1629.

Delgehyr, N., Sillibourne, J. and Bornens, M. (2005) Microtubule nucleation and anchoring at the centrosome are independent processes linked by ninein function. *Journal of Cell Science,* **118**: 1565-1575.

Delorenzi, M. and Speed, T. (2002) An HMM model for coiled-coil domains and a comparison with PSSM-based predictions. *Bioinformatics* **18**: 617-625.

Dibbayawan, T.P., Harper, J.D.I., Elliott, J.E., Gunning, B.E.S. and Marc, J. (1995) A gamma-tubulin that associates specifically with centrioles in HeLa cells and the basal body complex in *Chlamydomonas*. *Cell Biology International* **19**: 559-567.

Dictenberg, J.B., Zimmerman, W., Sparks, C.A., Young, A., Vidair, C., Zheng, Y.X., Carrington, W., Fay, F.S. and Doxsey, S.J. (1998) Pericentrin and gamma-tubulin form a protein complex and are organized into a novel lattice at the centrosome. *Journal of Cell Biology* **141**: 163-174.

Dietz, R. (1966) The dispensability of the centrioles in the spermatocyte division of *Pales ferrugenea* (Nematocera). In: Darlington, C.D. and Lewis, K.R. (eds.) *Chromosomes Today*. Edinburgh: Oliver and Boyd Ltd.

Ding, R., West, R.R., Morphew, M., Oakley, B.R. and McIntosh, J.R. (1997) The spindle pole body of *Schizosaccharomyces pombe* enters and leaves the nuclear envelope as the cell cycle proceeds. *Molecular Biology of the Cell* **8**: 1461-1479.

Dobbelaere, J., Josue, F., Suijkerbuijk, S., Baum, B., Tapon, N. and Raff, J. (2008) A genome-wide RNAi screen to dissect centriole duplication and centrosome maturation in *Drosophila*. *PLOS BIOLOGY* **6**: 1975-1990.

Doonan, J.H. and Grief, C. (1987) Mictroubule cycle in *Chlamydomonas reinhardtii*: an immunofluorescence study. *Cell Motility and the Cytoskeleton* **7**: 381-392.

Dos Santos, H.G., Abia, D., Janowski, R., Mortuza, G., Bertero, M.G., Boutin, M., Guarin, N., Mendez-Giraldez, R., Nunez, A., Pedrero, J.G., Redondo, P., Sanz, M., Speroni, S., Teichert, F., Bruix, M., Carazo, J.M., Gonzalez, C., Reina, J., Valpuesta, J.M., Vernos, I., Zabala, J.C., Montoya, G., Coll, M., Bastolla, U. and Serrano, L. (2013) Structure and non-structure of centrosomal proteins. *PLOS ONE* **8**: e62633. doi:10.1371/journal.pone.0062633.

Doxsey, S., Zimmerman, W. and Mikule, K. (2005) Centrosome control of the cell cycle. *Trends in Cell Biology* **15**: 303-311.

Doyle, P.S., Engel, J.C., Pimenta, P.F.P., Dasilva, P.P. and Dwyer, D.M. (1991) *Leishmania donovan*i: long-term culture of axenic amastigotes at 37°C. *Experimental Parasitology* **73**: 326-334.

Duboscq, O. and Tuzet, O. (1939) Les diverses formes des choanocytes des éponges calcaires hétérocoeles et leur signification. *Archives of Zoological Experimental Genetics* **80**: 353-388.

Dutcher, S.K. (1995) Flagellar assembly in two hundred and fifty easy-to-follow steps. *Trends in Genetics* **11**: 398-404.

Dutcher, S.K. (2001) The tubulin fraternity: alpha to eta. *Current Opinion in Cell Biology* **13**: 49-54.

Dutcher, S.K. and Trabuco, E.C. (1998) The UNI3 gene is required for assembly of basal bodies of *Chlamydomonas* and encodes delta-tubulin, a new member of the tubulin superfamily. *Molecular Biology of the Cell* **9**: 1293-1308.

Dute, R. and Kung, C. (1978) Ultrastructure of the proximal region of somatic cilia in *Paramecium tetraurelia*. *The Journal of Cell Biology* **78**: 451-464.

Eger-Mangrich, I., de Oliveira, M.A., Grisard, E.C., de Souza, W. and Steindel, M. (2001) Interaction of *Trypanosoma rangeli* (Tejera, 1920) with different cell lines *in vitro*. *Parasitology Research* **87**: 505-509.

Eperon, S. and McMahon-Pratt, D. (1989) Extracellular cultivation and morphological characterization of amastigote-like forms of *Leishmania panamensis* and *L. braziliensis*. *Journal of Protozoology* **36**: 502-510.

Eperon, S. and McMahon-Pratt, D. (1989) Extracellular amastigote-like forms of *Leishmania panamensis* and *Leishmania braziliensis* .II. Stage- and species-specific monoclonal antibodies. *Journal of Protozoology* **36**: 510-518.

Erlemann, S., Neuner, A., Gombos, L., Gibeaux, R., Antony, C. and Schiebel, E. (2012) An extended gamma-tubulin ring functions as a stable platform in microtubule nucleation. *Journal of Cell Biology* **197**: 59-74.

Ettinger, A.W., Wilsch-Brauninger, M., Marzesco, A.M., Bickle, M., Lohmann, A., Maliga, Z., Karbanova, J., Corbeil, D., Hyman, A.A. and Huttner, W.B. (2011) Proliferating versus differentiating stem and cancer cells exhibit distinct midbody-release behaviour. *Nature Communications* **2**: 503. doi:10.1038/ncomms1511.

Euteneuer, U., Graf, R., Kube-Granderath, E. and Schliwa, M. (1998) *Dictyostelium* gamma-tubulin: molecular characterization and ultrastructural localization. *Journal of Cell Science* **111**: 405-412.

Evans, J.E., Snow, J.J., Gunnarson, A.L., Ou, G.S., Stahlberg, H., McDonald, K.L. and Scholey, J.M. (2006) Functional modulation of IFT kinesins extends the sensory repertoire of ciliated neurons in *Caenorhabditis elegans. Journal of Cell Biology* **172**: 663-669.

Fairclough, S.R., Dayel, M.J. and King, N. (2010) Multicellular development in a choanoflagellate. *Current Biology* **20**: R875-R876.

Farina, M., Attias, M., Suoto-Padron, T. and de Souza, W. (1986) Further studies on the organisation of the paraxial rod of trypanosomatids. *Journal of Protozoology* **33**: 552-557.

Fawcett, D.W. (1968) Topographical relationship between plane of central pair of flagellar fibrils and transverse axis of head in guinea-pig spermatozoa. *Journal of Cell Science* **3**: 187-198.

Finn, R.D., Tate, J., Mistry, J., Coggill, P.C., Sammut, S.J., Hotz, H.R., Ceric, G., Forslund, K., Eddy, S.R., Sonnhammer, E.L.L. and Bateman, A. (2008) The Pfam protein families database. *Nucleic Acids Research* **36**: D281-D288.

Fitzpatrick, D.A., Logue, M.E., Stajich, J.E. and Butler, G. (2006) A fungal phylogeny based on 42 complete genomes derived from supertree and combined gene analysis. *BMC Evolutionary Biology* **6**. doi:10.1186/1471-2148-6-99.

Fjerdingstad, E.J. (1961a) The ultrastructure of choanocyte collars in *Spongilla lacustris*. *Zeitschrift Fur Zellforschung Und Mikroskopische Anatomie* **53**: 645-657.

Fjerdingstad, E.J. (1961b) Ultrastructure of the collar of the choanoflagellate *Codonosiga botrytis* (Ehrenb). *Zeitschrift Fur Zellforschung Und Mikroskopische Anatomie* **54**: 499-510.

Fliegauf, M., Benzing, T. and Omran, H. (2007) Mechanisms of disease - when cilia go bad: cilia defects and ciliopathies. *Nature Reviews Molecular Cell Biology* **8**: 880-893.

Flory, M.R. and Davis, T.N. (2003) The centrosomal proteins pericentrin and kendrin are encoded by alternatively spliced products of one gene. *Genomics* **82**: 401-405.

Flory, M.R., Moser, M.J., Monnat, R.J. and Davis, T.N. (2000) Identification of a human centrosomal calmodulin-binding protein that shares homology with pericentrin. *Proceedings of the National Academy of Sciences of the United States of America* **97**: 5919-5923.

Fong, J.H., Shoemaker, B.A., Garbuzynskiy, S.O., Lobanov, M.Y., Galzitskaya, O.V. and Panchenko, A.R. (2009) Intrinsic disorder in protein interactions: insights from a comprehensive structural analysis. *PLoS Computational Biology* **5**: e1000316. doi:10.1371/journal.pcbi.1000316.

Fridberg, A., Buchanan, K.T. and M, E.D. (2007) Flagellar membrane trafficking in kinetoplastids. *Parasitology Research* **100**: 205-212.

Friedlander, M. and Wahrman, J. (1970) The spindle as a basal body distributor: a study in the meiosis of the male silkworm moth, *Bombyx mori*. *Journal of Cell Science* **7**: 65-89.

Fry, A.M., Mayor, T., Meraldi, P., Stierhof, Y.D., Tanaka, K. and Nigg, E.A. (1998) C-Nap1, a novel centrosomal coiled-coil protein and candidate substrate of the cell cycle-regulated protein kinase Nek2. *Journal of Cell Biology* **141**: 1563-1574.

Fu, J.Y. and Glover, D.M. (2012) Structured illumination of the interface between centriole and peri-centriolar material. *Open Biology* **2**: 120104. doi:10.1098/rsob.120104 2046-2441

Fuentealba, L.C., Eivers, E., Geissert, D., Taelman, V. and De Robertis, E.M. (2008) Asymmetric mitosis: unequal segregation of proteins destined for degradation. *Proceedings of the National Academy of Sciences of the United States of America* **105**: 7732-7737.

Fuge, H. (1969) Electron microscopic studies on the intra-flagellar structures of trypanosomes. *Journal of Protozoology* **16**: 460-466.

Fukumoto, M. (2000) Acrosome differentiation in the ascidians *Clavelina lepadiformis* and *Ciona intestinalis*. *Cell Tissue Research* **302**: 105-114.

Funayama, N., Nakatsukasa, M., Hayashi, T. and Agata, K. (2005) Isolation of the choanocyte in the fresh water sponge, *Ephydatia fluviatilis* and its lineage marker, Ef annexin. *Development Growth and Differentiation* **47**: 243-253.

Gadelha, C., Rothery, S., Morphew, M., McIntosh, J.R., Severs, N.J. and Gull, K. (2009) Membrane domains and flagellar pocket boundaries are influenced by the cytoskeleton in African trypanosomes. *Proceedings of the National Academy of Sciences of the United States of America* **106**: 17425-17430.

Gadelha, C., Wickstead, B., de Souza, W., Gull, K. and Cunha-e-Silva, N. (2005) Cryptic paraflagellar rod in endosymbiont-containing kinetoplastid protozoa. *Eukaryotic Cell* **4**: 516-525.

Gadelha, C., Wickstead, B., McKean, P.G. and Gull, K. (2006) Basal body and flagellum mutants reveal a rotational constraint of the central pair microtubules in the axonemes of trypanosomes. *Journal of Cell Science* **119**: 2405-2413.

Gardener, P.J. (1974) Pellicle-associated structures in the amastigote stage of *Trypanosoma cruzi* and *Leishmania* species. *Annals of Tropical Medicine and Parasitology* **68**: 167-176.

Garnham, P.C.C. (1971) Genus *Leishmania*. *Bulletin of the World Health Organization* **44**: 477-489.

Garreau de Loubresse, N., Ruiz, F., Beisson, J. and Klotz, C. (2001) Role of delta-tubulin and the C-tubule in assembly of *Paramecium* basal bodies. *BMC Cell Biology* **2**: 4. doi:10.1186/1471-2121-2-4.

Geer, L.Y., Domrachev, M., Lipman, D.J. and Bryant, S.H. (2002) CDART: protein homology by domain architecture. *Genome Research* **12**: 1619-1623.

Gibbons, I.R. (1961) Structural asymmetry in cilia and flagella. *Nature* **190**: 1128-1129.

Gilula, N.B. and Satir, P. (1972) The ciliary necklace: a ciliary membrane specialization. *Journal of Cell Biology* **53**: 494-509.

Ginger, M.L., Portman, N. and McKean, P.G. (2008) Swimming with protists: perception, motility and flagellum assembly. *Nature Reviews Microbiology* **6**: 838-850.

Glauert, A.M., Baker, J.R. and Selden, L.F. (1982) Mechanism of entry and development of *Trypanosoma dionisii* in non-phagocytic cells. *Journal of Cell Science* **56**: 371-387.

Gluenz, E., Hoog, J.L., Smith, A.E., Dawe, H.R., Shaw, M.K. and Gull, K. (2010) Beyond 9+0: noncanonical axoneme structures characterize sensory cilia from protists to humans. The *FASEB Journal* **24**: 3117-3121.

Glyn, M. and Gull, K. (1990) Flagellum retraction and axoneme depolymerisation during the transformation of flagellates to amoebae in *Physarum*. *Protoplasma* **158**: 130-141.

Goetz, S.C. and Anderson, K.V. (2010) The primary cilium: a signalling centre during vertebrate development. *Nature Reviews Genetics* **11**: 331-344.

Gogendeau, D., Hurbain, I., Raposo, G., Cohen, J., Koll, F. and Basto, R. (2011) SAS-4 proteins are required during basal body duplication in *Paramecium*. *Molecular Biology of the Cell* **22**: 1035-1044.

Gomez-Conde, E., Lopez-Robles, M.C., Hernandez-Rivas, R., Hernandez-Jauregui, P. and Vargas-Mejia, M. (2000) Structural organization of gamma-tubulin in the microtubule organizing center (MTOC) during the nuclear division of *Entamoeba histolytica* trophozoites. *Archives of Medical Research* **31**: S205-S206.

Gonobobleva, E. and Maldonado, M. (2009) Choanocyte ultrastructure in *Halisarca dujardini* (Demospongiae, Halisarcida). *Journal of Morphology* **270**: 615-627.

Gould, R.R. and Borisy, G.G. (1977) The pericentriolar material in Chinese hamster ovary cells nucleates microtubule formation. *Journal of Cell Biology* **73**: 601-615.

Graf, R., Daunderer, C. and Schliwa, M. (2000) *Dictyostelium* DdCP224 is a microtubule-associated protein and a permanent centrosomal resident involved in centrosome duplication. *Journal of Cell Science* **113**: 1747-1758.

Graser, S., Stierhof, Y.D., Lavoie, S.B., Gassner, O.S., Lamla, S., Le Clech, M. and Nigg, E.A. (2007a) Cep164, a novel centriole appendage protein required for primary cilium formation. *Journal of Cell Biology* **179**: 321-330.

Graser, S., Stierhof, Y.D. and Nigg, E.A. (2007b) Cep68 and Cep215 (CDK5RAP2) are required for centrosome cohesion. *Journal of Cell Science* **120**: 4321-4331.

Grewal, M.S. (1957) The life cycle of the British rabbit trypanosome, *Trypanosoma nabiasi* (Railliet, 1895). *Parasitology* **47**: 100-118.

Guarguaglini, G., Duncan, P.I., Stierhof, Y.D., Holmstrom, T., Duensing, S. and Nigg, E.A. (2005) The forkhead-associated domain protein Cep170 interacts with Polo-like kinase 1 and serves as a marker for mature centrioles. *Molecular Biology of the Cell* **16**: 1095-1107.

Gueth-Hallonet, C., Antony, C., Aghion, J., Santa-maria, A., Lajoie-Mazenc, I., Wright, M. and Maro, B. (1993) γ-tubulin is present in acentriolar MTOCs during early mouse development. *Journal of Cell Science* **105**: 157-166.

Gull, K. (1999) The cytoskeleton of trypanosomatid parasites. *Annual Review of Microbiology* **53**: 629-655.

Gull, K. (2003) Host-parasite interactions and trypanosome morphogenesis: a flagellar pocketful of goodies. *Current Opinion in Microbiology* **6**: 365-370.

Gull, K., Briggs, L. and Vaughan, S. (2004) Basal bodies and microtubule organization in pathogenic protozoa. In: Nigg, E. (ed.) *Centrioles in Development and Disease*. Weinhein: Wiley-VCH.

Gupta, N., Goyal, N., Kumar, R., Agarwal, A.K., Seth, P.K. and Rastogi, A.K. (1996) Membrane characterization of amastigote-like forms of *Leishmania donovani*. *Tropical Medicine and International Health* **1**: 495-502.

Gupta, N., Goyal, N. and Rastogi, A.K. (2001) *In vitro* cultivation and characterization of axenic amastigotes of *Leishmania*. *Trends in Parasitology* **17**: 150-153.

Gupta, N., Goyal, N., Singha, U.K., Bhakuni, V., Roy, R. and Rastogi, A.K. (1999) Characterization of intracellular metabolites of axenic amastigotes of *Leishmania donovani* by 1H NMR spectroscopy. *Acta Tropica* **73**: 121-133.

Haag, J., O'Huigin, C. and Overath, P. (1998) The molecular phylogeny of trypanosomes: evidence for an early divergence of the Salivaria. *Molecular and Biochemical Parasitology* **91**: 37-49.

Habibi, P., Sadjjadi, S.M., Owji, M., Moattari, A., Sarkari, B., Naghibalhosseini, F., Hatam, G.R. and Kazemian, S. (2008) Characterization of *in vitro* cultivated amastigote-like of *Leishmania major*: a substitution for *in vivo* studies. *Iranian Journal of Parasitology* **3**: 6-15.

Haering, C.H. and Nasmyth, K. (2003) Building and breaking bridges between sister chromatids. *Bioessays* **25**: 1178-1191.

Hagiwara, H., Ohwada, N., Aoki, T., Suzuki, T. and Takata, K. (2008) The primary cilia of secretory cells in the human oviduct mucosa. *Medical Molecular Morphology* **41**: 193-198.

Hamilton, P.B., Gibson, W.C. and Stevens, J.R. (2007) Patterns of co-evolution between trypanosomes and their hosts deduced from ribosomal RNA and protein-coding gene phylogenies. *Molecular Phylogenetics and Evolution* **44**: 15-25.

Hamilton, P.B., Stevens, J.R., Gaunt, M.W., Gidley, J. and Gibson, W.C. (2004) Trypanosomes are monophyletic: evidence from genes for glyceraldehyde phosphate dehydrogenase and small subunit ribosomal RNA. *International Journal for Parasitology* **34**: 1393-1404.

Hashimoto, T., Nakamura, Y., Kamaishi, T., Adachi, J., Nakamura, F., Okamoto, K. and Hasegawa, M. (1995) Phylogenetic place of kinetoplastid protozoa inferred from a protein phylogeny of elongation factor 1 alpha. *Molecular and Biochemical Parasitology* **70**: 181-185.

Heath, I.B. (1980) Variant mitoses in lower eukaryotes: indicators of the evolution of mitosis. *International Review of Cytology* **64**: 1-80.

Hedges, S.B. (2002) The origin and evolution of model organisms. *Nature Reviews Genetics* **3**: 838-849.

Heiss, A.A., Walker, G. and Simpson, A.G.B. (2013) The microtubular cytoskeleton of the apusomonad *Thecamonas*, a sister lineage to the opisthokonts. *Protist* **164**: 598-621.

Hentzer, B. and Kobayasi, T. (1977) The ultrastructure of *Leishmania tropica* in skin lesions. *Acta Pathologica et Microbiologica Scandinavica Section B* **85**: 153-60.

Heuser, T., Raytchev, M., Krell, J., Porter, M.E. and Nicastro, D. (2009) The dynein regulatory complex is the nexin link and a major regulatory node in cilia and flagella. *Journal of Cell Biology* **187**: 921-933.

Hibberd, D.J. (1975) Observations on ultrastructure of choanoflagellate *Codosiga botrytis* (Ehr) Saville-Kent with special reference to flagellar apparatus. *Journal of Cell Science* **17**: 191-219.

Hinchcliffe, E.H. and Sluder, G. (2001) Centrosome duplication: three kinases come up a winner! *Current Biology* **11**: R698-R701.

Hiraki, M., Nakazawa, Y., Kamiya, R. and Hirono, M. (2007) Bld10p constitutes the cartwheel-spoke tip and stabilizes the 9-fold symmetry of the centriole. *Current Biology* **17**: 1778-1783.
Hirano, T. (2005) Condensins: organizing and segregating the genome. *Current Biology* **15**: R265-R275.
Hirano, T. (2006) At the heart of the chromosome: SMC proteins in action. *Nature Reviews Molecular Cell Biology* **7**: 311-322.
Hirano, T. (2012) Condensins: universal organizers of chromosomes with diverse functions. *Genes and Development* **26**: 1659-1678.
Hoare, C.A. (1972) The Trypanosomes of Mammals. Oxford: Blackwell Scientific.
Hoare, C.A. and Wallace, F.G. (1966) Developmental stages of trypanosomatid flagellates: a new terminology. *Nature* **212**: 1385-1386.
Hodges, M.E., Scheumann, N., Wickstead, B., Langdale, J.A. and Gull, K. (2010) Reconstructing the evolutionary history of the centriole from protein components. *Journal of Cell Science* **123**: 1407-1413.
Hodgkinson, V.H., Soong, L., Duboise, S.M. and McMahon-Pratt, D. (1996) *Leishmania amazonensis*: cultivation and characterization of axenic amastigote-like organisms. *Experimental Parasitology* **83**: 94-105.
Holzer, T.R., McMaster, W.R. and Forney, J.D. (2006) Expression profiling by whole genome interspecies microarray hybridization reveals differentiatial gene expression in procyclic promastigotes, lesion-derived amastigotes, and axenic amastigotes in *Leishmania mexicana*. *Molecular and Biochemical Parasitology* **146**: 198-218.
Hughes, A.L. and Piontkivska, H. (2003) Phylogeny of Trypanosomatidae and Bodonidae (Kinetoplastida) based on 18S rRNA: evidence for paraphyly of *Trypanosoma* and six other genera. *Molecular Biology and Evolution* **20**: 644-652.
Hutchings, N.R., Donelson, J.E. and Hill, K.L. (2002) Trypanin is a cytoskeletal linker protein and is required for cell motility in African trypanosomes. *Journal of Cell Biology* 156: 867-877.
Ibanez-Tallon, I., Heintz, N. and Omran, H. (2003) To beat or not to beat: roles of cilia in development and disease. *Human Molecular Genetics* 12: R27-R35.
Ibi, M., Zou, P., Inoko, A., Shiromizu, T., Matsuyama, M., Hayashi, Y., Enomoto, M., Mori, D., Hirotsune, S., Kiyono, T., Tsukita, S., Goto, H. and Inagaki, M. (2011) Trichoplein controls microtubule anchoring at the centrosome by binding to Odf2 and ninein. *Journal of Cell Science* **124**: 857-864.
Ichida, A.A. and Fuller, M.S. (1968) Ultrastructure of mitosis in the aquatic fungus *Catenaria anguillulae. Mycologia* **60**: 141-155.
Ishikawa, H., Kubo, A., Tsukita, S. and Tsukita, S. (2005a) Odf2-deficient mother centrioles lack distal/subdistal appendages and the ability to generate primary cilia. *Nature Cell Biology* **7**: 517-524.
Jaeckel-Williams, R.J. (1978) Nuclear divisions with reduced numbers of microtubules in Tetrahymena. *Journal of Cell Science* **34**: 303-319.
James-Clark, H. (1867) Conclusive proofs on the animality of the ciliate sponges, and their affinities with the Infusoria flagellata. *Memoirs of the Boston Society of Natural History* **1**: 305-340.
James, T.Y., Letcher, P.M., Longcore, J.E., Mozley-Standridge, S.E., Porter, D., Powell, M.J., Griffith, G.W. and Vilgalys, R. (2006) A molecular phylogeny of the flagellated fungi (Chytridiomycota) and description of a new phylum (Blastocladiomycota). *Mycologia* **98**: 860-871.
Januschke, J., Llamazares, S., Reina, J. and Gonzalez, C. (2011) *Drosophila* neuroblasts retain the daughter centrosome. *Nature Communications* **2**: 243. doi:10.1038/ncomms1245.
Jaspersen, S.L. and Winey, M. (2004) The budding yeast spindle pole body: structure, duplication, and function. *Annual Review of Cell and Developmental Biology* **20**: 1-28.
Jensen, K.G., Moestrup, O. and Schmid, A.M.M. (2003) Ultrastructure of the male gametes from two centric diatoms, *Chaetoceros laciniosus* and *Coscinodiscus wailesii* (Bacillariophyceae). *Phycologia* **42**: 98-105.

Jones, S. and Sgouros, J. (2001) The cohesin complex: sequence homologies, interaction networks and shared motifs. *Genome Biology* **2**. doi:10.1186/gb-2001-2-3-research0009

Jones, T.C. and Hirsch, J.G. (1972) Interaction between *Toxoplasma gondii* and mammalian cells .II. The absence of lysosomal fusion with phagocytic cacuoles containing living parasites. *Journal of Experimental Medicine* **136**: 1173-1194.

Joukov, V., De Nicolo, A., Rodriguez, A., Walter, J.C. and Livingston, D.M. (2010) Centrosomal protein of 192 kDa (Cep192) promotes centrosome-driven spindle assembly by engaging in organelle-specific Aurora A activation. *Proceedings of the National Academy of Sciences of the United States of America* **107**: 21022-21027.

Karpov, S.A. (1980) The pecularities of the life-cycle of *Monosiga ovata* (Choanoflagellida: Monosigidae). *Zoologichesky Zhurnal* **59**: 269-299.

Karpov, S.A. (1981) The ultra-thin structure of the choanoflagellate *Sphaeroeca volvox*. *Tsitologia* **23**: 991-996.

Karpov, S.A. (1982) The ultra-thin structure of the choanoflagellate *Monosiga ovata*. *Tsitologia* **24**: 400-404.

Karpov, S.A. (1985) The ultra-thin structure of the choanoflagellate *Kentrosiga thienemanni*. *Tsitologia* **27**: 947-949.

Karpov, S.A. and Leadbeater, B.S.C. (1997) Cell and nuclear division in a freshwater choanoflagellate, *Monosiga ovata* (Kent). *European Journal of Protistology* **33**: 323-334.

Karpov, S.A. and Leadbeater, B.S.C. (1998) Cytoskeleton structure and composition in choanoflagellates. *Journal of Eukaryotic Microbiology* **45**: 361-367.

Karpov, S.A. and Mylnikov, A.P. (1993) Preliminary observations on the ultrastructure of mitosis in choanoflagellates. *European Journal of Protistology* **29**: 19-23.

Keating, T.J. and Borisy, G.G. (2000) Immunostructural evidence for the template mechanism of microtubule nucleation. *Nature Cell Biology* **2**: 352-357.

Kerr, S.F. (2006) Molecular trees of trypanosomes incongruent with fossil records of hosts. *Memorias Do Instituto Oswaldo Cruz* **101**: 25-30.

Khodjakov, A., Cole, R.W., Oakley, B.R. and Rieder, C.L. (2000) Centrosome-independent mitotic spindle formation in vertebrates. *Current Biology* **10**: 59-67.

Kim, K., Lee, S., Chang, J. and Rhee, K. (2008) A novel function of CEP135 as a platform protein of C-NAP1 for its centriolar localization. *Experimental Cell Research* **314**: 3692-3700.

Kima, P.E. (2007) The amastigote forms of *Leishmania* are experts at exploiting host cell processes to establish infection and persist. . *International Journal for Parasitology* **37**: 1087-1096.

King, N. (2004) The unicellular ancestry of animal development. *Developmental Cell* **7**: 313-325.

King, N., Westbrook, M.J., Young, S.L., Kuo, A., Abedin, M., Chapman, J., Fairclough, S., Hellsten, U., Isogai, Y., Letunic, I., Marr, M., Pincus, D., Putnam, N., Rokas, A., Wright, K.J., Zuzow, R., Dirks, W., Good, M., Goodstein, D., Lemons, D., Li, W.Q., Lyons, J.B., Morris, A., Nichols, S., Richter, D.J., Salamov, A., Bork, P., Lim, W.A., Manning, G., Miller, W.T., McGinnis, W., Shapiro, H., Tjian, R., Grigoriev, I.V. and Rokhsar, D. (2008) The genome of the choanoflagellate *Monosiga brevicollis* and the origin of metazoans. *Nature* **451**: 783-788.

Klotz, C., Ruiz, F., de Loubresse, N.G., Wright, M., Dupuis-Williams, P. and Beisson, J. (2003) Gamma-tubulin and MTOCs in *Paramecium*. *Protist* **154**: 193-209.

Kobayashi, T. and Dynlacht, B.D. (2011) Regulating the transition from centriole to basal body. Journal of Cell Biology **193**: 435-444.

Kohl, L., Robinson, D. and Bastin, P. (2003) Novel roles for the flagellum in cell morphogenesis and cytokinesis of trypanosomes. *The EMBO Journal* **22**: 5336-46.

Kollman, J.M., Merdes, A., Mourey, L. and Agard, D.A. (2011) Microtubule nucleation by gamma-tubulin complexes. *Nature Reviews Molecular Cell Biology* **12**: 709-21.

Krampitz, H.E. (1970) Reproductive activity and multiple divisions of trypanosomes of subgenus *Herpetosoma* (Doflein 1901) in placental blood of specific host. *Zeitschrift Fur Parasitenkunde* **34**: 296-309.

Kress, Y., Bloom, B.R., Wittner, M., Rowen, A. and Tanowitz, H. (1975) Resistance of *Trypanosoma cruzi* to killing by macrophages. *Nature* **257**: 394-396.

Kubo, A., Sasaki, H., Yuba-Kubo, A., Tsukita, S. and Shiina, N. (1999) Centriolar satellites: molecular characterization, ATP-dependent movement toward centrioles and possible involvement in ciliogenesis. *Journal of Cell Biology* **147**: 969-979.

Kubo, A. and Tsukita, S. (2003) Non-membranous granular organelle consisting of PCM-1: subcellular distribution and cell-cycledependent assembly/disassembly. *Journal of Cell Science* **116**: 919-928.

Kuo, T.C., Chen, C.T., Baron, D., Onder, T.T., Loewer, S., Almeida, S., Weismann, C.M., Xu, P., Houghton, J.M., Gao, F.B., Daley, G.Q. and Doxsey, S. (2011) Midbody accumulation through evasion of autophagy contributes to cellular reprogramming and tumorigenicity. *Nature Cell Biology* **13**: 1214-1223

Kyttala, M., Tallila, J., Salonen, R., Kopra, O., Kohlschmidt, N., Paavola-Sakki, P., Peltonen, L. and Kestila, M. (2006) MKS1, encoding a component of the flagellar apparatus basal body proteome, is mutated in Meckel syndrome. *Nature Genetics* **38**: 155-157.

Lambert, J.D. and Nagy, L.M. (2002) Asymmetric inheritance of centrosomally localized mRNAs during embryonic cleavages. *Nature* **420**: 682-686.

Landfear, S.M. and Ignatushchenko, M. (2001) The flagellum and flagellar pocket of trypanosomatids. *Molecular and Biochemical Parasitology* **115**: 1-17.

Lang, B.F., O'Kelly, C., Nerad, T., Gray, M.W. and Burger, G. (2002) The closest unicellular relatives of animals. *Current Biology* **12**: 1773-1778.

Lang, T., Hellio, R., Kaye, P.M. and Antoine, J.C. (1994) *Leishmania donovani*-infected macrophages: characterization of the parasitophorous vacuole and potential role of this organelle in antigen presentation. *Journal of Cell Science* **107**: 2137-2150.

Larsen, P.S. and Riisgard, H.U. (1994) The sponge pump. *Journal of Theoretical Biology* **168**: 53-63.

Laurent, T., Van der Auwera, G., Hide, M., Mertens, P., Quispe-Tintaya, W., Deborggraeve, S., De Doncker, S., Lectipteux, T., Banuls, A.L., Buscher, P. and Dujardin, J.C. (2009) Identification of Old World *Leishmania spp.* by specific polymerase chain reaction amplification of cysteine proteinase B genes and rapid. *Diagnostic Microbiology and Infectious Disease* **63**: 173-181.

Leadbeater, B.S.C. (1972) Fine-structural observations on some marine choanoflagellates from coast of Norway. *Journal of the Marine Biological Association of the United Kingdom* **52**: 67-79.

Leadbeater, B.S.C. (1977) Observations on life-history and ultrastructure of marine choanoflagellate *Choanoeca perplexa* Ellis. *Journal of the Marine Biological Association of the United Kingdom* **57**: 285-301.

Leadbeater, B.S.C. (1983) Life-history and ultrastructure of a new marine species of *Proterospongia* (Choanoflagellida). *Journal of the Marine Biological Association of the United Kingdom* **63**: 135-160.

Leadbeater, B.S.C. (1987) Developmental studies on the loricate choanoflagellate *Stephanoeca diplocostata* (Ellis). V. The cytoskeleton and the effects of microtubule poisons. *Protoplasma* **136**: 1-15.

Leadbeater, B.S.C. (1994) Developmental studies on the loricate choanoflagellate *Stephanoeca diplocostata* (Ellis). VIII. Nuclear division and cytokinesis. *European Journal of Protistology* **30**: 171-183.

Lee, K. and Rhee, K. (2011) PLK1 phosphorylation of pericentrin initiates centrosome maturation at the onset of mitosis. *Journal of Cell Biology* **195**: 1093-1101.

Letunic, I., Doerks, T. and Bork, P. (2009) SMART 6: recent updates and new developments. *Nucleic Acids Research* **37**: D229-D232.

Letunic, I., Doerks, T. and Bork, P. (2011) SMART 7: recent updates to the protein domain annotation resource. *Nucleic Acids Research* **40**: D302-D305.

Lewis, D.H. and Peters, W. (1977) Resistance of intracellular *Leishmania* parasites to digestion by lysosomal enzymes. *Annals of Tropical Medicine and Parasitology* **71**: 295-312.

Leys, S.P. and Degnan, B.M. (2002) Embryogenesis and metamorphosis in a haplosclerid demosponge: gastrulation and transdifferentiation of larval ciliated cells to choanocytes. *Invertebrate Biology* **121**: 171-189.

Leys, S.P. and Hill, A. (2012) The physiology and molecular biology of sponge tissues. *Advances in Marine Biology* **62**: 1-56.

Liang, A.H., Ruiz, F., Heckmann, K., Klotz, C., Tollon, Y., Beisson, J. and Wright, M. (1996) Gamma-tubulin is permanently associated with basal bodies in ciliates. *European Journal of Cell Biology* **70**: 331-338.

Libusova, L., Sulimenko, T., Sulimenko, V., Hozak, P. and Draber, P. (2004) Gamma-tubulin in *Leishmania*: cell cycle-dependent changes in subcellular localization and heterogeneity of its isoforms. *Experimental Cell Research* **295**: 375-386.

Litowski, J.R. and Hodges, R.S. (2001) Designing heterodimeric two-stranded alpha-helical coiled-coils: the effect of chain length on protein folding, stability and specificity. *Journal of Peptide Research* **58**: 477-492.

Liu, J. and Rost, B. (2001) Comparing function and structure between entire proteomes. *Protein Science* **10**: 1970-1979.

Longcore, J. (1999) *Batrachochytrium dendrobatidis* gen. et sp. nov., a chytrid pathogenic to amphibians. *Mycologia* **91**: 219-227.

Losada, A. and Hirano, T. (2005) Dynamic molecular linkers of the genome: the first decade of SMC proteins. *Genes and Development* **19**: 1269-1287.

Luders, J. and Stearns, T. (2007) Microtubule-organizing centres: a re-evaluation. *Nature Reviews Molecular Cell Biology* **8**: 161-167.

Lukes, J., Jirku, M., Dolezel, D., Kralova, I., Hollar, L. and Maslov, D.A. (1997) Analysis of ribosomal RNA genes suggests that trypanosomes are monophyletic. *Journal of Molecular Evolution* **44**: 521-527.

Lumsden, R. and Shaw, J.J. (1987) Evolution, classification and geographical distribution. In: Peters, W. and Killick-Kendrick, R. (eds.) *The Leishmaniases in Biology and Medicine*. Orlando: Academic Press.

Lumsden, W.H.R. (1974) Leishmaniasis and trypanosomiasis: the causative organisms compared and contrasted. In: Elliot, K., O'Connor, M. and Wolstenholme, G.E.W. (eds.) *Ciba Foundation Symposium 20 - Trypanosomiasis and Leishmaniasis (with Special Reference to Chagas' Disease).* Chichester: John Wiley and Sons, Ltd.

Lupas, A., Vandyke, M. and Stock, J. (1991) Predicting coiled coils from protein sequences. *Science* **252**: 1162-1164.

Lyons, K.M. (1973a) Collar cells in planula and adult tentacle ectoderm of solitary coral *Balanophyllia regia* (Anthozoa Eupsammiidae). *Zeitschrift Fur Zellforschung Und Mikroskopische Anatomie* **145**: 57-74.

Lyons, K.M. (1973b) Evolutionary implications of collar cell ectoderm in a coral planula. *Nature* **245**: 50-51.

Mack, G.J., Ou, Y.C. and Rattner, J.B. (2000) Integrating centrosome structure with protein composition and function in animal cells. *Microscopy Research and Technique* **49**: 409-419.

Maga, J.A., Sherwin, T., Francis, S., Gull, K. and LeBowitz, J.H. (1999) Genetic dissection of the *Leishmania* paraflagellar rod, a unique flagellar cytoskeleton structure. *Journal of Cell Science* **112**: 2753-63.

Maldonado, M. (2004) Choanoflagellates, choanocytes, and animal multicellularity. *Invertebrate Biology* **123**: 1-22.

Marchler-Bauer, A., Lu, S., Anderson, J.B., Chitsaz, F., Derbyshire, M.K., DeWeese-Scott, C., Fong, J.H., Geer, L.Y., Geer, R.C., Gonzales, N.R., Gwadz, M., Hurwitz, D.I., Jackson, J.D., Ke, Z., Lanczycki, C.J., Lu, F., Marchler, G.H., Mullokandov, M., Omelchenko, M.V., Robertson, C.L., Song, J.S., Thanki, N., Yamashita, R.A., Zhang, D., Zhang, N., Zheng, C.M. and Bryant, S.H. (2011) CDD: a

Conserved Domain Database for the functional annotation of proteins. *Nucleic Acids Research* **39**: D225-229.
Mardin, B.R., Lange, C., Baxter, J.E., Hardy, T., Scholz, S.R., Fry, A.M. and Schiebel, E. (2010) Components of the Hippo pathway cooperate with Nek2 kinase to regulate centrosome disjunction. *Nature Cell Biology* **12**: 1166-76.
Margulis, L. (1981) *Symbiosis in Cell Evolution*. New York: W.H. Freeman.
Marinkelle, C.J. and Abdalla, R.E. (1978) The multiplication stages of *Trypanosoma* (Herpetosoma) *xeri* in the liver of the Sudanese ground squirrel *Xerus* (Euxerus) *erythropus*. *Journal of Wildlife Diseases* **14**: 11-14.
Marshall, W.F. and Nonaka, S. (2006) Cilia: tuning in to the cell's antenna. *Current Biology* **16**: R604-614.
Matsuura, K., Lefebvre, P.A., Kamiya, R. and Hirono, M. (2004) Bld10p, a novel protein essential for basal body assembly in *Chlamydomonas*: localization to the cartwheel, the first ninefold symmetrical structure appearing during assembly. *Journal of Cell Biology* **165**: 663-671.
Mayor, T., Stierhof, Y.D., Tanaka, K., Fry, A.M. and Nigg, E.A. (2000) The centrosomal protein C-Nap1 is required for cell cycle-regulated centrosome cohesion. *Journal of Cell Biology* **151**: 837-846.
Mcconville, M.J. and Ferguson, M.A.J. (1993) The structure, biosynthesis and function of glycosylated phosphatidylinositols in the parasitic protozoa and higher eukaryotes. *Biochemical Journal* **294**: 305-324.
McConville, M.J., Mullin, K.A., Ilgoutz, S.C. and Teasdale, R.D. (2002) Secretory pathway of trypanosomatid parasites. *Microbiology and Molecular Biology Reviews* **66**: 122-154.
McDonnell, A.V., Jiang, T., Keating, A.E. and Berger, B. (2006) Paircoil2: improved prediction of coiled coils from sequence. *Bioinformatics* **22**: 356-358.
McKean, P.G., Baines, A., Vaughan, S. and Gull, K. (2003) Gamma-tubulin functions in the nucleation of a discrete subset of microtubules in the eukaryotic flagellum. *Current Biology* **13**: 598-602.
Mcneely, T.B. and Turco, S.J. (1990) Requirement of lipophosphoglycan for intracellular survival of *Leishmania donovani* within human monocytes. *Journal of Immunology* **144**: 2745-2750.
Melkonian, M., Robenek, H. and Rassat, J. (1982) Flagellar membrane specializations and their relationship to mastigonemes and microtubules in *Euglena gracilis*. *Journal of Cell Science* **55**: 115-135.
Meyer, H., de Oliveira Musacchio, M. and de Andrade Mendonça, I. (1958) Electron microscopic study of *Trypanosoma cruzi* in thin sections of infected tissue cultures and of blood-agar forms. *Parasitology* **48**: 1-8.
Meyer, H. and de Souza, W. (1976) Electron microscopic study of *Trypanosoma cruzi* periplast in tissue cultures. I. Number and arrangement of the peripheral microtubules in the various forms of the parasite's life cycle. *Journal of Protozoology* **23**: 385-390.
Meyer, H. and Queiroga, L.T. (1960) Submicroscopical aspects of *Schizotrypanum cruzi* in thin sections of tissue culture forms. *Journal of Protozoology* **7**: 124-127.
Michaud, E.J. and Yoder, B.K. (2006) The primary cilium in cell signaling and cancer. *Cancer Research* **66**: 6463-6467.
Michod, R.E. (2007) Evolution of individuality during the transition from unicellular to multicellular life. *Proceedings of the National Academy of Sciences of the United States of America* **104**: 8613-8618.
Mitchell, D.R. (2003) Orientation of the central pair complex during flagellar bend formation in Chlamydomonas. *Cell Motility and the Cytoskeleton* **56**: 120-129.
Mitchell, D.R. (2004) Speculations on the evolution of 9+2 organelles and the role of central pair microtubules. *Biology of the Cell* **96**: 691-696.
Mitchell, D.R. (2007) The evolution of eukaryotic cilia and flagella as motile and sensory organelles. *Advances in Experimental Medicine and Biology* **607**: 130-40.

Modarressi, M.H., Behnam, B., Cheng, M., Taylor, K.E., Wolfe, J. and van der Hoorn, F.A. (2004) *Tsga*10 encodes a 65-kilodalton protein that is processed to the 27-kilodalton fibrous sheath protein. *Biology of Reproduction* **70**: 608-615.

Moestrup, O. (2000) The flagellate cytoskeleton: introduction of a general terminology for microtubular flagellar roots in protists. In: Leadbeater, B.S.C. and Green, J.C. (eds.) *The Flagellates: Unity, Diversity and Evolution.* New York: Taylor and Francis.

Molyneux, D.H. (1969a) Morphology and biology of *Trypanosoma* (Herpetosoma) *evotomys* of the bank-vole, *Clethrionomys glareolus*. *Parasitology* **59**: 843-857.

Molyneux, D.H. (1969b) Morphology and life-history of *Trypanosoma* (Herpetosoma) *microti* of the field-vole, *Microtus agrestis*. *Annals of Tropical Medicine and Parasitology* **63**: 229-244.

Molyneux, D.H. (1969c) Reproduction of *Trypanosoma nabiasi* in the rabbit. *Transactions of the Royal Society of Tropical Medicine and Hygiene* **63**: 10.

Molyneux, D.H. (1970) Studies on the reproductive stages of trypanosomes of the subgenus *Herpetosoma*. *Transactions of the Royal Society of Tropical Medicine and Hygiene* **64**: 165-166.

Molyneux, D.H. (1976) Biology of trypanosomes of the subgenus *Herpetosoma*. In: Lumsden, W.H.R. and Evans, D.A. (eds.) *Biology of the Kinetoplastida*. London: Academic Press.

Moran, D.T., Rowley, J.C., Jafek, B.W. and Lovell, M.A. (1982) The fine-structure of the olfactory mucosa in man. *Journal of Neurocytology* **11**: 721-746.

Moritz, M., Braunfeld, M.B., Fung, J.C., Sedat, J.W., Alberts, B.M. and Agard, D.A. (1995) Three-dimensional structural characterization of centrosomes from early *Drosophila* embryos. *The Journal of Cell Biology* **130**: 1149-1159.

Moritz, M., Braunfeld, M.B., Guenebaut, V., Heuser, J. and Agard, D.A. (2000) Structure of the gamma-tubulin ring complex: a template for microtubule nucleation. *Nature Cell Biology* **2**: 365-370.

Morrissette, N.S. and Sibley, L.D. (2001) Disruption of microtubules uncouples budding and nuclear division in *Toxoplasma gondii*. *Journal of Cell Science* **115**: 1017-1025.

Morrissette, N.S. and Sibley, L.D. (2002) Cytoskeleton of apicomplexan parasites. *Microbiology and Molecular Biology Reviews* **66**: 21-38.

Mottier-Pavie, V. and Megraw, T.L. (2009) *Drosophila* Bld10 is a centriolar protein that regulates centriole, basal body, and motile cilium assembly. *Molecular Biology of the Cell* **20**: 2605-2614.

Moudjou, M., Bordes, N., Paintrand, M. and Bornens, M. (1996) Gamma-tubulin in mammalian cells: the centrosomal and the cytosolic forms. *Journal of Cell Science* **109**: 875-887.

Mykytyn, K. and Sheffield, V.C. (2004) Establishing a connection between cilia and Bardet-Biedl syndrome. *Trends in Molecular Medicine* **10**: 106-109.

Nakamura, A., Arai, H. and Fujita, N. (2009) Centrosomal Aki1 and cohesin function in separase-regulated centriole disengagement. *Journal of Cell Biology* 187: 607-614.

Newman, J.R.S., Wolf, E. and Kim, P.S. (2000) A computationally directed screen identifying interacting coiled coils from *Saccharomyces cerevisiae*. *Proceedings of the National Academy of Sciences of the United States of America* **97**: 13203-13208.

Nicastro, D. (2006) The molecular architecture of axonemes revealed by cryoelectron tomography. *Science* **313**: 944-948.

Nicastro, D., McIntosh, J.R. and Baumeister, W. (2005) 3D structure of eukaryotic flagella in a quiescent state revealed by cryo-electron tomography. *Proceedings of the National Academy of Sciences of the United States of America* **102**: 15889-15894.

Nielsen, C. (1987) Structure and function of metazoan ciliary bands and their phylogenetic significance. *Acta Zoologica* **68**: 205-262.

Nielsen, C. (2008) Six major steps in animal evolution: are we derived sponge larvae? *Evolution and Development* **10**: 241-257.

Nigg, E.A. and Raff, J.W. (2009) Centrioles, centrosomes, and cilia in health and disease. *Cell* **139**: 663-678.

Nitsche, F., Carr, M., Arndt, H. and Leadbeater, B.S.C. (2011) Higher level taxonomy and molecular phylogenetics of the choanoflagellatea. *Journal of Eukaryotic Microbiology* **58**: 452-462.

Nohynkova, E., Draber, P., Reischig, J. and Kulda, J. (2000) Localization of gamma-tubulin in interphase and mitotic cells of unicellular eukaryote*, Giardia intestinalis*. *European Journal of Cell Biology* **79**: 438-445.

Norrevang, A. and Wingstrand, K.G. (1970) On the occurence and structure of choanocyte-like cells in some echinoderms. *Acta Zoologica* **51**: 249-270.

Norris, R.E. (1965) Neustonic marine Craspedomondales (choanoflagellates) from Washington and California. *Journal of Protozoology* **12**: 589-602.

O'Toole, E.T., McDonald, K.L., Mantler, J., McIntosh, J.R., Hyman, A.A. and Muller-Reichert, T. (2003) Morphologically distinct microtubule ends in the mitotic centrosome of *Caenorhabditis elegans*. *Journal of Cell Biology* **163**: 451-456.

Oakley, B.R. (1992) Gamma-tubulin: the microtubule organizer? *Trends in Cell Biology* **2**: 1-5.

Oakley, B.R., Oakley, C.E., Yoon, Y.S. and Jung, M.K. (1990) Gamma-tubulin is a component of the spindle pole body that is essential for microtubule function in *Aspergillus nidulans*. *Cell* **61**: 1289-1301.

Oakley, C.E. and Oakley, B.R. (1989) Identification of gamma-tubulin, a new member of the tubulin superfamily encoded by mipA Gene of *Aspergillus nidulans*. *Nature* **338**: 662-664.

Oda, T., Hirokawa, N. and Kikkawa, M. (2007) Three-dimensional structures of the flagellar dynein-microtubule complex by cryoelectron microscopy. *Journal of Cell Biology* **177**: 243-252.

Odgren, P.R., Harvie, L.W. and Fey, E.G. (1996) Phylogenetic occurrence of coiled coil proteins: implications for tissue structure in Metazoa via a coiled coil tissue matrix. *Proteins: Structure, Function and Genetics* **24**: 467-484.

Odor, D.L. and Blandau, R.J. (1985) Observations on the solitary cilium of rabbit oviductal epithelium: its motility and ultrastructure. *American Journal of Anatomy* **174**: 437-453.

Ohta, T., Essner, R., Ryu, J.H., Palazzo, R.E., Uetake, Y. and Kuriyama, R. (2002) Characterization of Cep135, a novel coiled-coil centrosomal protein involved in microtubule organization in mammalian cells. *Journal of Cell Biology* **156**: 87-99.

Omoto, C.K., Gibbons, I.R., Kamiya, R., Shingyoji, C., Takahashi, K. and Witman, G.B. (1999) Rotation of the central pair microtubules in eukaryotic flagella. *Molecular Biology of the Cell* **10**: 1-4.

Ono, T., Losada, A., Hirano, M., Myers, M.P., Neuwald, A.F. and Hirano, T. (2003) Differential contributions of condensin I and condensin II to mitotic chromosome architecture in vertebrate cells. *Cell* **115**: 109-121.

Orme, B.A.A., Blake, J.R. and Otto, S.R. (2003) Modelling the motion of particles around choanoflagellates. *Journal of Fluid Mechanics* **475**: 333-355.

Ostrowski, L.E., Blackburn, K., Radde, K.M., Moyer, M.B., Schlatzer, D.M., Moseley, A. and Boucher, R.C. (2002) A proteomic analysis of human cilia: identification of novel components. *Molecular and Cell Proteomics* **1**: 451-465.

Ou, Y.Y., Mack, G.J., Zhang, M.F. and Rattner, J.B. (2002) CEP110 and ninein are located in a specific domain of the centrosome associated with centrosome maturation. *Journal of Cell Science* **115**: 1825-1835.

Overath, P., Haag, J., Lischke, A. and O'Huigin, C. (2001) The surface structure of trypanosomes in relation to their molecular phylogeny. *International Journal for Parasitology* **31**: 468-471.

Overath, P., Stierhof, Y.D. and Wiese, M. (1997) Endocytosis and secretion in trypanosomatid parasites: tumultuous traffic in a pocket. *Trends in Cell Biology* 7: 27-33.

Palacios, M.J., Joshi, H.C., Simerly, C. and Schatten, G. (1993) Gamma-tubulin reorganization during mouse fertilization and early development. *Journal of Cell Science* **104**: 383-389.

Palazzo, R.E., Vogel, J.M., Schnackenberg, B.J., Hull, D.R. and Wu, X.Y. (2000) Centrosome maturation. *Centrosome in Cell Replication and Early Development* **49**: 449-470.

Pan, A.A. (1984) *Leishmania mexicana*: serial cultivation of intracellular stages in a cell-free medium. *Experimental Parasitology* **58**: 72-80.
Pan, A.A., Duboise, S.M., Eperon, S., Rivas, L., Hodgkinson, V., Traubcseko, Y. and McMahon-Pratt, D. (1993) Developmental life-cycle of *Leishmania* : cultivation and characterization of cultured extracellular amastigotes. *Journal of Eukaryotic Microbiology* **40**: 213-223.
Pan, A.A. and Pan, S.C. (1986) *Leishmania mexicana*: comparative fine structure of amastigotes and promastigotes *in vitro* and *in vivo*. *Experimental Parasitology* **62**: 254-65.
Pazour, G.J., Agrin, N., Leszyk, J. and Witman, G.B. (2005) Proteomic analysis of a eukaryotic cilium. *Journal of Cell Biology* **170**: 103-113.
Pazour, G.J. and Witman, G.B. (2003) The vertebrate primary cilium is a sensory organelle. *Current Opinion in Cell Biology* **15**: 105-110.
Pelletier, L., Ozlu, N., Hannak, E., Cowan, C., Habermann, B., Ruer, M., Muller-Reichert, T. and Hyman, A.A. (2004) The *Caenorhabditis elegans* centrosomal protein SPD-2 is required for both pericentriolar material recruitment and centriole duplication. *Current Biology* **14**: 863-873.
Pelletier, L. and Yamashita, Y.M. (2012) Centrosome asymmetry and inheritance during animal development. *Current Opinion in Cell Biology* **24**: 541-546.
Pereira, G. and Schiebel, E. (1997) Centrosome-microtubule nucleation. *Journal of Cell Science* **110**: 295-300.
Perkins, L.A., Hedgecock, E.M., Thomson, J.N. and Culotti, J.G. (1986) Mutant sensory cilia in the nematode *Caenorhabditis elegans*. *Developmental Biology* **117**: 456-487.
Pettitt, M.E., Orme, B.A.A., Blake, J.R. and Leadbeater, B.S.C. (2002) The hydrodynamics of filter feeding in choanoflagellates. *European Journal of Protistology* **38**: 313-332.
Pham, T.D., Azar, H.A., Moscovic, E.A. and Kurban, A.K. (1970) The ultrastructure of *Leishmania tropica* in the oriental sore. *Annals of Tropical Medicine and Parasitology* **64**: 1-4.
Pickett-Heaps, J.D. (1971) The autonomy of the centriole: fact or fallacy? *Cytobios* **3**: 205-214.
Pickett-Heaps, J.D. (1973) Cell division in *Tetraspora*. *Annals of Botany* **37**: 1017-1025.
Piontkivska, H. and Hughes, A.L. (2005) Environmental kinetoplastid-like 18S rRNA sequences and phylogenetic relationships among Trypanosomatidae: paraphyly of the genus *Trypanosoma*. *Molecular and Biochemical Parasitology* **144**: 94-99.
Praetorius, H.A. and Spring, K.R. (2001) Bending the MDCK cell primary cilium increases intracellular calcium. *Journal of Membrane Biology* **184**: 71-79.
Pral, E.M.F., Bijovsky, A.T., Balanco, J.M.F. and Alfieri, S.C. (1993) *Leishmania mexicana*: proteinase activities and megasomes in axenically cultured amastigote-like forms. *Experimental Parasitology* **77**: 62-73.
Prensier, G., Vivier, E., Goldstein, S. and Schrevel, J. (1980) Motile flagellum with a "3 + 0" ultrastructure. *Science* 207: 1493-1494.
Pullen, T.J., Ginger, M.L., Gaskell, S.J. and Gull, K. (2004) Protein targeting of an unusual, evolutionarily conserved adenylate kinase to a eukaryotic flagellum. *Molecular Biology of the Cell* **15**: 3257-3265.
Punta, M., Coggill, P.C., Eberhardt, R.Y., Mistry, J., Tate, J., Boursnell, C., Pang, N., Forslund, K., Ceric, G., Clements, J., Heger, A., Holm, L., Sonnhammer, E.L.L., Eddy, S.R., Bateman, A. and Finn, R.D. (2011) The Pfam protein families database. *Nucleic Acids Research* **40**: D290-D301.
Rackham, O.J., Madera, M., Armstrong, C.T., Vincent, T.L., Woolfson, D.N. and Gough, J. (2010) The evolution and structure prediction of coiled coils across all genomes. *Journal of Molecular Biology* **403**: 480-493.
Raikov, I.B. (1982) *The protozoan nucleus.* Berlin: Springer-Verlag.
Ralston, K.S. and Hill, K.L. (2008) The flagellum of *Trypanosoma brucei*: new tricks from an old dog. *International Journal for Parasitology* **38:** 869-884.
Rattner, J.B. (1992) Integrating chromosome structure with function. *Chromosoma*: **101,** 259-264.

Rehberg, M. and Graf, R. (2002) *Dictyostelium* EB1 is a genuine centrosomal component required for proper spindle formation. *Molecular Biology of the Cell* **13**: 2301-2310.
Reilein, A., Yamada, S. and Nelson, W.J. (2005) Self-organization of an acentrosomal microtubule network at the basal cortex of polarized epithelial cells. *Journal of Cell Biology* **171**: 845-855.
Rieder, C.L. and Borisy, G.G. (1982) The centrosome cycle in PtK2 cells: asymmetric distribution and structural changes in the pericentriolar material. *Biology of the Cell* **44**: 117-132.
Riparbelli, M.G., Cabrera, O.A., Callaini, G. and Megraw, T.L. (2013) Unique properties of *Drosophila* spermatocyte primary cilia. *Biology Open* 2: 1137-1147
Roghanian, A., Jones, D.C., Pattisapu, J.V., Wolfe, J., Young, N.T. and Behnam, B. (2010) Filament-associated TSGA10 protein is expressed in professional antigen presenting cells and interacts with vimentin. *Cellular Immunology* **265**: 120-126.
Romio, L., Fry, A.M., Winyard, P.J.D., Malcolm, S., Woolf, A.S. and Feather, S.A. (2004) OFD1 is a centrosomal/basal body protein expressed during mesenchymal-epithelial transition in human nephrogenesis. *Journal of the American Society of Nephrology* **15**: 2556-2568.
Rose, A. (2007) Open mitosis: nuclear envelope dynamics. In: Verma, D.P.S. and Hong, Z. (eds.) *Cell Division Control in Plants (Plant Cell Monographs)*. Berlin: Springer.
Rose, A., Schraegle, S.J., Stahlberg, E.A. and Meier, I. (2005) Coiled-coil protein composition of 22 proteomes: differences and common themes in subcellular infrastructure and traffic control. *BMC Evolutionary Biology* **5**: 66. doi:10.1186/1471-2148-5-66
Rosenbaum, J.L. and Witman, G.B. (2002) Intraflagellar transport. *Nature Reviews Molecular Cell Biology* **3**: 813-825.
Rozen, S. amd Skaletsky, H.J. (2000) Primer3 on the WWW for general users and biologist programmers. In: Krawetz, S. and Misener, S. (eds.) *Bioinformatics Methods and Protocols: Methods in Molecular Biology*. Totowa: Humana Press.
Rudzinska, M.A., D, A.P. and Trager, W. (1964) The fine structure of *Leishmania donovani* and the role of the kinetoplast in the leishmania-leptomonad transformation. *Journal of Protozoology* 11: 166-191.
Ruiz-Trillo, I., Roger, A.J., Burger, G., Gray, M.W. and Lang, B.F. (2008) A phylogenomic investigation into the origin of metazoa. *Molecular Biology and Evolution* **25**: 664-672.
Rupp, G. and Porter, M.E. (2003) A subunit of the dynein regulatory complex in *Chlamydomonas* is a homologue of a growth arrest-specific gene product. *Journal of Cell Biology* **162**: 47-57.
Ruthmann, A., Behrendt, G. and Wahl, R. (1986) The ventral epithelium of *Trichoplax adhaerens* (Placozoa): cytoskeletal structures, cell contacts and endocytosis. *Zoomorphology* **106**: 115-122.
Sádlová, J., Price, H.P., Smith, B.A., Votýpka, J., Volf, P. and Smith, D.F. (2010) The stage-regulated HASPB and SHERP proteins are essential for differentiation of the protozoan parasite *Leishmania major* in its sand fly vector, *Phlebotomus papatasi*. *Cellular Microbiology* **12**: 1765-1779.
Sale, W.S. (1986) The axonemal axis and Ca2+-induced asymmetry of active microtubule sliding in sea-urchin sperm tails. *Journal of Cell Biology* **102**: 2042-2052.
Sanabria, A. (1963) Ultrastructure of *Trypanosoma cruzi* in mouse myocardium. I. Trypanosome form. *Experimental Parasitology* **14**: 81-91.
Sanabria, A. (1964) Ultrastructure of *Trypanosoma cruzi* in mouse myocardium. II. Crithidial and leishmanial forms. *Experimental Parasitology* **15**: 125-137.
Sanabria, A. (1966) Ultrastructure of *Trypanosoma cruzi* in the rectum of *Rhodnius prolixus*. *Experimental Parasitology* **19**: 276-299.
Sanabria, A. (1968) Ultrastructure of *Trypanosoma cruzi* in mouse brain. *Experimental Parasitology* **23**: 379-391.
Sanabria, A. (1971) Ultrastructure of *Trypanosoma cruzi* in mouse liver. *Experimental Parasitology* **30**: 187-198.

Santrich, C., Moore, L., Sherwin, T., Bastin, P., Brokaw, C., Gull, K. and LeBowitz, J.H. (1997) A motility function for the paraflagellar rod of *Leishmania* parasites revealed by PFR-2 gene knockouts. *Molecular and Biochemical Parasitology* **90**: 95-109.

Sanyal, A.B. and Sen Gupta, P.C. (1967) Fine structure of *Leishmania* in dermal leishmanoid. *Transactions of the Royal Society of Tropical Medicine and Hygiene* **61**: 211-216.

Sapiro, R., Kostetskii, I., Olds-Clarke, P., Gerton, G.L., Radice, G.L. and Strauss, J.F. (2002) Male infertility, impaired sperm motility, and hydrocephalus in mice deficient in sperm-associated antigen 6. *Molecular and Cellular Biology* **22**: 6298-6305.

Satir, P. (1963) Studies on cilia: fixation of metachronal wave. *Journal of Cell Biology* **18**: 345-365.

Satir, P. (1989) The role of axonemal components in ciliary motility. *Comparative Biochemistry and Physiology Part A: Physiology* **94**: 351-357.

Satir, P. and Christensen, S.T. (2007) Overview of structure and function of mammalian cilia. *Annual Review of Physiology* **69**: 377-400.

Satir, P., Mitchell, D.R. and Jekely, G. (2008) How did the cilium evolve? *Ciliary Function in Mammalian Development* **85**: 63-82.

Schatten, H. (2008) The mammalian centrosome and its functional significance. *Histochemistry and Cell Biology* **129**: 667-686.

Schliwa, M. (1982) Action of cytochalasin D on cytoskeletal networks. *Journal of Cell Biology* **92**: 79-91.

Schneider, P., Rosat, J.P., Ransijn, A., Ferguson, M.A.J. and Mcconville, M.J. (1993) Characterization of glycoinositol phospholipids in the amastigote stage of the protozoan parasite *Leishmania major*. *Biochemical Journal* **295**: 555-564.

Schockel, L., Mockel, M., Mayer, B., Boos, D. and Stemmann, O. (2011) Cleavage of cohesin rings coordinates the separation of centrioles and chromatids. *Nature Cell Biology* **13**: 966-972.

Schrevel, J. and Besse, C. (1975) A functional flagella with a 6+0 pattern. *Journal of Cell Biology* **66**: 492-507.

Schulz, I., Erle, A., Graf, R., Kruger, A., Lohmeier, H., Putzler, S., Samereier, M. and Weidenthaler, S. (2009) Identification and cell cycle-dependent localization of nine novel, genuine centrosomal components in *Dictyostelium discoideum*. *Cell Motility and the Cytoskeleton* **66**: 915-928.

Scott, V., Sherwin, T. and Gull, K. (1997) Gamma-tubulin in trypanosomes: molecular characterisation and localisation to multiple and diverse microtubule organising centres. *Journal of Cell Science* **110**: 157-168.

Sebé-Pedrós, A., Burkhardt, P., Sánchez-Pons, N., Fairclough, S.R., Lang, B.F., King, N. and Ruiz-Trillo, I. (2013) Insights into the origin of metazoan filopodia and microvilli. *Molecular Biology and Evolution* **30**: 2013-2023.

Shlomai, J. (2004) The structure and replication of kinetoplast DNA. *Current Molecular Medicine* **4**: 623-647.

Silflow, C.D., Liu, B., LaVoie, M., Richardson, E.A. and Palevitz, B.A. (1999) Gamma-tubulin in *Chlamydomonas*: characterization of the gene and localization of the gene product in cells. *Cell Motility and the Cytoskeleton* **42**: 285-297.

Silverman, J., Clos, J., De'Oliveira, C., Shirvani, O., Fang, Y., Wang, C., Foster, L. and Reiner, N. (2010) An exosome-based secretion pathway is responsible for protein export from. *Journal of Cell Science* **123**: 842-852.

Simpson, A.G., Gill, E.E., Callahan, H.A., Litaker, R.W. and Roger, A.J. (2004) Early evolution within kinetoplastids (euglenozoa), and the late emergence of trypanosomatids. *Protist* **155**: 407-422.

Simpson, A.G. and Roger, A.J. (2004) The real 'kingdoms' of eukaryotes. *Current Biology* **14**: R693-R696.

Simpson, A.G.B., Stevens, J.R. and Lukes, J. (2006) The evolution and diversity of kinetoplastid flagellates. *Trends in Parasitology* **22**: 168-174.

Simpson, C.F., Harvey, J.W. and French, T.W. (1982) Ultrastructure of amastigotes of *Leishmania donovani* in the bone marrow of a dog. *American Journal of Veterinary Research* **43**: 1684-1686.

Sinden, R.E., Canning, E.U., Bray, R.S. and Smalley, M.E. (1978) Gametocyte and gamete development in *Plasmodium falciparum*. *Proceedings of the Royal Society of London Series B: Biological Sciences* **201**: 375-399.

Sinden, R.E., Canning, E.U. and Spain, B. (1976) Gametogenesis and fertilization in *Plasmodium yoelii nigeriensis*: a transmission electron microscope study. *Proceedings of the Royal Society of London Series B: Biological Sciences* **193**: 55-76.

Singh, S. (2006) New developments in diagnosis of leishmaniasis. *Indian Journal of Medical Research* **123**: 311-330.

Singla, V. and Reiter, J.F. (2006) The primary cilium as the cell's antenna: signaling at a sensory organelle. *Science* **313**: 629-633.

Sir, J.H., Barr, A.R., Nicholas, A.K., Carvalho, O.P., Khurshid, M., Sossick, A., Reichelt, S., D'Santos, C., Woods, C.G. and Gergely, F. (2011) A primary microcephaly protein complex forms a ring around parental centrioles. *Nature Genetics* **43**: 1147-1153.

Smith, E.F. and Lefebvre, P.A. (1996) PF16 encodes a protein with armadillo repeats and localizes to a single microtubule of the central apparatus in *Chlamydomonas* flagella. *Journal of Cell Biology* **132**: 359-370.

Smith, E.F. and Lefebvre, P.A. (1997) PF20 gene product contains WD repeats and localizes to the intermicrotubule bridges in *Chlamydomonas* flagella. *Molecular Biology of the Cell* **8**: 455-467.

Smith, J.C., Northey, J.G., Garg, J., Pearlman, R.E. and Siu, K.W. (2005) Robust method for proteome analysis by MS/MS using an entire translated genome: demonstration on the ciliome of *Tetrahymena thermophila*. *Journal of Proteome Research* **4**: 909-919.

Soppa, J. (2001) Prokaryotic structural maintenance of chromosomes (SMC) proteins: distribution, phylogeny, and comparison with MukBs and additional prokaryotic and eukaryotic coiled-coil proteins. *Gene* **278**: 253-264.

Southworth, D. and Cresti, M. (1997) Comparison of flagellated and non-flagellated sperm in plants. *American Journal of Botany* **84**: 1301-1311.

Spang, A., Geissler, S., Grein, K. and Schiebel, E. (1996) Gamma-tubulin-like Tub4p of *Saccharomyces cerevisiae* is associated with the spindle pole body substructures that organize microtubules and is required for mitotic spindle formation. *Journal of Cell Biology* **134**: 429-441.

Spektor, A., Tsang, W.Y., Khoo, D. and Dynlacht, B.D. (2007) Cep97 and CP110 suppress a cilia assembly program. *Cell* **130**: 678-690.

Stanley, S.M. (1973) Ecological theory for sudden origin of multicellular life in late Precambrian. *Proceedings of the National Academy of Sciences of the United States of America* **70**: 1486-1489.

Stearns, T., Evans, L. and Kirschner, M. (1991) Gamma-tubulin Is a highly conserved component of the centrosome. *Cell* **65**: 825-836.

Stearns, T. and Kirschner, M. (1994) *In vitro* reconstitution of centrosome assembly and function: the central role of gamma-tubulin. *Cell* **76**: 623-637.

Steenkamp, E.T., Wright, J. and Baldauf, S.L. (2006) The protistan origins of animals and fungi. *Molecular Biology and Evolution* **23**: 93-106.

Stevens, J.R., Noyes, H., Dover, G.A. and Gibson, W.C. (1999) The ancient and divergent origins of the human pathogenic trypanosomes, *Trypanosoma brucei* and *T. cruzi*. *Parasitology* **118**: 107-116.

Stevens, J.R., Noyes, H.A., Schofield, C.J. and Gibson, W. (2001) The molecular evolution of Trypanosomatidae. *Advances in Parasitology* **48**: 1-56.

Stevens, N.R., Raposo, A.A.S.F., Basto, R., St Johnston, D. and Raff, J.W. (2007) From stem cell to embryo without centrioles. *Current Biology* **17**: 1498-1503.

Straube, A., Weber, I. and Steinberg, G. (2005) A novel mechanism of nuclear envelope break-down in a fungus: nuclear migration strips off the envelope. The *EMBO Journal* **24**: 1674-1685.
Strelkov, S.V., Herrmann, H. and Aebi, U. (2003) Molecular architecture of intermediate filaments. *Bioessays* **25**: 243-251.
Stuart, K., Brun, R., Croft, S., Fairlamb, A., Gurtler, R.E., McKerrow, J., Reed, S. and Tarleton, R. (2008) Kinetoplastids: related protozoan pathogens, different diseases. *Journal of Clinical Investigation* **118**: 1301-1310.
Su, J.Y., Hodges, R.S. and Kay, C.M. (1994) Effect of chain-length on the formation and stability of synthetic alpha-helical coiled coils. *Biochemistry* 33: 15501-15510.
Suga, H., Chen, Z., de Mendoza, A., Sebe-Pedros, A., Brown, M.W., Kramer, E., Carr, M., Kerner, P., Vervoort, M., Sanchez-Pons, N., Torruella, G., Derelle, R., Manning, G., Lang, B.F., Russ, C., Haas, B.J., Roger, A.J., Nusbaum, C. and Ruiz-Trillo, I. (2013) The *Capsaspora* genome reveals a complex unicellular prehistory of animals. *Nature Communications* **4**: 2325. doi:10.1038/ncomms3325.
Summers, K.E. and Gibbons, I.R. (1971) Adenosine triphosphate induced sliding of tubules in trypsin-treated flagella of sea-urchin sperm. *Proceedings of the National Academy of Sciences of the United States of America* **68**: 3092-3096.
Szappanos, B., Suveges, D., Nyitray, L., Perczel, A. and Gaspari, Z. (2010) Folded-unfolded cross-predictions and protein evolution: the case study of coiled-coils. *FEBS Letters* **584**: 1623-1627.
Szöllösi, A., Ris, H., Szöllösi, D. and Debec, A. (1986) A centriole-free *Drosophila* cell line: a high voltage EM study. *European Journal of Cell Biology* **40**: 100-104.
Szöllösi, D., Calarco, P. and R.P., D. (1972) Absence of centrioles in the first and second meitotic spindles of mouse oocytes. *Journal of Cell Science* **11**: 521-541.
Tamm, S.L. and Tamm, S. (1981) Ciliary ceversal without rotation of axonemal structures in ctenophore comb plates. *Journal of Cell Biology* **89**: 495-509.
Tetley, L. and Vickerman, K. (1985) Differentiation in *Trypanosoma brucei* : host-parasite cell-junctions and their persistence during acquisition of the variable antigen coat. *Journal of Cell Science* **74**: 1-19.
Thein, K.H., Kleylein-Sohn, J., Nigg, E.A. and Gruneberg, U. (2007) Astrin is required for the maintenance of sister chromatid cohesion and centrosome integrity. *Journal of Cell Biology* **178**: 345-354.
Theisen, U., Straube, A. and Steinberg, G. (2008) Dynamic rearrangement of nucleoporins during fungal "open" mitosis. *Molecular Biology of the Cell* **19**: 1230-1240.
Tsang, W.Y., Bossard, C., Khanna, H., Peraenen, J., Swaroop, A., Malhotra, V. and Dynlacht, B.D. (2008) CP110 suppresses primary cilia formation through its interaction with CEP290, a protein deficient in human ciliary disease. *Developmental Cell* **15**: 187-197.
Tsang, W.Y., Spektor, A., Luciano, D.J., Indjeian, V.B., Chen, Z.H., Salisbury, J.L., Sanchez, I. and Dynlacht, B.D. (2006) CP110 cooperates with two calcium-binding proteins to regulate cytokinesis and genome stability. *Molecular Biology of the Cell* **17**: 3423-3434.
Tsou, M.F. and Stearns, T. (2006) Mechanism limiting centrosome duplication to once per cell cycle. *Nature* **442**: 947-951.
Tulu, U.S., Rusan, N.M. and Wadsworth, P. (2003) Peripheral, non-centrosome-associated microtubules contribute to spindle formation in centrosome-containing cells. *Current Biology* **13**: 1894-1899.
Tyler, K.M. andEngman, D.M. (2001) The life cycle of *Trypanosoma cruzi* revisited. *International Journal for Parasitology* **31**: 472-481.
Ueda, M., Schliwa, M. and Euteneuer, U. (1999) Unusual centrosome cycle in *Dictyostelium*: correlation of dynamic behavior and structural changes. *Molecular Biology of the Cell* **10**: 151-160.

Uhlmann, F., Lottspeich, F. and Nasmyth, K. (1999) Sister-chromatid separation at anaphase onset is promoted by cleavage of the cohesin subunit Scc1. *Nature* **400**: 37-42.

Urdaneta-Morales, S. and Tejero, F. (1985) *Trypanosoma* (Herpetosoma) *rangeli* Tejera, 1920: mouse model for high, sustained parasitemia. *Journal of Parasitology* **71**: 409-414.

Vacelet, J., Bouryesnault, N., Devos, L. and Donadey, C. (1989) Comparative study of the choanosome of *Porifera*. II. The keratose sponges. *Journal of Morphology* **201**: 119-129.

Vacelet, J. and Duport, E. (2004) Prey capture and digestion in the carnivorous sponge *Asbestopluma hypogea* (Porifera: Demospongiae). *Zoomorphology* **123**: 179-190.

Varmark, H., Liamazares, S., Rebollo, E., Lange, B., Reina, J., Schwarz, H. and Gonzalez, C. (2007) Asterless is a centriolar protein required for centrosome function and embryo development in *Drosophila*. *Current Biology* **17**: 1735-1745.

Vickerman, K. (1969) Fine structure of *Trypanosoma congolense* in its bloodstream phase. *Journal of Protozoology* **16**: 54-69.

Vickerman, K. (1994) The evolutionary expansion of the trypanosomatid flagellates. *International Journal for Parasitology* **24**: 1317-1331.

Wainright, P.O., Hinkle, G., Sogin, M.L. and Stickel, S.K. (1993) Monophyletic origins of the Metazoa: an evolutionary link with fungi. *Science* **260**: 340-342.

Wang, H., Xu, Z., Gao, L. and Hao, B. (2009a) A fungal phylogeny based on 82 complete genomes using the composition vector method. *BMC Evolutionary Biology* **9**: 195. doi:10.1186/1471-2148-9-195

Wang, X., Tsai, J.W., Imai, J.H., Lian, W.N., Vallee, R.B. and Shi, S.H. (2009b) Asymmetric centrosome inheritance maintains neural progenitors in the neocortex. *Nature* **461**: 947-955.

Wargo, M.J., McPeek, M.A. and Smith, E.F. (2004) Analysis of microtubule sliding patterns in *Chlamydomonas* flagellar axonemes reveals dynein activity on specific doublet microtubules. *Journal of Cell Science* **117**: 2533-2544.

Wargo, M.J. and Smith, E.F. (2003) Asymmetry of the central apparatus defines the location of active microtubule sliding in *Chlamydomonas* flagella. *Proceedings of the National Academy of Sciences of the United States of America* **100**: 137-142.

Watanabe, K. (1978) Structure and formation of the collar in choanocytes of *Tetilla sertca* (Lebwohl), Demosponge. *Development, Growth and Differentiation* **20**: 79-91.

Webster, P. and Russell, D.G. (1993) The flagellar pocket of trypanosomatids. *Parasitology Today* **9**: 201-206.

Westbrook, M.W. (2011) *Introns and alternative splicing in choanoflagellates*. PhD Dissertation. University of California, Berkeley.

Wickstead, B. and Gull, K. (2007) Dyneins across eukaryotes: a comparative genomic analysis. *Traffic* **8**: 1708-1721.

Wiese, C. and Zheng, Y.X. (2000) A new function for the gamma-tubulin ring complex as a microtubule minus-end cap. *Nature Cell Biology* **2**: 358-364.

Wilkerson, C.G., King, S.M., Koutoulis, A., Pazour, G.J. and Witman, G.B. (1995) The 78,000-*Mr* intermediate chain of *Chlamydomonas* outer arm dynein Is a WD-repeat protein required for arm assembly. *Journal of Cell Biology* **129**: 169-178.

Wilkinson, C.J., Andersen, J.S., Mann, M. and Nigg, E.A. (2004) A proteomic approach to the inventory of the human centrosome. In: Nigg, E.A. (ed.) *Centrosomes in Development and Disease*. Weinhein: Wiley-VCH.

Williams, B.D., Velleca, M.A., Curry, A.M. and Rosenbaum, J.L. (1989) Molecular cloning and sequence analysis of the *Chlamydomonas* gene coding for radial spoke protein-3: flagellar mutation PF-14 is an ochre allele. *Journal of Cell Biology* **109**: 235-245.

Wilson, D., Madera, M., Vogel, B., Chothia, C. and Gough, J. (2007) The SUPERFAMILY database in 2007: families and functions. *Nucleic Acids Research* **35**: D308-D313.

Wilson, V.C.L.C., Viens, P., Targett, G.A.T. and Edwards, C.I. (1973) Comparative studies on persistence of *Trypanosoma* (Herpetosoma) *musculi* and *T. (H) lewisi* in immune hosts. *Transactions of the Royal Society of Tropical Medicine and Hygiene* 67: 271-272.

Wolf, E., Kim, P.S. and Berger, B. (1997) MultiCoil: a program for predicting two- and three-stranded coiled coils. *Protein Science* **6**: 1179-1189.

Woods, A., Sherwin, T., Sasse, R., Macrae, T.H., Baines, A.J. and Gull, K. (1989) Definition of individual components within the cytoskeleton of *Trypanosoma brucei* by a library of monoclonal antibodies. *Journal of Cell Science* **93**: 491-500.

Woodward, R. and Gull, K. (1990) Timing of nuclear and kinetoplast DNA replication and early morphological events in the cell cycle of *Trypanosoma brucei*. *Journal of Cell Science* **95**: 49-57.

Woollacott, R.M. (2005) Spermatozoa of *Ciona intestinalis* and analysis of ascidian fertilization. *Journal of Morphology* **152**: 77-88

Woollacott, R.M. and Pinto, R.L. (1995) Flagellar basal apparatus and its utility in phlogenetic analysis of the Porifera. *Journal of Morphology* **226**: 247-265.

Xiong, Y. and Oakley, B.R. (2009) *In vivo* analysis of the functions of gamma-tubulin-complex proteins. *Journal of Cell Science* **122**: 4218-4227.

Yamashita, Y.M., Mahowald, A.P., Perlin, J.R. and Fuller, M.T. (2007) Asymmetric inheritance of mother versus daughter centrosome in stem cell division. *Science* **315**: 518-521.

Yang, J., Adamian, M. and Li, T.S. (2006) Rootletin interacts with C-Nap1 and may function as a physical linker between the pair of centrioles/basal bodies in cells. *Molecular Biology of the Cell* **17**: 1033-1040.

Zheng, Y.X., Jung, M.K. and Oakley, B.R. (1991) Gamma-tubulin is rresent in *Drosophila melanogaster* and *Homo sapiens* and is associated with the centrosome. *Cell* **65**: 817-823.

Zhu, F., Lawo, S., Bird, A., Pinchev, D., Ralph, A., Richter, C., Muller-Reichert, T., Kittler, R., Hyman, A.A. and Pelletier, L. (2008) The mammalian SPD-2 ortholog Cep192 regulates centrosome biogenesis. *Current Biology* **18**: 136-141.

Zilberstein, D. and Shapira, M. (1994) The role of pH and temperature in the development of *Leishmania* parasites. *Annual Review of Microbiology* **48**: 449-470.

Zimmerman, W., Sparks, C.A. and Doxsey, S.J. (1999) Amorphous no longer: the centrosome comes into focus. *Current Opinion in Cell Biology* **11**: 122-128.

Zimmerman, W.C., Sillibourne, J., Rosa, J. and Doxsey, S.J. (2004) Mitosis-specific anchoring of gamma tubulin complexes by pericentrin controls spindle organization and mitotic entry. *Molecular Biology of the Cell* **15**: 3642-3657.